Synthesis and Characterization of Nafion Composite Membrane for Reduced Methanol Crossover in DMFC

Submitted in partial fulfilment of the requirements for the degree of

Doctor of Philosophy

by

LEPAKSHI BARBORA

CENTRE FOR ENERGY

INDIAN INSTITUTE OF TECHNOLOGY GUWAHATI

Guwahati – 781 039

December, 2013

Synthesis and Characterization of Nafion Composite Membrane for Reduced Methanol Crossover in DMFC

Submitted by

Lepakshi Barbora

Centre for Energy

Indian Institute of Technology Guwahati

Guwahati – 781 039

December, 2013

Dedicated to my family...

Centre for Energy
Indian Institute of Technology Guwahati
Guwahati – 781 039
Assam, India

STATEMENT

I do hereby declare that the matter embedded in this thesis is the result of investigations carried out by me in the Centre for Energy, Indian Institute of Technology Guwahati, Guwahati, Assam, India, under the supervision of Dr. Anil Verma, Department of Chemical Engineering, Indian Institute of Technology Guwahati, Guwahati, Assam, India.

In keeping with the general practice of reporting scientific observations, due acknowledgement has been made wherever the work described is based on the findings of other investigators.

_ _ _ _ _ _ _ _ _ _ _ _ _ _ _ _ _ _ _ _

Dated:
IIT Guwahati

Lepakshi Barbora
Roll No. 06615104
Centre for Energy
Indian Institute of Technology Guwahati
Guwahati – 781 039

Centre for Energy
Indian Institute of Technology Guwahati
Guwahati – 781 039
Assam, India

CERTIFICATE

It is certified that the work contained in the thesis entitled "Synthesis and Characterization of Nafion Composite Membrane for Reduced Methanol Crossover in DMFC", by Mrs. Lepakshi Barbora (Roll No. 06615104), for the award of degree of Doctor of Philosophy, has been carried out under my supervision and that this work has not been submitted elsewhere for a degree.

Dated:
IIT Guwahati

_ _ _ _ _ _ _ _ _ _ _ _ _ _ _ _ _ _ _ _

Dr. Anil Verma
Associate Professor
Department of Chemical Engineering
Indian Institute of Technology Guwahati
Guwahati – 781 039

Preface

This thesis is an attempt to develop Nafion® composite membrane for reduced methanol crossover in direct methanol fuel cell (DMFC). The thesis provides detailed experimental techniques, characterization, and investigations to develop effective nafion composite membrane for DMFC applications.

Historical background of fuel cell, working principle, fuel cell types, description of the various components of DMFC with special emphasis on the various types of polymer electrolyte membrane used in DMFC is provided in the 1st chapter.

A detailed literature review on the important scientific findings on the nafion composite membranes developed for DMFC is given in 2nd chapter. The outcomes of a few significant literatures are summarized at the end of the chapter and the objective of the thesis is formulated based on the literature review.

Description on the materials used for synthesis of nafion composites along with the methodology of membrane preparation and membrane characterization both by ex-situ techniques as well as evaluation of the composite membranes in a DMFC test set-up is given in the 3rd chapter.

The results and discussion of the research is included in the 4th chapter. The effects of the various additives on the properties of the membranes are discussed in this chapter. Moreover, the performance of the synthesized nafion composite membranes in a DMFC test set-up has also been discussed.

The 5th chapter describes an approach to reduce the effect of crossed-over methanol through the nafion composite membranes by modifying the platinum cathode with a biocatalyst (laccase). The performance of the bio-electrodes, methanol tolerance, and the fuel cell performance is evaluated.

An overall conclusion of the research work is included in the 6th chapter. Moreover, it also includes the future scope towards extension of the research work. The chapter will help the future researchers in formulating the objective to further enhance the DMFC performance.

Lepakshi Barbora
Roll No. 06615104
Guwahati – 39

Acknowledgement

I would like to take this opportunity to express my gratitude to them, whose contribution has made this thesis possible.

The first and foremost appreciation goes to my supervisor Dr. Anil Verma for his valuable guidance throughout the research work. I thank him for his encouragement, guidance and moral support throughout, which enabled me to work towards a successful completion. I would like to acknowledge my sincere gratitude to my doctoral committee members, Dr. G. Pugazhenthi, Prof. P. Goswami, and Dr. S. Khijwania, for their insightful advices and suggestions throughout the research. I also acknowledge the kind support of Prof. P. Mahanta during my research work.

My sincere thanks go to Prof. A.K. Ghoshal, Head, Centre for Energy, for his moral support and inspiration. I would also like to extend my sincere thanks to the Head of the Department of Chemical Engineering for permitting me to use the facilities of the department. The kind and constant help of the staff member of the Department of Chemical Engineering is also duly acknowledged. As a staff member, I am thankful to the Indian Institute of Technology Guwahati for permitting me to pursue Ph.D and for providing me with the infrastructure and facilities for advanced research. I would also like to convey my sincere thanks to the Head of Central Instruments Facility (CIF), IIT Guwahati, for providing me the analytical facilities. My sincere thanks go to Dr. Kula Kamal Senapati, Chandan Borgohain and Madhurjya Borah for their help in using the analytical facilities of CIF.

I extend my sincerest thanks to S. Kaalwa, A. Difoe, Simadri, Rupesh, and Nivedita for extending helping hands in various part of the research work. Moreover, my special thanks go to Biraj, Leela, Avijit, Surya, and Shyam for their constant encouragement and help during the course of the research. I would also like to acknowledge the support and

encouragement of Preety, Mithilesh, Jayashree, and Vigya. I am also thankful to Pankaj, Dhiren Huzuri, Gitanjali, Dipti, and Madhuri for their constant help and motivation.

I gratefully acknowledge the financial support of the Department of Science and Technology, Government of India through the project (SR/FTP/ETA-29/2007).

At last but not least, I am highly indebted to my husband Jagat for his patience, endless support, sacrifice, love and inspiration towards the completion of my Ph.D thesis. My heartfelt love and appreciation to my son Avinash for bearing with me through the period. I extend my sincere gratitude to my parents, parents-in-law, Mridul, and Mayuri for their constant support and encouragement. My sincere apology goes to them whom I forget to mention but helped me at any part of the research work.

_ _ _ _ _ _ _ _ _ _ _ _ _ _ _ _ _ _ _

Lepakshi Barbora
Roll No. 06615104
Guwahati – 39

Abstract

The polymer electrolyte membrane (PEM) is a key component in a direct methanol fuel cell (DMFC). The primary characteristics desired of a PEM for DMFC are low methanol crossover (MCO), high proton conductivity, high mechanical, thermal and chemical stability, sufficient water uptake and moderate swelling, easy fabrication to form the membrane electrode assembly (MEA), competitive low-cost, and sufficient long-term durability. The state of the art membrane, Nafion® by DuPont possesses almost all of the desirable properties except the low MCO and low cost. Low MCO through nafion in DMFC is a challenging issue. Subsequently, a lot of research has been directed to the modification of nafion for DMFC application for reducing the MCO and simultaneously there has also been a search for alternative membrane with all the desirable properties of nafion including low MCO. As a contribution to the research on nafion modification for DMFC application, this thesis aims to synthesize nafion composite membranes with inorganic additives. Six different inorganic additives namely, titanium dioxide (TiO_2), neodymium oxide (Nd_2O_3), magnesium silicate hydroxide or talc $H_2Mg_3(SiO_3)_4$, erbium triflate (ErTfO), neodymium triflate (NdTfO), and molecular sieve (MS), have been used for nafion modification by the casting method. Each additive selected had a characteristic property, which was anticipated to modify nafion by lowering its MCO while maintaining its other desirable properties especially proton conductivity, thermal, chemical and mechanical stability. TiO_2, Nd_2O_3, and talc are hygroscopic and crystalline and consist of –OH groups on the surface. Both ErTfO and NdTfO are rare earth lanthanide triflates, resembles nafion in structure, have high coordination number, are hygroscopic, thermally stable, resistant to redox environment, and is anticipated to lower MCO without compromising proton conductivity and the other desirable properties of nafion. MS is

hygroscopic and crystalline in nature with pore size of 3 Å, which is anticipated to act as barrier to methanol having molecular size of 4.4 Å.

All the six additives were studied for morphological analysis using particle size analyzer, X-ray diffraction (XRD), BET surface area analyzer, and scanning electron microscope (SEM). The volume median diameters of the particles were determined using particle size analyzer.

The developed composite nafion membranes were characterized under ex-situ conditions by scanning electron microscopy (SEM), for thickness, X-ray diffraction (XRD) analysis, thermogravimetric analysis (TGA), Fourier transform infrared (FTIR) spectrometer analysis, ion exchange capacity (IEC), water uptake, methanol uptake, swelling, tensile strength, oxidative stability, proton conductivity, and methanol crossover. SEM images of the membranes indicated the formation of dense nafion composite membranes with no pore formation. XRD analysis of the nafion composite membranes indicated that the TiO_2/nafion and talc/nafion membranes are more crystalline than pure cast nafion membrane. TGA thermograms of the nafion composite membranes indicated that all the composite membranes were stable upto a temperature of 310 °C. FTIR analysis of the composite membranes indicated shifting of peaks for S-O stretching and water stretching frequency to higher wavenumbers and broader peak for water bending vibration for the composite membranes compared to pure cast nafion membrane. It is indicative of structural changes in the nafion polymer due to incorporation of the additives, increase in hydrogen bond association, and increase in water content, etc. Ion exchange capacity, water uptake and methanol uptake of the composite membranes were, in general, higher than pure cast nafion membrane. The tensile strength of the nafion composite membranes

was at par or slightly lower than pure cast nafion membrane. Comparison of the oxidative stability of the membranes showed that the composite membranes with lower additive loadings were chemically more stable than pure cast nafion membrane, though the optimum percent of loading varied for each type of additive. The proton conductivity of the composite membranes increased significantly, the highest being 0.127 S/cm for 1% TiO_2/nafion, which is about 42.7% higher than pure cast nafion membrane followed by 0.123 S/cm for 3% ErTfO/nafion membrane, which is about 38.2% higher than pure cast nafion membrane. The other composites almost retained the proton conductivity value of pure cast nafion membrane. Appreciable reduction in MCO was observed for the composite membranes; the highest being 80% by ErTfO/nafion. Both increase in methanol concentration as well as temperature led to an increase in MCO. The selectivity was highest for ErTfO/nafion membranes followed by TiO_2/nafion membranes.

Once the membrane was thoroughly characterized using ex-situ techniques, the membrane was used in the DMFC (in-situ characterization) to evaluate the performance of the fuel cell. The composite membranes exhibited higher power density than pure cast nafion membrane attributed to the decrease in MCO and increased proton conductivity. The maximum power density with 1 M methanol and at 30 °C was obtained with 1% talc/nafion membrane and 5% ErTfO/nafion (~8 mW/cm^2). Increase in methanol concentration led to an increase in power density, however the open circuit voltage decreased slightly. The maximum power density of 11.33 mW/cm^2 was obtained with 1% talc/nafion membrane with 4 M methanol solution at 30 °C. Increase in fuel cell temperature also led to an increase in the power density, the highest being 92.48 mW/cm^2 by 1% talc/nafion membrane with 1 M methanol at 80 °C.

The composite membranes decreased the MCO up to 80% as compared to pure cast nafion membrane. However, the methanol, which crosses over through the composite membrane affects the DMFC performance. Therefore, an attempt was made to circumvent the affect of crossed-over methanol by use of a methanol tolerant enzyme (laccase) in combination with Pt at the cathode. Laccase showed high tolerance to methanol, and the use of laccase in combination with Pt in the cathode showed better performance than Pt alone.

Keywords: Nafion; Composite; Methanol; Fuel Cell; Methanol Crossover; Proton conductivity

Contents

List of tables

List of figures

List of symbols

E	ion exchange capacity (meq/g)
P	potential (V)
V_{NaOH}	volumes of NaOH (mL)
V_{HCl}	volumes of HCl (mL)
W_d	weight of dry membrane (g)
W_w	weight of wet membrane (g)
σ	proton conductivity of the membrane (S/cm)
L_d	length of dry membrane (cm)
L_w	length of wet membrane (cm)
L	distance between the electrodes (cm)
R	resistance (ohm)
A	area (cm^2)
ρ	methanol crossover (cm^2/s)
C_A	initial methanol concentration (mol/L)
C_B	methanol concentration (mol/L) at time t (s)
V_B	volume of solution (cm^3)
l	thickness of the membrane (cm)
φ	selectivity (Ss/cm^3)
D(v,0.5)	volume median diameter (μm)
λ	wavelength of the X-ray (cm)
κ	constant
θ	diffraction angle (°)
β	full width at half maxima (cm)

List of abbreviations

3-APTES	(3-aminopropyl)triethoxysilane
ATRP	atom transfer radical polymerization
CV	cyclic voltammetry
DMF	dimethylformamide
DMFC	direct methanol fuel cell
DPS	diphenylsilicate
ErTfO	erbium triflate
FTIR	Fourier transform infra-red
FWHM	full width at half maxima
GDL	gas diffusion layer
HPAs	heteropolyacids
IEC	ion exchange capacity
MCO	methanol crossover
MEA	membrane electrode assembly
MoPh-a	molybdophosphoric acid
MPL	microporous layer
MPMDMS	(3-mercaptopropyl) methyldimethoxysilane
MPTMS	mercaptopropyltrimethoxysilane
MS	molecular sieve
MWCNT	multi walled carbon nanotube
NAFB	acid functionalized zeolite β/nafion
NdTfO	neodymium triflate
OCV	open circuit voltage
ORR	oxygen reduction reaction
PBI	polybenzimidazole
PEEK	poly(etheretherketone)

PEM	proton exchange membrane
PEMFC	proton exchange membrane fuel cell
PFA	polyfurfuryl alcohol
PFI	perfluorinated ionomer
PMA	phosphomolybdic
PPSQ	polyphenylsilsesquioxane
PSF	polysulfone
PTFE	poly tetra fluoro ethylene
PTFE	polytetrafluoroethylene
PVA	poly vinyl alcohol
PWA	phosphotungstic acid
REOs	rare earth oxides
RH	relative humidity
SEM	scanning electron microscopy
SHE	standard hydrogen electrode
SiWA	silicotungstic acid
SPAEK	sulfonated poly(aryl ether ketone)
SPEEK	sulfonated poly(ether ether ketone)
TEOS	tetraethylorthosilicate
TGA	thermogravimetric analyzer
VCC	voltage current curves
XRD	X-ray diffractometer

Chapter 1

Introduction

Chapter 1: Introduction

The global demand for energy is on the rise, while the fossil fuel reserves, which are the major sources of primary energy, are limited. Presently, around 80% of the primary energy is obtained from conventional fossil fuels (oil, natural gas, and coal). It is reported that the total energy demand is expected to increase by about 56% towards 2040 [DOE/EIA-0484, 2013]. The total world energy use will rise from 524 quadrillion British thermal units (Btu) in 2010 to 630 quadrillion Btu in 2020 and to 820 quadrillion Btu in 2040 [DOE/EIA-0484, 2013]. Thus severe energy crisis is predicted in the near future if the need is solely dependent on the fossil fuel reserves. Another major concern associated with the usage of fossil fuels is the emissions. The emissions from fossil fuel include large amounts of carbon dioxide (CO_2), nitrogen oxides (NOx), sulphur oxides (SOx), volatile organic compounds (VOCs), and particulates etc. These emissions are inflicting enormous impacts on the environment. Thus a secure and accessible supply of energy becomes very crucial not only for the sustainability but also for the growth of the society. Moreover, environmental concerns necessitate that new energy sources must be highly efficient and have zero (or very low) emissions. Thus, the need is clear and well recognized for clean, safe, and reliable forms of energy, which have instigated scientists and technologists to search for alternate energy sources [Martinot and Sawin, 2009].

Fuel cells have been identified as one of the potential power generation devices that may reduce the dependency on fossil fuel usage while simultaneously abating environmental pollution. Fuel cells have been recognized as one of the most stringent and promising energy conversion devices for mobile and residential applications in future [Li and Sabir, 2005]. In essence, fuel cell is an electrochemical device that consumes fuel and oxygen in

an electrochemical process to produce electricity and water. The fuel cell directly converts the chemical energy of the fuel to electrical energy and thus much more efficient than conventional heat engine. Its efficiency can reach as high as 60% in electrical energy conversion and overall 80% in co-generation of electrical and thermal energies with >90% reduction in major pollutants [Wang et al., 2011]. Fuel cell consists of an anode and a cathode, with an electrolyte in between, similar to a battery but unlike batteries the fuel cells can generate power continuously as long as the fuel and oxidant are supplied. High efficiency of energy conversion, low pollution level, low noise, and low maintenance costs render fuel cells preferable over other energy conversion devices. Therefore, fuel cell is being recognized as one of the promising candidates for the next generation power conversion devices for transportation, stationary, and portable applications [Dillon et al., 2004].

1.1 Brief history of fuel cell

The principle of the fuel cell was discovered by German scientist Christian Friedrich Schönbein in 1838 [Wand, 2008]. Based on his work, the first fuel cell was demonstrated by Welsh scientist and barrister Sir William Robert Grove in 1839 [O'Hayre et al., 2004]. In 1889, Ludwig Mond and Carl Langer developed a hydrogen-oxygen fuel cell, with thin perforated platinum electrode, which could produce current density of around 6.45 mA/cm^2 at 0.73 V [Zhang, 2005]. They were the first to demonstrate the practical hardware to sustain the fuel cell reactions. In 1893, Friedrich Wilhelm Ostwald experimentally determined the interrelated roles of the electrodes, anions and cations, electrolyte, as well as oxidizing and reducing agents in the fuel cells [Andujar and Segura, 2009]. Ostwald explained the correlation of physical properties and chemical reactions at the point of contact among electrode, gas, and electrolyte. His exploration of the

underlying chemistry of fuel cells laid the foundation for fuel cell researchers. Francis Thomas Bacon, a British engineer, began work on alkaline fuel cells in the late 1930s, and by 1939 a fuel cell was built using nickel electrodes operating under pressure as high as 3000 psi [Bacon, 1969; Demirbas, 2009]. During World War II, Bacon worked on developing a fuel cell that could be used in Royal Navy submarines, and in 1958 demonstrated an alkaline fuel cell stack of 10-inch diameter electrodes. Later, Pratt and Whitney licensed Bacon's work for the Apollo spacecraft fuel cells [Bacon, 1985].

Emil Baur of Switzerland and his group conducted extensive research on the electrolyte for high temperature fuel cell. They used molten silver and a solid electrolyte of clay and metal oxides [website[1]]. In 1955, W. Thomas Grubb, a chemist working for the General Electric Company (GE), further modified the original fuel cell design using a sulphonated polystyrene ion-exchange membrane as an electrolyte. Three years later another GE chemist, Leonard Niedrach, devised a way for depositing platinum onto the membrane, which served as catalyst for the necessary hydrogen electro-oxidation and oxygen electro-reduction reactions. GE went on to develop this technology with NASA and McDonnell Aircraft, leading to its use during Project Gemini. This was the first commercial use of a fuel cell. However, the sulphonated polystyrene ion-exchange membrane used as an electrolyte in these fuel cells exhibited brittleness in the dry state and were later replaced with crosslinked polystyrene-divinyl benzene sulphonic acid membranes [Zaidi, 2009]. This material also lacked stability and underwent degradation and suffered other problems. Also, the main problem encountered with these membranes was that proton conductivity was not sufficiently high to reach a power density even as low as 100 mW/cm^2 .

In 1959, Francis Thomas Bacon successfully developed a 5 kW stationary hydrogen fuel cell. A team led by Harry Ihrig built a 15 kW fuel cell stack, which used potassium hydroxide as the electrolyte and compressed hydrogen and oxygen as the reactants. This was used in a fuel cell tractor and demonstrated across the USA at state fair. Later, Bacon and his colleagues demonstrated a practical 5 kW fuel cell unit capable of powering a welding machine. In 1960s, Pratt and Whitney licensed Bacon's USA patents for use in the USA space program to supply electricity and drinking water [Gross, 2010].

In 1966, sulphonated polystyrene membranes were replaced by Nafion®, which proved to be superior in performance and durability to sulphonated polystyrene. At this early stage of development, the nafion membrane showed lifetimes of up to 3,000 h at low current densities and temperatures of 50 °C [Zaidi, 2009]. After Gemini program, NASA decided to operate the next space programme with alkaline fuel cell systems [Stone and Morrison, 2002]. However, GE continued working on its proton exchange membrane fuel cell (PEMFC) units and by the mid 1970s water electrolysis technology using polymer electrolyte membrane (PEM) was developed for USA Navy Oxygen Generating Plant [Appleby, 1996]. In 1980s, the British Navy adopted PEM electrolyzer for its submarine fleet and other companies also started to look at PEMFC systems for the commercial development and end-use applications. The PEMFC technology has evolved a lot since the first commercial development of the PEMFC unit in the 1960s. PEMFC units are considered to be the most prevalent alternative for automotive and stationary applications [Hogarth and Ralph, 2002]. In 1991, the first hydrogen fuel cell automobile was developed by Roger Billings. United Technologies Corporation's UTC Power subsidiary was the first company to manufacture and commercialize a large, stationary fuel cell system to use as a co-generation power plant in hospitals, universities, and large office

buildings. UTC Power marketed their 200 kW fuel cell system, the PureCell 200, which is now replaced by a 400 kW version, the PureCell Model 400 [Fuel cell industry review, 2012].

In 1990, Jet Propulsion Laboratory in Pasadena, California, in collaboration with the University of Southern California, developed a Direct Methanol Fuel Cell (DMFC) as a variant of PEMFC [Surampudi et al., 1994]. It was designed to supply electricity for field troops in the armed forces and for applications in NASA. Currently, DMFC is the technology of choice for the majority of portable appliances. DMFC with liquid-feed (methanol solution) offers promising alternative to hydrogen gas consuming fuel cell (PEMFC) as they allow easy handling and storage of the liquid fuel for applications in portable and mobile electronic devices [Surampudi et al., 1994]. Many liquid fuels such as methanol [Wang et al., 2006], ethanol [Zhou et al., 2004; Lobato et al., 2011; Datta et al., 2012], formic acid [Ha et al., 2005], and ethylene glycol [Neto et al., 2005] are being tested as a fuel in PEM based fuel cells. Among all the investigated possible fuels, methanol [Rice et al., 2002; Difoe et al., 2008] is the most favorite due to various reasons. A few of the reasons include, generation of 6 moles of electron per mole of methanol, comparatively easy electro-oxidation than higher alcohols, and very high energy density as compared to hydrogen gas. Moreover, methanol can be obtained through biomass, thus is sustainable and environment friendly in production and use [Basak et al., 2010].

1.2 Basic principle of direct methanol fuel cell

The main components of a DMFC are the electrodes (anode and cathode) comprising of catalyst layers on the gas diffusion layers (backing layers), an electrolyte, end plates, fittings and necessary connectors. The catalyst layers, gas diffusion layers and the PEM

make up what is known as membrane electrode assembly (MEA). The catalyst layers typically consist of platinum or platinum alloys. The anode catalyzes the methanol electro-oxidation reaction as shown in eq.1.1, and provides a pathway through which the generated electrons are conducted to cathode via external circuit through a load. Protons generated at the anode migrate to cathode through the PEM. At cathode, the protons, electrons, and oxygen react as per eq.1.2 to form water. The overall reaction is shown in eq.1.3.

$$CH_3OH\,(l) + H_2O\,(l) \longrightarrow 6H^+ + 6e^- + CO_2\,(g) \quad \text{(anodic reaction)} \quad (1.1)$$

$$3/2O_2\,(g) + 6H^+ + 6e^- \longrightarrow 3H_2O\,(l) \quad \text{(cathodic reaction)} \quad (1.2)$$

$$CH_3OH\,(l) + 3/2\,O_2\,(g) \longrightarrow 2H_2O\,(l) + CO_2\,(g) \quad \text{(overall reaction)} \quad (1.3)$$

The standard reversible potential for methanol oxidation is 1.18 V [Deluca and Elabd, 2006].

The electrodes are made up of gas diffusion layer (GDL) and catalyst layer. The GDL regulates the uniform distribution of reactant over the catalyst layer [Wang et al., 2006]. The PEM typically consists of strong acidic groups in a polymer structure, which aid in proton transport through the membrane and serves as a barrier to unwanted species transport through it. A discussion on the PEM is given in the next section.

1.3 Nafion membrane

The polymer electrolyte membrane is a crucial part in DMFC, which governs its performance. One of the major challenges in current DMFC research is the development of suitable PEM for improving the performance of DMFCs [Othman et al., 2010]. The

polymer membrane should simultaneously maintain high proton conductivity; a low permeability to reactants; and have reasonable chemical, thermal, and mechanical stability [Neburchilov et al., 2007]. A lot of researches have been conducted in attempting to develop a membrane having all of these properties. Some researchers have proposed thermoplastic polymers such as poly(etheretherketone) (PEEK), polysulfone (PSF) and polybenzimidazole (PBI) as good PEM for DMFC [Ahmad et al., 2010]. However, nafion, a perfluorinated ionomer (PFI) membrane developed by DuPont in 1960s for PEMFC has been the preferred electrolyte for DMFC to date [Othman et al., 2010]. Other PFI membranes like Flemion (Asahi Glass), Aciplex (Asahi Chemical), and Dow (Dow Chemical), were developed but their primary applications remained for PEMFC. The starting raw material for developing PFI is polyethylene. The hydrogen molecules of polyethylene are substituted with fluorine and the product obtained is polytetrafluoroethylene or PTFE, also referred to as Teflon [Larminie and Dicks, 2000]. The strong C-F bonds make PTFE mechanically durable and resistant to chemical attacks [Othman et al., 2010]. A perfluorinated side chain with ionically bonded sulphonic acid (SO_3H) group is added to the PTFE and the resulting polymer is referred to as PFI.

Nafion has both hydrophobic and hydrophilic domains. The long chain molecules of PTFE contribute to the hydrophobic domain and the sulphonic acid side chains contribute to the hydrophilic domain. Two models have been proposed to describe the morphology of nafion namely, the cluster network model by Gierke, (1981) (fig.1.1) and the three-region model by Yeager and Steck, (1981) (fig.1.2).

As per the cluster network model (fig 1.1) the morphology of hydrated nafion shows the formation of spherical clusters (pores), which are connected by short narrow channels,

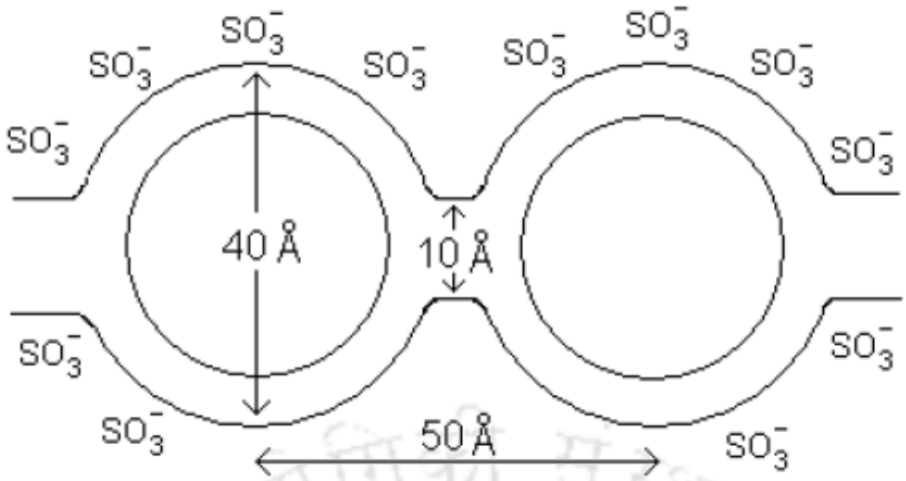

Fig.1.1 The microstructure of nafion according to Gierke's cluster-network model [Heitner-Wirguin, 1996]

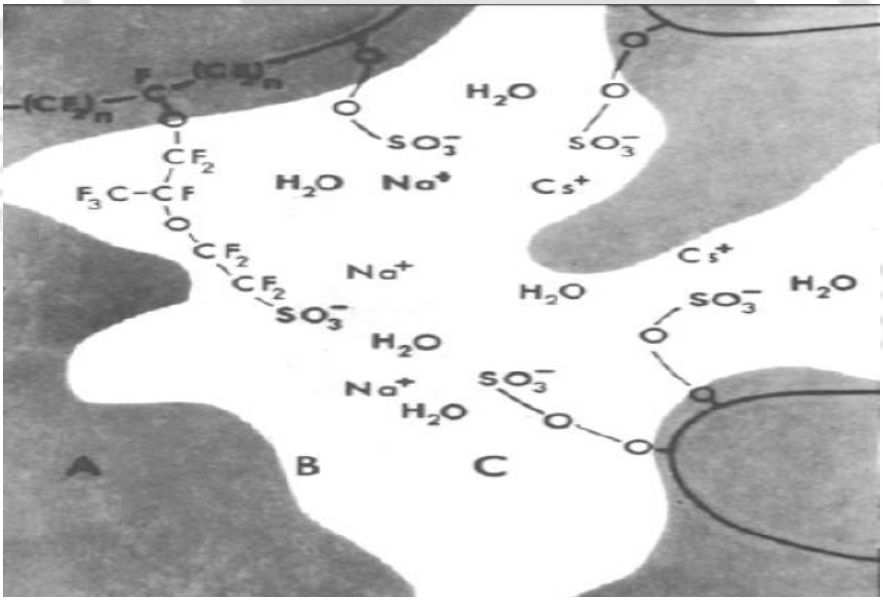

A- Polymer backbone **B-** Transition region **C-** Proton conducting region

Fig.1.2 Illustration of Yeager and Steck's three region model of nafion [Yeager and Steck,1981]

due to the separation of ion-exchange sites from the fluorocarbon backbone [Gierke, 1981]. When the membrane is dry, an average cluster has a radius of about 1.8 nm and it contains about 26 SO_3^- groups distributed on the inner pore surface. In the swollen state, the diameter increases to about 4 nm and the number of fixed SO_3^- groups goes up to about 70. Under these conditions, each pore is filled with about 1000 water molecules [Smitha et al., 2005].

The morphology of nafion as described by the three-region model distinguishes polymer backbone regions, proton conducting (aqueous) regions, and narrow bridge-like transition regions connecting the large aqueous regions and PTFE polymer backbone [Yeager and Steck, 1981]. Within the hydrated regions for both the models, the H^+ ions are relatively weakly attached to the SO_3^- group and move freely to enable the membrane in transferring hydrogen ions through the membrane from anode to the cathode. The migration of hydrogen ion from anode to cathode takes space by diffusion and/or by the hoping mechanism via hydronium or Zundel and Eigen ions [Kreuer, 2001]. The hydrophobic region primarily makes the nafion highly chemically resistive and mechanically strong. The hydrophilic region of the nafion primarily helps to attain acidity, sufficiently absorptive to water, as well as good proton conductivity [Othman et al., 2010].

Despite showing an effective performance in PEMFC, the nafion membrane has many limitations when used in DMFC. The limitations of the nafion hamper the emergence of the DMFC design. One of the main limitations of nafion is methanol crossover (MCO) through the nafion membrane from the anode to the cathode side [Tricoli, 1998]. The

MCO is a major problem since it has two detrimental effects on the DMFC. Firstly, the crossed methanol is oxidized by the cathodic electro-catalyst, which depolarizes the electrode. Secondly, it severely lowers the efficiency of fuel utilization [Neburchilov et al., 2007]. Since the energy resulting from crossed-over methanol oxidation is not extracted as electricity, it all ends up as waste heat that increase the cooling load on the cell [Othman et al., 2010]. Nafion is also susceptible to water and methanol uptake and thus experience swelling, which is determinative factor in the longevity and performance of a DMFC.

Various polymers are being investigated to replace nafion for reduced methanol crossover while maintaining high proton conductivity, chemical resistance, mechanical strength etc. comparable to nafion. However, till now no membrane has achieved all the desired properties to surpass nafion membrane. Any new polymeric membrane suitable to DMFC should possess low fuel crossover, high mechanical and thermal stability along with high chemical or oxidation stability, and high proton conductivity. Besides, these properties must be achieved while maintaining low cost. Nafion, as of date, is the only membrane which has many properties up to the desired level. Therefore, nafion is the most widely accepted PEM for DMFC. However, one of the main challenges to nafion is the reduction of MCO in order to make it suitable for DMFC. The investigators are trying various routes to modify the nafion for reduced MCO. A brief description of these routes is provided in the next section.

1.4 Routes to nafion modification

Passive approaches to reduce MCO through nafion in DMFC such as increase in membrane thickness and/or equivalent weight of membrane have been reported. These

approaches reduce the methanol crossover. However, increased thickness and equivalent weight adversely affect the DMFC performance due to higher ohmic resistance and lower proton conductivity, respectively [Neburchilov et al., 2007]. Various approaches to alter the physical geometry (or size) and chemical functionality (or acidity) of the ionic clusters in the nafion membrane has also been tried to lower the MCO of nafion. Some of the important routes are nafion coating, nafion blending, nafion impregnation, and nafion composite.

A number of investigators have coated nafion with a thin barrier layer through a variety of deposition techniques with the primary objective to reduce the methanol crossover in a DMFC. Nafion coating with thin barrier layers of palladium, poly(1-methyl pyrrole), poly vinyl alcohol, nano silica, sulfonated poly(ether ether ketone) etc. has been attempted [Tang et al., 2005; Kadirgan et al., 2004; Hobson et al., 2001; Kim et al., 2004; Ren et al., 2005]. Usually it has been observed that coating reduces the MCO of nafion but the proton conductivity also decreases resulting in a lower power density of DMFC. The nano silica coated nafion membrane could decrease MCO by 67%, but proton conductivity decreased by 21% compared to commercial nafion-115 with a lower DMFC performance compared to nafion-115 [Kim et al., 2004]. Moreover, formation of crack free barrier layer is also an issue with nafion coated membranes [Ma et al., 2003]. Probably because of these reasons, it has been observed that the membranes have not been thoroughly characterized for fuel cell applications.

A number of researchers have impregnated polymers within nafion by in-situ polymerization and sorption technique. Impregnating nafion with solvent resistant polymer membranes like polypyrrole (PPy), polybenzimidazole (PBI), poly(furfuryl

alcohol) etc. has been reported [Easton et al., 2003; Hobson et al., 2002; Park et al., 2005; Liu et al., 2005]. Easton et al., (2003) impregnated PPy by in-situ polymerization and polymerization in hydrogen peroxide with Fe(III) as an oxidizing agent (in in-situ polymerization, peroxide is used as the free-radical initiator, PPy was impregnated with and without Fe(III) as an oxidizing agent). The composite membranes exhibited low MCO compared to pure nafion but had lower proton conductivity than pure nafion. The membranes modified via Fe(III) oxidation exhibited poor performance in comparison with pure nafion based DMFCs due to poor electrode bonding. Hobson et al., (2002) used a variety of methods such as spin coating, dipping, and screen printing, to incorporate acid-doped PBI into nafion membrane. All the PBI/nafion composites could reduce MCO. However, the membranes prepared by coating and dipping showed reduced proton conductivity. Screen printing could maintain the proton conductivity at par with pure nafion. However, it is reported that the maintenance of the right experimental conditions is required to prevent increase in the impedance of the resultant MEA. Liu et al., (2005) impregnated nafion with polyfurfuryl alcohol (PFA) through in-situ polymerization of PFA. PFA/nafion membranes could reduce MCO by a factor of 2.7 compared to nafion-115 but the proton conductivity reduced by 26%. However, they have reported higher cell performance with the composite membrane, which may be due to suppression of lower proton conductivity effect by reduced MCO. However, these membranes exhibited reduced proton conductivities and compatibility with the electrodes.

A number of investigators have blended nafion with poly vinyl alcohol (PVA) or sulfonated poly(aryl ether ketone) (SPAEK) or Sulfonated poly(ether ether ketone) (SPEEK) with the goal to reduce MCO [Shao and Hsing, 2005; Deluca and Elabd, 2006; Kim et al. 2007; Tsai et al., 2009]. Assessment of PVA/nafion membranes annealed at

high temperature (230 °C) showed increased selectivity (proton conductivity/methanol crossover) when compared with pristine nafion at similar or higher proton conductivity values, attributed to increased interaction between the hydroxyl groups in PVA and the sulphonic acid groups in nafion and subsequent increase in cross-linking. However, the PVA/nafion membranes with increased cross-linking (due to high temperature annealing) become brittle in dry state, which is problematic for the DMFC application. On the other hand, the PVA/nafion membranes annealed at lower temperature did not show similar performance. SPAEK/nafion and SPEEK/nafion membranes exhibited lower MCO but exhibited lower proton conductivity. Another significant issue with the nafion blends could be the problem of phase separation, if nafion and the polymer used for blending are immiscible. Similar problem was faced with SPAEK/nafion membranes as SPAEK and nafion are immiscible. Study of the crucial parameters like mechanical stability and chemical or oxidation stability of these nafion blends have not been reported or performed.

Another significant approach widely investigated by researchers to improve the performance of nafion membrane by reducing MCO, is the synthesis of nafion composite membranes. Nafion composite membranes may be macrocomposite, nanocomposite, and/or hybrid organic-inorganic membranes with organic or inorganic fillers incorporated as a modifier. Organic–inorganic composites, which reduce methanol crossover and increase conductivity have been investigated [Neburchilov et al., 2007]. The idea is that the fillers will make the path more tortuous and block the methanol transport channel. Composite nafion membranes are prepared either by impregnation of commercial nafion membrane with organic or inorganic materials or their precursors followed by in-situ synthesis or by solution-casting a nafion solution mixed with organic or inorganic

particles. In case of modification of the commercial nafion, the hydrophilic regions of nafion membrane provide the reaction cage for the fillers and the original structure of nafion membrane is maintained. The use of casting method allows the modifiers to participate in forming the membrane structure easily [Jones and Roziere, 2008]. More intensive efforts are needed to modify nafion with inorganic fillers than with organic fillers [Zhang and Shen, 2012]. Composite membranes with inorganic compounds are attractive because physical properties, such as thermal and mechanical behavior etc. may be controlled by combining the properties of nafion and the inorganic compounds. The inorganic material has the ability to enhance the properties of nafion and has the potential to have required balance between the two important characteristics in DMFC namely, proton conductivity and methanol permeability apart from various other properties. Hence, amongst the various routes to nafion modification, special attention has been given to the fabrication of inorganic/nafion composite membrane.

The next chapter presents the research and development status of the composite nafion membrane using inorganic compounds.

Chapter 2

Literature Review

Chapter 2: Literature Review

Nafion composite membrane for direct methanol fuel cell (DMFC) is expected to meet the following primary requirements-

(i) low methanol crossover (MCO), (ii) high proton conductivity, and (iii) good thermal stability. The MCO and proton conductivity together determine the cell performance in a DMFC [Zhang et al., 2012]. The performance of DMFC commonly depends on low MCO (preferably) and high proton conductivity (typically 0.1 S/cm at 90 °C) [Ahmad et al., 2010]. Increase in DMFC temperature improves the fuel cell performance, which is attributed to increase in electro-oxidation and electro-reduction kinetics along with alleviation of CO poisoning of the platinum catalyst. Additionally, the composite membrane is expected to possess (iv) excellent electrochemical stability, (v) substantial morphological and dimensional stability, (vi) outstanding mechanical properties, (vii) sufficient water uptake and moderate swelling, (viii) suppressed water transport through diffusion and electro-osmosis, (ix) easy fabrication to form the MEA, and finally, more importantly from a practical point of view, (x) a competitive low-cost and sufficient long-term durability [Zhang et al., 2012].

Different types of inorganic material have been explored as additives for nafion modification. However, the success achieved so far is limited and various new additives are being investigated to meet the objectives. It would be easier if the inorganic additives used in nafion modification can be classified under three categories: (i) hygroscopic additives, (ii) bi-functional additives, and (iii) methanol impermeable and/or proton conducting additives. The following sections will address on points of relevance such as a comparative as well as parallel understanding of the unmodified nafion membrane with the composite membranes in terms of membrane properties. Now onwards the nafion

with any inorganic filler will be called nafion composite membrane or nafion composites. Similarly, the inorganic fillers may be reported as additives also.

2.1. Hygroscopic additives

The most commonly used additives under this category for nafion modification for DMFC include silica (SiO_2), and titania (TiO_2). It is anticipated that MCO can be reduced if inorganic additives are placed along the diffusion pathways, i.e., within the polar clusters of the membrane [Xi et al., 2007]. Moreover, it is believed that such modification of nafion membrane would allow its application at low humidity or high temperatures as these inorganic additives enhance the water retention of the nafion composites [Amjadi et al., 2012].

2.1.1. *Nafion composites with SiO_2 additives*

Modification of nafion through the addition of SiO_2 is a common approach utilized for the improvement of membrane performance in DMFC applications. SiO_2/nafion membranes have been prepared according to several methods by casting mixtures such as: silica powder [Dimitrova et al., 2002], dithenylsilicate (DPS) [Liang et al., 2006], sol-gel reaction with tetraethylorthosilicate (TEOS) followed by solution casting of the nafion solution [Jiang et al., 2006], and phosphotungstic acid (PWA) dopes composite SiO_2/nafion/PWA [Staiti et al., 2001]. The 3% SiO_2/nafion membrane prepared by casting method exhibited improved performance with increase in temperature attributed to the hygroscopic property of SiO_2 with reduced MCO [Antonucci et al., 1999]. A maximum power density of 240 mW/cm^2 and 150 mW/cm^2 was obtained with oxygen and air feed supply, respectively, with 2 M methanol at 145 °C. Nafion composites with 10–20 wt.% dithenylsilicate (DPS) prepared by casting method exhibited a nanolayered microstructure

resulting in low MCO. Increased DPS content in the composite membrane improved the proton conductivity attributed to its hydrophobic characteristics responsible for reduction in water adsorption and flooding at the cathode [Liang et al., 2006].

According to Xi et al., (2007) the SiO_2/nafion membranes prepared using sol-gel have been successfully used in DMFCs due to the simple handling procedure and lower MCO attributed to the filling of polar clusters (pores) of the unmodified nafion membrane with SiO_2 nanoparticles during the in situ sol-gel reaction with TEOS. A 5% SiO_2/nafion membrane prepared by employing the sol-gel method utilizing TEOS exhibited MCO of 4.17×10^{-7} cm^2/s compared to 9.7×10^{-7} cm^2/s for pure cast nafion. Moreover, the thermal stability of the composite nafion membrane was improved along with higher water uptake than pure cast nafion [Jiang et al., 2006]. The maximum power density of 64 mW/cm^2 at 300 mA/cm^2 was achieved with 1M methanol at 60 °C and air (1 atm) as feed, which was around 10 mW/cm^2 higher when pure cast nafion membrane was used in the DMFC. However, the proton conductivity of the SiO_2/nafion membranes was found to be slightly lower than pure cast nafion membrane.

Lin et al., (2008) modified the surface of a nafion-117 membrane with mesoporous silica layers through an in-situ surfactant-templated sol-gel reaction. All the SiO_2 modified samples had a higher water uptake value than that of the nafion-117. The modified membranes had more dimensional stability and reduced swelling than nafion-117. They found that the aging time, along with the number of the SiO_2 layers, influenced the proton conductivity and MCO. The nafion composite with a second SiO_2 layer coated on SiO_2/nafion membrane after 5 minutes, exhibited the best performance in terms of proton conductivity and MCO. They showed elevated proton conductivity of 0.049 and 0.069

S/cm at 25 and 80 °C, respectively, while possessing the lowest MCO at both the temperatures. Moreover, the diffusion coefficients of methanol through the membrane was 1.75×10^{-8} and 6.95×10^{-8} cm^2/s, which were about three orders lower compared to nafion-117 at the similar conditions. However, they are of the opinion that the technique of application of mesoporous silica layer in modifying nafion membranes through dip-coating is a facile route in improving the said criteria simultaneously.

Rodgers et al., (2008) incorporated SiO_2 nanoparticles into nafion-115 membrane using the sol-gel method to study several transport properties such as water transport and proton conductivity. Swelling of the SiO_2/nafion composite membranes in water was less than that of unmodified nafion-115 membrane although water uptake was high. Xi et al., (2007) reported good chemical stability for the SiO_2/nafion membrane prepared by in-situ sol-gel method in vanadium and acid solutions. The nafion composites have been reported to exhibit low vanadium ions permeability compared to nafion-117, attributed to the filling of its polar clusters with SiO_2 nanoparticles. However, the authors have not reported MCO results.

Tang et al., (2007) reported that by optimizing the SiO_2 content in SiO_2/nafion membrane or by using organically modified silicate (ORMOSIL) to replace SiO_2, the performance of the nafion composite could be further improved. The 5% SiO_2/nafion membrane based on self-assembled SiO_2 nanoparticles formed through a reformative sol-gel process showed significantly improved performance in terms of stability and durability at cell/humidifying temperatures of 100/60 °C under a current density of 600 mA/cm^2 and has a degradation rate of 0.12 mV/min, which is almost 20 times smaller than 2.33 mV/min measured on nafion-212 membrane under the same conditions.

Nafion membranes modified by 3.3% molybdophosphoric acid (MoPh-a) and 4.3% SiO_2 exhibited slightly higher MCO than nafion-117 but enhanced the proton conductivity by 2-2.5 times (0.23 and 0.12; 0.29 and 0.15 S/cm for nafion composite and nafion-117 respectively at 60 and 90 °C) [Dimitrova et al., 2002].

SiO_2 has been used to modify nafion in combination with polyaniline (polyaniline/nafion/ SiO_2 or PaniNC) through sol-gel method and redox polymerization for deposition of polyaniline. Polyaniline, an electronically conductive polymer, modifies the membrane structure and correspondingly reduces the MCO, while the silica nanocomposite improves the conductivity [Neburchilov et al., 2007]. The SiO_2/nafion membrane with 5% filler prepared by sol-gel method showed improved performance in a H_2/O_2 fuel cell than nafion-117 membrane (720 mA/cm^2 with 5% SiO_2/nafion as compared to 390 mA/cm^2 with nafion-117 at 0.2 V), at 110 °C and in low humid conditions, attributed to the water holding capacity of the SiO_2/nafion membranes [Amjadi et al., 2012]. The authors were able to obtain the minimum amount of leaching of SiO_2 at a reaction temperature of 60 °C. Some important properties of nafion and SiO_2/nafion membranes reported in different literature are listed in Table 2.1. On comparison of the SiO_2/nafion membranes synthesized and characterized by various research groups in table 2.1, it is observed that SiO_2/nafion membranes demonstrated improved thermal and mechanical stability as well as maintained adequate water uptakes at elevated temperatures. Addition of silica reduced MCO but also reduced proton conductivity by a large extent.

The swelling of SiO_2/nafion membranes have been reported to be less than unmodified nafion but moderate level of swelling is desirable to prevent delamination of membranes in the MEA.

Table 2.1 Comparison of critical properties of nafion composite membranes with SiO_2 additives

Reference	Preparation technique	Water uptake (%)	Proton conductivity (S/cm)	MCO	DMFC performance
Antonucci et al., 1999	Casting	NR	NR	4×10^{-6} mol/min/cm^2 with 2 M methanol for 3% SiO_2/nafion	Maximum of 240 mW/cm^2 and 150 mW/cm^2 with oxygen and air feed supply, respectively, for 3% SiO_2/nafion (145 °C, 2 M methanol)
Jiang et al., 2006	Sol-gel	20 for pure cast nafion and 22 for 5% SiO_2/nafion	0.045 for pure cast nafion and 0.034 for 5% SiO_2/nafion	9.7×10^{-7} cm^2/s for pure cast nafion and 4.17×10^{-7} cm^2/s for 5% SiO_2/nafion	Maximum of 54 mW/cm^2 for pure cast nafion and 64 mW/cm^2 for 5% SiO_2/nafion (60 °C, 1 M methanol)
Xi et al., 2007	Sol-gel	26 for nafion-117 and 21.5 for 9.2% SiO_2/nafion	0.059 for nafion-117 and 0.056 for 9.2% SiO_2/nafion	NR	NR
Lin et al., 2008	Dip-coating technique (in-situ surfactant templated sol-gel reaction)	18.8 for nafion-117 and 36.9 for SiO_2/nafion with second SiO_2 layer	0.037 and 0.062 for nafion-117 at 25 °C and 80 °C, respectively. 0.048 and 0.068 for SiO_2/nafion with second SiO_2 layer at 25 °C and 80 °C respectively.	1.75×10^{-8} and 6.95×10^{-8} cm^2/s, for SiO_2/nafion with second SiO_2 layer at 25 °C and 80 °C respectively.	NR
Amjadi et al., 2012	Sol-gel	31 for nafion-117 and 38 for 5% SiO_2/nafion	0.011 for nafion-117 and 0.004 for 5% SiO_2/nafion	NR	390 mA/cm^2 for nafion-117 and 750 mA/cm^2 for 5% SiO_2/nafion at 0.2 V (110 °C and 30 % RH, H_2/O_2 fuel cell)

NR: Not reported

Moreover, DMFC performance of the SiO_2/nafion composites have been reported to be inferior or at par with unmodified nafion at low temperature but remarkably good at temperatures beyond 100 °C attributed to the water holding capacity of SiO_2. Leaching of SiO_2 from membranes prepared by sol-gel method could be an issue though only a few research groups have tried to check and reported about it.

2.1.2. *Nafion composites with TiO_2 additives*

TiO_2 is another hygroscopic filler employed extensively for membrane modification for fuel cell applications [Lobato et al., 2011]. TiO_2 differ from SiO_2 in the nature and electronic environment of the surface functional groups (surface acid-base behavior, the amount and strength of the surface functionalities, as well as the water adsorption density behavior) [Baglio et al., 2004, Arico et al., 2004]. Besides, TiO_2 has advantage to be tailored, the crystallographic structure allowing to modulate the physico-chemical characteristics and thus the water adsorption properties, which facilitate proton conductivity. The composite membranes based on mesoporous anatase TiO_2 powders and nafion show large improvements in DMFC performance under low relative humidity and elevated temperature.

Santiago et al., (2009) incorporated TiO_2 into nafion by sol-gel method to form a composite membrane that improved the PEMFC performance at 130 °C. However, no morphological study has been reported in their work. Baglio et al., (2004) synthesized TiO_2 nanometric powder via a sol-gel procedure, and calcined them at various temperatures to vary the powder particle size as well as crystalline phase to modify nafion by casting method to evaluate the effect of filler content on high temperature DMFCs. The composite membranes showed superior power densities at higher temperature with

respect to pure cast nafion membrane. The improved performance of the cell may be attributed to the higher conductivity of the cell using TiO_2/nafion membranes as compared to pure cast nafion membrane, which was confirmed by the cell resistance measurements. Maximum power density of 350 mW/cm^2 was achieved in the presence of oxygen feed at 145 °C for the composite membranes containing 3-5 wt.% TiO_2; whereas, the maximum power density with air feed was about 210 mW/cm^2. The DMFC performance increased as the mean particle size of the TiO_2 filler decreased, which was attributed to the influence of the filler morphology on the electrochemical properties of the composite membranes.

Sacca et al., (2005) prepared 3% TiO_2/nafion membranes prepared by casting method with TiO_2 prepared by sol-gel technique and calcined at 400 °C exhibited higher water uptake, ion exchange capacity (IEC) and proton conductivity than nafion-115 and pure cast nafion. The enhanced proton conductivity of the composite membrane was attributed to the hygroscopic property and proton conducting ability of TiO_2.

Crack free nafion composite membranes with nano-TiO_2 films, fabricated by deposition of TiO_2 nanoparticles from a sol solution of TiO_2 on the surface of nafion-112 by spin coating exhibited reduced MCO (2.9×10^{-6} cm^2/s at 25 °C) than nafion-112 (3.6×10^{-6} cm^2/s at 25 °C) and a maximum power density of 44 mW/cm^2 with TiO_2 coated nafion membrane containing 0.009 mg/cm^2 TiO_2, with 2 M methanol at 80 °C [Liu et al., 2006]. The protonic conductivity of the composite membranes decreased with increased TiO_2 content, which was contrary to the results of Sacca et al., (2005) and may be attributed to the difference in synthesis method. Nafion composites prepared with mesoporous TiO_2 provided the best cell performance in the temperature range of 80-120 °C under 50% and

95% relative humidities (669 mW/cm^2 under 50% RH at 120 °C in a H_2/O_2 fuel cell, which was 5.7 times higher than the value obtained from the pure cast nafion membrane) [Chen et al., 2007]. The enhanced performance was attributed to the high surface area and the large amount of mesopores with the small pore sizes. According to them, in the lower temperatures of 80 °C and 90 °C the surface area of the filler, which reflects its water retention capacity, played a key factor in enhancing cell performance and at the higher temperatures of 110 °C and 120 °C under lower relative humidity (RH), the size and the amount of mesopores in the filler, which influence the reduction of the dehydration rate of the nafion composite, became more important. Nafion composites with sulphonated TiO_2 particles (6%), prepared by casting method exhibited improved performance with 5 M methanol feed compared to pure cast nafion attributed to the reduced MCO by the composite membranes [Wu et al., 2008]. Daiko et al., (2006) synthesized nafion composite membrane with combination of both TEOS and TBT alkoxides and tested them in direct methanol fuel cell. They concluded that infiltrated oxides improve the membrane barrier property against methanol. Table 2.2 shows a comparative study of various properties of TiO_2/nafion composites reported in different literature. It is observed that the introduction of TiO_2 particles endows the nafion composite membrane with good mechanical and thermal resistance and improves the water uptake and ion-exchange capacity in comparison with pure nafion membranes. Modifiation of nafion with TiO_2 additives resulted in a change in structure of the membrane, causing the blockade of the proton migrating channels and narrowing of the water channels thereby lowering the MCO and electroosmotic drag coefficient. However, other problems such as reduction in mechanical stability (becomes brittle) when the inorganic component loading reached a critical level, decrease in proton conductivity and decreased fuel cell performances were encountered.

Table 2.2 Comparison of critical properties of nafion composite membranes with TiO_2 additives

Reference	Preparation technique	Water uptake (%)	Proton conductivity (S/cm)	MCO	DMFC performance
Baglio et al., 2004	Casting	NR	NR	NR	Maximum of 350 mW/cm^2 for 5% TiO_2/nafion with oxygen feed (2 M methanol, 145 °C)
Sacca et al., 2005	Casting	29 for 3% TiO_2/nafion, 27 for nafion-115 and 20 for pure cast nafion	0.150-0.180 for 3% TiO_2/nafion and 0.120-0.140 for pure cast nafion	NR	NR
Liu et al., 2006	Spin coating	NR	0.027 and 0.041 for nafion-112 at 25 °C and 85 °C, respectively. 0.022 and 0.036 for TiO_2/nafion with 0.009 mg/cm^2 TiO_2 at 25 °C and 85 °C, respectively.	3.6 × 10^{-6} cm^2/s for nafion-112 and 2.9 × 10^{-6} cm^2/s for TiO_2/nafion with 0.009 mg/cm^2 TiO_2 at 25 °C. 13 × 10^{-6} cm^2/s for nafion-112 and 11 × 10^{-6} cm^2/s for TiO_2/nafion with 0.009 mg/cm^2 TiO_2 at 85 °C.	Maximum of 37 mW/cm^2 for nafion 112 and 44 mW/cm^2 for TiO_2/nafion with 0.009 TiO_2 mg/cm^2 (2 M methanol, 80 °C)
Wu et al., 2008	Casting	37 for pure cast nafion, 35 for 3% TiO_2–SO_4^{2-}/nafion and 36 for 6% TiO_2–SO_4^{2-}/nafion	0.095 for pure cast nafion, 0.089 for 3% TiO_2–SO_4^{2-}/nafion and 0.089 for 6% TiO_2–SO_4^{2-}/nafion	4.05 × 10^{-6} cm^2/s for pure cast nafion, 2.83 for 3% TiO_2–SO_4^{2-} /nafion and 2.73 × 10^{-6} cm^2/s for 6% TiO_2–SO_4^{2-} /nafion	Maximum of 99 mW/cm^2 for pure cast nafion and 119 mW/cm^2 for 6% TiO_2–SO_4^{2-} /nafion (5 M methanol, 70 °C)

NR: Not reported

2.2. Bi-functional additives

2.2.1. *Nafion composites with silicon, including silica and polysiloxane additives*

Recently, more attention has been paid to nafion composite membranes doped with bi-functional inorganic additives. The nafion composite containing silicon, including silica and polysiloxane are reported to exhibit better membrane properties such as improved water management, a different proton conducting kinetic mechanism, and a lower MCO than unmodified nafion, attributed to the hygroscopic and proton-conductive properties of the bi-functional additives [Pereira et al., 2008]. Tay et al., (2008) prepared nanoparticles with a core-shell structure consisting of a silica core (<10 nm) and a densely grafted oligomeric ionomer layer. The resultant core-shell filler is used to synthesize nafion composite membrane, which displayed improved proton conductivity considerably and also repressed MCO by a factor of almost four. However, to obtain the core−shell structured nanoparticles, three steps including silylation, bromination, and atom transfer radical polymerization were required, which renders the synthesis process complex and may result in non-uniform membrane synthesis thereby affecting the fuel cell performance [Tay et al., 2008].

The nafion nanocomposite membrane containing 3 wt.% phosphoric acid-functionalized (3-aminopropyl)triethoxysilane (3-APTES) has an MCO at least 50% lower than that of nafion and a maximum proton conductivity of 0.07 S/cm, which is comparable with the conductivity of nafion. However, the stability of the phosphoric acid group on 3-APTES has not been evaluated [Kang et al., 2008].

Polyphenylsilsesquioxane (PPSQ) is a class of polysiloxane which has high heat stability, high crystallinity, and low fuel permeability. Polysiloxanes incorporated in nafion are

commonly synthesized by an in-situ sol-gel technique within nafion membranes through corresponding organically functionalized silicon alkoxide precursors containing a thiol (−SH) group (e.g., mercaptopropyltrimethoxysilane (MPTMS) and (3-mercaptopropyl) methyldimethoxysilane (MPMDMS) to give a nafion composite membrane that is further treated with H_2O_2 solution to convert the −SH to $-SO_3H$ [Yen et al., 2007]. It is interesting to note that the nafion composite membranes with 5 wt.% Sulphonated PPSQ gave a proton conductivity of 1.57×10^{-1} S/cm at 120 °C and yielded a better DMFC performance than nafion-115 at temperatures ranging from 100 to 120 °C and at pressures from 1 to 2 bar [Nam et al., 2008]. Selectivity, defined as the ratio of proton conductivity to methanol permeability, and often used to evaluate the potential performance of membranes, was higher for the modified nafion membrane with 13.9 wt.% poly(MPMDMS) and was approximately 5.88 times that of nafion-117, attributed to its higher proton conductivity and lower MCO [Su et al., 2009a, b]. Usually, a high value of selectivity corresponds to good performance [Dan et al., 2010]. Apparently, nafion composites synthesized by using polysiloxane additives has great potential for DMFC application. However, extensive characterization is lacking and durability of this composite membrane is still questionable.

2.2.2. *Nafion composites with ZrO_2 additives*

Sulphonated zirconia ($SZrO_2$) is accepted as a useful bifunctional filler to a nafion membrane as it improves water retention characteristics as well as maintains proton conductivity for higher temperature operation of DMFCs. $SZrO_2$ is a strong superacid and it has been demonstrated that the proton conductivity of $SZrO_2$, as well as its surface and crystallographic properties, varies largely depending on the method of preparation, in particular on the thermal treatments [D'Epifanio et al., 2010]. Introducing $SZrO_2$ in

nafion membranes, a general enhancement was revealed in a H_2/O_2 fuel cell response, both in terms of power density delivered and reduction of ohmic resistance, compared to unmodified nafion membranes. Moreover, the high-temperature impedance response of the $SZrO_2$-doped nafion based fuel cell was highly improved, showing a well-controlled charge-transfer resistance [Siracusano et al., 2012]. The proton conductivity of nafion-115 membrane was 1.5×10^{-2} S/cm at 25 °C, while that of the S–ZrO_2/nafion membrane was decreased to 5.0×10^{-3} S/cm. However, at or above 110 °C, the proton conductivity of the S–ZrO_2/nafion membrane was more than one-half that of the pure cast nafion membrane.

The ZrO_2/nafion membranes prepared by casting method were found to possess high thermal stability (T_g =188-192 °C) and conductivity (0.30-0.93 S/cm) [Mokhtaruddin et al., 2011]. The incorporation of sulfated zirconia into nafion membrane increases the amount of water uptake and provides additional acid sites for proton transportation, which results in higher proton conductivity compared to the host membrane at higher temperature [Ren et al., 2006]. The recast nafion composite membrane containing ZrO_2−SiO_2 binary oxides gives a maximum cell performance of 683 mW/cm^2 in a H_2/air fuel cell at 120 °C, 50% RH, and 2 atm pressure [Zhang et al., 2012].

Di Noto et al., (2008, 2010) prepared two nano additives with core shell structure consisting of harder core covered by softer shell. The highest conductivities for these two core shell nanoadditives/nafion membranes are 4.3×10^{-2} and 5.0×10^{-2} S/cm, respectively at 135 °C, whereas under the same conditions, pure cast nafion shows a conductivity of only 2.8×10^{-2} S/cm. The MCO of ZrO/nafion membrane is not reported. However Silva et al., (2004) reported a good balance between high proton conductivity, good chemical stability and low methanol permeability for the sulphonated poly(ether

ether ketone) (SPEEK) polymer with a 7.5% (w/w) ZrO_2 content and sulfonation degrees of 87%. Compared to nafion-112, the composite membrane was 3-times more impermeable towards water/methanol and had similar proton conductivity (0.081 S/cm compared to 0.088 S/cm).

2.2.3. *Nafion composites modified with ZrP additives*

Zirconium phosphates, $Zr(HPO_4)_2$, (ZrP), a Bronsted acid have the dual role of being both hydrophilic and proton conducting [Viswanathan and Helen, 2007]. The ZrP particles have the ability to donate protons, can increase water retention of nafion composite membranes at elevated temperatures by acting as nanotanks, and thus improve membrane conductivity. Bauer and Porada, (2004) examined the DMFC performance of ZrP-modified nafion membranes and found that the inorganic fraction slightly enhanced water content as compared to the unmodified nafion membrane and reduced the MCO. Yang et al., (2001) introduced ZrP into nafion through ion exchange of Zr^{4+} followed by precipitation of zirconium phosphate by immersion of the membrane in H_3PO_4 solution, which entrapped ZrP in the pores of the nafion membrane. The composite membranes were thermally stable. The maximum power density of 380 mW/cm^2 and 260 mW/cm^2 for a DMFC with the nafion composites was achieved with oxygen and air feeds, respectively. The ZrP additive enhanced water retention characteristics, raised the maximum working temperature, and increased the dry weight and thickness of the membrane. The $Zr(HPO_4)_2$/nafion membranes prepared by solution casting exhibited lower resistance than pure cast nafion attributed to the proton conducting property of $Zr(HPO_4)_2$ [Si et al., 2002]. According to the authors, the existence of $Zr(HPO_4)_2$ in the nafion structure provided more exchange sites for proton conduction and reduced the reliance of the membrane's conductivity on water content. Exfoliated-ZrP/nafion (e-

ZrP/nafion) membrane prepared by dispersing e-ZrP nanosheet in nafion solution exhibited 15.38% lower MCO than pure cast nafion with better thermal properties [Chen et al., 2004]. However, the proton conductivity of the composite membranes 0.055 S/cm were slightly lower than pure cast nafion membrane (0.06 S/cm).

The increase in the ZrP loading is associated with an enhancement of the elastic modulus and with a decrease in the membrane conductivity, especially at low RH values [Casciola et al., 2008]. However, temperatures above 130 °C, the conductivity of nafion-117 was lower than the composite. Moreover, the incorporation of ZrP into nafion was reported to significantly enhance the mechanical properties of the nafion-117 membrane [Bauer and Porada, 2005]. As a consequence of the higher elastic modulus values, the composite membranes exhibited enlarged stability region at higher temperature and RH values in comparison to the nafion-117 membrane [Casciola et al., 2008]. However, the polarization curve of the nafion composite in a DMFC was slightly decreased as compared to nafion-117 membrane. ZrP/nafion membranes with 25% ZrP exhibited lower water flux than nafion-115, attributed to low water diffusion, and displayed higher power density than nafion-115 in a H_2/O_2 fuel cell when operated at reduced humidity [Yang et al., 2004].

ZrP/nafion membranes developed by ion exchange method exhibited markedly increased IEC (0.909 meq/g for nafion-115, and 1.93 meq/g for ZrP/nafion), and 50% less MCO than nafion-115 [Hou et al., 2008]. The single cell performance evaluation with ZrP/nafion membranes demonstrated better fuel cell performance than nafion-115 at 75 °C with higher methanol concentration (10 M) attributed to reduced MCO. The reported peak power density of DMFC with 10 M methanol as fuel at 75 °C using α-

ZrP/nafion composite membrane is 76.19 mW/cm^2, which is approximately two times higher than that of nafion-115. The preliminary result of durability test showed that the single cell with composite membrane can stably be run 100 h above 0.4 V when 1 M methanol solution was used as fuel. Moreover, the stability was found to be at least 7 h at high methanol concentration (5 M and 10 M). Subsequent treatment with phosphoric acid enhanced elastic modulus but reduced the conductivity of the composite membranes as compared to nafion-117 [Casciola et al., 2008]. Partial replacement of the phosphate groups of ZrP with sulphophenylphosphonate groups led to a significant improvement of conductivity and stiffness. Similar composite membranes prepared by casting gels of exfoliated *a*-zirconium phosphate reduced MCO and swelling and improved thermal stability than pure cast nafion [Casciola et al., 2009a]. Further treatment with aqueous solutions of meta-sulphophenylphosphonic acid (H_2SPP) rendered the composite membranes more hydrophilic than pure nafion, and increased their stiffness, elastic modulus and proton conductivity than the parent ZrP/nafion membranes [Casciola et al., 2009b]. The MCO of unmodified nafion-117 was 2.3 × 10^{-6} cm^2/s at ambient temperature while that of the zirconium sulphophenyl phosphate membrane, (ZrSPP)/nafion, decreased to 6.5 × 10^{-7} cm^2/s [Kim et al., 2008].

The 10% ZrSPP/nafion membranes delivered constant power output of 104 mW/cm^2 at 0.4 V using 1 M MeOH at 70 °C. Table 2.3 compares the critical parameters of ZrO/nafion and ZrP/nafion developed by various researchers. The success of ZrO/nafion and ZrP/nafion membranes so far remains limited. The interaction between the inorganic phase and proton conductor stands vaguely understood. Besides, there are many other significant issues that need to be resolved, which include standard operating parameters

such as mechanical strength, durability, cyclability, synthetic conditions, and design issues including catalyst compatibility and scale-up.

2.2.4. *Nafion composites with heteropolyacids (HPAs) additives*

In recent years, significant efforts have been made to utilize heteropolyacids (HPAs) as both electrolyte and surface promoters for low temperature fuel cells. These materials are proton conductors with high intrinsic ionic conductivity [Staiti et al., 2001].

England et al., (1980) reported exceptionally high conductivity of approximately 0.17 S/cm at room temperature. HPA is generally impregnated into silica particles and then used for nafion modification. The hydration sphere is connected to impart conducting behaviour and thus it is essential to maintain the hydrated state of HPA in the polymer matrices to exploit their conductivity. Therefore, the conductivity drops drastically once it is heated and dehydrated.

Tazi and Savadogo, (2000) prepared silicotungstic acid/nafion (SiWA/nafion) membrane by casting and compared the characteristics of the composite membrane with nafion-117. The SiWA/nafion membrane exhibited enhanced water uptake and proton conductivity compared to nafion-117. The mechanical strength and chemical stability of the SiWA/nafion membrane were also excellent. The fuel cell performance of the SiWA/nafion membrane in a H_2/O_2 cell was inferior compared to nafion-117. At a voltage of 0.60 V, SiWA/nafion membrane exhibited a current density of 55 mA/cm^2 compared to 640 mA/cm^2 by nafion-117. However, on addition of thiophene to the SiWA/nafion membrane, the current density increased to 810 mA/cm^2 at 0.60 V.

Table 2.3 Comparison of critical properties of nafion composite membranes with ZrO and ZrP additives

Reference	Preparation technique	Water uptake (%)	Proton conductivity (S/cm)	MCO	DMFC performance
Ren et al., 2006	Ion exchange and precipitation	58 for S-ZrO/nafion, 37.50 for nafion-115 at 100 °C	0.009 for S-ZrO/nafion, 0.003 for nafion-115, 100 °C	NR	20 mA/cm^2 at 0.2 V for S-ZrO/nafion (1 M methanol at 105 °C)
Chen et al., 2004	Casting	NR	0.060 for nafion-117 and 0.055 for eZrP/nafion	2.6×10^{-6} cm^2/s for pure nafion and 0.4×10^{-6} cm^2/s for eZrP/nafion	NR
Yang et al., 2004	Ion exchange	18 for nafion-115 and 25 for 25% ZrP/nafion at 80 °C	0.140 for nafion-115 and 0.120 for 25% ZrP/nafion	NR	NR
Bauer and Porada, 2005	Ion exchange	NR	0.032 for nafion-117 and 0.025 for 21% ZrP/nafion at 130 °C	0.4 A/cm^2 for nafion-117, 0.25 A/cm^2 for 13% ZrP/nafion, and 0.3 A/cm^2 for 26% ZrP/nafion at 130 °C	30 mA/cm^2 for nafion-117 and 21 mA/cm^2 for 13% and 26% ZrP/nafion at 0.35 V (1.5 M methanol, 130 °C)
Hou et al., 2008	Ion exchange	NR	0.102 for nafion-115 and 0.084 for 23% ZrP/nafion	55 mA/cm^2 for nafion-115 and 24 mA/cm^2 for 23% ZrP/nafion at 30 °C	Maximum of 96.3 mW/cm^2 for nafion-115 and 91.6 mW/cm^2 for 23% ZrP/nafion (75 °C, 5 M methanol) 42.4 mW/cm^2 for nafion-115 and 76.19 mW/cm^2 for 23% ZrP/nafion (75 °C, 10 M methanol)
Casciola et al., 2009a	Casting	NR	0.054 for pure cast nafion and 0.036 for 1% ZrP/nafion (40 °C, 100% RH)	2.6×10^{-6} cm^2/s for pure cast nafion and 2.5×10^{-7} cm^2/s for 1% ZrP/nafion (40 °C, 100% RH)	NR

NR: Not reported

They further extended their approach to the preparation and characterization of polymer electrolyte membrane based on modified nafion and included phosphotungstic acid (PWA) and phosphomolybdic acid (PMA) as modification additives [Tazi and Savadogo, 2001]. The SiWA/nafion membrane exhibited mechanical properties similar to nafion-117, while PWA/nafion and PMA/nafion exhibited lower mechanical properties than nafion-117 and SiWA/nafion membrane.

Water uptake was highest for PMA/nafion (95%) followed by PWA/nafion (70%), SiWA/nafion (60%), and nafion-117 (30%). The ionic conductivity and conductance of the SiWA/nafion membranes were higher than those of PWA/nafion, PMA/nafion, and nafion-117. The PEMFC performance was best for PMA/nafion followed by PWA/nafion, SiWA /nafion, and nafion-117. A maximum power density of 400 mW/cm^2 at 145 °C in the presence of oxygen feed, and 250 mW/cm^2 in the presence of air feed was obtained with nafion composite with phosphotungstic acid (PWA) impregnated into silica particles [Staiti et al., 2001]. The authors also reported that PWA has a promoting effect on the kinetics of electrochemical reduction of oxygen attributed to the high oxygen solubility in the PWA electrolyte. CO-like products, which form at the anode during methanol oxidation reaction giving rise to a strong chemisorption on surface catalyst, are removed efficiently in the presence of PWA.

Xu et al., (2005) reported an open circuit potential of 0.75 V at 80 °C with the PWA/silica/nafion composite membrane compared to 0.68 V for pure cast nafion membrane and a maximum power density of 70 mW/cm^2 and 62 mW/cm^2, respectively. The composite membrane exhibited higher proton conductivity than nafion-117. A

methanol diffusion coefficient of 2.8×10^{-7} cm^2/s could be obtained with the composite membrane as compared to 5.2×10^{-7} cm^2/s with nafion-117.

Thermogravimetric analysis (TGA) results indicated that nafion composite membranes like PWA/SiO_2/nafion and SiO_2/nafion composite membranes are thermally more stable than pure cast nafion membrane. However, the nafion composites with inorganic additives like titanium dioxide (TiO_2), tungsten oxide (WO_3) accelerated the decomposition of the composite membrane at an earlier temperature than pure cast nafion membrane [Shao et al., 2006]. The water uptake was higher for PWA/SiO_2/nafion membrane compared to the other modified nafion membranes and the pure cast nafion membrane. The proton conductivity of the modified membranes, except that of the TiO_2/nafion, was found to be close to pure cast nafion membrane at high temperature and at 100% relative humidity (RH), however, it was much higher at low RH. PWA/SiO_2/nafion membrane exhibited higher proton conductivity than the other nafion composites as well as pure cast nafion membrane. The performance of these modified membranes in the PEMFC operated at 110 °C and 70% RH was better than pure cast nafion membrane and was found in the order of PWA/SiO_2/nafion > SiO_2/nafion > WO_3/nafion > TiO_2/nafion.

Nafion composite membranes with sulfonic acid groups onto the surface of SiO_2 of HPA/SiO_2 were thermally stable up to 290 °C [Kim et al., 2006]. The maximum power density was 33 mW/cm^2 at 80 °C, 39 mW/cm^2 at 160 °C and 44 mW/cm^2 at 200 °C, respectively, with 4 M methanol. However, the authors reported that the fuel cell performance was lower than that with pure cast nafion membrane and insisted on the modification of the method of MEA preparation as the composite membrane has different

surface as compared to the nafion membrane. Modification of nafion with cesium hydrogen salt of heteropolyacids ($Cs_{2.5}H_{0.5}PMo_{12}O_{40}$) (CsPMo) and $Cs_{2.5}H_{0.5}PW_{12}O_{40}$ (CsPW) was done in an attempt to alter the membrane surface acidity and water solubility. Enhanced proton conductivity of the composite membranes was found, which may be attributed to the hygroscopic nature of CsHPs [Amirinejad et al., 2011]. The performances of the composite membranes in a PEMFC were superior to unmodified nafion. However, the composite membranes had lower thermal stability and lower IEC than pure nafion attributed to the covering of the nafion active sites (sulfonic groups) by the salts and decreasing the effective number of replaceable ion exchange sites. Moreover, there are some issues in general with the HPA/nafion membranes relating to operational and mechanical stability of the composites. Table 2.4 compares some of the critical parameters of HPA/nafion membranes developed by various researchers.

2.2.5. *Nafion composites with zeolite additives*

Zeolites are a class of hygroscopic, microporous, proton conducting, crystalline aluminosilicates [Sanni, 2011]. Tricoli and Nannetti, (2003) tried to exploit the molecular sieving properties of zeolites to design nafion membranes with low MCO. Two natural zeolites chabazite and clinoptilolite of considerably smaller size (40-50 nm) were selected as additives and both types were proton conductive as well as impermeable to methanol. Composite nafion membranes were made by evaporating the solvents from a suspension of small zeolite crystals of various concentrations (maximum 40 wt.%) in a nafion solution. The composites were studied in both Na^+ and H^+ form and characterized for surface morphology, particle distribution, proton conductivity, and MCO. The composite membranes retained reasonable flexibility when saturated with water but were rather brittle in the dry state indicating a decrease in mechanical stability.

Table 2.4 Comparison of critical properties of nafion composite membranes with HPA additives

Reference	Preparation technique	Water uptake (%)	Proton conductivity (S/cm)	MCO	DMFC performance
Staiti et al., 2001	Casting	NR	NR	NR	Maximum of 400 mW/cm^2 for 30% PWA/SiO_2/nafion and 340 mW/cm^2 for 3% SiO_2/nafion (145 °C, oxygen feed, 2 M methanol) Maximum of 250 mW/cm^2 for both 30% PWA/SiO_2/nafion and 3% SiO_2/nafion (145 °C, air feed, 2 M methanol)
Xu et al., 2005	Sol-gel	NR	0.015 for nafion-117 and 0.024 for 70.2 μg/g PWA/SiO_2/nafion	5.2×10^{-7} cm^2/s for nafion-117 and 2.8×10^{-7} cm^2/s for 38.2 μg/g PWA/SiO_2/nafion	Maximum of 62 mW/cm^2 for nafion-117 and 70 mW/cm^2 for 38.2 μg/g PWA/SiO_2/nafion (80 °C, 2 M Methanol)
Shao et al., 2006	Casting	38 for 10% PWA/SiO_2/nafion, 26 for nafion-115 and 32 for pure cast nafion respectively	0.027 for 10% PWA/SiO_2/nafion and 0.008 for nafion-115 (110 °C and 70% RH)	NR	NR
Kim et al., 2006	Casting	More than pure cast nafion (value not reported)	More than pure cast nafion (value not reported)	Lower than pure cast nafion (value not reported)	Maximum of 33 mW/cm^2 at 80 °C, 39 mW/cm^2 at 160 °C and 44 mW/cm^2 at 200 °C, 4 M methanol for 10% HPA/SiO_2/nafion
Amirinejad et al., 2011	Casting	33 for pure cast nafion, 62 for 10% CsPW/nafion and 76 CsPMo/nafion	0.037 for pure cast nafion, 0.055 for 10% CsPW/nafion and 0.058 CsPMo/nafion	NR	NR

NR: Not reported

The three-dimensional network of small size pores (3.8 Å) of chabazite and relatively high Al/Si ratio (1:2) that translates into notable ion-exchange capacity (2.5 meq/g) was expected to contribute to good ion conductivity coupled to low MCO to the nafion composite membranes compared to pure cast nafion. However, both MCO and proton conductivity of the nafion composite membranes were lower than nafion-117 and pure cast nafion membrane.

Acid functionalized zeolite β/nafion (NAFB) nanocomposite membranes by in-situ hydrothermal crystallization exhibited slightly lower proton conductivity than nafion-115 but markedly lower MCO (ca. 40% reduction) [Chen et al., 2006]. The proton conductivity of 2.5% zeolite β (AFB)/nafion membrane was higher than nafion-117 and the selectivity ratio (conductivity/MCO) of 2.5% and 5% AFB/nafion membranes were as much as 93% higher than nafion-117 at 21 °C, and 63% higher at 80 °C, attributed to the large reduction in MCO [Holmerg et al., 2008]. These membranes also performed well as compared to nafion-117 membrane in DMFC performance evaluations. The current density at 0.3 V were 150, 80 and 65 mA/cm^2 for 2.5% AFB/nafion, 5% AFB/nafion and nafion-117, respectively. Similarly, the NAFB composite membranes when tested with 1 M methanol feed, exhibited higher open circuit voltage (OCV) (3%) and much higher maximum power density (21%) than those with the nafion-115 membranes [Chen et al., 2006]. With a higher methanol concentration (5 M), the DMFCs with the NAFB composite membranes demonstrated a 14% higher OCV and a 93% higher maximum power density than those with the nafion-115 membrane. However, compared with the nafion-115 membrane, the NAFB composite membranes had slightly lower tensile strength but higher elastic modulus. Maximum power densities ranging from 350-370 mW/cm^2 and 200-210 mW/cm^2 were recorded at 140 °C with 3% chabazite/nafion and

6% clinoptilolite/nafion membranes, under oxygen and air operation, respectively. The high performances obtained were attributed to the enhancement of water retention of the composite membranes compared to pure cast nafion membrane caused by the presence of the hygroscopic additive, which was confirmed by cell resistance measurements [Baglio et al., 2005].

Montmorillonite (MMT) is another form of zeolite, a layered alumino-silicate mineral that has large surface areas (220-270 m^2/g) with a negative layer charge. Rhee et al., (2005) synthesized nafion composites with organic sulfonic acid group modified MMT (HSO_3-MMT). The HSO_3-MMT/nafion membranes exhibited lower proton conductivities compared to nafion-115 but exhibited substantial improvement in DMFC performance by reducing the MCO drastically. The relative permeabilities of methanol and water were reduced by up to 90% and 80%, respectively, relative to nafion-115 membrane.

Lin et al., (2005) cited that silicate clays are hydrophilic and have little affinity for hydrophobic polymers and an organic modification is required to enhance their compatibility with nafion. The nafion composites with modified MMT (Poly(oxyproplene)-backboned (POP) quaternary ammonium salts of POPD400-PS as intercalating agents) exhibited 60% reduction in MCO and improved the proton conductivity of pure cast nafion, which significantly enhanced the DMFC performance [Lin et al., 2007].

Nafion composites with MMT functionalized with Krytox, bearing nafion like poymer chain (Krytox–MMT/nafion) exhibited improvement in water retention and thermal resistance, reduced MCO by 50%, but lowered the proton conductivity as compared to

unmodified nafion membrane [Gosalawit et al., 2007]. The reduction in proton conductivity is attributed to the blocking effect of MMT additive confining the continuum of sulfonic acid groups of nafion responsible for proton conductivity. Table 2.5 gives a comparison of some critical parameters of zeolite/nafion membranes developed by various researchers.

2.3. Methanol impermeable and/or proton conducting additives

2.3.1. *Nafion composites with palladium (Pd) additives*

Palladium (Pd) is known to be an effective storage medium for hydrogen and can easily form palladium hydride [Choi et al., 2001]. Prabhuram et al., (2005) has reported Pd to be a methanol impermeable and proton conducting (MIPC) additive, which has been adopted by several researchers for nafion modification. Choi et al., (2001) combined plasma-modification of the nafion surface and palladium-sputtering techniques in an attempt to reduce the MCO problem.

Three types of modified membranes, i.e. plasma-etched membrane, Pd-sputtered membrane, and plasma etched and Pd-sputtered membrane, were prepared. All the modified membranes could effectively reduce the MCO. The MCO for the Pd-sputtered membrane was lower than that of the plasma etched membrane, while the membrane modified by both plasma etching and Pd sputtering exhibited the lowest MCO. The Pd sputtered membrane exhibited the highest proton conductivity, followed by the plasma etched membrane, unmodified nafion membrane, and the combination of plasma etched and Pd sputtered membrane. However, the findings of this work was contrary to that of Yoon et al., (2002), who observed that the proton conductivity for the modified membrane decreased as compared to the unmodified nafion membrane, despite using the

Table 2.5 Comparison of critical properties of nafion composite membranes with zeolite additives

Reference	Preparation technique	Water uptake (%)	Proton conductivity (S/cm)	MCO	DMFC performance
Tricoli and Nannetti, 2003	Casting	NR	0.018 for 40% chabazite/nafion (Na^+ form), 0.022 for 40% clinoptilolite/nafion (Na^+ form) at 22 °C, 0.101 for pure cast nafion (H^+ form) at 25 °C	1.85×10^{-6} cm^2/s for 40% chabazite/nafion (Na^+ form), 2.28×10^{-6} cm^2/s 40% clinoptilolite/nafion (Na^+ form) at 22 °C, 1.99×10^{-6} cm^2/s for pure cast nafion (H^+ form) at 21 °C	NR
Baglio et al., 2005	Casting	NR	NR	NR	Maximum of 370 mW/cm^2 for the 6% clinoptilolite/nafion, 350 mW/cm^2 for 6% chabazite/nafion, and 260 mW/cm^2 for pure cast nafion (oxygen feed, 2 M methanol, 140 °C)
Chen et al., 2006	In situ hydrothermal crystallization	NR	0.088 for NAFB membranes, 0.091 for nafion-115	1.40×10^{-6} cm^2/s for NAFB membranes, 2.36×10^{-6} cm^2/s for nafion-115	Maximum of 98 mW/cm^2 for NAFB membranes and 81 mW/cm^2 for nafion-115 (1 M methanol, 70 °C). 120 mW/cm^2 for NAFB membranes and 62 mW/cm^2 for nafion-115 membrane (5 M methanol, 70 °C)

NR: Not reported

Reference	Preparation technique	Water uptake (%)	Proton conductivity (S/cm)	MCO	DMFC performance
Holmberg et al., 2008	Casting	NR	0.061 for 2.5% AFB/nafion, 0.047 for 5% AFB/nafion and 0.037 for nafion-117 at 21 °C	5.68×10^{-7} cm^2/s for 2.5% AFB/nafion, 8.30×10^{-7} cm^2/s for 5% AFB/nafion and 1.26×10^{-6} cm^2/s for nafion-117 at 21 °C	150 mA/cm^2 for 2.5% AFB/nafion, 80 mA/cm^2 for 5% AFB/nafion and 65 mA/cm^2 for nafion-117 at 0.3 V (1 M methanol, 70 °C)
Rhee et al., 2005	Casting	NR	0.36 for 5% HSO_3-MMT/nafion, 0.52 for nafion-115	NR	336 mA/cm^2 for 5% HSO_3-MMT/nafion and 244 mA/cm^2 for nafion-115 at 0.2 V (2 M methanol, 40 °C)
Lin et al., 2007	Casting	NR	0.118 for 6% MMT-POPD400-PS/nafion, and 0.095 for pure cast nafion	1.2×10^{-6} cm^2/s for 6% MMT-POPD400-PS/nafion, and 3.1×10^{-6} cm^2/s for pure cast nafion	95 mA/cm^2 for 6% MMT-POPD400-PS/nafion, and 51 mA/cm^2 for pure cast nafion at 0.2 V (2 M methanol, 40 °C)
Gosalawit et al., 2007	Casting	26.4 for 2.5% Krytox–MT/nafion, 31.6 for 5% Krytox–MMT/nafion, and 20.8 for pure cast nafion	0.025–0.048 for 2.5% Krytox–MMT/nafion, 0.023–0.032 for 5% Krytox–MMT/nafion, and 0.029–0.062 for pure cast nafion	1.2×10^{-6} cm^2/s for 2.5% Krytox–MMT/nafion, 8.7×10^{-7} cm^2/s for 5% Krytox–MMT/nafion, and 8.7×10^{-6} cm^2/s for pure cast nafion at 25 °C	NR

NR: Not reported

same modification technique. Nafion composites with deposition of a thin Pt/Pd-Ag/Pt alloy film by sputtering method on the surface of the nafion-117 effectively reduced MCO and gave a higher DMFC performance than that of unmodified nafion-117 membrane [Ma et al., 2003]. However, the composite membranes synthesized developed cracks. Modification of nafion-117 with Pd nanophases permitted the use of higher molar concentration of methanol in DMFC without any power loss and the performance was superior to nafion-117 [Kim et al., 2003]. This has numerous advantages such as the reduction of the volume of the system and long-term usage of fuel through the circulation of high concentrated methanol. The power densities of unmodified nafion membrane and Pd/nafion with 2 M methanol and at 30 °C were 60 mW/cm^2 and 65 mW/cm^2, respectively. The maximum power density of the Pd/nafion was slightly increased or maintained with increasing concentrations of methanol, while the maximum power density of the pure cast nafion membrane was abruptly decreased. The Pd-Nafion showed an increment of 23% while the maximum power density of nafion-117 was reduced by 43% when 10 M methanol was used as a fuel compared to 2 M methanol at 30 °C.

Subjecting nafion-117 to γ-ray radiation caused membrane cross-linking and reduced the swelling of membrane along with reduction in MCO compared to unmodified nafion [Liu et al., 2006]. Electroless Pd deposition further reduced the MCO and produced reasonable power density performance as high as 4.9 mW/cm^2 with 2 M methanol solution at room temperature in a μDMFC. Modification of nafion-115 with Pd alloyed with Group 1B metals, to prevent hydrogen embrittlement, did not show significant improvement in DMFC performance compared to unmodified nafion-115 membranes [Prabhuram et al., 2005]. The Pd-sputtered membrane yielded a power density of 14 mW/cm^2, while the Pd-Cu-sputtered and bare membranes gave power densities of 13 mW/cm^2 and 11 mW/cm^2,

respectively. Though Pd modified nafion membranes were proving to be a potential method of nafion modification for DMFC, Prabhuram et al., (2005) opined that the prolonged hydride formation and its conversion into protons during cell operation can lead to hydrogen embrittlement in the Pd thin layer, which can eventually cause mechanical degradation of the Pd layers from the surface of the membrane. According to them, the problem of the occurrence of hydrogen embrittlement in Pd can be ceased if it is alloyed with metals like Ag (30 wt.%), Au (5 wt.%), and Cu (40 wt.%) (Group 1B metals); at the same time, the hydrogen diffusion rate can be maintained in these Pd alloys.

2.3.2. *Nafion composites with Platinum (Pt) additives*

Watanabe et al., (1998) successfully employed Pt modified nafion-112 for self-humidification and suppression of gas-crossover in a PEMFC. Similar concept was employed and extended for DMFC [Uchida et al., 2000]. The advantages brought about, by the presence of Pt particles in nafion were not significant at the high methanol feed rate, which was attributed to a higher MCO rate than the rate of catalytic oxidation in Pt/nafion. The Pt/nafion membranes synthesized by exchange between the tetraammineplatinum (II) cations ($[Pt(NH_3)_4]^{2+}$) and sulfonic groups in the nafion molecules, exhibited increased proton conductivity and open circuit voltage compared with the pure cast nafion membrane [Lee et al., 2008]. The maximum power density was enhanced by 29% by the composite membrane attributed to the oxidation of methanol passing through the proton-exchange membrane, which lowered the MCO. However, at a high loading of Pt (over 3 wt.%), the Pt/nafion membranes exhibited lower water uptake and proton conductivity attributed to the reduction in the nafion clusters and this hypothesis was also supported by the increased ohmic resistance in the fuel cell

polarization curve. Table 2.6 compares some critical parameters of nafion composite membranes developed with methanol impermeable and/or proton conducting additives.

2.4. Summary of literature review

Nafion composites have great potential in achieving a polymer electrolyte membrane with the ideal characteristics desired for DMFC. Composites are attractive because they allow blending or modification of the different properties of each component to improve an overall material performance. Basically, the inorganic additives utilized in nafion modification for DMFC usually possess a few of the important properties, namely hygroscopic property, proton conducting property, methanol impermeability, and methanol oxidizing ability. The two primary parameters targeted by the researchers during nafion modification are reduction of MCO while maintaining the proton conductivity of nafion membrane. The addition of hygroscopic additives resulted in a change in structure of the membrane, where the particles block part of the hydrophilic polymer channels through which protons migrate. At the same time narrowing of water channels facilitated low solvent permeation and electroosmotic drag coefficient, which simultaneously reduced MCO. The water uptake by the oxide containing membrane was higher than that of the pure nafion. They also exhibited improved thermal and mechanical stability than the parent polymer, and in most cases exhibited reduced proton conductivity compared to pure nafion membrane. However, other problems such as reduction in mechanical stability when the inorganic component loading reached a critical level, and decreased fuel cell performances were encountered. Proton conductive additive could reduce MCO while maintaining the proton conductivity but showed improved performance only at high operating temperatures.

Table 2.6 Comparison of critical properties of nafion composite membranes with Pd and Pt additives

Reference	Preparation technique	Water uptake (%)	Proton conductivity (S/cm)	MCO	DMFC performance
Ma et al., 2003	Sputtering	NR	Improved (value not reported)	Reduced (value not reported)	Maximum of 2.8 mW/cm^2 for 1 µm Pd-Ag/nafion, and 0.9 mW/cm^2 for nafion-117 (1 M methanol, ambient temperature)
Kim et al., 2003	Casting	NR	4.9 for nafion-117, and 3.2 for 0.90 mg/cm^2 Pd/nafion	3.2×10^{-6} cm^2/s for nafion-117, 4.3×10^{-7} cm^2/s for 0.90 mg/cm^2 Pd/nafion	Maximum of 60 mW/cm^2 for nafion-117 and 65 mW/cm^2 for 0.90 mg/cm^2 Pd/nafion (2 M methanol, 30 °C) Maximum of 34 mW/cm^2 for nafion-117 and 79 mW/cm^2 for 0.90 mg/cm^2 Pd/nafion (10 M methanol, 30 °C)
Prabhuram et al., 2005	Sputtering	NR	NR	NR	300 mA/cm^2 for nafion-115, 220 mA/cm^2 for Pd/nafion, 280 mA/cm^2 for (60:40) Pd-Cu/nafion at 0.12 V (2 M methanol, 70 °C)
Lee et al., 2008	Cation exchange	22.93 for pure cast nafion and 41.98 for 2% Pt/nafion	0.033 for pure cast nafion, and 0.038 for 2% Pt/nafion	NR	Maximum of 77.7 mW/cm^2 for pure cast nafion, and 100 mW/cm^2 for 2% Pt/nafion (1 M Methanol, 70 °C)

NR: Not reported

Modification of nafion with zeolite, and their derivatives could increase thermal and mechanical properties and reduce MCO. However, increasing impermeable filler content usually resulted in a simultaneous reduction in proton conductivity and mechanical failure. The composite membranes containing the impermeable additives were found to have increased MCO when loading increased, attributed to lack of interactions between the filler and the polymer creating a crude dispersion impairing the transport trend. Pd modified nafion membranes could lower MCO while maintaining the proton conductivity and also allowed usage of higher methanol concentrations without depreciating the fuel cell performance. However, it has been indicated that prolonged hydride formation and its conversion into protons during cell operation can lead to hydrogen embrittlement in the Pd thin layer, which can eventually cause mechanical degradation of the Pd layers from the surface of the membrane. Alloying Pd with other metals could alleviate the problem of hydrogen embrittlement but the composite showed increased MCO than Pd/nafion membranes. Modification of nafion with methanol oxidizing catalyst like Pt is a good strategy. However, the performances of the composite membranes are limited by factors such as high methanol concentration and high flow rate of methanol. Besides, Pt is very expensive and would increase the cost of the composite membranes.

Therefore, the search for a nafion composite possessing the physic-chemical properties of nafion with the additional property of methanol selectivity is still going on and there have been efforts globally by the researchers to meet the set criterion. For a proper assessment of the nafion composites a detailed characterization of the composite membranes both under ex-situ environment and fuel cell conditions is necessary. Another significant point to be noted is that DMFC has applications for automotive, stationary, and portable devices. Hence, as pointed out by Zang and Shen, (2012), it would be impractical to

expect that a single type of membrane can meet all the requirements. If the application of DMFC is for portable devices like camera, laptops, thermometers, i-pods, mobile phones, etc., which are operated at ambient temperature, performance of the composite membranes at ambient temperature is noteworthy rather than that at high temperature. Thus, for enhanced DMFC performance at ambient temperature both the parameters namely, low MCO and high proton conductivity will play a crucial role. The mechanical properties of the composite membranes namely, tensile strength and swelling have also not been taken into consideration while studies have shown that the mechanical properties of the membranes are extremely important to the performance and longevity of the fuel cell. Nafion is a polymeric membrane, which means that it responds to stress in a time dependant manner. The membrane of a fuel cell is subject to various stresses, including those due to solvent mass uptake and clamping between flow plates. Hence, an accurate knowledge of the physico-chemical properties of the synthesized nafion composite membrane under a range of environmental conditions is crucial to identify the potential composite membranes for DMFC. Moreover, the degradation of nafion in polymer electrolyte membrane fuel cells has caused widespread concern. However, there are barely any reports on the analysis of nafion composites for chemical stability or oxidative stability.

It is an undeniable fact that in the foreseeable future, it will be difficult to completely replace nafion membranes, especially at temperatures less than 80 °C, because of their excellent oxidative stability and superior proton conductivity. Besides, the nafion membranes reinforced by filling pores offer a cost-effective option. So, in order to improve the performance of nafion composites, there is the need for extensive research with new type of additives that would contribute to low MCO, acceptable proton

conductivity, high thermal, chemical and mechanical durability, moderate swelling and, high power density. It is also desirable for the additives to have some kind of bond with the nafion matrices so as to enhance the durability of the composites. Therefore, the objective of the current research is set as per the above literature survey and discussed in the next section.

2.5. Aim and objectives

In this study, we have identified a few of the novel additives, which have the potential to reduce not only MCO but may also help to achieve the other desirable properties of the composite nafion membrane for DMFC application.

Hence, the main objective of this thesis is to develop a composite nafion membrane for reduced MCO keeping other vital properties of the membrane at least at par with the cast nafion membrane. The research work was started with cast nafion and TiO_2/nafion composite membranes. The study and the result helped to standardize and develop a protocol for various processes and techniques starting from additive characterization, membrane casting, various membrane characterization techniques, and DMFC development along with the MEA fabrication.

Therefore, in order to achieve the objective the additives were characterized first and then using the additive and nafion dispersion the composite nafion membrane was synthesized. The synthesized membrane was characterized thoroughly under ex-situ conditions. Further, a direct methanol fuel cell was designed for evaluating the composite membrane performance in the DMFC. The details of the work are given below.

►Characterization of additives by,

a. Particle size,

b. X-ray diffraction (XRD) ,

c. BET surface area, and

d. Scanning electron microscopy (SEM).

►Synthesis of nafion composite membrane using casting technique

►Characterization of the developed nafion composite membrane by,

a. Scanning electron microscopy (SEM),

b. Thickness,

c. X-ray diffraction (XRD),

d. Thermogravimetric analysis (TGA),

e. Fourier transform infrared (FTIR) spectrometer analysis,

f. Ion exchange capacity,

g. Water uptake,

h. Methanol uptake

i. Swelling,

j. Tensile strength,

k. Oxidative stability,

l. Proton conductivity,

m. Methanol crossover, and

n. Selectivity.

►Fuel cell development

a. Development of MEA

b. Fabrication of DMFC setup

►**Performance evaluation of DMFC using developed membranes**

Once the above methodologies and techniques were set using cast nafion and TiO_2/nafion membranes, the next step was to choose suitable and novel additive. The following additives were chosen,

- TiO_2 (Titanium dioxide)
- Nd_2O_3 (Neodymium oxide)
- $H_2Mg_3(SiO_3)_4$ (Magnesium silicate hydroxide)
- $Er(SO_3CF_3)_3$ (Erbium triflate)
- $Nd(SO_3CF_3)_3$ (Neodymium triflate)
- $0.4K_2O:0.6Na_2OAl_2O_3:2.OSiO_2:24.5H_2O$ (Molecular sieve, 3Å)

The above additives are grouped in to three categories as shown below,

i) Crystalline hygroscopic additive (TiO_2, Nd_2O_3, and $H_2Mg_3(SiO_3)_4$)
   - these three additives are crystalline in nature, adsorb water and form –OH groups on the surface.

ii) Bi-functional additive (ErTfO, and NdTfO)
   - both the additives have SO_3^- as the functional group attached to the trifluoromethane ($-CF_3$) chain as in nafion. Both Er^{3+} and Nd^{3+} have high coordination numbers and can form coordination bonds with the anion (SO_3^-) of triflate as well as nafion.

iii) Size selective additive (molecular sieve)
   - MS has a pore size of 3 Å, which is smaller than the diameter of methanol molecule and hence should act as size selective additive.

► Reduction of crossed-over methanol effect at cathode using hybrid Pt/laccase

Next chapter provides the various materials used along with the details of the experimental methodologies.

Chapter 3

Experimental

Chapter 3: Experimental

The major materials used for the synthesis of nafion composite membranes are discussed in the first part of the chapter. The experimental methodologies for characterization of the additives, composite membranes, and DMFC along with the fabrication of membrane, electrodes, and membrane electrode assemblies are discussed in the later part of the chapter.

3.1 Materials

3.1.1 *Crystalline, hygroscopic additive*

Three different additives under this category namely, titanium dioxide, neodymium oxide, and magnesium silicate hydroxide have been used in this work for the nafion modification. A brief discussion on the properties of these additives is provided in the subsequent sections.

3.1.1.1 *Titanium dioxide (TiO_2)*

Titanium dioxide (fig. 3.1 a), also known as titanium (IV) oxide or titania, is the naturally occurring oxide of titanium. Titanium dioxide occurs in nature in three different forms, rutile; brookite; and anatase [Dachille, 1968]. TiO_2 is crystalline and hygroscopic in nature. The strong oxidation potential of TiO_2 oxidizes the water molecules associated to it, which results in the formation of hydroxyl (fig. 3.1 b) groups on the surface of the particles [Fujishima et al., 2000; Staiti et al., 2001]. In the present work, TiO_2 was obtained from Merck, Germany. A few of the general properties of TiO_2 is presented in table 3.1.

(a) (b)

Fig. 3.1 Chemical structure of (a) titanium dioxide and (b) titanium hydroxide

Table 3.1: General properties of TiO_2

Properties	Values
Molar mass	79.87 g/mol
Appearance	White solid powder
Density	4.23 g/cm^3
Melting point	1843 °C
Boiling point	2972 °C
Solubility in water	Insoluble

3.1.1.2 *Neodymium oxide (Nd_2O_3)*

Electrical and chemical properties of rare earth oxides (REOs) have been recognized as of great technological importance [Dakhel, 2004]. REOs find applications in a large variety of research areas, including medical or biochemical systems, property enhancements of materials as fillers and catalysis [Rill et al., 2008]. These are the main constituents of the solid electrolytes and widely used as additives for improving their ion-conducting characteristics and thus play a major role in the field of solid state ionics [Adachi et al., 2002]. Neodymium (III) oxide or neodymium sesquioxide is a rare earth oxide and neodymium (Nd) belongs to the lanthanide (III) series.

Neodymium is one of the most abundant rare earth elements and neodymium oxide is a very light grayish blue chemical compound composed of neodymium and oxygen with the formula Nd_2O_3 (fig. 3.2a) [Lide, 1998]. There is evidence in the literature that the lanthanide oxides may act as either Lewis acids or Lewis bases [Read, 1972]. Nd_2O_3 is crystalline, thermally stable [Kepin´ski et al., 2004], hygroscopic compound, which is insoluble in water [Nagao et al., 2003]. The hygroscopic nature of Nd_2O_3 leads to the formation of neodymium hydroxide [$Nd(OH)_3$] (fig. 3.2b), and the presence of OH^- groups, which can act as proton conducting domains and render it conductive [Dakhel, 2004; Nagao et al., 2003]. Wang and Kumar, (2004) used Nd_2O_3 as a proton conductor in a novel solid electrochemical sensor for monitoring HCl gas [Wang and Kumar, 2004]. Various researchers synthesized urea silicates and dissolved large quantities of neodymium salt to get the conductive films. The free-standing polymer films showed moderate levels of ionic conductivity (approximately 10^{-5} S/cm at room temperature) over a wide range of salt concentration [Silva et al., 1998]. Nd_2O_3 used in the present

work was obtained from Alfa Aesar (Lancaster). A few of the general properties of Nd_2O_3 is presented in table 3.2.

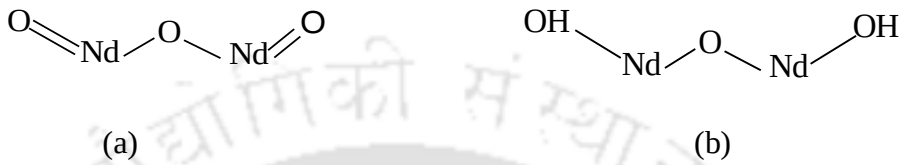

(a) (b)

Fig.3.2 Chemical structure of (a) neodymium oxide, and (b) neodymium hydroxide

Table 3.2: General properties of Nd_2O_3

Properties	Values
Molar mass	336.48 g/mol
Appearance	Light bluish gray powder
Density	7.24 g/cm^3
Melting point	2233 °C
Boiling point	3760 °C
Solubility in water	Insoluble

3.1.1.3 *Magnesium silicate hydroxide or talc [$H_2Mg_3(SiO_3)_4$]*

Talc is a crystalline, hygroscopic material having bimatellic oxide. The co-existence of magnesium and silica in its oxide form (fig. 3.3) in talc has been anticipated to be advantageous for improving the characteristics of the nafion membrane. There are several reports in the literature where the individual effects of these oxides have been evaluated for fuel cell applications. The contribution of SiO_2 in SiO_2/nafion membranes in terms of MCO and proton conductivity for DMFC has already been discussed in the previous chapter. However, magnesium oxide (MgO) has been used for modification of Pt/C catalyst for direct oxidation of ethanol in direct ethanol fuel cell (DEFC) [Xu et al., 2005] but not in electrolyte. MgO is hygroscopic in nature and forms magnesium hydroxide [$Mg(OH)_2$] in the presence of water [Merwe and Strydom, 2006]. The magnesium silicate hydroxide (talc) for the present work was procured from Loba Chemie, India. A few of the general properties of talc is presented in table 3.3.

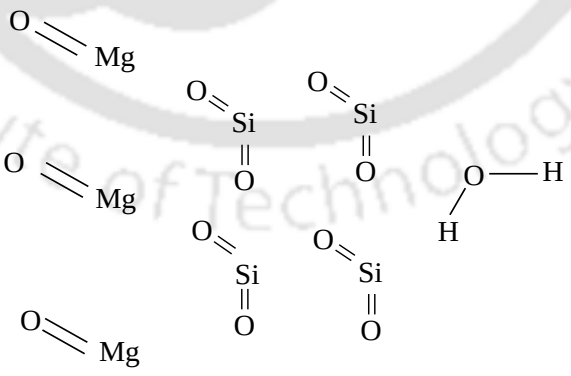

Fig.3.3 Chemical structure of magnesium silicate hydroxide

Table 3.3: General properties of magnesium silicate hydroxide

Properties	Values
Molar mass	379.27 g/mol
Appearance	White powder
Density	2.7 g/cm^3
Melting point	1500 °C
Boiling point	1557 °C
Solubility in water	Insoluble

3.1.2 *Bi-functional additive*

Two additives under this category namely, erbium triflate and neodymium triflate have been used in this work for nafion modification. A brief discussion on the properties of these two additives is given below.

3.1.2.1 *Erbium triflate [Er $(SO_3CF_3)_3$] and Neodymium triflate [Nd $(SO_3CF_3)_3$]*

Erbium triflate (ErTfO) and neodymium triflate (NdTfO) are rare earth lanthanide triflates and are regarded as environment friendly Lewis acid catalyst [Kobayashi, 1994; Inanaga et al., 1993]. The lanthanide (III) triflates, $La(TfO)_3$, where TfO represents $-SO_3CF_3$ group, have high coordination number, are hygroscopic, thermally stable, and resistant to redox environment [Katsuhara et al., 2006; Shroti et al., 2011]. Trifluoromethanesulphonic acid or triflate acid (CF_3SO_3H), is regarded as one of the strongest acids, which resembles nafion in structure [Barbora et al., 2009b]. Therefore, $La(TfO)_3$ may contribute to protonic conductivity. Recently, lanthanide triflates have been

widely investigated as solid polymer electrolytes in high performance battery because of their high Lewis acidity and coordination number [Silva et al., 1995]. Studies carried out on materials containing lanthanide salts have demonstrated that novel applications in the fields of flexible phosphors and solid state lasers may also be possible [Silva et al., 1998]. Silva et al., (1995) prepared solid polymer electrolytes from poly(ethylene oxide) and lanthanide triflates. They reported relatively high ionic conductivity for neodymium triflate as compared to the other lanthanide triflates. Further, they prepared polymer electrolytes for optical applications by the sol-gel method containing neodymium triflate and reported ionic conductivity of the composite membrane in the range of 10^{-5} S/cm [Silva et al., 1998]. ErTfO and NdTfO used in this work were obtained from Sigma Aldrich, USA. Figure 3.4 shows the chemical structure of the two inorganic triflates and the general properties are given in table 3.4.

(a) (b)

Fig.3.4 Chemical structure of (a) ErTfO, and (b) NdTfO

Table 3.4: General properties of ErTfO and NdTfO

Properties	Values	
	ErTfO	**NdTfO**
Molar mass	614.47 g/mol	591.45 g/mol
Appearance	Pink powder	Purple powder
Density	1.6 g/cm^3	1.7 g/cm^3
Coordination number	7-10	12
Boiling point	160 °C	162 °C
Solubility in water	Soluble	Soluble

3.1.3. *Size selective additive (Molecular sieve)*

Molecular sieve (MS) is the material containing tiny and uniform size pores, and is generally used as an adsorbent for gases and liquids. Molecular species smaller than the pores of MS pass through whereas others are retained. These size selective additives are usually crystalline and hydrophilic in nature. MS is relatively stable at high temperature and pressure environments, and shows good chemical stability [Malherbe, 2009]. Recently, several reports have demonstrated that some surface modified mesoporous molecular sieves may be employed as proton conducting solid materials, which are of great interest due to their potential applications in electrochemical devices such as batteries and fuel cells [Coutinho et al., 2005]. A molecular sieve can adsorb water up to 22% of its own weight, which is quite similar to nafion [Ramaswamy et al., 2013]. Thus considering the size selective nature, the MS was used as an additive for nafion

modification. MS may be classified based on the pore size such as 3A, with pore size 3 Å; 4A, with pore size 4 Å; 5A, with pore size 5 Å; 10×, with pore size 8 Å; and 13×, with pore size 10 Å and accordingly, the MS has varied applications.

In the present work, 3A MS was procured from Merck, India. The molecular formula of 3A MS is $0.4K_2O:0.6Na_2OAl_2O_3:2.OSiO_2:24.5H_2O$. 3A MS was selected as the additive for the nafion modification due to the following reasons: pore size (3 Å) has smaller diameter than that of methanol (4.4 Å) and is expected to play a role as size-selective barrier, and hygroscopic nature is expected to assist in proton conductivity. It has been anticipated that both methanol and the water will be adsorbed strongly to the molecular sieve in the composite membranes, the size of water being less than the pore size of MS will adsorb to the surface area within the pores and might create larger resistance to methanol molecule to pass through. Thus, water (1.93 Å) will enter the 3Å pore size of the additive, while methanol (4.4 Å) will largely be excluded [Nadykto and Yu, 2003, Chiou et al., 2009]. The 3A MS used in the study was ground to obtain fine particles. The grounded MS was used to synthesize the nafion composite membrane. Chemical structure of MS is shown in fig.3.5 and the general properties of the 3A MS is given in table 3.5.

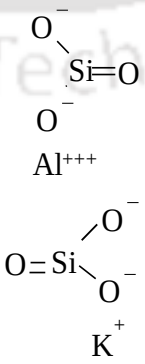

Fig.3.5 Chemical structure of MS

Table 3.5: General properties of 3A MS

Properties	Values
Molar mass	697.23 g/mol
Appearance	Beige or light tan
Bulk density	760 g/cm^3
Melting point	> 600 °C
Solubility in water	Insoluble
Pore diameter	3Å

Nafion dispersion (5 wt.%) and poly tetra fluoro ethylene (PTFE) dispersion (40 wt.%), were purchased from DuPont, USA. Dimethylformamide (DMF) was purchased from Merck, India. Methanol, HCl, NaOH, isopropyl alcohol, H_2O_2, and H_2SO_4 were procured from Merck, India. Pt (40%) and Pt/Ru (40/20) were purchased from Electrochem. Inc. (USA). Carbon paper was purchased from Toray. All the chemicals in the study were used without further purification and de-ionized water was used in all the experiments.

3.2 Synthesis of membrane

3.2.1 *Pure cast nafion membrane*

The nafion membrane was prepared using nafion dispersion (5 wt%). In order to synthesize the nafion membrane, a measured amount of the dispersion was first dried in a petridish at 30 °C. The obtained dried nafion residue was then solubilized in dimethyl formamide to obtain nafion solution. The nafion solution was used to cast the nafion membrane in a petridish using a well aligned oven to get a uniform film of definite

thickness. The temperature of the oven was kept at 165 °C [Silva et al., 2005]. The membrane synthesis process is described in fig. 3.6. The membrane thus prepared is now referred to as pure cast nafion membrane.

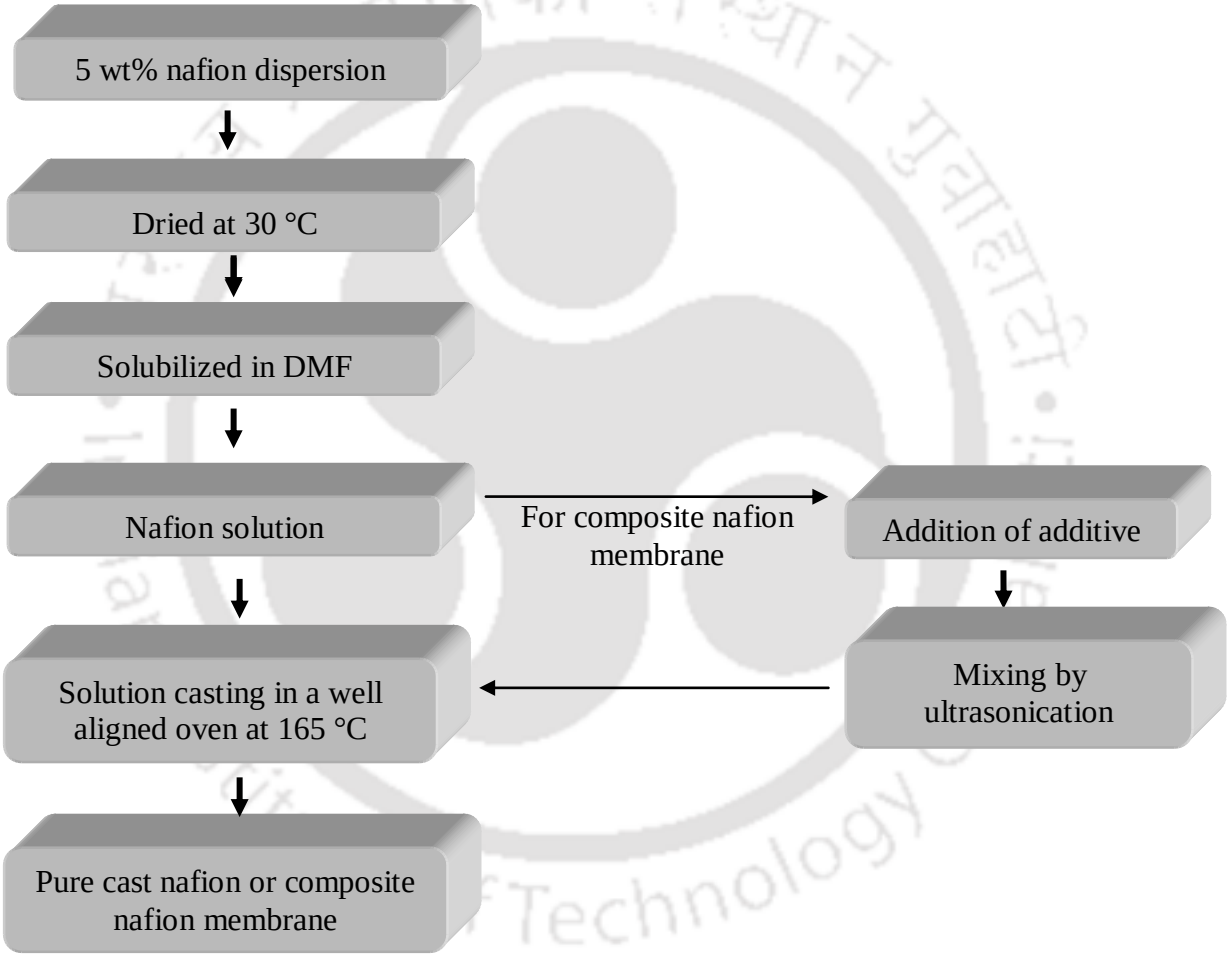

Fig. 3.6 Schematic of membrane preparation process

3.2.2 *Composite nafion membrane*

Block diagram in the fig. 3.6 describes solution casting process for synthesis of composite nafion membrane by addition of the additive in the nafion solution. The nafion solution and the additive were thoroughly mixed to get a homogeneous dispersion of additive in the nafion solution using ultrasonication. The obtained mixture was then solution cast in a similar way as pure cast nafion membrane so as to get the composite nafion membrane.

3.3 Treatment of membrane

The synthesized membrane obtained in the above process was chemically treated using conventional method before any characterization or application [Zawodzinski et al., 1993]. Block diagram for the membrane treatment process is given in fig. 3.7. The membrane was rinsed with distilled water and kept in 3% H_2O_2 solution at 80 °C for 2h to remove any trace organic impurity. The membrane was taken out, rinsed and then immersed in distilled water maintained at 80 °C for 2h for removal of excess H_2O_2. Thereafter, the membrane was kept in 0.5 M H_2SO_4 solution maintained at 80 °C in order to convert the sulphonic side chains to the acid form, $SO_3^-H^+$. Excess H_2SO_4 was removed from the membrane by thoroughly rinsing with distilled water followed by immersion in water maintained at 80 °C for 2h to remove any remaining free acid. Finally, the membranes were stored in 18 MΩ water at ambient temperature. All the properties of the membrane were evaluated at 30 °C, unless otherwise mentioned. The additive loading is reported in terms of weight percentage.

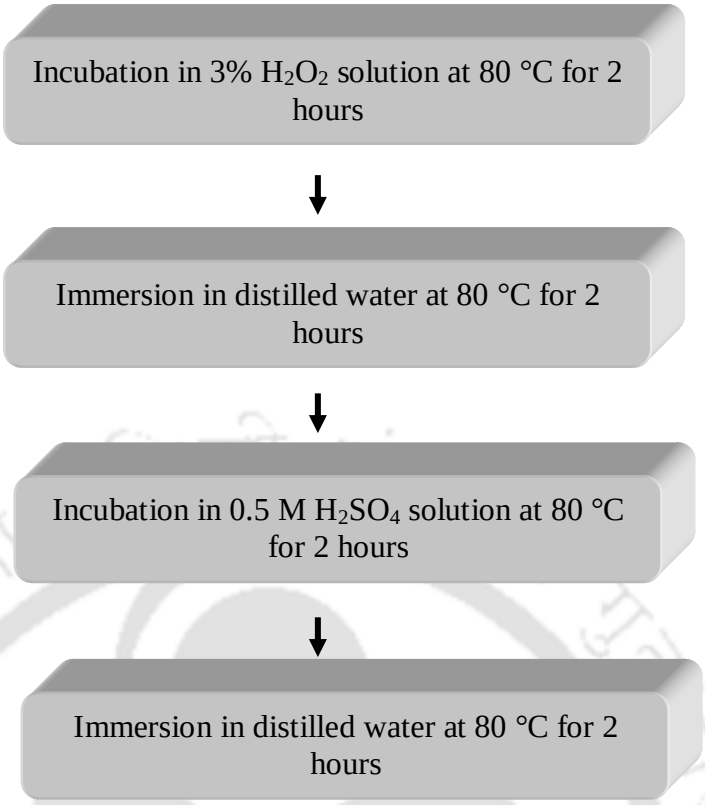

Fig.3.7 Schematic of membrane treatment process

3.4 Characterizations

The additives used for the synthesis of the composite nafion membranes were studied for morphological analysis using particle size analyzer, X-ray diffraction (XRD), BET surface area analyzer, and Scanning electron microscope (SEM). The developed composite nafion membranes were characterized under ex-situ conditions by SEM, for thickness, XRD, Thermogravimetric analysis (TGA), Fourier transform infrared (FTIR) spectrometer analysis, ion exchange capacity (IEC), water uptake, methanol uptake, swelling, tensile strength, oxidative stability, proton conductivity, and methanol crossover. Once the membrane was thoroughly characterized ex-situ, the membrane was used in the direct methanol fuel cell (in-situ characterization) to evaluate the performance of the fuel cell. The detailed procedure for the fabrication of the membrane electrode assembly (MEA) and characteristics of the fuel cell is provided in the relevant sections.

The following subsection describes the various techniques used for the additive characterization.

3.4.1 *Characterization of additives*

3.4.1.1 *Particle size analysis*

Particle size analyses of TiO_2, Nd_2O_3, talc, and MS were carried out in a laser particle size analyzer (make: Malvern Instruments; model: MASTERSIZER 2000) by dispersing the sample in water using ultra sonication. The instrument was corrected for background correction prior to the particle size analysis. The particle size analyses of ErTfO and NdTfO were not conducted as these additives get dissolved by ionizing in the nafion solution.

3.4.1.2 *X-ray diffraction (XRD) analysis*

X-ray diffraction (XRD) analyses of the additives were carried out in an advanced diffractometer (make: Brucker; model: D8 Advanced X-ray diffractometer). The sample was kept over a slide, which was later fixed in the XRD analyzer. The X-ray guns in the XRD analyzer used a monochromatized Cu-Kα radiation. The wavelength of the Cu-Kα X-ray was approximately 1.54 Å at 40 kV and 40 mA. The XRD gun was swept from 5–80° with a step size of 0.05° and scan rate of 0.5/s.

3.4.1.3 *BET surface area analysis*

Surface area of the additives was measured in BET surface area analyzer (make: Beckman-Coulter; model: SA 3100) using nitrogen adsorption isotherm at 350 °C. The relative pressure used to obtain the BET area is in the range of 0.05–0.2 mm of Hg. Prior

to nitrogen purging, the sample was thoroughly de-gassed for 3 h at 300 °C to remove any moisture or volatile content.

3.4.1.4 *Scanning electron microscopy (SEM) analysis*

Surface morphologies of the additives used in the study were evaluated using scanning electron microscope (make: LEO; model: 1430vp). The powder samples were mounted on a stub and subjected to gold coating to make them conductive for SEM analysis.

3.4.2 *Characterization of membrane*

The pure cast nafion membrane and the composite nafion membranes were characterized using SEM and XRD as discussed in the previous section. The details of the other characterization techniques are given below.

3.4.2.1. *Thickness analysis*

Membrane thickness was analyzed by using a screw gauge and confirmed by SEM analysis. Transverse sections of the membrane sample were mounted on a SEM stub and subjected to gold plating for making the sample conductive for thickness measurement using SEM. The thickness was measured at many locations and the measurements were repeated at least five times for each sample and the arithmetic mean is reported. The variations in the experimental values were in the range of ±7%. The thickness of the membrane was kept same for all the experiments, unless otherwise stated.

3.4.2.2. *Thermogravimetric analysis (TGA)*

Thermal behavior of the membrane was studied using thermogravimetric analyzer (make: Mettler Toledo; model: SDTA 851e). Approximately 5 mg of the membrane was cut into

very small pieces and taken in the alumina crucible of the analyzer. A heating rate of 10 °C/min was used in the range of 25-800 °C under nitrogen atmosphere to study the thermal behavior of the membrane.

3.4.2.3. Fourier transform infrared (FTIR) spectrometer analysis

The membranes were analyzed in a Fourier Transform Infrared (FTIR) spectrometer (make: Perkin–Elmer; model: Spectrum One Spectrometer) to identify the presence of functional groups. The transmission spectra of the membrane was recorded in a spectral range of 450-4000/cm at a resolution of 4/cm [Barbora et al., 2009].

3.4.2.4. *Ion exchange capacity*

The ion exchange capacity (IEC) of the membrane was determined by volumetric titration method. The membrane was immersed in 0.1N NaOH solution for 24 hours under continuous stirring. To assure complete ion exchange, the membrane was immersed again in another 0.1N NaOH solution for an additional 24 hour. In the process, H^+ from the sulphonic sites of the membrane were replaced by Na^+ using NaOH solution. The two solutions were then mixed and a sample was taken from the solution mixture. The sample was then titrated against 0.1N HCl solution using phenolphthalein as an indicator to determine the displaced H^+ ions present in the sample. The ion exchange capacity of the membrane, E (meq/g), was calculated using eq. (3.1), [Rhim et al., 2004; Barbora et al., 2009].

$$E(\text{meq/g}) = \frac{(V_{NaOH} N_{NaOH} - V_{HCl} N_{HCl})}{W_d} \tag{3.1}$$

where, V_{NaOH} and V_{HCl} are the volumes (in ml) of NaOH and HCl solutions, respectively, used in the titration. N_{NaOH} and N_{HCl} are the normalities of NaOH and HCl solutions. W_d is the weight of the dry membrane in gram.

3.4.2.5. *Water and methanol uptake*

Water uptake of the membrane was evaluated by suspending a dry membrane sample of known weight in de-ionized water for 24 hours. Thereafter, the membrane was removed from the water and the excess surface water was quickly wiped off from both the surfaces. The weight of the wet membrane sample was measured and the water uptake of the membrane was calculated by eq. (3.2),

$$Water\ uptake = \frac{(W_w - W_d)100}{W_d} \tag{3.2}$$

where, W_w and W_d are the weights of wet and dry membranes, respectively. The similar method was performed to estimate the methanol uptake [Barbora et al., 2009].

The methanol uptake was measured by the similar method except three different molar concentration of aqueous methanol solution (0.5 M, 1 M, 2 M) was used in place of pure de-ionized water. The measurement was repeated at least five times and the arithmetic mean is reported. The variations in the experimental values were in the range of ± 5%.

3.4.2.6 *Swelling*

The swelling of the membrane (3 cm^2) was determined by measuring changes of the membrane length upon equilibrating the membrane in water or methanol solution at room

temperature [Satterfield et al., 2006]. Determination of linear expansion is an effective method to interpret the swelling [Affoune et al., 2005]. Therefore, the linear expansion factor (L%) was calculated using eq. (3.3),

$$L(\%) = \frac{(L_w - L_d)100}{L_d} \tag{3.3}$$

where, L_w and L_d are the lengths of wet and dry membranes, respectively.

The measurements were repeated at least five times for each sample and the arithmetic mean is reported. The variations in the experimental values were in the range of ± 5%.

3.4.2.7 *Tensile strength*

The membrane was cut into ASTM (D-638) standard dog-bone samples with a gauge length of 2.2 cm and a width of 0.5 cm [Satterfield et al., 2006]. The tensile strength of the dry membrane was examined under ambient conditions using a universal tensile tester.

3.4.2.8 *Oxidative stability*

The oxidative stability was characterized by immersing membrane in a 3% H_2O_2 solution at 80 °C and measuring the weight of the membrane over a period of time [Fu et al., 2008; Barbora et al., 2010]. The membrane was cut in a size of 1 cm × 4 cm and immersed in the solution. The membrane was taken out at an interval of 24 hours and its weight was measured after the excess surface water was wiped off from both the surfaces. The study was conducted for 30 days. The variation in membrane weight with time was evaluated

for the oxidative stability and reported as degradation rate (percent change in weight/day). The error in the measurement was within ±3%.

3.4.2.9 *Proton conductivity*

Through-plane proton conductivity of the membrane was determined in a conductivity cell shown in fig. 3.8 [Barbora et al., 2009]. The conductivity cell was fabricated using perspex. Two cylinders of 3.2 cm internal diameter and 30 cm length were taken. A perspex flange was attached to one end of each of the cylinders. The other ends were sealed by the teflon blocks. Silicon gasket was used in between the flanges. Both the cylindrical compartments have the arrangements to fix various electrodes as well as stirrer as shown in fig. 3.8. These arrangements were also used to pour the solutions into the cell compartments.

The conductivity was measured at 30 ^{o}C by AC impedance technique over a frequency range of 10 kHz to 100 mHz using a potentiostat (Autolab, PGSTAT 302N) [Barbora et al., 2010]. The proton conductivity measurements were performed after hydrating the membrane in de-ionized water for 24 hours. The membrane was fixed between flanges of the two chambers of the conductivity cell. A platinum foil electrode (0.25 cm^2) was placed in one of the chambers, facing the membrane. The electrode was marked as the working electrode. Another platinum foil electrode (0.25 cm^2) was placed in the other chamber facing the membrane, which was marked as the counter electrode. Both of these two electrodes were kept near to the membrane. A third electrode (reference electrode) was placed in the chamber where the working electrode was kept. The reference electrode was kept very near to the working electrode. Chamber A of the cell was filled with 0.25 M of H_2SO_4 solution, whilst chamber B was filled with distilled water. Proper mixing of

the solution in the chambers was done all the time in order to increase the mass transfer to the electrode. The proton conductivity of the membrane, σ (S/cm), was calculated using eq. (3.4) after background correction for each measurement [Barbora et al., 2010],

$$\sigma = \frac{L}{RA} \tag{3.4}$$

where *L*, *R*, and *A* denote the distance between the electrodes (cm), the measured resistance (ohm), and the area of the membrane (cm^2) perpendicular to proton flow, respectively.

3.4.2.10 *Methanol crossover (MCO)*

MCO through the membrane was investigated in the two chamber cell discussed in the section 3.4.2.9. The membrane was placed between flanges separating the two chambers of the MCO cell. Chamber A of the cell was filled with methanol of known concentration (1, 2, 3 and 4 M) in 0.5 M sulfuric acid, while chamber B was filled with the 0.5 M sulfuric acid only. The MCO through the membrane was measured by chronoamperometric method using a Potentiostat/Galvanostat (Autolab, PGSTAT 302N) [Offer et al., 2008].

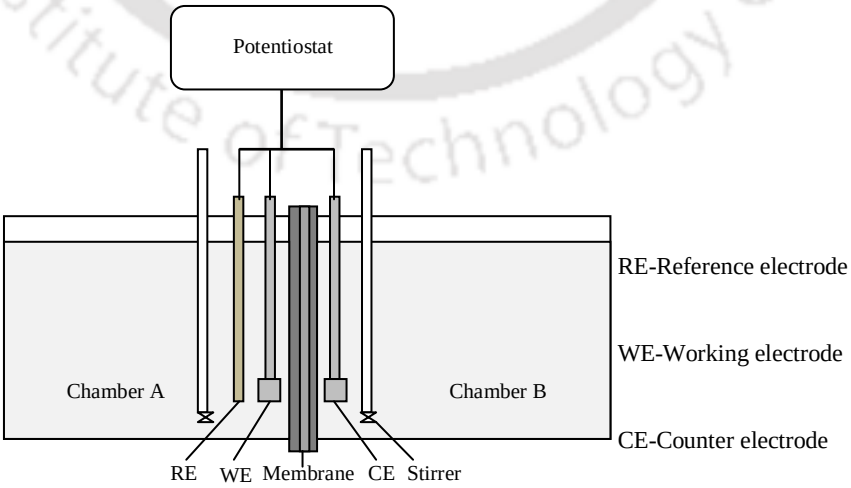

Fig.3.8 Schematic of the two chambered cell for measurement of proton conductivity and MCO

To determine the methanol crossover, the chamber containing only the dilute sulphuric acid was stirred continuously and the methanol concentration was measured in this chamber at regular intervals. The methanol permeability (ρ) reported as MCO was obtained using the following relationship (eq. 3.5) [Barbora et al., 2009].

$$C_B = \frac{A\rho C_A t}{V_B l} \tag{3.5}$$

where, C_A is the initial methanol concentration (mol/L); C_B is the methanol concentration (mol/L) in the second compartment at time t (sec); V_B is the volume of electrolyte solution in the second compartment (cm^3); l is the thickness of the membrane (cm); and A is the exposed area of the membrane (cm^2).

3.4.2.11 *Selectivity*

The polymer electrolyte membrane for DMFC applications ought to have the lowest MCO and highest proton conductivity possible [Rhim et al., 2004]. Thus a relationship between the MCO and proton conductivity is an important factor in evaluating membrane potential for DMFC application. This relationship is expressed as the selectivity [Tricoli, 1998], ϕ, and is calculated by using eq. (3.6),

$$\phi = \frac{\sigma}{\rho} \tag{3.6}$$

where, σ is the proton conductivity (S/cm) and ρ is the methanol crossover (cm^2/s) of the membrane.

3.5 Fuel cell testing

The synthesized membranes were tested in a direct methanol fuel cell (DMFC) developed in the laboratory. The fuel cell was used to study and compare the *I-V* performance of the membranes as discussed in the subsequent sections.

3.5.1 *Fabrication of MEA*

Porous carbon paper or GDL (TGP-H-120) from Toray, USA, was used as support for the microporous layers as well as for anode and cathode catalysts of the DMFC. Microporous layer was developed on the carbon paper by depositing a thin carbon layer with the help of a spray gun. The microporous layer on the anode side was kept hydrophilic and for the cathode side it was made hydrophobic [Li et al., 2009; Wang et al., 2011]. The hydrophilic microporous layer (MPL) at the anode comprised of Vulcan XC72 grade carbon black and 5 wt.% nafion ionomer. On the other hand, the hydrophobic microporous layer for the cathode side was prepared by using 40 wt.% PTFE along with the carbon black [Alcaide et al., 2009]. The carbon loading in MPL for both the anode and cathode was maintained at 1 mg/cm^2. The prepared slurry of MPL was then sprayed uniformly over the respective carbon papers at a temperature of 110 °C. The anode electrode was dried at 135 °C for 30 minutes. However, the cathode electrode containing PTFE was sintered at a temperature step of 110 °C, 280 °C, and 360 °C, each for 30 min [Easton, 2003; Lindermeir et al., 2004]. Sintering allows the PTFE to form an evenly distributed gas/liquid diffusion network.

MPL over the carbon paper worked as a support for the electrode catalysts. Catalyst slurry was prepared by mixing isopropyl alcohol and the nafion dispersion with 40 wt% Pt/C for the cathode ink, and 60 wt.% Pt/Ru (2:1)/C for anode ink followed by sonication

for 20 min. The metal catalyst loading was maintained at 2 mg/cm^2 for both the electrodes. Nitrogen gas was used as a carrier gas for spraying the catalyst dispersion onto the MPL of the electrode. The electrodes with the catalyst layer were heat treated in an air oven for about 12 h at 80 °C to obtain the final electrodes.

The treated membrane as discussed in section 3.3 was then placed in between anode and cathode electrodes and the assembly was then hot pressed at 100 °C for 3 min under 70 kg/cm^2 pressure to obtain membrane electrode assembly. The MEA was then cooled to room temperature by setting a cooling time of 30 min in the hot press machine. Figure 3.9 shows the sequence of the different layers of MEA and a snapshot of a MEA. The final MEA was then ready to be tested in the DMFC. The details of the experimental setup of DMFC are given in the next section.

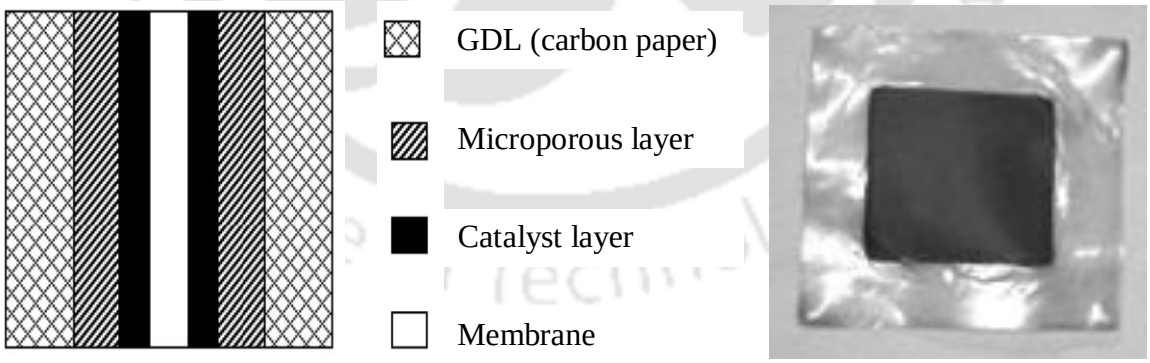

(a) (b)

Fig. 3.9 Schematic of (a) the developed MEA, and (b) its snapshot

3.5.2 *Fabrication of DMFC setup*

Direct methanol fuel cell hardware was developed and fabricated to study the performance of the composite nafion membrane in real environment of the direct methanol fuel cell. Two graphite plates were used to fabricate the monopolar plates or end plates and machined to deliver the reactants at anode and cathode. Figure 3.10 shows the picture of a machined graphite plate along with parallel channels and ribs and an assembly of single DMFC. The channels are connected to a supply-head at one end and outlet at other end so as the reactant can be fed in as well as the product and unreacted reactant can be taken out from the fuel cell. The ribs serve the purpose of collecting the electron from the anode and supplying them to the cathode via the external circuit. The electrons collected by the ribs at anode migrate to the gold plated terminal attached at the anode monopolar plate. Similarly, the electrons that are transported to the cathode via the external circuit and reaching to the cathode are first received by the gold plated terminal attached at the cathode monopolar plate then transported to the ribs. One of such graphite plates with flow arrangement along with the gold plated terminals can be seen in the fig.3.10a. The developed membrane electrode assembly (MEA), as described in section 3.5.1, was sandwiched between these two aligned graphite monopolar plates. Temperature controlled silicon heating pads were attached on the opposite faces of the plates as shown in the fig. 3.10b. Two stainless steel plates were used to integrate the full assembly using tie rods. It can also be seen in the fig.3.10b that teflon sheets and teflon/rubber sleeves were used to make the fuel cell isolated for any short-circuiting. The DMFC was checked for any short-circuiting as well as leakage of any of the reactants.

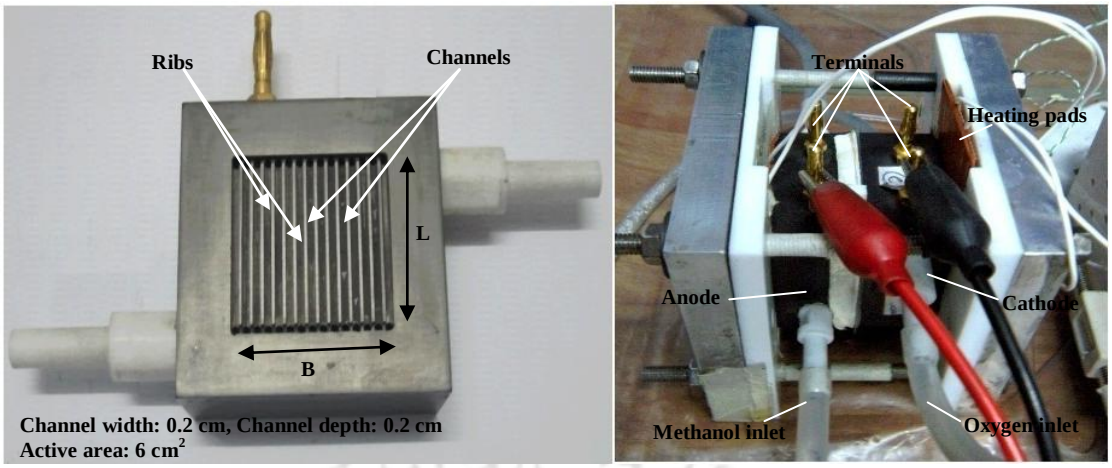

(a) (b)

Fig. 3.10 Snapshot of (a) a machined graphite plate along with parallel channels and ribs, (b) DMFC assembly

3.5.3 *Performance evaluation of DMFC*

The developed MEA was sandwiched between two similar monopolar plates and tested for *I-V* performance of the fuel cell. The methanol solution kept on a heating mantle to maintain the desired temperature of the solution was fed to the anode side, whereas oxygen was fed to the cathode side of the DMFC cell. For conducting experiments above ambient temperature, the methanol solution was kept on a heating mantle to maintain the desired temperature, and the methanol tank as well the carrier tubes were insulated with aluminum coated glass wool sheets to prevent heat loss. The flow rate of methanol was maintained with the help of a peristaltic pump whereas oxygen flow rate was maintained with the help of a rotameter. The methanol and oxygen flow rates were maintained at 0.5 mL/min and 0.7 L/min, respectively. The temperature of the fuel cell was controlled with the help of two silicon heating pads, connected to a digital temperature controller. The heating pads were attached in between the graphite plate and stainless steel casing. The output current and voltage across the cell was monitored with the help of two high

precision digital multimeters (make: Sanwa, model: PC 5000). Prior to evaluating the performance, the fuel cell was activated by circulating the methanol solution at the desired temperature till obtaining a constant open circuit voltage (OCV). Thereafter, the circuit was closed with a rheostat for providing variable load to obtain resulting current and cell voltage from the fuel cell. The *I-V* performance of the fuel cell using the developed membranes was recorded at various methanol concentrations as well as at different operating temperatures.

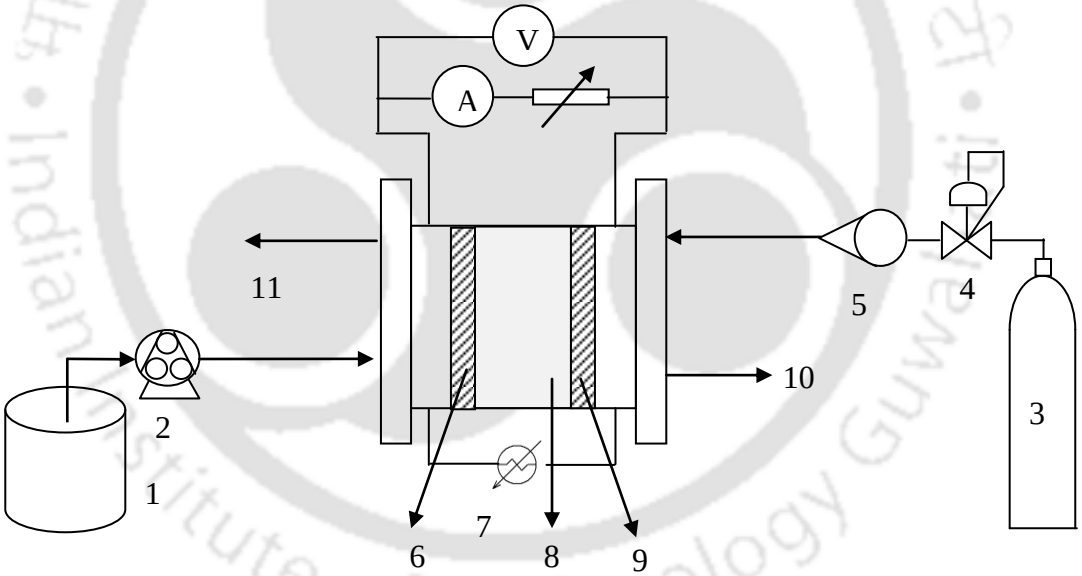

1) Methanol tank, 2) Peristaltic pump, 3) O_2 cylinder, 4) Pressure regulator, 5) Rotameter, 6) Anode, 7) Heater, 8) Membrane, 9) Cathode, 10) Cathode outlet, 11) Anode outlet

Fig. 3.11 Schematic of the DMFC experimental set-up

Chapter 4

Results and Discussion

Chapter 4: Results and Discussion

The additives and the developed composite nafion membranes have been characterized by various techniques. Details of the procedure used for characterization of the additives and the developed membranes have been described in the previous chapter. In this chapter, the characterization results obtained by various techniques are analyzed and discussed.

4.1 Characterization of additives

4.1.1. *Particle size analysis*

The particle size of a powder affects its dispersions and consequently contributes to the property of the composite membrane containing the powder. The particle size analyses of the additives (TiO_2, Nd_2O_3, talc, and MS) were performed as per the methodology described in section 3.4.1.1. Table 4.1 shows the volume median diameter [D(v,0.5)] for the additives. The particle size of ErTfO and NdTfO are not reported as these additives dissolve into the nafion solution. Amongst TiO_2, Nd_2O_3, and talc the D(v,0.5) of TiO_2 (21.30 µm) and talc (20.37 µm) are comparable. The D(v,0.5) of Nd_2O_3 (06.39 µm) is about one third than TiO_2 and talc, which may prove to be advantageous, as reduced size of the inorganic additives are crucial to the compatibility between the inorganic additive and nafion, which has significant effects on the properties of the composite membranes. It may be noted that the laser particle size analyzer was used for the study. Therefore, the aspect ratio may also come into consideration. The talc particles were flaky in nature as can be seen later in SEM image of the talc. The D(v,0.5) of MS (07.39 µm) particles is slightly greater than Nd_2O_3. Overall, it is observed that the results are in agreement with the SEM images of the particles (section 4.1.4).

Table 4.1 Volume median diameter [D(v,0.5)] for TiO_2, Nd_2O_3, talc, and MS

Additive	**D(v,0.5) (µm)**
TiO_2	21.30
Nd_2O_3	06.39
Talc	20.37
MS	07.39

4.1.2. *X-ray diffraction (XRD) analysis*

XRD analyses of the additives were performed to obtation information about the morphological properties, mainly to assess the phase identification of a crystalline material as it is an important parameter that would influence the physical properties of nafion composite. Figure 4.1 shows the XRD pattern of the six additives. The XRD pattern of TiO_2 shows strong diffraction peaks at 25°, 38.1° and 48°, which indicates that the TiO_2 is in anatase phase [Thamaphat et al., 2008; Wongkaew et al., 2010]. The XRD pattern of Nd_2O_3 shows sharp peaks at 15.81°, 27.78°, 28.70°, 30.73°, and 40.30°, which indicates the characteristic crystalline nature of the Nd_2O_3. The XRD pattern of talc shows sharp peak at 25.28° indicating the crystalline character of the talc. Similarly, for ErTfO a peak is observed at 8.07° in fig. 4.1, indicative of its crystalline nature. The XRD pattern of NdTfO shows two broad peaks at 6.20° and 14.80°, attributed to the amorphous nature of the NdTfO powder. Several sharp peaks are visible in the XRD profile of MS powder with the three major peaks at 23.36°, 26.49°, and 30.92°, which indicate that the MS is highly crystalline in nature.

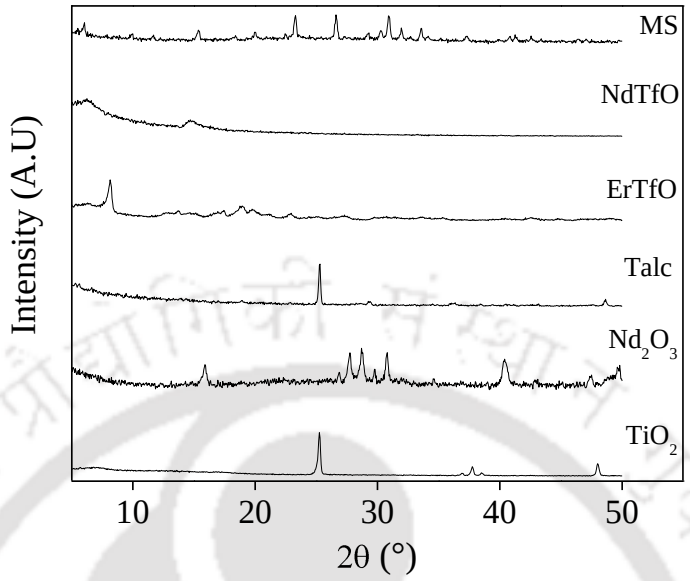

Fig.4.1 XRD profile of different additives

The crystal size of the additives was estimated using the Debye Scherrer equation (eq.4.1),

$$D = \kappa\lambda / \beta\cos\theta \tag{4.1}$$

where, λ is wavelength of the X-ray, κ is a constant taken as 0.9, θ is the diffraction angle, and β is the full width at half maxima (FWHM). The crystallite size of the additives derived from the XRD data (except NdTfO), are given in table 4.2. The crystallite size of NdTfO could not be obtained using Debye Scherrer equation due to absence of sharp peak.

4.1.3. *BET surface area analysis*

Apart from particle size and XRD analysis, surface area is a key physical parameter of the additive powder used for nafion modification. The BET surface area analyses of the additives

Table 4.2 Crystal size by Debye Scherrer equation

Additive	**Size (nm)**
Titanium dioxide (TiO_2)	34.65
Neodymium oxide (Nd_2O_3)	26.65 ± 8
Talc	36.08
Erbium triflate (ErTfO)	19.8
Molecular sieve (MS)	27.90 ± 3

were carried out as per the procedure described in section 3.4.1.3. The surface areas of the additives are reported in table 4.3. The BET surface areas are not in close agreement with the particle size analysis because particle size shown in table 4.1 is evaluated using laser particle analyzer.

4.1.4. *Scanning electron microscopy (SEM) analysis*

Figure 4.2 shows the SEM images of the TiO_2, Nd_2O_3, and talc particles. In fig. 4.2(a), the SEM image of TiO_2 particles can be seen as small irregular shaped particles. Because of their hydrophilic surface characteristics, TiO_2 powder is extremely sensitive to atmospheric conditions such as moisture and have tendency to agglomerate [Lin, 2006]. Thus, TiO_2 clusters are visible in the SEM image. Fig. 4.2(b) shows the SEM image of Nd_2O_3 particles. The Nd_2O_3 particles appear irregular shaped. Small as well as large agglomerates are also visible, which may be attributed to the hygroscopic nature of Nd_2O_3. The SEM image of talc

Table 4.3 BET surface area of the additives

Additive	**BET surface area (m^2/g)**
Titanium dioxide (TiO_2)	6.54
Neodymium oxide (Nd_2O_3)	5.71
Talc	3.07
Erbium triflate (ErTfO)	11.37
Neodymium triflate (NdTfO)	9.63
Molecular sieve (MS)	4.02

is shown in fig. 4.2(c). The talc appears as large, flaky and irregular shaped particles. Small and big flakes along with agglomeration are also visible.

Figure 4.3 shows the SEM image of ErTfO and NdTfO particles. The SEM image of ErTfO in fig. 4.3(a) appears to be white lumps of varying sizes. Fig. 4.3(b) shows the SEM image of NdTfO, which appear as loosely stacked sheets. Figure 4.4 shows the SEM image of MS particles. Well dispersed and uniformed size of the particles may be seen in the figure.

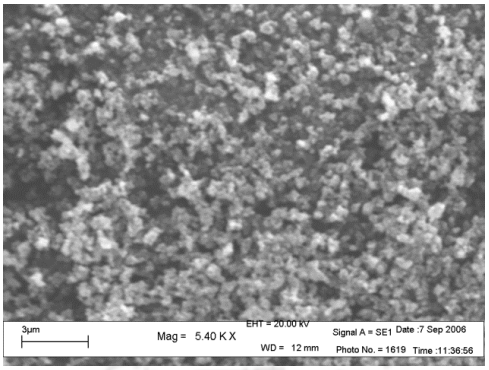

(a)

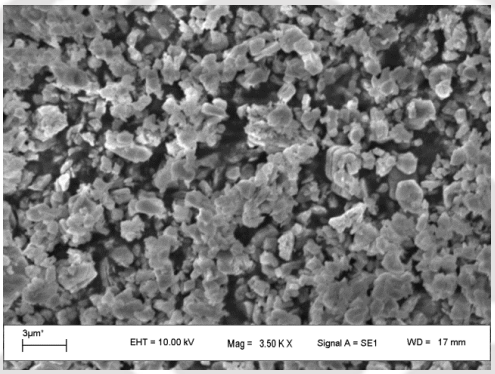

(b)

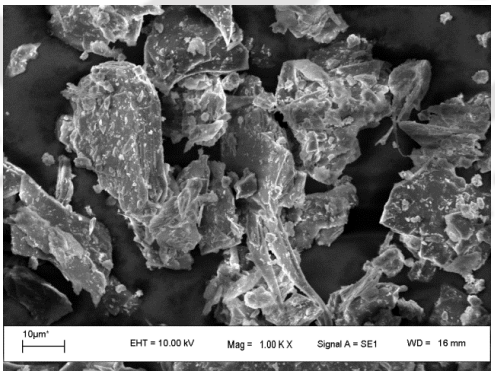

(c)

Fig.4.2 SEM image of (a) TiO_2, (b) Nd_2O_3, and (c) talc powder

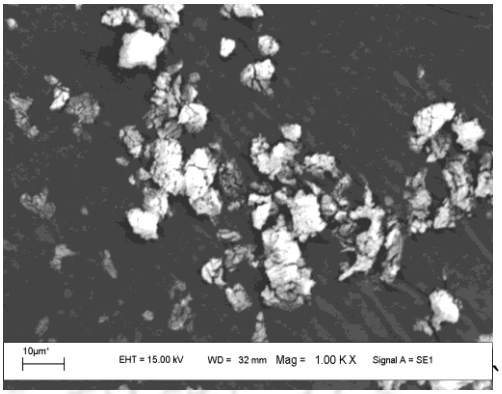

(a)

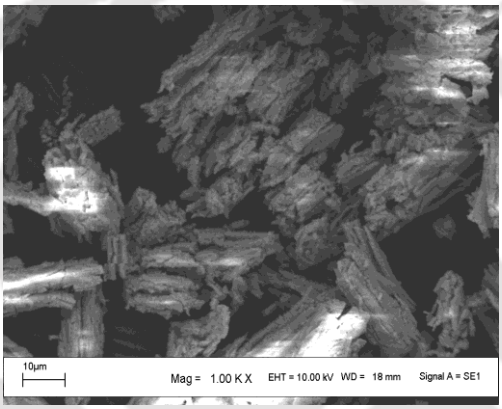

(b)

Fig.4.3 SEM image of (a) ErTfO, and (b) NdTfO powder

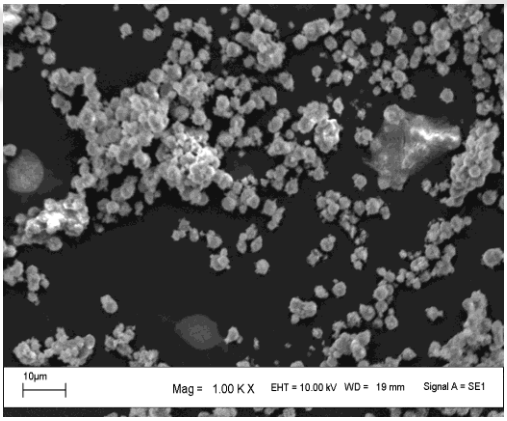

Fig.4.4 SEM image of MS powder

4.2 Characterization of membrane

4.2.1. *Scanning electron microscopy (SEM) analysis*

SEM images of the membranes were obtained for studying the surface morphology, for determination of membrane thickness (using SEM of membrane cross-section, not shown in figures), and for ascertaining the physical compatibility between nafion and the additives in the composite membranes. Figure 4.5 shows the SEM image of pure cast nafion membrane. The surface morphology of the nafion membrane appears uniform without formation of pores or cracks.

Figure 4.6 shows the SEM image of TiO_2/nafion composite membranes at varying loadings of TiO_2 ranging from 1% to 9%. Distribution of TiO_2 particles appear uniform and the distribution gets denser with increase in loading percentage. No pores or cracks are visible in the membranes. However, large agglomerates are visible in case of 7%, and 9% TiO_2/nafion membranes. Size of the agglomerates increases with increase in TiO_2 loading in the composite membrane.

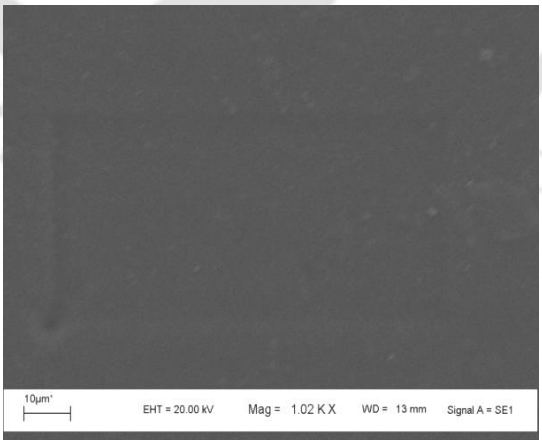

Fig.4.5 SEM image of pure cast nafion membrane

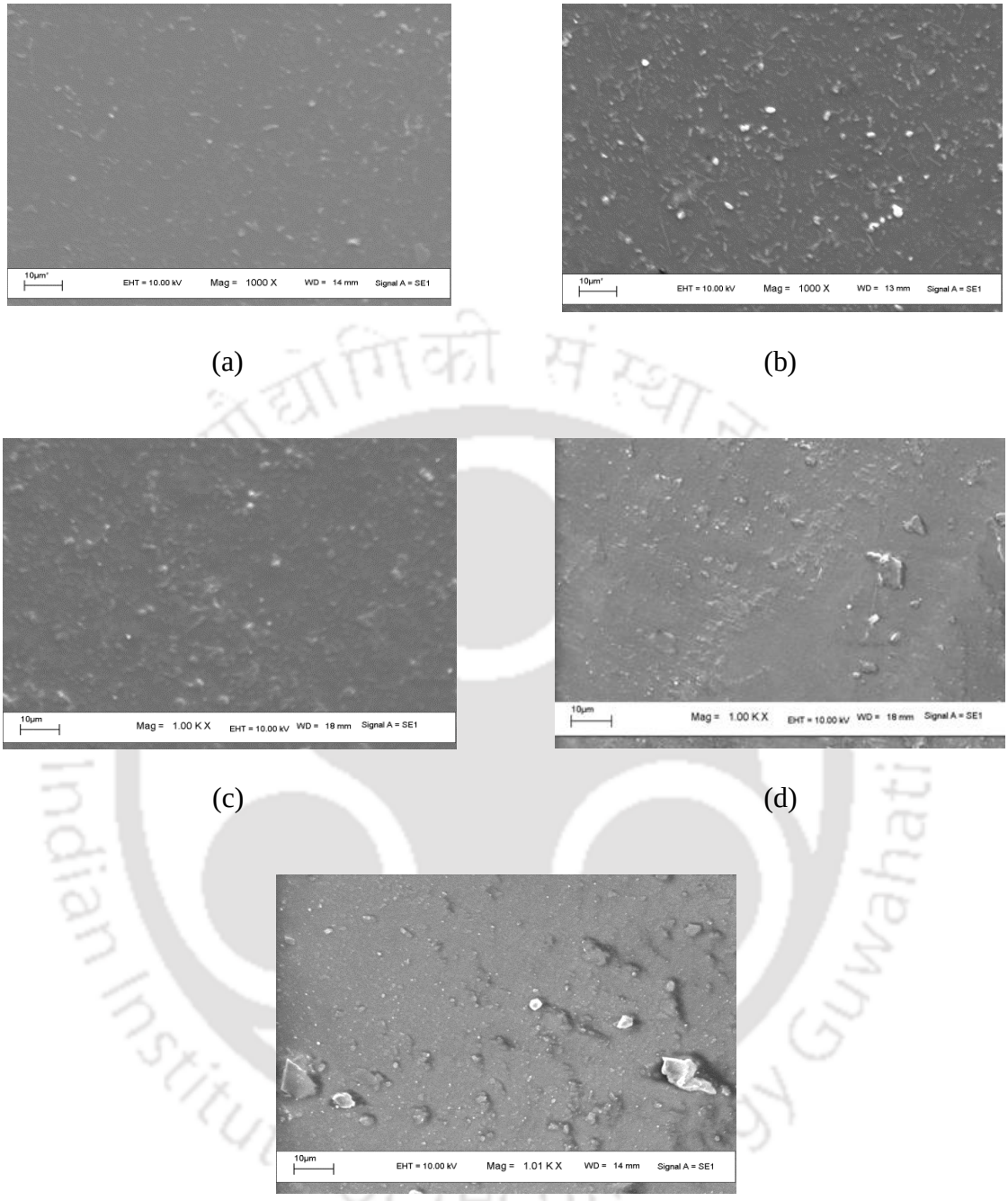

(a) (b)

(c) (d)

(e)

Fig.4.6 SEM image of (a) 1% TiO_2/nafion, (b) 3% TiO_2/nafion, (c) 5% TiO_2/nafion, (d) 7% TiO_2/nafion, and (e) 9% TiO_2/nafion composite membranes

Figure 4.7 shows the SEM images of Nd_2O_3/nafion composite membranes with varying loading of Nd_2O_3 from 1% to 9%. The Nd_2O_3 are uniformly distributed in the Nd_2O_3/nafion membranes for 1%, 3% and 5% Nd_2O_3 loadings. The distribution of Nd_2O_3 particles in the composite membranes appears uniform with no formation of pores or cracks in these composites. However, agglomerate formation can be seen in case of 7% and 9% Nd_2O_3/nafion composite membranes.

Figure 4.8 shows the SEM images of talc/nafion composite membranes with additive loading varying from 1% to 9%. The distribution of the talc particles gets denser with increase in talc loading. No crack or pore formation is visible. Small agglomerates can be seen in all the membranes.

The surface morphology of 1% ErTfO/nafion and 1% NdTfO/nafion composites is shown in fig. 4.9 and 4.10, respectively. The membranes appear smooth and uniform. There is no evidence of pore or crack formation. The similarity in appearance of these composites with pure cast nafion may be attributed to the ionization of the additives in the nafion cast solution and thus uniformity in nafion composite membranes without any appearance of the particles in the membranes. The increase in additive loading did not show any marked difference in surface morphology. Thus, the SEM images at other loadings of ErTfO and NdTfO are not shown here. However, the images may be seen in annexure A (figs. A.1 and A.2, respectively).

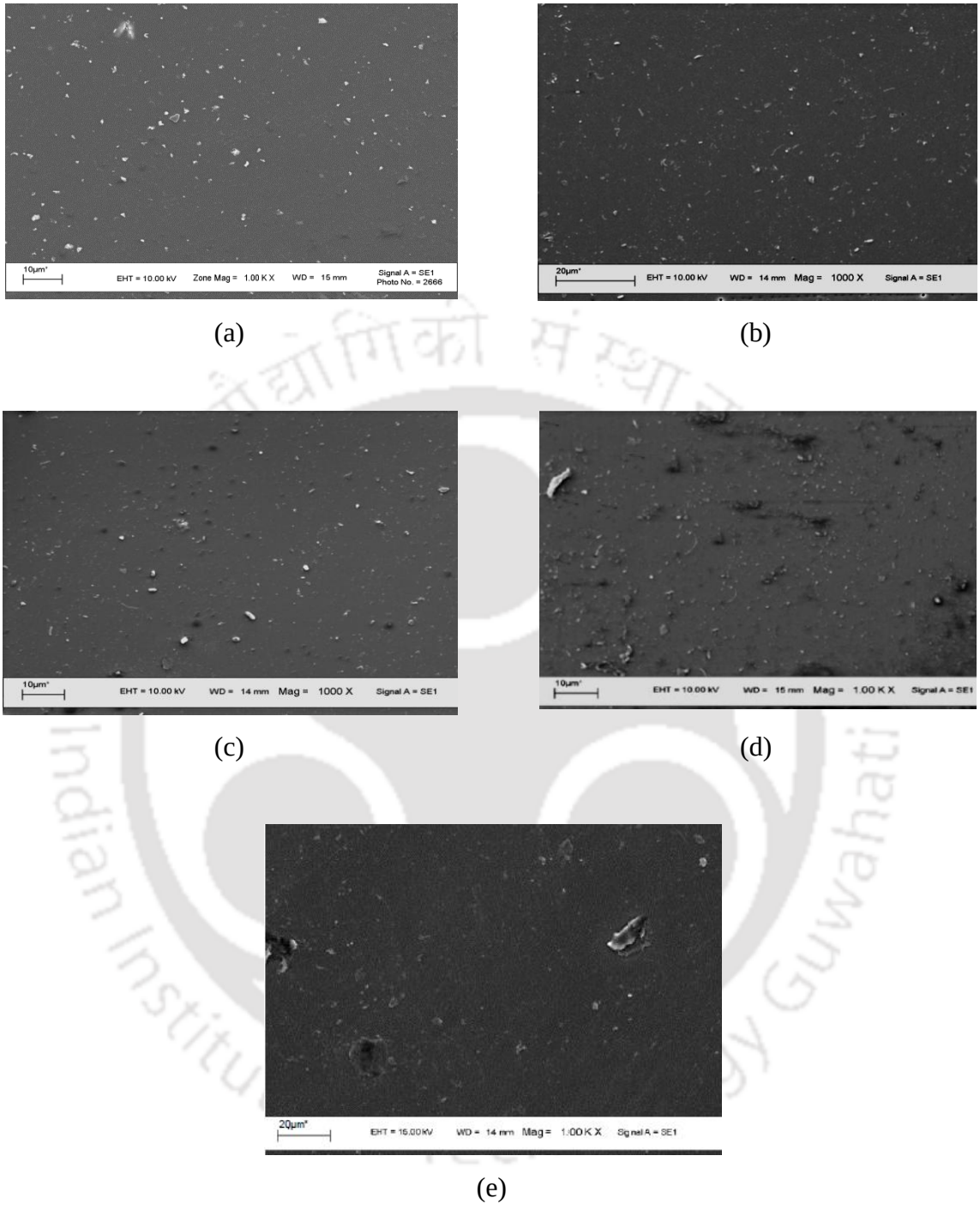

Fig.4.7 SEM image of (a) 1% Nd_2O_3/nafion, (b) 3% Nd_2O_3/nafion, (c) 5% Nd_2O_3/nafion, (d) 7% Nd_2O_3/nafion, and (e) 9% Nd_2O_3/nafion composite membranes

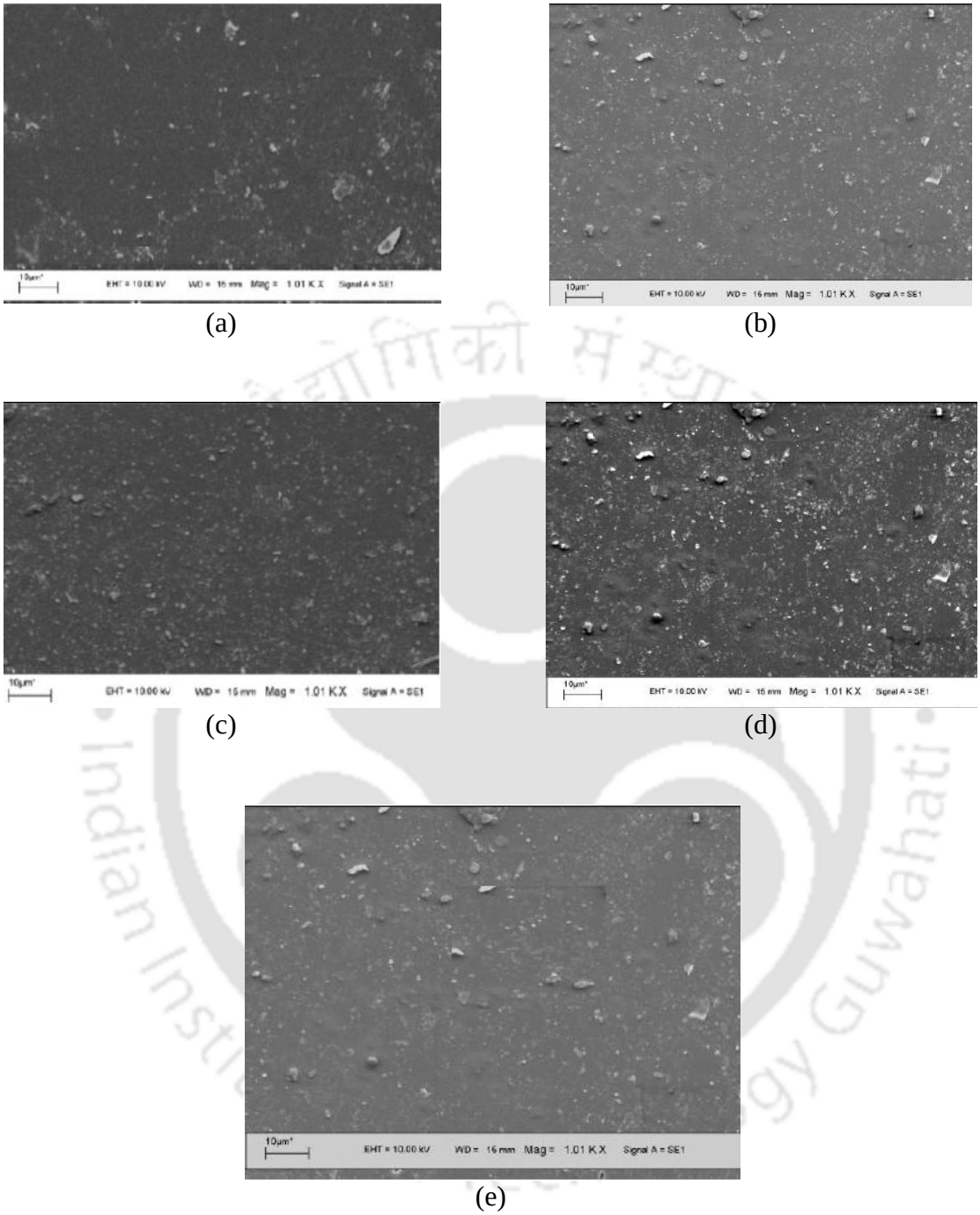

Fig.4.8 SEM image of (a) 1% talc/nafion, (b) 3% talc/nafion, (c) 5% talc/nafion, (d) 7% talc/nafion, and (e) 9% talc/nafion composite membranes

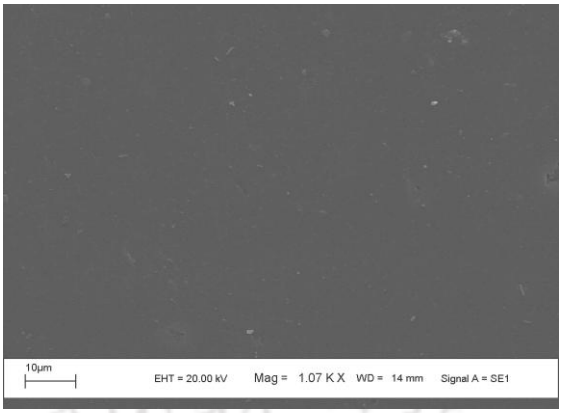

Fig.4.9 SEM image of 1% ErTfO/nafion composite membrane

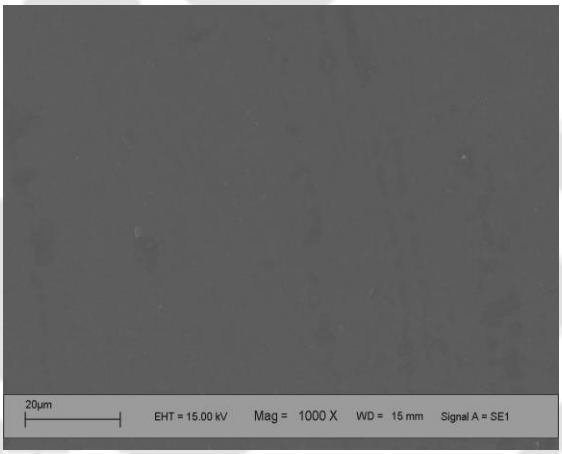

Fig.4.10 SEM image of 1% NdTfO/nafion composite membrane

Figure 4.11 shows the SEM images of MS/nafion composite membranes with additive loading varying from 1% to 9%. Small agglomerates are seen in case of the composite membranes with the loading of 1%, 3%, and 5% MS; large agglomerates are visible with MS loading of 7% and 9%. The surface morphology of the membranes does not appear uniform. Some wrinkles are also visible for 3%, 5%, and 7% MS/nafion composite membranes.

Membrane thickness was measured at several cross-sections of the nafion and composite nafion membrane samples. Increase in additive content did not significantly change the membrane thickness. Infact the average thickness of all the membranes were found to be between 65-70 µm with a maximum error of ±7%.

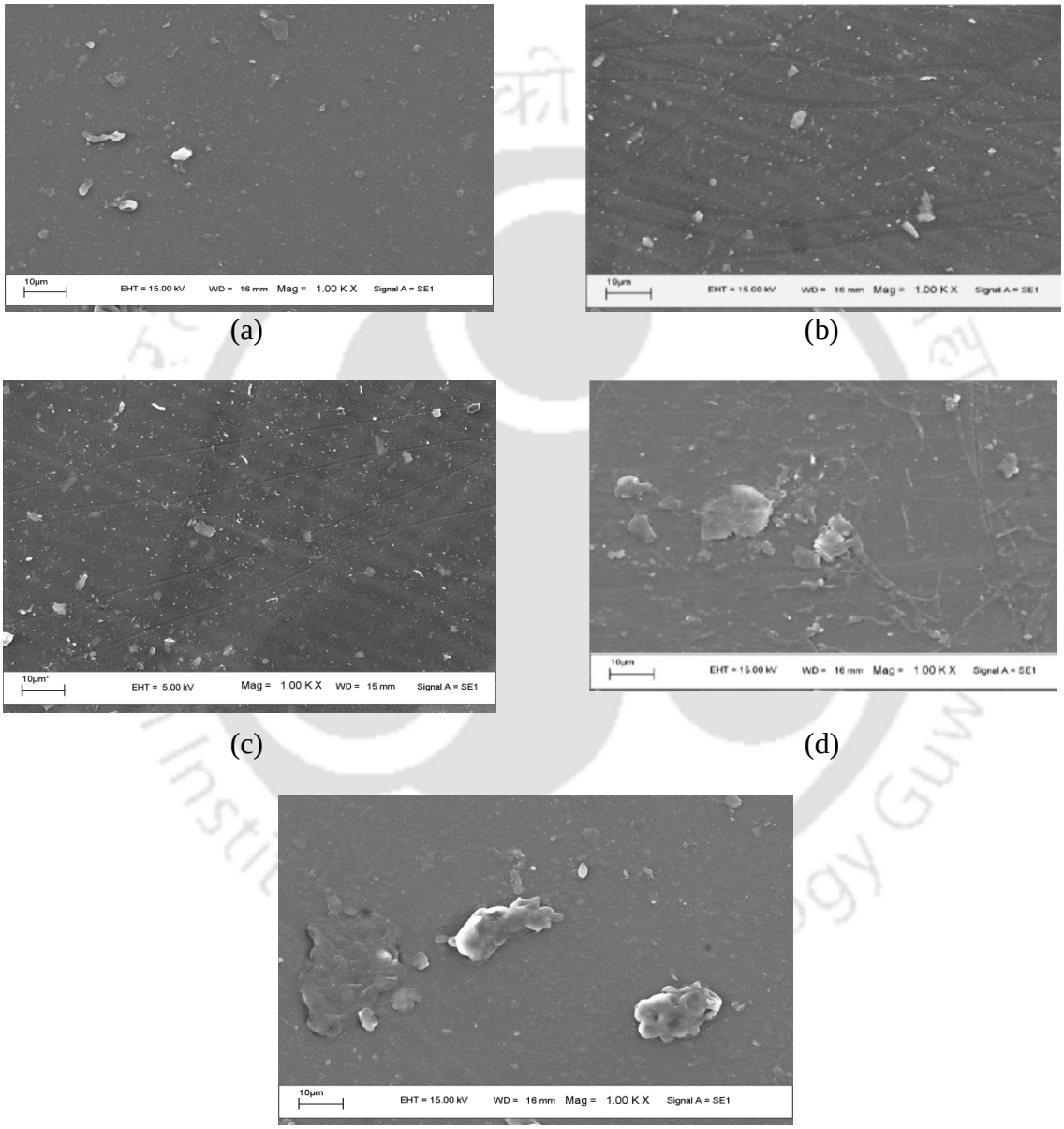

Fig.4.11 SEM image of (a) 1% MS/nafion, (b) 3% MS/nafion, (c) 5% MS/nafion, (d) 7% MS/nafion, and (e) 9% MS/nafion composite membranes

4.2.2. *X-ray diffraction (XRD) analysis*

Figure 4.12 shows the representative XRD patterns of pure cast nafion membrane and the additive/nafion composite membranes with 1% additive. The pure cast nafion membrane shows a broad peak at 14–18° (2θ). According to the literature [Dimitrova et al., 2002], this broad peak can be deconvoluted into two peaks, assigned to amorphous (2θ =16°) and crystalline (2θ = 17.5°) scattering from the polycarbon chains of nafion.

The XRD pattern of the TiO_2/nafion membrane shows the characteristic peak of anatase phase of TiO_2 at 2θ = 25°, 38.1°, and 48° indicating the presence of the TiO_2 in the nafion composite membranes [Barbora et al., 2009a; Wongkaew et al., 2010]. On comparing the XRD patterns of pure cast nafion and TiO_2/nafion membrane, it can be inferred that the crystallinity of the nafion membrane increased with the incorporation of TiO_2. However, the

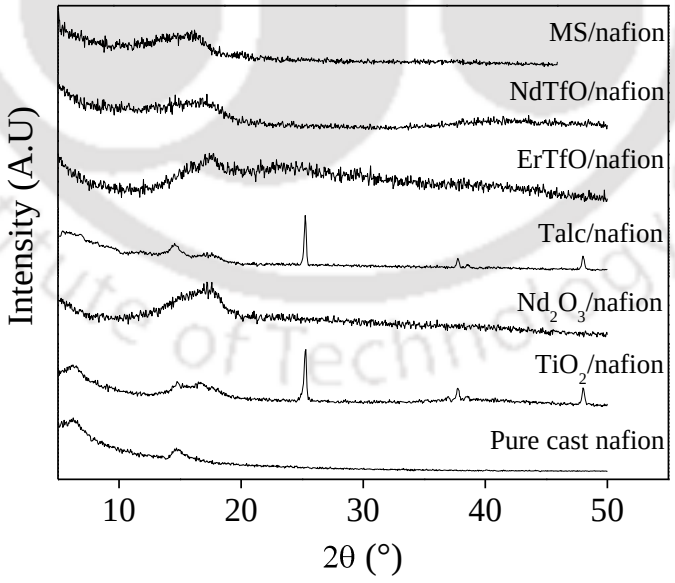

Fig.4.12 XRD profile of pure cast nafion and composite membrane with 1% additive loading

XRD pattern of Nd_2O_3/nafion membrane did not reveal the characteristic peaks of the Nd_2O_3. Moreover, the broad peak of nafion at 2θ = 14−18° is increased in the composite membrane, indicating some kind of interaction between nafion side chain and Nd_2O_3 particles [Jin et al., 2007; Barbora et al., 2010]. The XRD pattern of talc/nafion membrane shows the characteristic peak of talc powder at 2θ = 25.28° as well as the broad peaks of nafion between 14−18°. Thus the talc has contributed its crystallinity to the nafion composites. A peak at 38° is observed for talc/nafion membrane but is not seen in the XRD profile of talc powder (fig. 4.1). Similar peak from about 35° to about 38° has also been reported by Tseng et al., (2012) for sintered talc for blending of epoxy resin. During preparation of talc/nafion membranes by the casting technique, it was kept at 165 °C, which justifies the additional peak at 38° for the composite membrane.

The ErTfO/nafion membrane did not reveal the characteristic peaks of ErTfO, but rather exhibited very broad peak in the region of 2θ = 13-20°, which may be due to the involvement of the Er^{3+} ions of ErTfO in bond formation with the SO_3^- groups of nafion. Similar to ErTfO powder, the NdTfO/nafion membrane too did not reveal any sharp peak. The peak is rather broad compared to that of pure cast nafion membrane. Thus it may be inferred that incorporation of NdTfO has contributed its amorphous nature to the composite membrane [Shroti et al., 2011].

The XRD pattern of MS/nafion composite membrane can also be seen in fig. 4.12. The broad peak between 11° to 18° is attributed to the increase in the particle size of MS due to

agglomerate formation in the composite membranes [Ruslimie et al., 2010], which is also confirmed in the SEM images of MS/nafion membranes in fig. 4.11.

4.2.3. *Thermogravimetric analysis (TGA)*

TGA of the nafion composite membrane was conducted to evaluate the thermal stability of the membrane. Typically, the operating temperature of the DMFC is upto 80 °C. However, maximum temperature experienced by the membrane is 165 °C during synthesis process of the membrane (section 3.2). Therefore, TGA was conducted to know the thermal stability of the membrane atleast upto 200 °C. Figure 4.13 to 4.15 represents the thermograms of pure cast nafion membranes and different composite membrane at 1% loading of the additive. The trend of TGA for other loadings of the additives is same. Therefore, the TGA of the composites at all other loadings are shown in annexure A (figs A.3 to A.8).

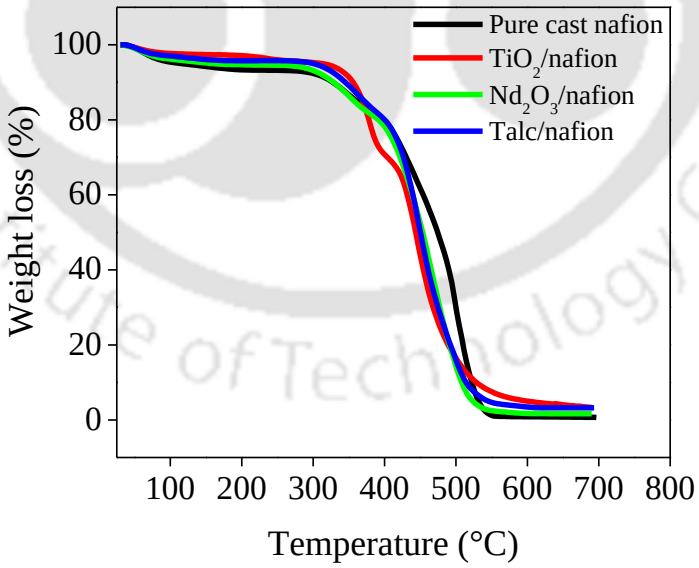

Fig. 4.13 Thermogram of pure cast nafion and composite membrane with 1% loading of TiO_2, Nd_2O_3, and talc

Figure 4.13 shows the TGA thermograms of pure cast nafion membrane and nafion composite membranes with 1% loading of TiO_2, Nd_2O_3, and talc. The initial weight loss upto 100 ºC is due to removal of residual water. The weight loss in the temperature range of 100−200 ºC corresponds to dehydration of the bound water in the membranes [Barbora et al., 2009a]. It can be seen that addition of TiO_2 or Nd_2O_3 or talc increases the bound water. It will be further confirmed by water uptake of the membranes in the subsequent section. However, it may be noted that when the temperature was in the range of 300-400 ºC the weight loss of the composite membrane was more as compared to pure cast nafion membrane, which is due to the decomposition of SO_3^- groups within the membranes [Babu et al., 2007; Barbora et al., 2010]. On further increase in the temperature, the weight loss increases drastically due to the degradation of the polymer main chain [Chen et al., 2006]. On comparison of the TGA thermograms, it is observed that all the membranes retain more than 90% of its weight up to a temperature of about 310 (±10) °C at which sulphonic groups detach from the polymer backbone. Beyond that the composite membranes start decomposing and loose weight quite rapidly. It can be seen that above 360 °C the degradation of the composite membrane is faster than the pure cast nafion membrane.

Figure 4.14 compares the TGA thermograms of 1% ErTfO/nafion and 1% NdTfO/nafion with pure cast nafion membrane. It can be seen in the figure that the thermograms of the nafion composites are almost similar to the pure cast nafion membrane with no noticeable change in thermal stability. However, above 440 °C onwards, degradation of the composite membrane was higher as compared to the pure cast nafion membrane.

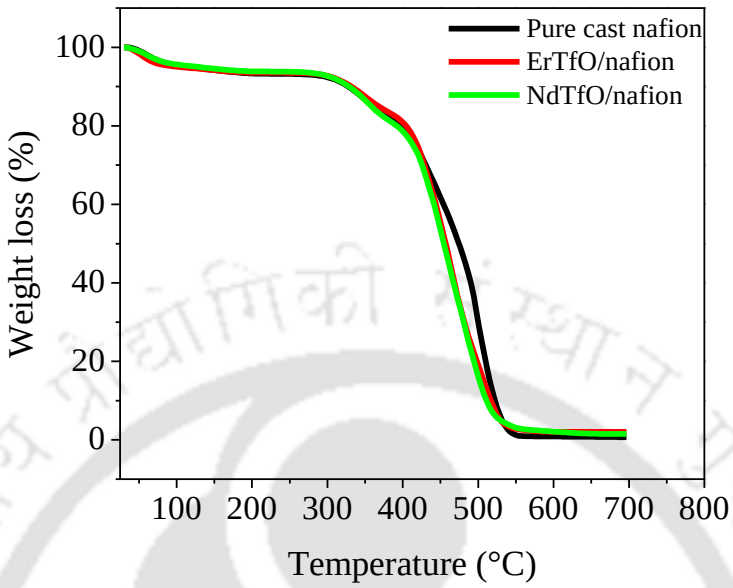

Fig. 4.14 Thermogram of pure cast nafion and composite membrane with 1% loading of ErTfO and NdTfO

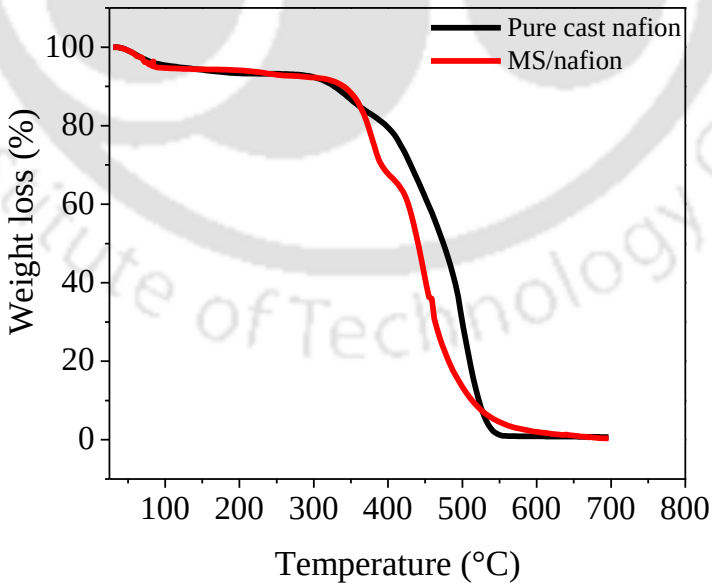

Fig. 4.15 Thermogram of pure cast nafion and composite membrane with 1% loading of MS

A similar trend of the thermal stability can be seen in the fig. 4.15 in which the thermograms of pure cast nafion membrane and 1% MS/nafion composite membranes are compared. The thermal stability trend was same for pure cast nafion and 1% MS/nafion composite membranes upto 360 °C. However, above 360 °C the thermal degradation of the composite was higher as compared to pure cast nafion membrane as well as other nafion composites (fig. 4.13 and fig. 4.14).

4.2.4. *Fourier transform infrared (FTIR) spectrometer analysis*

FTIR spectra were obtained to find out the changes in the structure of composite membranes on incorporation of the additive as compared to the pure cast nafion membrane. The FTIR spectra of pure cast nafion and nafion composite membranes are shown in figs. 4.16 to 4.18.

Figure 4.16 shows a comparison of the FTIR spectra of pure cast nafion membrane with that of TiO_2/nafion, Nd_2O_3/nafion, and talc/nafion membranes. The FTIR spectra of pure cast nafion shows five major bands, namely, SO_3^- or $-SO_3H$ band, C=O and C-O-C band, C-F band, band for H_2O bending, and a band for stretching vibration of water. The observations made for pure cast nafion and nafion composites for each type of band are discussed below.

The peaks at 518 and 633 cm^{-1} for the pure cast nafion membrane (fig. 4.16) may be assigned to SO_3^- and at 718 cm^{-1} to C=O bending [Kumutha and Alias, 2006]. A peak is observed at 982 cm^{-1} for the vibration of C-O-C bending in pure cast nafion membrane [Mahreni et al., 2009]. Similarly, the peak for the stretching vibration of SO_3^- is observed at 1055 cm^{-1}

[Ramani et al., 2005]. A band for water bending vibration occurs in the region 1400−2000 cm^{-1} [Park and Yamazaki, 2005] and the peak for stretching vibration of water molecules is obtained within 3200 and 3700 cm^{-1} [Ludvigsson et al., 2000]. It may be seen in the fig. 4.16 that the presence of TiO_2, Nd_2O_3, and talc in the nafion membrane show marked difference in the FTIR, when compared to pure cast nafion. The presence of TiO_2 and Nd_2O_3 additives led to a shift of some of the peaks of nafion membrane and also caused changes in the relative intensities. In case of TiO_2 additive, the peak for the stretching vibration of SO_3^- at 1055 cm^{-1} is shifted to 1067 cm^{-1}. These obvious changes suggest that an interaction exist between TiO_2 particles and nafion because titanium (a transition metal) has tendency to form coordination

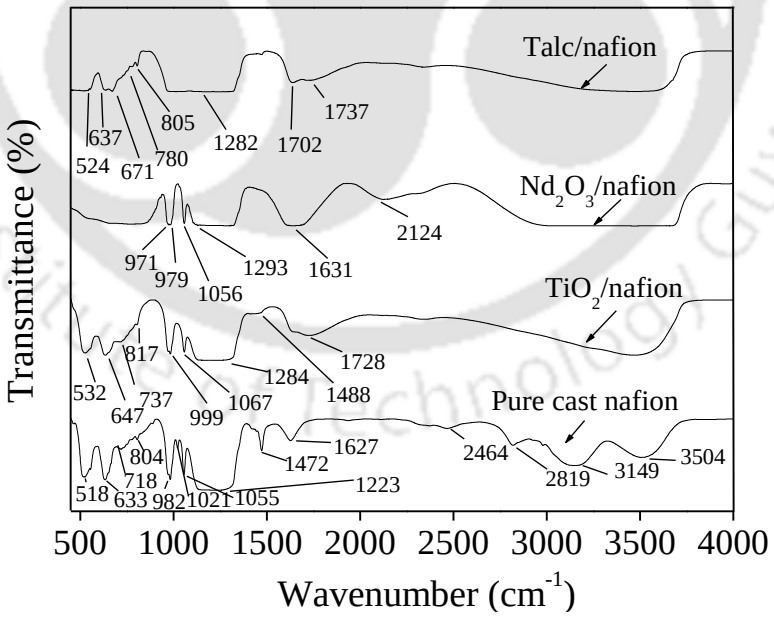

Fig. 4.16 FTIR spectra of pure cast nafion and composite membrane with 1% loading of TiO_2, Nd_2O_3, and talc

bond with sulphur atom of the sulphonic acid group in the nafion [Bian et al., 2007]. The peak between 800 and 465 cm^{-1} is broadened in case of TiO_2/nafion and may be assigned to the Ti–O–Ti stretching vibrations [Yeo et al., 2005] with a valley centered at 517 cm^{-1}. The broad band of Ti–OH can be observed below 3500 cm^{-1} indicating the existence of hydrogen bonding [Wu et al., 2006]. This interaction between the organic and inorganic phase is favorable for the improvement of the thermal stability [Wu et al., 2006]. A broad band for water bending vibration in the region 1400–2000 cm^{-1} is assigned to the bending modes of hydroxyl group of TiO_2 [Park and Yamazaki, 2005]. The broad peak for stretching vibration of water molecules within 3200 and 3700 cm^{-1} [Ludvigsson et al., 2000] is assigned to the stretching mode of the hydroxyl groups of TiO_2. Altogether both indicate increased water content in the nafion composite membrane.

Shifting of peaks could also be observed in fig. 4.16 for the Nd_2O_3/nafion membrane due to the presence of the inorganic moiety [Barbora et al., 2010]. A broad peak compared to that of pure cast nafion is observed from 500 to 800 cm^{-1} for the Nd_2O_3/nafion membrane. The vibration of C−O−C bending for pure cast nafion membrane at the wavenumber of 982 cm^{-1} shifted to lower wave number for the Nd_2O_3/nafion membrane (971 and 979 cm^{-1}), which may be attributed to the interaction of SO_3^- of nafion and –OH groups of Nd_2O_3 [Mahreni et al., 2009]. A similar change was observed for the stretching vibration of SO_3^- 1055 cm^{-1}, which may also be associated with the rearrangement of molecule or the backbone structure in the composite, probably as a result in the rearrangement of the hydrophilic clusters [Ramani et al., 2005]. The band for water bending vibration in the region 1400−2000 cm^{-1} is

much broader with greater intensity for the composite membrane as compared to pure cast nafion membrane, which indicates the increased water content in the composite membrane. The shift in water bending frequency from 1627 cm^{-1} in pure cast nafion to 1631 cm^{-1} in the composite membrane indicates the increase in hydrogen bond association [Laporta et al., 1999]. Similarly, the peak for stretching vibration of water molecules ranging from 3200 to 3700 cm^{-1} [Ludvigsson et al., 2000] is broader for the composite membrane than for the pure cast nafion membrane and indicates that the composite membrane has a higher water uptake than the pure cast membrane. This may be due to the presence of –OH groups on the neodymium surface [Barbora et al., 2010].

The FTIR spectra of talc/nafion membrane in fig. 4.16 shows the characteristic bands for water bending vibration at 1702 and 1737 against 1472 and 1628 cm^{-1} for pure cast nafion membrane. The shift of the bending frequency is due to the increase in hydrogen bond strength [Mizuno et al., 1997]. Peaks in the higher wavenumber region can be assigned to water molecules characterized by strong hydrogen bonding, whilst at lower wavenumber it could be assigned to weaker hydrogen-bonded water molecules [Laporta et al., 1999]. Similarly, the peak for stretching vibration of water molecules ranging from 3200 to 3700 cm^{-1} [Ludvigsson et al., 2000] is much broader for the talc/nafion membrane than for the pure cast nafion membrane. This data indicates that the talc/nafion membrane had a higher water uptake than the pure cast membrane, which is in agreement with the water uptake results discussed in later section of the thesis. The peaks of Si-OH (960 cm^{-1}) and Si-O-Si (1084 cm^{-1} and 1035 cm^{-1}) are visible only for the talc/nafion membrane and shown in annexure A (fig. A.9) [Jung et al., 2002]. Similarly, the Mg-O absorption peaks [Raj et al.,

2007] expected in the region of 400-600 cm^{-1} is observed only for the talc/nafion and shown in annexure A (fig. A.10).

Figure 4.17 represents the FTIR results of ErTfO/nafion and NdTfO/nafion composite and compared with the FTIR results of pure cast nafion membrane [Barbora et al., 2009b; Shroti et al., 2011]. The nafion and ErTfO have similar structures except for the long chain of nafion with ether linkages. The spectral region between 1000 and 1350 cm^{-1}, with a band at around 1055 cm^{-1} indicate symmetric S–O stretching for both pure cast nafion and ErTfO/nafion membranes [Kujawski et al., 1992; Park and Yamazaki, 2005]. The shift in band for the ErTfO/nafion membrane, from 1021 to 1030 cm^{-1}, may be attributed to stretching of S-O involved in coordination bond with Er^{3+} ions. A band for water bending vibration occurs in the region 1400–2000 cm^{-1} [Park and Yamazaki, 2005]. On comparison of the FTIR spectra of pure cast nafion and ErTfO/nafion membranes, it is observed that characteristic bands appear at 1472 and 1628 cm^{-1} for pure cast nafion whilst in case of the composite membrane (ErTfO/nafion), there are close peaks at 1440, 1472, 1500, and another at 1660 cm^{-1}, respectively. The band area is much larger for these composite membranes as compared to pure cast nafion membrane, which indicate increased water content in the composite membrane. The shift in water bending frequency from 1628 cm^{-1} in pure cast nafion to 1660 cm^{-1} in the composite membrane indicates the increase in hydrogen bond association [Laporta et al., 1999]. The shift of the bending frequency from 1628 to 1660 cm^{-1} is due to the increase in hydrogen bond strength [Mizuno et al., 1997]. The observed widening of band is due to the increase in hydrogen bond strength that results from the increase in hydrogen bond distribution because of the presence of ErTfO in the nafion matrix

[Hankins et al., 1970]. The peak for stretching vibration of water molecules ranging from 3200 to 3700 cm^{-1} [Ludvigsson et al., 2000] is much broader for the composite membrane indicating higher water uptake than the pure cast nafion membrane, which is in agreement with water uptake results shown in later section of the thesis.

The similar results are also found for the FTIR spectra of NdTfO/nafion membrane (fig.4.17) with some slight shifting of the bands for the NdTfO/nafion composites. The spectral regions between 1000 and 1350 cm^{-1}, with a band at 1055 cm^{-1} for pure cast nafion membrane and at 1058 cm^{-1} for NdTfO/nafion, indicate symmetric S-O stretching [Lowry and Mauritz, 1980; Kujawski et al., 1992]. The shift in band for the NdTfO/nafion composite membrane, from 1223 cm^{-1} - 1294 cm^{-1}, may be attributed to stretching of S-O involved in coordination bond with Nd^{3+} ions. A band for water bending vibration occurs in the region 1400-2000 cm^{-1} [Park and Yamazaki, 2005]. On comparison of the FTIR spectra of pure cast nafion and NdTfO/nafion membrane, it is observed that characteristic bands appear at 1472 and 1627 cm^{-1} for pure cast nafion whilst in case of composite membrane, a broad peak appears at 1642 cm^{-1}. The increase in band area indicates increased water content in the composite membrane. The shift in water bending frequency from 1627 cm^{-1} in pure cast nafion to 1642 cm^{-1} in the composite membrane indicates the increase in hydrogen bond association [Laporta et al., 1999)]. Similarly, the peak for stretching vibration of water molecules ranging from 3200 - 3700 cm^{-1} [Ludvigsson et al., 2000] is much broader for the composite membrane than for the pure cast nafion membrane, which indicates increased water content in the composite membrane. Moreover, it may be noted that the NdTfO/nafion composite membranes is expected to exhibit lower water uptake as compared to the ErTfO/nafion

composite membranes, and this is in agreement in the water uptake results shown in later section of the thesis .

Figure 4.18 shows the comparison of FTIR spectra of MS/nafion membrane and pure cast nafion for comparsion. The spectral region between 1000 to 1350 cm^{-1}, with a band at 1055 cm^{-1} for pure cast nafion membrane and at 1057 cm^{-1} for MS/nafion indicates symmetric S-O stretching [Kujawski et al., 1992]. The shift in band from 1223 cm^{-1} in pure cast nafion to 1271 cm^{-1} in MS/nafion composite membrane indicates the changes in structure due to the incorporation of MS in pure cast nafion membrane. On comparison of the FTIR spectra of pure cast nafion membrane and MS/nafion composite membrane, it is observed that characteristic bands for water bending vibration appear at 1472 and 1627 cm^{-1} for pure cast nafion membrane whilst in case of the composite membrane, a broad peak appears at 1638 cm^{-1}. The FTIR results of MS/nafion membrane also indicate the increased water content as compared to the pure cast nafion membrane, which is in concurrence with the water uptake results found in the later section of the thesis.

Table 4.4 summarizes the FTIR bands of nafion and the composite nafion membranes. It can be seen that the FTIR spectra of the composite membranes showed band shifts attributed to the presence of the inorganic moiety.

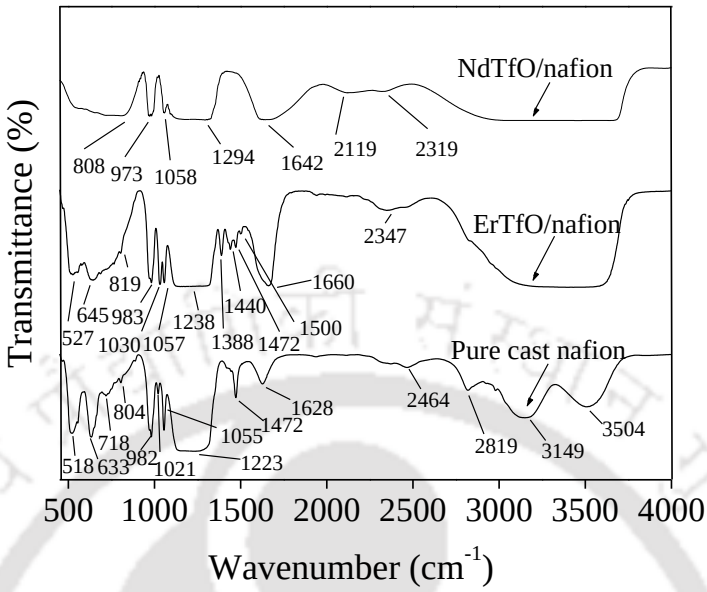

Fig. 4.17 FTIR spectra of pure cast nafion and composite membrane with 1% loading of ErTfO and NdTfO

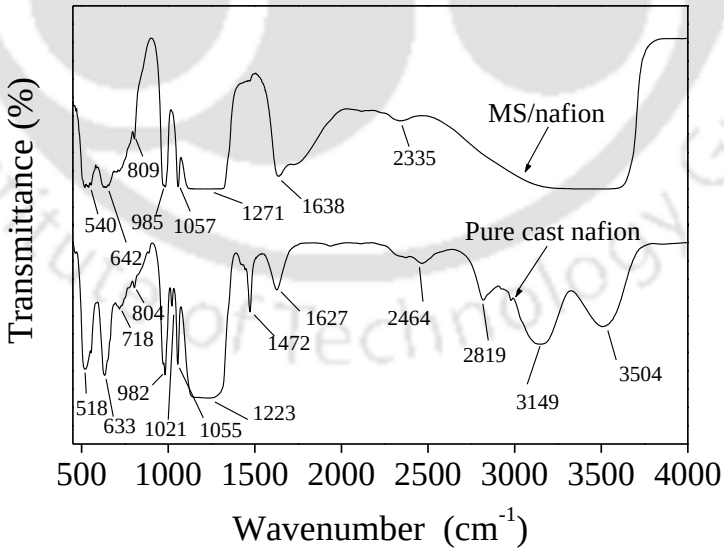

Fig. 4.18 FTIR spectra of pure cast nafion and composite membrane with 1% loading of MS

Table 4.4 FTIR bands of pure cast nafion and nafion composite membranes

Membrane	**Wavenumber (cm^{-1})**					
	500-800	1000 - 1350	718, 982	1223	1400–2000	3200 - 3700
	SO_3^- or $-SO_3H$ band	*Stretching vibration of SO_3^- group*	*C=O bending and C-O-C band*	*C-F band*	*H_2O bending*	*Stretching vibration of water*
Pure cast nafion	518, 633,	1021,1055	718, 804, 982	1223	1472, 1627	3504
TiO_2/nafion	532, 647,	1067	737, 817, 999	1284	1488, 1728	Broad band between 3200 - 3700 cm^{-1}
Nd_2O_3/nafion	Broad band between 500-800	1056	971, 979	1293	1631	Broad band between 3200 - 3700 cm^{-1}
Talc/nafion	524, 637, 671	-	780, 805	1282	1702, 1737	Broad band between 3200 - 3700 cm^{-1}
ErTfO/nafion	527, 645	1030, 1057	819, 983	1284	1440, 1472, 1500, 1660	Broad band between 3200 - 3700 cm^{-1}
NdTfO/nafion	Broad band between 500-800	1058	808, 973	1294	1642	Broad band between 3200 - 3700 cm^{-1}
MS/nafion	540, 642	1057	809, 985	1271	1638	Broad band between 3200 - 3700 cm^{-1}

4.2.5. *Ion exchange capacity*

Ion exchange capacity (IEC) is defined as the number of replaceable ions (H^+) per unit mass of the dry membrane. It is one of the very important characteristics of the polymer electrolyte membrane as it provides an estimate of the acid groups having replaceable H^+ ions. These H^+ ions are relatively weakly attached to SO_3^- groups and thus able to move from anode to cathode via the Grotthuss mechanism, which involves rapid 'hopping' of protons amongst neighboring sites involving solvated H^+ ions [Sandhu et al., 2005; Barbora et al., 2009a] or through vehicular mechanism using hydronium, Zundel, and/or Eigen ions [Kreuer, 2001; Barbora et al., 2010]. Figures 4.19 to 4.21 show the effect of additives on ion exchange capacity of the nafion composite membrane.

Figure 4.19 shows the effect of TiO_2, Nd_2O_3, and talc on ion exchange capacity of the nafion composite membrane. It can be seen in the figure that the IEC initially increases with the addition of additives. However, the IEC reduces with further increase in the additive loading. The maximum IEC was found at 1% of TiO_2 (1.17 meq/g) and 5% of Nd_2O_3 (1.34 meq/g) and talc loading (1.17 meq/g) [Barbora et al., 2009a; Barbora et al., 2010; Barbora et al., 2012]. The reason for the increase in IEC is due to the presence of –OH groups on the surface of TiO_2, Nd_2O_3, and talc. Hydroxyl groups form on to the TiO_2 surface because of the strong oxidation potential of TiO_2, which oxidizes the water molecule associated with it [Staiti et al., 2001]; The hygroscopic nature of Nd_2O_3 leads to the formation of neodymium hydroxide [$Nd(OH)_3$] and a weak hydrogen bond develops between the water molecules and the –OH group of $Nd(OH)_3$ [Glushkova and Suglobov, 1965]; the SiO_2 present in talc is hydrophilic and forms Si-OH, which has affinity for proton adsorption [Jun et al., 2007; Tang

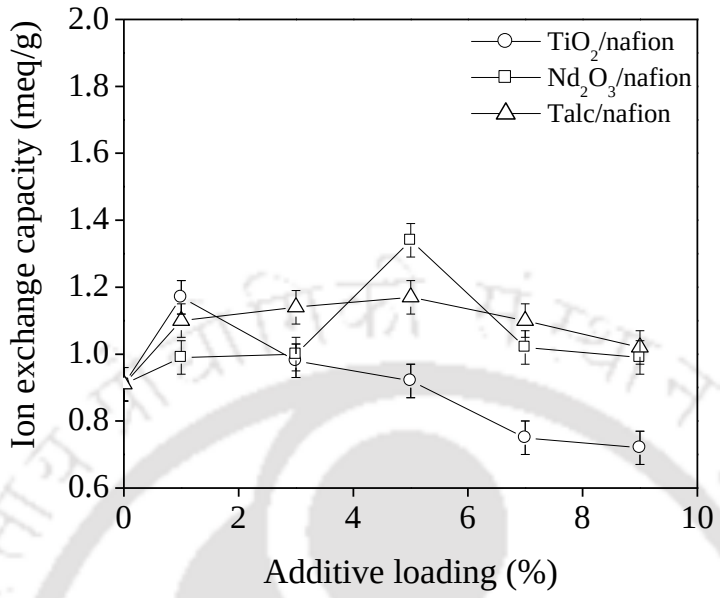

Fig. 4.19 Effect of TiO_2, Nd_2O_3, and talc on ion exchange capacity of the composite membranes

et al., 2007], which may simultaneously improve the ion exchange capacity of the composite membrane. Besides, MgO in talc contributes to the hygroscopic nature of talc. These additional –OH groups on the surface of the additives coordinate with the significant number of water molecules and thus increase the water content inside the composite membranes. The increased amount of water helps to loosen the interaction between proton and SO_3^- ion. Thus more number of replaceable protons is available. However, further increase in the additive loading forms agglomerates of the additive in the composite membrane. The agglomerate formation was evidenced from the SEM image (fig. 4.6-4.8). Moreover, according to Falk, (1980), three quarter of all –OH groups can participate in the hydrogen bonding, and one-quarter in non hydrogen bonding [Falk, 1980]. Thus, the effective number of replaceable ion

exchange sites reduces in the composite membranes above the loading for 1% TiO_2, 5% Nd_2O_3, and 5% talc.

Figure 4.20 shows the effect of ErTfO and NdTfO on IEC of the composite membrane. The figure shows that IEC of the ErTfO composite is maximum at 1% with a value of around 1.82. Higher loadings of the ErTfO do not help to increase the IEC further and IEC reduces on further increase in the ErTfO loading. At the same time, it is observed that IEC of the NdTfO composite slowly increases upto 3% loading and thereafter the increase in the loading hardly have any influence on the IEC. The IEC of the NdTfO composite is 1.13 meq/g at 3% loading of NdTfO in the composite membrane. The reason of increasing IEC may be explained in light of the fact that in both the cases the triflate ions as well as nafion have SO_3^- as functional group in the molecular structure. The ionic character of triflates and stabilizing effect of the polymer matrix enable the SO_3^- group of triflate ion, not involved in coordination bond with Er^{3+} of ErTfO or Nd^{3+} of NdTfO, to act as ion exchange domains [Barbora et al., 2009b; Barbora et al., 2010], which is probably responsible for the increase in IEC of the NdTfO/nafion membrane compared to pure cast nafion membrane.

It may be noted that Er^{3+} and Nd^{3+} ions show a striking tendency to coordinate with polymer or oxygen of triflate ion. The average coordination number of ErTfO (or Er^{3+}) is 9 as compared to 12 for NdTfO. That means Er^{3+} and Nd^{3+} ions coordinate to both nafion and triflate ions involving 9 SO_3^- and 12 SO_3^- groups. The presence of SO_3^- groups not involved in bonding with Er^{3+} ions increase the ion exchange capacity (in the presence of water) of the

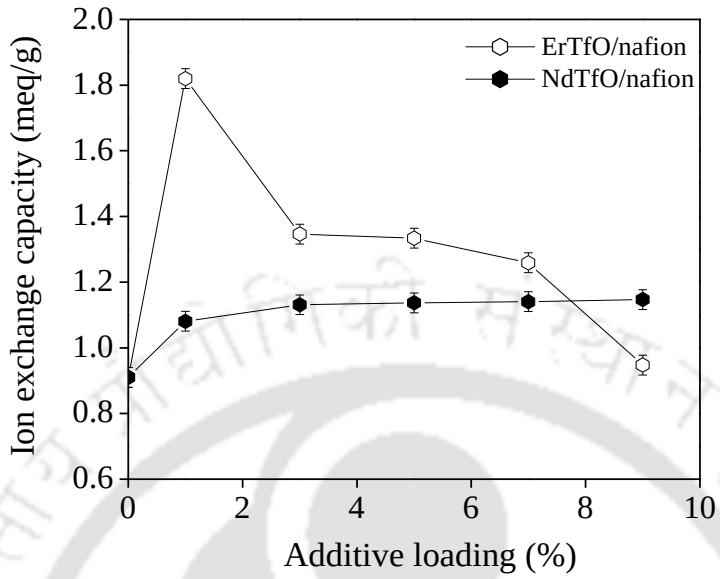

Fig. 4.20 Effect of ErTfO, and NdTfO loading on ion exchange capacity of composite membranes

composite membrane (fig. 4.20) with the increased number of ion exchange domains. Whereas, the decrease in IEC with the increase in ErTfO (above 1%) and NdTfO (above 3%) loading was due to the decrease in the effective number of replaceable ion exchange sites with the increased ErTfO loading, as more and more SO_3^- sites were bonded [Barbora et al., 2009b].

The effect of higher coordination number can be seen by the results of Nd^{3+} as compared to Er^{3+}, where the IEC values of NdTfO were less than the IEC of the ErTfO almost in all the composites. The effect of additional SO_3^- groups is almost suppressed, due to the high coordination number of Nd^{3+} ion. Figure 4.21 compares the IEC of pure cast nafion

membrane with MS/nafion membranes. The MS/nafion membranes exhibited slight improvement in IEC compared to pure cast nafion membrane, attributed to the ion exchange characteristic property manifested by molecular sieves [Townsend and Harjula, 2002]. The porous structure of the molecular sieves can accommodate a wide variety of cations, such as Na^+, K^+ and others that are rather loosely held and can readily be exchanged for others in a contact solution [Lin et al., 2011]. In our case the ion is H^+, as the membranes were protonated before testing. However, the increase in IEC was not very high as expected, which might have been due to the poor physical compatibility (agglomeration) of the additive with nafion as obvious from the SEM images shown earlier. The maximum IEC value (1.04 meq/g) was obtained at a loading of 3%.

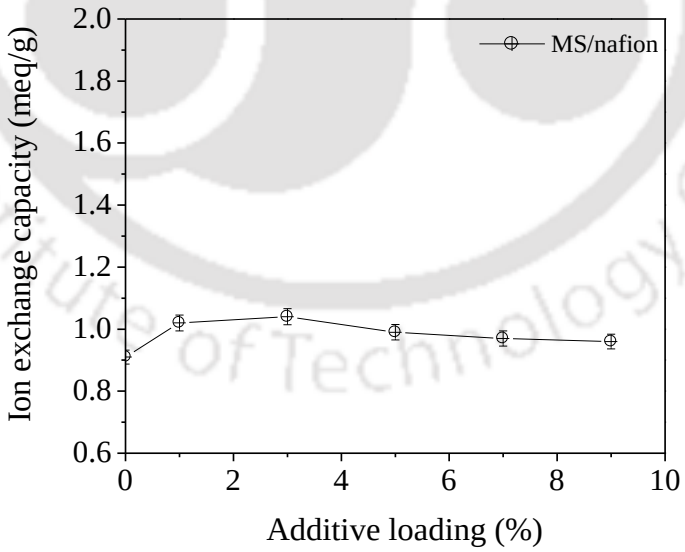

Fig. 4.21 Effect of MS loading on ion exchange capacity of composite membranes

4.2.6. *Water uptake*

Water uptake is closely related to the basic membrane properties and plays an important role in the membrane behavior. Proton conductivity and fuel permeation across the membrane depend to a large extent on the amount of water absorbed by the membrane. Presence of water in the membrane influences the ionomer microstructure, cluster, channel size, plasticizes, and modifies the mechanical properties [Baglio et al., 2005]. It may be noted that very high value of water uptake is not desirable due to adverse effect on strength and swelling.

Figure 4.22 shows the water uptake profile of TiO_2/nafion, Nd_2O_3/nafion, and talc/nafion membranes with varying percentage of additive loading. All the three composites exhibited higher water uptake than pure cast nafion membrane, which is in agreement to the FTIR bands for water bending and water stretching vibrations (fig. 4.16). The enhanced water uptake may be attributed to the hygroscopic nature of the additives [Watanabe et al., 1996]. A significant number of water molecules could be coordinated by hydrogen bonding with the –OH groups present on the surface of the additives [Sandhu et al., 2005]. Therefore, the water uptake of the pure cast nafion membrane increased with the addition of the additive. The water uptake follows almost similar trend to that of IEC. The maximum water uptake was found at 1% of TiO_2 loading (36.82%). Wheras, for Nd_2O_3 (31.93%), and talc (24.42%), the maximum water uptake was observed at 5%. However, the composite membranes with TiO_2 loadings in the range of 7% to 9% showed water uptake lower than the pure cast nafion membrane. This may be attributed to the distribution of TiO_2 and the availability of active

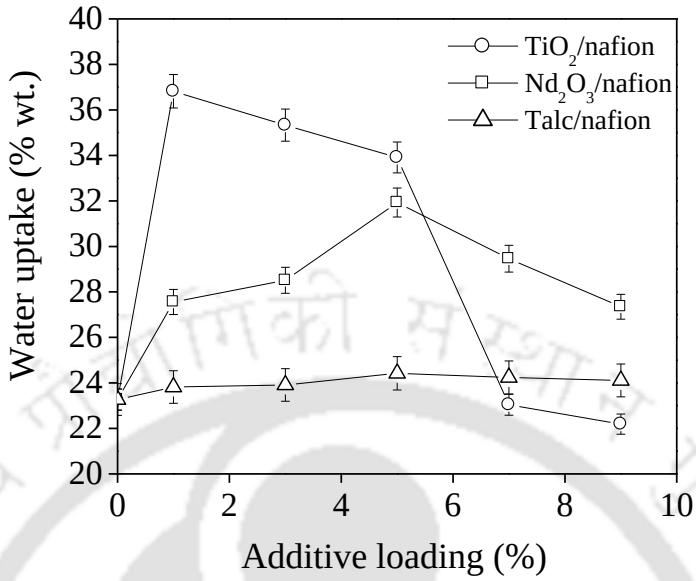

Fig. 4.22 Effect of TiO_2, Nd_2O_3, and talc on water uptake of composite membranes

sites (–OH attached with TiO_2) on the surface of the composite membrane for hydrogen bonding with water. As can be seen from the SEM images (figures 4.6a to 4.6e), with increase in TiO_2 loading by 7% in the composite membranes, the formation of agglomerations increased and thus the surface area of the TiO_2 decreased. Over and above non-hydrogen bonding between adjacent –OH groups may be responsible for the decrease of free –OH groups on the composite surface for hydrogen bonding with water. However, at any time the water uptake was observed to be more than the pure cast nafion membrane for Nd_2O_3/nafion and talc/nafion membranes [Barbora et al., 2009a; Barbora et al., 2010; Barbora et al., 2012].

Figure 4.23 shows the water uptake of ErTfO/nafion and NdTfO/nafion membranes with different percentage of the additive loading in the composite nafion membrane. The

composite membranes with both the additives exhibited higher water uptake than pure cast nafion, attributed to the coordination of SO_3^- group of ErTfO and NdTfO with water molecules through hydrogen bonding. The SO_3^- groups involved in coordination bonding with Er^{3+} or Nd^{3+} though did not contribute much to IEC, but the weakly bonded SO_3^- groups could still attract water by weak hydrogen bonding [Barbora et al., 2009b; Shroti et al., 2011]. The lower uptake of NdTfO support the results of lower IEC discussed previously. The higher water uptake for ErTfO/nafion membranes as compared to NdTfO/nafion membranes is in agreement with FTIR results (section 4.2.4). The nafion composites with the inorganic triflates showed a continuous increase in the water content with the additive loading. It may be noted that in earlier case (inorganic hygroscopic fillers), the water uptake reached upto a maxima, then decreased due to agglomeration of the particles.

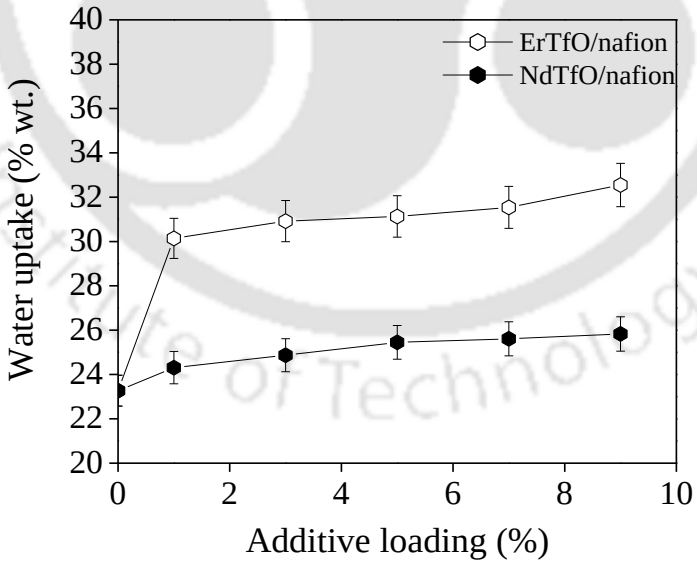

Fig. 4.23 Effect of ErTfO and NdTfO on water uptake of composite membranes

However, in this case there was no agglomeration due to soluble nature of the ErTfO and NdTfO in the nafion solution and thus the water uptake kept on slowly increasing with the additive loading. If we correlate the maximum IEC found in section 4.2.5, it may be found that the water uptakes were 30.14% and 24.87% for the nafion composites with 1% ErTfO and 3% NdTfO, respectively.

Figure 4.24 shows the water uptake of MS/nafion membranes with varying percentage of MS loading. The water uptake of the MS/nafion membranes was slightly higher than pure cast nafion, which may be attributed to the water adsorbing capacity of the additive [Mohamadbeigy et al., 2007]. The water uptake of the composite membranes increased with a loading of up to 3% and then gradually decreased with the increase in additive loading. The water uptake corresponding to 3% loading is 27.76%.

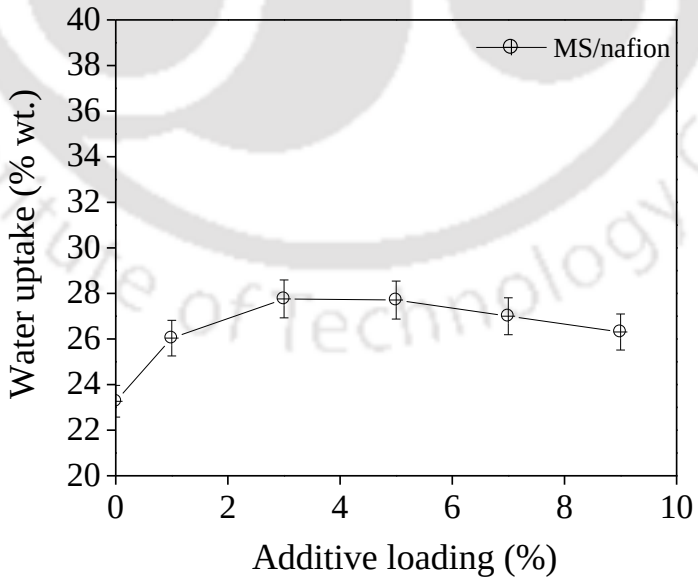

Fig. 4.24 Effect of MS on water uptake of composite membranes

The decrease in water uptake at higher additive loading might have been due to agglomeration of the additive as observed in the SEM images (fig. 4.11a to 4.11e).

4.2.7. *Methanol uptake*

Evaluation of methanol uptake is one of the important characteristics of a solid polymer electrolyte membrane for DMFC. Ideally, methanol uptake is not desired as it would increase the methanol crossover as well as may increase the swelling as discussed in the subsequent section. Figures 4.25 to 4.27 show the effect of additives on the methanol uptake by the pure cast nafion membrane and composite nafion membrane for different concentration of methanol solution. It may be noted that for evaluating the methanol uptake as well as the swelling characteristics (section 4.2.8) of the membranes, three different concentrations (0.5 M, 1 M, and 2M) of methanol solution have been selected. The reason for selecting these methanol concentrations is that the DMFC is generally fed with these methanol solutions as a fuel [Vaivars et al., 2004; Jiang et al., 2006; Shen et al., 2007; Arbizzani et al., 2010]. It has been observed in the figs. 4.25-4.27 that the trend of methanol uptake is almost similar to that of water uptake discussed in section 4.2.6.

Figure 4.25 shows the effect of TiO_2, Nd_2O_3, and talc loading on the methanol uptake at the three concentrations of methanol. It can be seen that for any of the additives at any particular loading the methanol uptake increases with the increase in the methanol concentration, which is in agreement to previous reports in the literature [Godino, 2006]. The reason for this behavior is that the nafion has both hydrophobic and hydrophilic domains, water being more polar has high accessibility to the hydrophilic domains, which covers about 25 to 35% of the

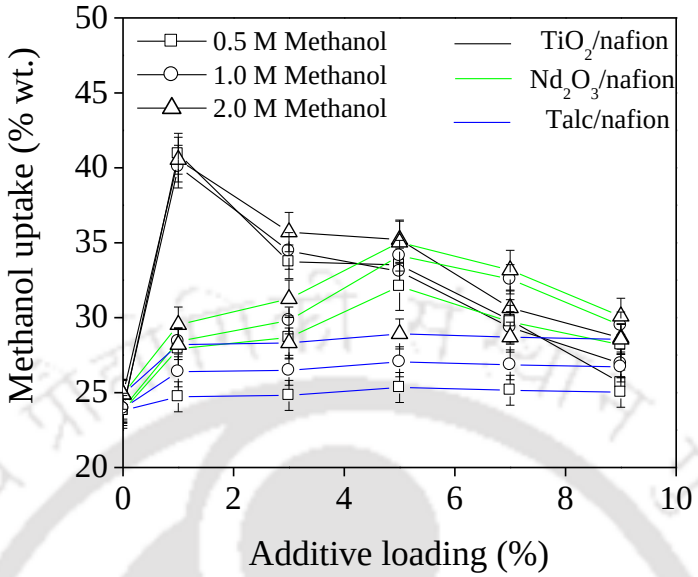

Fig. 4.25 Effect of TiO_2, Nd_2O_3, and talc loading on methanol solution uptake of composite membranes

membrane mass as is obvious from the water uptake results shown in figs. 4.22 to 4.24 [Barbora et al., 2009a]. Methanol being less polar than water has accessibility to hydrophilic domains along with the hydrophobic domains. Hence, the uptake of methanol was slightly higher than water for pure cast nafion membrane as well as the composite nafion membranes. Similar trends of methanol uptake can be seen in the fig 4.26 and 4.27 for ErTfO and NdTfO, and MS, respectively.

4.2.8. *Swelling*

During DMFC operation the protons along with water molecules (hydrated protons) transport from anode to cathode. The generation of water at the cathode and aqueous methanol solution at anode keep the membrane hydrated. The membrane hydration is very important

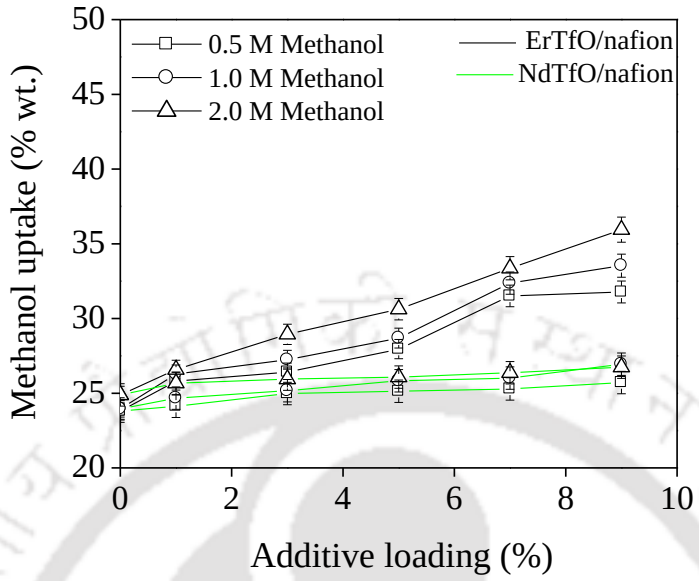

Fig. 4.26 Effect of ErTfO, and NdTfO loading on methanol solution uptake of composite membranes

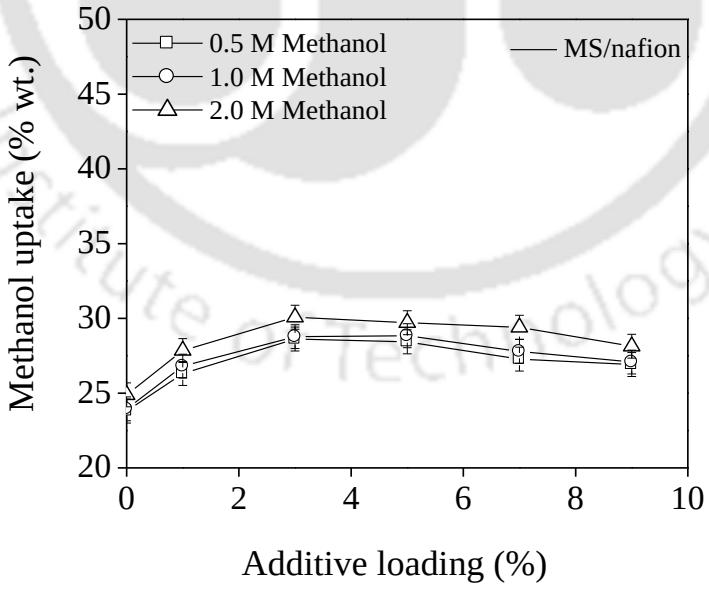

Fig. 4.27 Effect of MS loading on methanol solution uptake of composite membranes

for the transport of protons through the proton exchange membrane (nafion). However, the nafion membrane swells up due to the presence of water and methanol because of water and methanol uptakes (section 4.2.6 and 4.2.7) by the membrane. The hydration level in the membrane decreases when the fuel cell is not in operation, which leads to shrinkage of the nafion membrane. Therefore, during on/off cycles of the fuel cell there may be high chances that MEA may not only be delaminated but may develop cracks in the MEA [Velankar et al., 2012]. Thus leakage of the methanol solution may occur through the MEA and reduce the DMFC performance drastically. However, the presence of inorganics in the nafion composites is likely to prevent the shrinkage of nafion membrane as they have a higher water uptake than pure nafion and unlike nafion would not loose water so easily. The water retained by the inorganics would keep the membrane in the hydrated state even when the fuel cell is turned off and thereby prevent delamination as well as cracks in the MEA [Adjemian et al., 2002]. However, there should be a balance between the water uptake (a desired property, upto certain extent, to have proton conductivity) and the swelling (an undesired property) due to water and methanol uptake. Therefore, swelling is one of the most important properties, which is to be evaluated for the nafion composite membrane.

Figures 4.28-4.30 show the swelling characteristics of the membrane in water and in the three different concentrations (0.5 M, 1 M, and 2M) of methanol solution for various additives at different loadings. However, for better clarity of the figures the swelling results for water are separately tabulated in tables 4.5-4.7.

Figure 4.28 and table 4.5 shows the effect of methanol solution and water on percentage swelling for nafion composites using TiO_2, Nd_2O_3, and talc. It can be seen that the swelling is invariably more for any of the nafion composites in methanol solution as compared to water [Barbora et al., 2009a]. Exposing nafion or its composite to methanol solution results in methanol uptake apart for water uptake by the membrane as discussed in the previous sections, which results in more swelling. According to Affoune et al., (2005), nafion structure undergoes high modification due to the swelling of the methanol. The presence of hydrophilic and hydrophobic zones in the nafion makes the interaction between the nafion surface and methanol differently as compared to when contacted to only water. Methanol has access to both the hydrophilic and hydrophobic zones in nafion as discussed. This makes nafion expand much more in methanol solution than in water. Amongst the three additives, talc/nafion composite membrane show the highest swelling followed by TiO_2, and Nd_2O_3, respectively. The trend followed somewhat match with that of water and methanol uptake (fig. 4.22 and fig. 4.25). It may be noted that both TiO_2 and Nd_2O_3 are more hydrophilic (greater water uptake) than talc even then the composites with these two additives exhibited reduced swelling than talc. This may be attributed to the difference in talc size, which is flaky in nature [Wang et al., 2013].

The swelling of the composite membranes with ErTfO and NdTfO using methanol solution and water is shown in the figure 4.29 and table 4.6. It is observed that swelling is slightly more in ErTfO/nafion as compared to NdTfO/nafion composite membranes and follows the water and methanol uptake patterns. The higher coordination number of Nd, which produced more compact and dense composite ultimately develop more resistance to swelling.

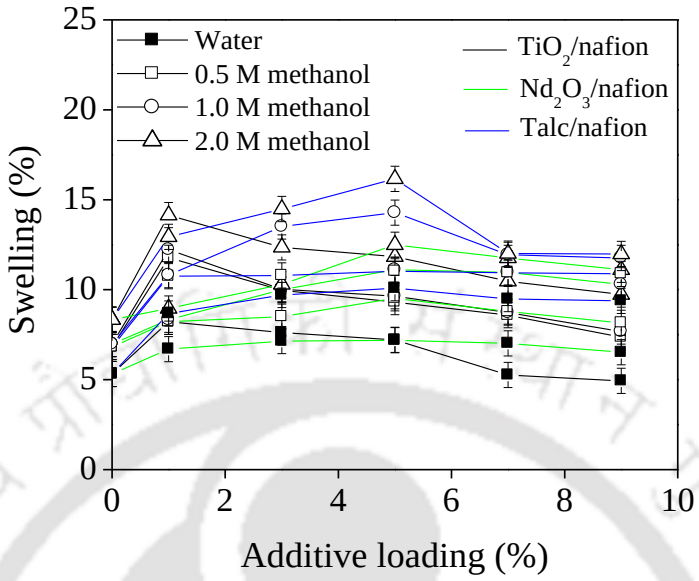

Fig. 4.28 Effect of TiO_2, Nd_2O_3, and talc on membrane swelling by water and by different concentrations of methanol solution

Table 4.5 Effect of TiO_2, Nd_2O_3, and Talc on membrane swelling by water

Additive loading (%)	Swelling (%)		
	TiO_2	Nd_2O_3	Talc
0	05.32	05.32	05.32
1	08.22	06.70	08.68
3	07.62	07.14	09.71
5	07.21	07.19	10.09
7	05.26	07.02	09.48
9	04.93	06.52	09.38

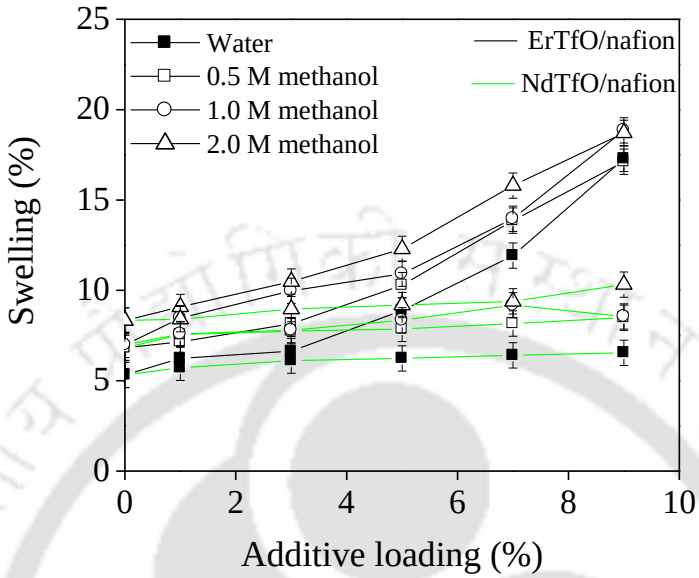

Fig. 4.29 Effect of ErTfO and NdTfO on membrane swelling by water and by different concentrations of methanol solution

Table 4.6 Effect of ErTfO and NdTfO on membrane swelling by water

Additive loading (%)	Swelling (%)	
	ErTfO	NdTfO
0	05.32	05.32
1	06.24	05.72
3	06.64	06.11
5	08.89	06.24
7	11.92	06.41
9	17.28	06.55

Figure 4.30 and table 4.7 show the swelling of pure cast nafion membrane with MS/nafion membranes. The pattern followed is similar to the other composite membranes. Overall the percentage of swelling in the membranes was in the range of 10 (±5)%.

4.2.9. *Tensile strength*

It has been already discussed that the membrane is sandwiched between the electrodes and placed into the fuel cell casing under a particular pressure. The nafion and nafion composite membrane have different compressive strength. However, once the fuel cell operation commences, the swelling occur, which may produce linear variation in the longitudinal direction. Thus, the membrane is generally tested for its mechanical strength using tensile strength [Liu et al., 2003; Park et al., 2012]. Therefore, tensile strength is one of the important properties of the fuel cell membrane, which needs to be evaluated. In fig. 4.31, the tensile strength of TiO_2/nafion, Nd_2O_3/nafion, and talc/nafion composite membranes is compared with that of pure cast nafion membrane. As can be seen from the figure, nafion membrane with 1% loading of Nd_2O_3 has a higher tensile strength than pure cast nafion membrane. However, the tensile strength slowly decreases with the further increase in the Nd_2O_3 loading. Nonetheless, the tensile strength of Nd_2O_3/nafion membranes is much higher than the composites with TiO_2 and talc, which is attributed to the comparatively smaller size of Nd_2O_3 particles (table 4.1). The fine Nd_2O_3 particles along with evenly distributed particles in the Nd_2O_3/nafion composite membranes might have enhanced its physical compatibility with nafion and thus the strength [Barbora et al., 2010]. It can be seen that the tensile strength of the membrane with TiO_2 and talc reduces gradually with the addition of the additive [Barbora et al., 2009a].

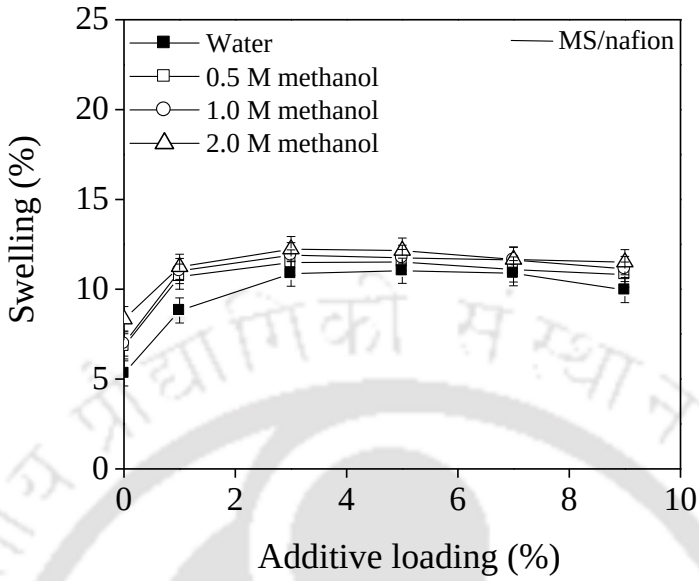

Fig. 4.30 Effect of MS on membrane swelling by water and by different concentrations of methanol solution

Table 4.7 Effect of MS on membrane swelling by water

Additive loading (%)	Swelling (%)
	MS
0	05.32
1	08.82
3	10.87
5	11.03
7	10.89
9	09.96

In case of the inorganic triflate/nafion membranes, the nafion composites with 1% ErTfO shows slight improvement in tensile strength over pure cast nafion membrane (fig.4.32), which decreases with the increase in the ErTfO loading may be due to the miscibility of these two additives in nafion solution [Barbora et al., 2009]. However, at higher percentage of loading, the tensile strength of the nafion composites deteriorated. Higher cross-linking at higher loading apparently increased the stiffness of the membrane and reduced its tensile strength. It can be seen that due to higher coordination number, NdTfO hardly increases the tensile strength at 1% loading. Whereas, as the NdTfO loading increases above 1%, the tensile strength decreases compared to nafion membrane. Moreover, ErTfO has lower coordination number as compared to the NdTfO and thus have higher tensile strength than NdTfO/nafion composites for all the compositions.

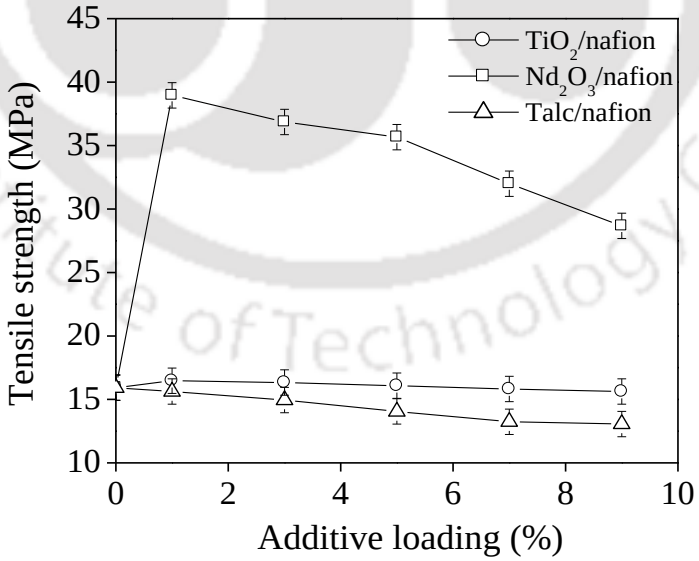

Fig. 4.31 Effect of TiO_2, Nd_2O_3, and talc on tensile strength of composite membranes

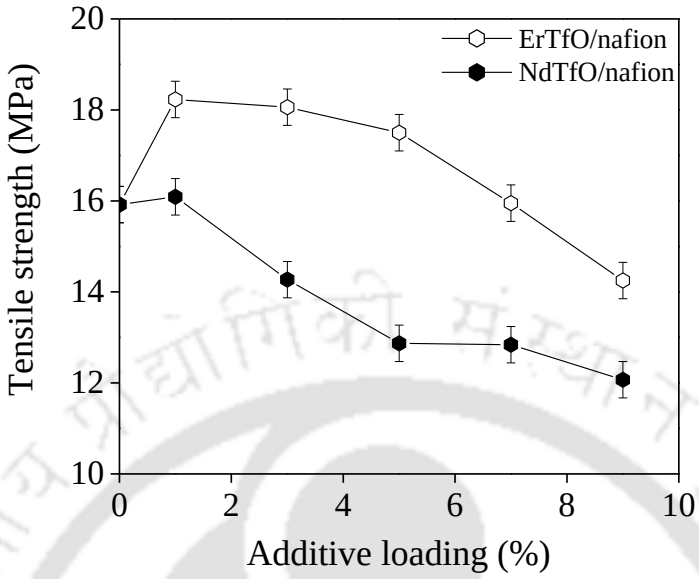

Fig. 4.32 Effect of ErTfO, and NdTfO on tensile strength of composite membranes

The tensile strength of MS/nafion membranes was slightly lower than that of pure cast nafion membrane (14 MPa vs ~16 MPa) (fig.4.33). The formation of MS agglomerates in the composites might have apparently weakened the integrity of the nafion membrane and reduced its tensile strength.

4.2.10. *Oxidative stability*

Various studies show that hydrogen peroxide forms as a reaction intermediate in the oxygen reduction process at cathode [Song and Zhang, 2008]. Two reaction pathways are generally considered for the oxygen reduction reaction (ORR); the one is the four-electron pathway and the other is 2+2 electron pathway or peroxide pathway. In acidic medium, as in case with DMFC using nafion, the ORR proceeds through peroxide pathway where reactive oxygen

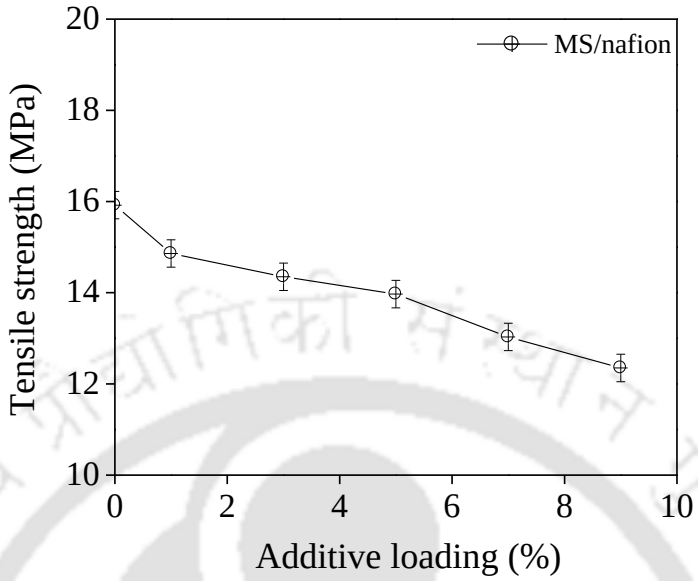

Fig. 4.33 Effect of MS on tensile strength of composite membranes

species are generated in-situ during the ORR in an operating direct methanol fuel cell [Fang et al., 2009].These reactive oxygen species namely hydroxyl (·OH) and hydroperoxyl (·OOH) radicals are amongst the strongest oxidizing agents. These reactive oxygen species may diffuse over the time into the polymer electrolyte membrane and degrade the membrane. The concentration of these reactive species, which diffuse into the membrane, is in ppm range generated over a long duration of time [Sethuraman et al., 2008]. The reactive oxygen species initiate oxidative degradation of membrane side chains (primarily) that contain ionic groups, which are essential for ion conduction [Curtin et al., 2004]. The adverse consequences of these degradation modes (e.g., membrane thinning, pin-hole formation, and loss of ionic conductivity) eventually contribute to catastrophic cell and stack failure. However, the degradation process is so slow that it is not convenient to perform the study in

the DMFC. Therefore, an accelerated test (ex-situ) was performed in H_2O_2 solution as described in the experimental chapter (section 3.4.2.8).

The membrane was immersed in the hydrogen peroxide (H_2O_2) solution and change in the weight percent (wt.%) was measured with time (in days). The pattern of change of weight loss followed by the pure cast nafion membrane is shown in fig 4.34. It may be noted that the initial dry membrane weight was considered as 100%. After first day the membrane weight increased by 30%. This particular increase in weight (excess weight) was due to the uptake of H_2O_2 solution by the dry membrane [Barbora et al., 2009b]. The degradation rate of the pure cast membrane was calculated from the figure 4.34 and was found to be around 0.28 wt.% per day [Barbora et al., 2009]. It is reported that the oxidative degradation of nafion membrane was due to the degradation of sulphonated polychains in the presence of H_2O_2 [Chen et al., 2006].

Figure 4.35 to 4.37 shows the degradation rates of nafion composite membranes with various loadings of the different additives in comparison to pure cast nafion membrane. It can be seen that almost all the composites for all the compositions show lower degradation rate as compared to pure cast nafion membrane. It infers that the composites are chemically more stable than pure cast nafion membrane though the optimum percent of loading varies for each type of additive. The degradation rates of the composite nafion membrane using TiO_2, Nd_2O_3, and talc are shown in fig. 4.35. It can be seen that the degradation rate initially reduces with the additive loading but for a higher loading of the additives the degradation

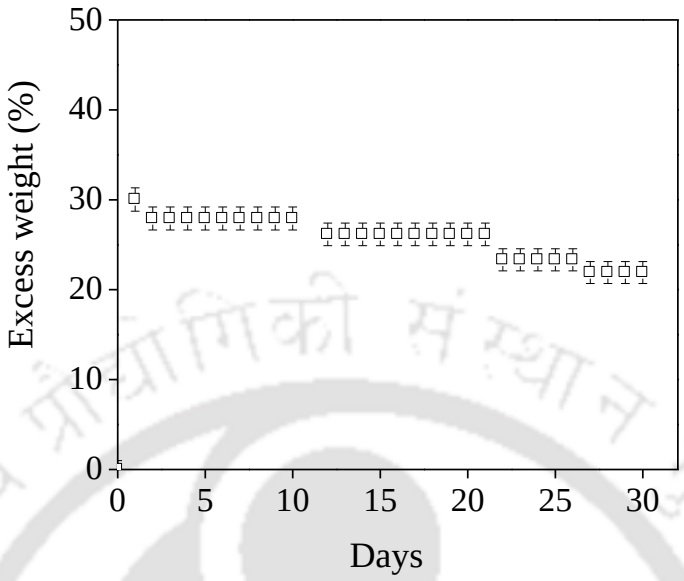

Fig.4.34 Pattern of pure cast nafion membrane weight change during incubation of membrane in H_2O_2 and its degradation rate

rate increases. This may be attributed to the weakening of chemical bonds of the polymer due to incorporation of the additive at higher loadings of the additive [Shroti et al., 2011]. The lowest degradation rate was found for 1% TiO_2, 5% Nd_2O_3, and 5% talc loading in the nafion membrane [Barbora et al., 2010]. However, in any of the composition (except 9% TiO_2) the degradation rate of the composite was lower than the cast nafion membrane. Similar trends were found for ErTfO and NdTfO (fig. 4.36) composites as well as for MS (fig. 4.37) composites [Barbora et al., 2009b; Shroti at al., 2011]. The minimum degradation rate was observed at 1% for ErTfO and NdTfO composites wheras 5% for MS composites.

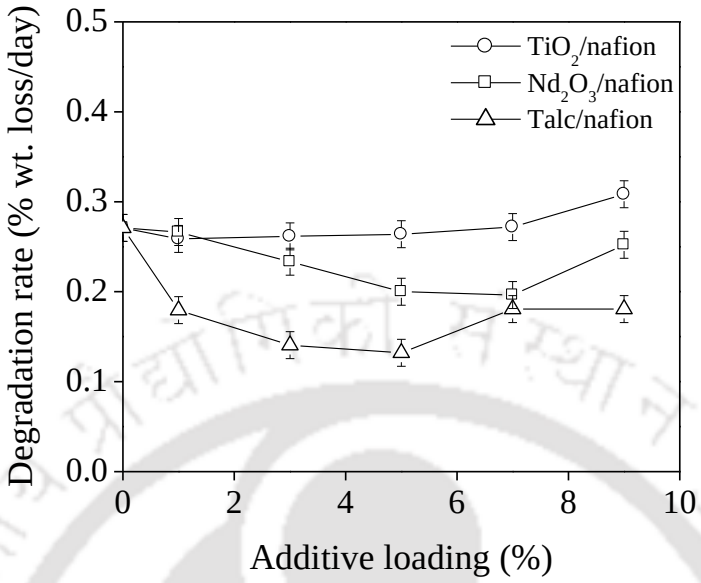

Fig. 4.35 Effect of TiO_2, Nd_2O_3, and talc on the oxidative stability of composite membranes

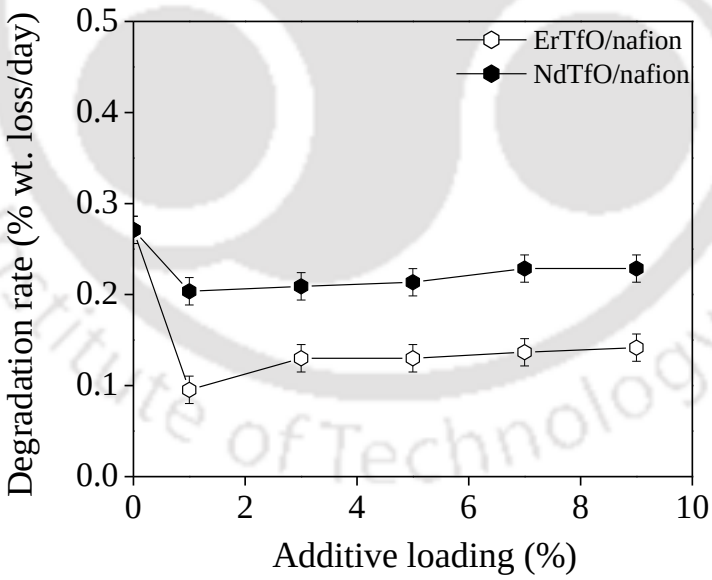

Fig. 4.36 Effect of ErTfO, and NdTfO loading on the oxidative stability of composite membranes

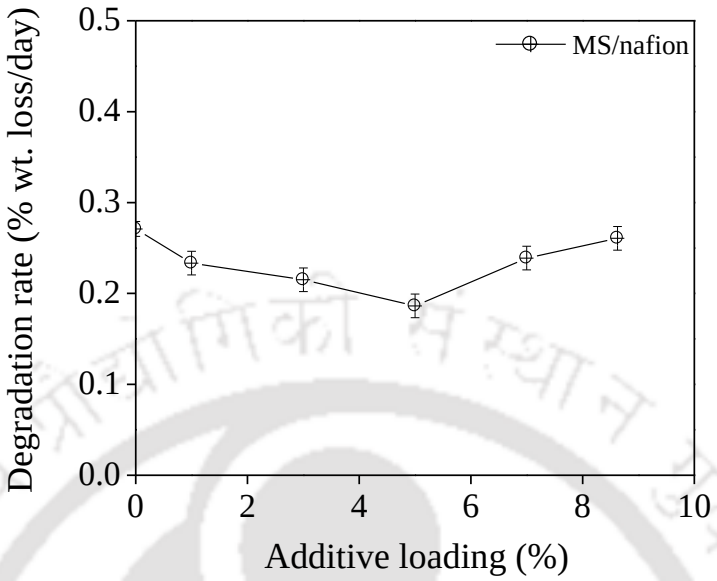

Fig. 4.37 Effect of MS loading on the oxidative stability of composite membranes

4.2.11. *Proton conductivity*

The proton conductivity of the fuel cell membrane is a key property that directly affects operational fuel cell voltage. Nafion membrane is a good proton conductor due to the presence of loosely held hydrogen ions (protons), which are attached to the fixed sulphonic acid sites, pending with the polymer chain. The protons along with the surrounded water molecules available in the membrane form hydronium ions and diffuse through the flooded pore channel of the membrane to contribute for the proton conductivity. Moreover, the protons also transport through hopping mechanism via hydronium, Zundel and/or Eigen ions [Kreuer, 2001, Barbora et al., 2009b]. Thus water is important for the transport of proton whether vehicular or hopping mechanism. Moreover, as these protons should be loosely held with the sulphonic acid groups, the IEC also plays an important role as discussed previously.

The replaceable characteristic of the hydrogen ion from the sulphonic site has been discussed in terms of the IEC (4.2.5). The fixed charged (SO_3^-) sites within the main polymer chain provide the centers where the moving ions (protons) can be accepted or released. In a polymer structure, maximizing the concentration of these charged sites is critical to ensure high conductivity. However, excessive addition of ionically charged side chains may significantly decrease the mechanical stability of the polymer, making it unsuitable for the fuel cell.

Usually the trend followed by proton conductivity is similar to IEC and water uptake. Nevertheless, this may not necessarily be the rule of thumb as increase in water uptake or ion exchange capacity may not necessarily increase the proton conductivity of the membranes. The IEC and water uptake contribute to proton conductivity by facilitating the transfer of protons while at the same time the connectivity of the ion exchange channels within the membrane is also crucial for effective proton conductivity [Kreuer, 2001]. Inclusion of additives in nafion changes the morphology of the membrane by changing the shape of the ionic cluster and water content, which subsequently result in variation of the proton conductivity of the composite membranes.

Figure 4.38 shows the effect of TiO_2, Nd_2O_3, and talc loading on the proton conductivity of the composite membrane. The proton conductivity of the composite membrane increases initially and then gradually decreases with the increase in the additives loading [Barbora et al., 2009a; Barbora et al., 2010]. The maximum proton conductivity varies with the loading of the additive for the nafion composites. The maximum proton conductivity of 0.127 S/cm is

obtained for 1% TiO_2/nafion membrane. Lvov et al., (2004) reported proton conductivity of 0.11 S/cm for 5% TiO_2/nafion membranes at 20 °C. It can be seen in the fig. 4.38 that Nd_2O_3 and talc nafion composites show the maximum proton conductivity of 0.119 S/cm and 0.113 S/cm, respectively, at 5% loading in the composite membrane.

Figure 4.39 and 4.40 show the similar pattern of proton conductivity for ErTfO/nafion, NdTfO/nafion, and MS/nafion composite membranes. The maximum proton conductivity of 0.123 S/cm and 0.101 S/cm is obtained for ErTfO/nafion (fig. 4.39) and MS/nafion (fig. 4.40) at 3% additive loading. However, it can also be seen that the proton conductivity of the NdTfO/nafion membrane sharply increases for the 1% NdTfO loading and on further increase in the NdTfO loading the proton conductivity increases marginally. Therefore, the maximum proton conductivity (0.113 S/cm) of the NdTfO/nafion membrane is considered at 1% NdTfO loading.

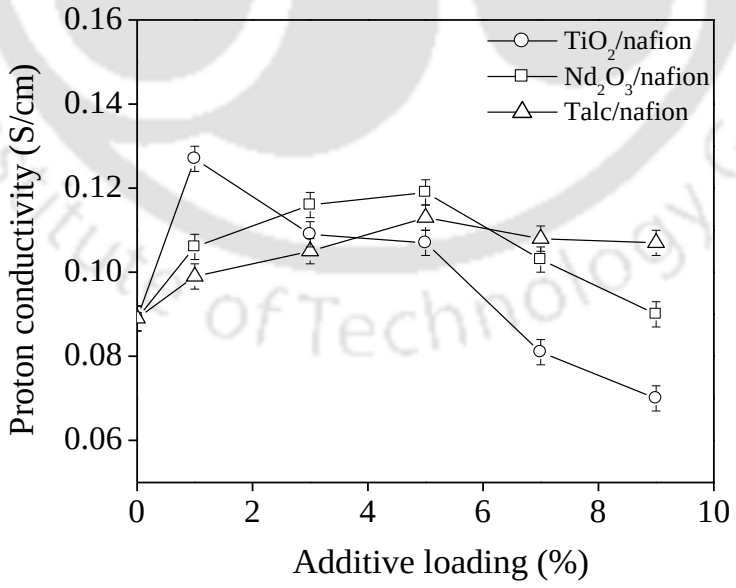

Fig. 4.38 Effect of TiO_2, Nd_2O_3, and talc on the proton conductivity of composite membranes

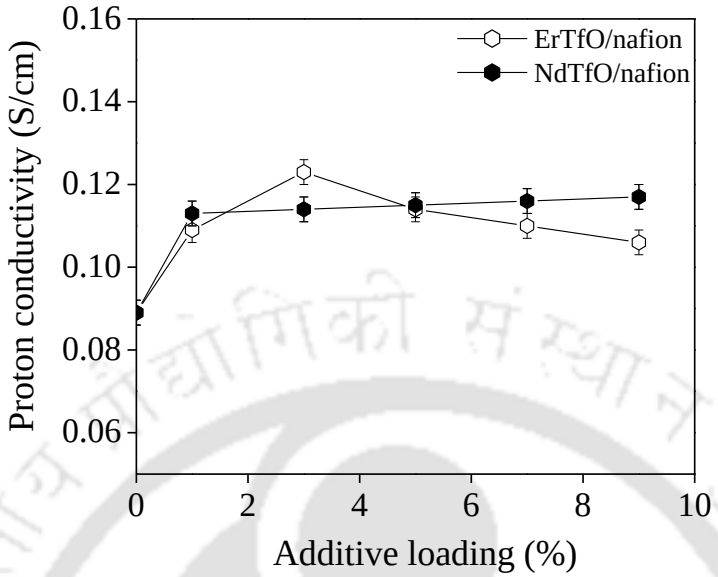

Fig. 4.39 Effect of ErTfO, and NdTfO on the proton conductivity of composite membranes

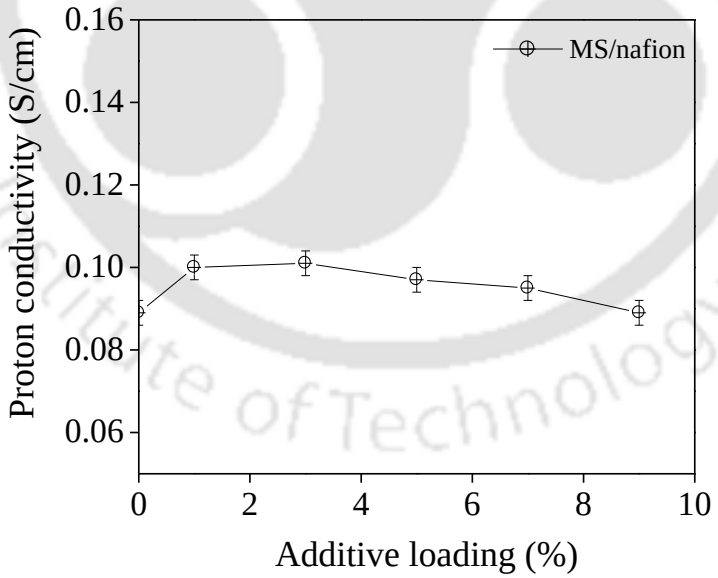

Fig. 4.40 Effect of MS on the proton conductivity of composite membranes

It is shown that the proton conductivity of the composite membrane increases upto a certain loading of the additive (except NdTfO/nafion composite). Beyond this optimum percentage of additive loading, the proton conductivity of the nafion composite drops. The probable reason is explained in the fig. 4.41. It can be seen that with the increase in additive amount beyond an optimum value, there might be some disruption in the continuum of hydrophilic channels or the sulfonic group clusters. Thus the proton movement either takes a longer path or the hindered movement results in the drop of the proton conductivity [Gierke, 1981]. Infact, on comparing the ion exchange capacity (fig. 4.19-4.21), water uptake (fig. 4.22-4.24), and proton conductivity (fig. 4.38-4.40) of the nafion composite membranes, it is noticed that higher water uptake does not inevitably result into higher proton conductivity. It is not only the total water uptake, but also the distribution of water between surface and hydrophilic channels of the membrane, which determines the effective proton conduction [Choi et al., 2005].

Fugure 4.42 shows the relative proton conductivity of the composite membranes with optimum loading of the various additives with pure cast nafion membrane. It is observed that 1% TiO_2/nafion membrane exhibited the highest proton conductivity and improved the proton conductivity of the pure cast nafion membrane by 43% followed by the nafion composite membrane with 3% ErTfO loading, which improved the proton conductivity of pure cast nafion membrane by 38%. The nafion composites with a loading of 5% Nd_2O_3 and 1% NdTfO improved the proton conductivity of pure cast nafion by 33.7% and 31.5%, respectively. Similarly, the nafion composites with 5% talc improved the proton conductivity of nafion by 27% and by 13.5% with MS loading of 3% [Barbora et al., 2012].

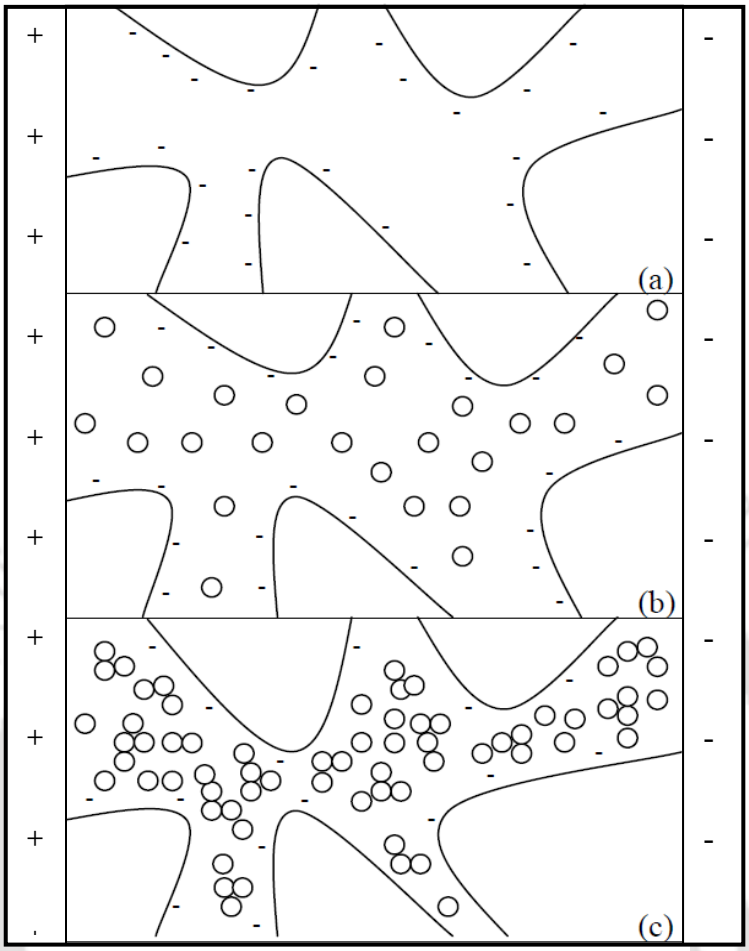

Fig. 4.41 Conceptual schematic of the pathway for proton conduction (positive electrode to negative electrode) in (a) pure cast nafion, (b) nafion composite with optimum additive loading, and (c) nafion composite beyond optimum additive loading

4.2.12. *Methanol crossover*

Methanol crossover (MCO) through the proton exchange membrane adversely affects the performance of the fuel cell due to polarization of the cathode. Therefore, a vital characteristic of the membrane in direct methanol fuel cell is to possess ideally no methanol crossover or very low methanol crossover.

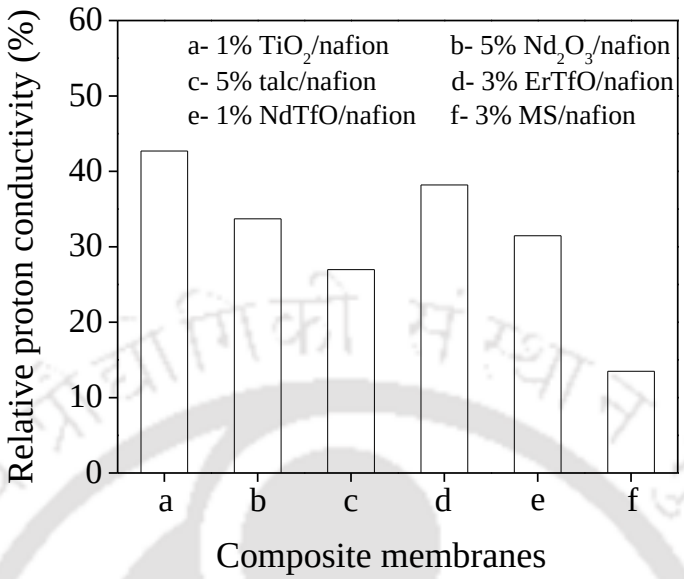

Fig. 4.42 Relative proton conductivity of composite membrane with respect to pure cast nafion membrane for optimum loading of TiO_2, Nd_2O_3, talc, ErTfO, NdTfO, and MS compared to pure cast nafion

Hence, MCO of pure cast nafion membrane and the nafion composite membranes was investigated with 1 M, 2 M, 3 M, and 4 M methanol solutions at 30 °C and compared to that of pure cast nafion membrane. Figures 4.43 to 4.48 show the MCO pattern using 1 M methanol solution for pure cast nafion and nafion composite membranes with various additives. Figure 4.43 shows the MCO for pure cast nafion membrane and nafion composite membranes with TiO_2, Nd_2O_3, and talc as the additive. As can be seen from the fig. 4.43, all the three types of nafion composite membranes could reduce the MCO as compared to the pure cast nafion membrane. The pattern followed is almost similar for all the composite nafion membranes. However, the optimum loading in terms of lowest MCO varied for each type of nafion composite. The 5% TiO_2/nafion decreased the MCO value by 75% (fig. 4.44)

compared to pure cast nafion membrane [Barbora et al., 2009a]. However, further increase in TiO_2 loading to 7% and 9% did not show significant improvement, which may be due to agglomerate formation of TiO_2 particles within the composite membrane as shown in SEM analysis. Figure 4.44 is a reproduction of data using fig. 4.43 for better clarity.

Similar to TiO_2/nafion membranes, the optimum loading for Nd_2O_3 in the Nd_2O_3/nafion membrane is 5%. The MCO is reduced by about 55% (fig. 4.44) at the loading of 5% Nd_2O_3 when compared to pure cast nafion membrane [Barbora et al., 2010]. This may be due to partial blocking of the hydrophilic channels present in the nafion or the reduction in ionic cluster size as a result of non-hydrogen bonding amongst the –OH groups on the surface of neodymium. Moreover, there is possibility of the change in pore channel microstructure of the composite membrane that might have resisted the crossover through the membrane [Kreuer, 2001]. Further increase in loading however led to an increase in methanol crossover, which may be attributed to the agglomeration of Nd_2O_3 particles as shown in SEM analysis (fig. 4.7).

It may be seen in the fig. 4.44 that the incorporation of talc into nafion polymer has significantly suppressed the MCO. A reduction of around 45% in MCO by 1% talc/nafion composite membrane was found as compared to pure cast nafion membrane. This may be attributed to the surface modification by the crystalline talc, which created obstruction in the flow channels of the composite membrane. The composite membrane with 1% talc loading exhibited the lowest crossover; the crossover increases with the talc loading above 1% but for all the studied compositions the crossover was lower than pure cast nafion membrane.

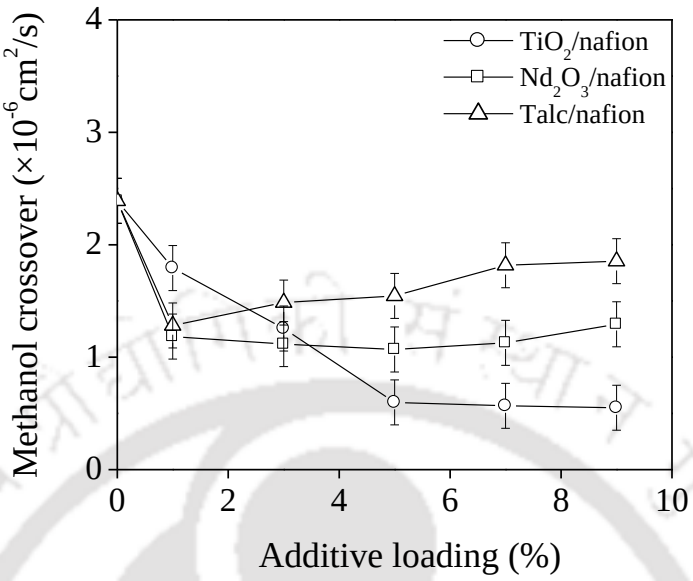

Fig. 4.43 Effect of TiO_2, Nd_2O_3, and talc loading on MCO of composite membranes

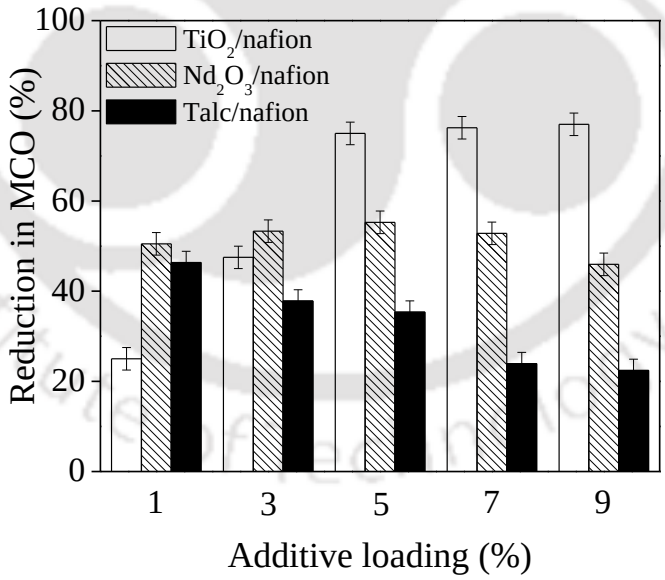

Fig. 4.44 Reduction in MCO of composite membrane at various loading of TiO_2, Nd_2O_3, and talc compared to pure cast nafion membranes

As can be seen from the SEM image, 1% talc/nafion membrane appears flaky (fig.4.8), which help to reduce the MCO. However, the MCO slowly increases due to non-uniform and agglomerated talc particles in the composite nafion membranes.

Figure 4.45 shows the MCO pattern of ErTfO/nafion and NdTfO/nafion composite membranes. The composite membrane with 1% ErTfO reduces the MCO by approximately 77.5% (fig. 4.46). This may be attributed to the reduced size of ionic clusters because of increased cross-linking within the ErTfO/nafion membranes, owing to the Er^{3+} ions forming coordination bond with the oxygen atom of SO_3^- group of both triflic acid as well as nafion matrix [Barbora et al., 2009b].

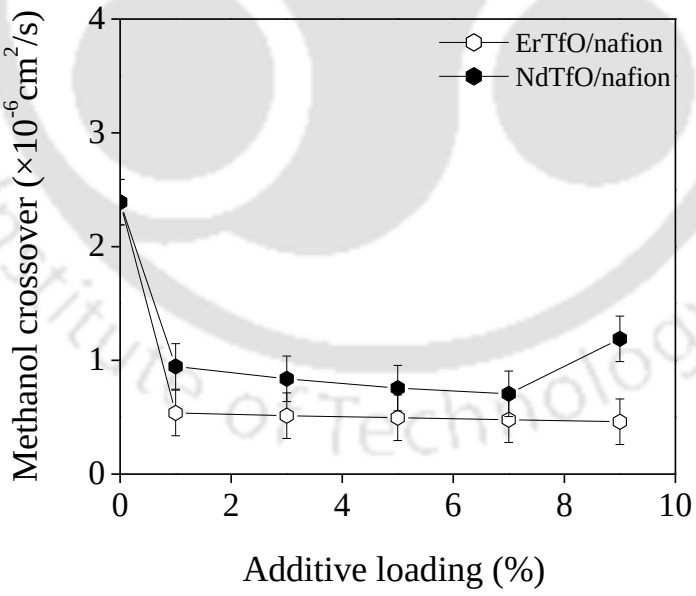

Fig. 4.45 Effect of ErTfO, and NdTfO loading on MCO of composite membrane

Thereafter, an increase in ErTfO loading decreased the MCO insignificantly, the maximum reduction in MCO being 80.75% for 9% ErTfO/nafion membrane as compared to nafion membrane. This behavior may be attributed to the denser composite membrane as a result of increased cross-linking and reduction of free space.

In case of NdTfO/nafion membranes, the methanol crossover is reduced by about 70.5% (fig. 4.46) at a loading of 7% NdTfO when compared to pure cast nafion membrane. The reduction in MCO using NdTfO is comparable to ErTfO, as both the additives are structurally similar except for the inorganic ions. Further increase in NdTfO loading did not exhibit marked difference. However, when loading was increased to 9% there was an increase in methanol crossover. It was observed during synthesis that the 9% NdTfO/nafion membrane shrank owing to intensive cross-linking, resulting in a smaller and thicker hard polymer membrane with increased thickness. As a result the 9% NdTfO/nafion membrane was synthesized at an annealing temperature of 110 °C instead of 165 °C (the temperature at which all the other membranes were synthesized) [Shroti et al., 2011]. It has been reported that membranes annealed at lower temperature has higher methanol crossover and vice-versa [Luan et al., 2008].

Figure 4.47 shows the MCO pattern of MS/nafion membranes. As can be seen from the figure, at 1% MS loading the MCO of pure cast nafion was reduced by around 25% (fig.4.48), which may be attributed to the size selective adsorbent property of the MS. However, increased MS loading showed increase in MCO, which may be due to the poor physical association of the polymer and additive due to agglomerate formation as was

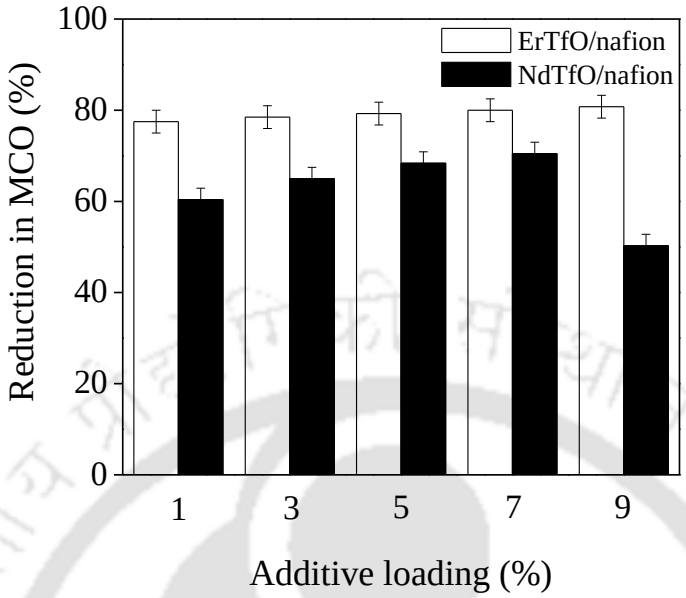

Fig. 4.46 Reduction in MCO of composite membrane at various loading of ErTfO, and NdTfO compared to pure cast nafion membrane

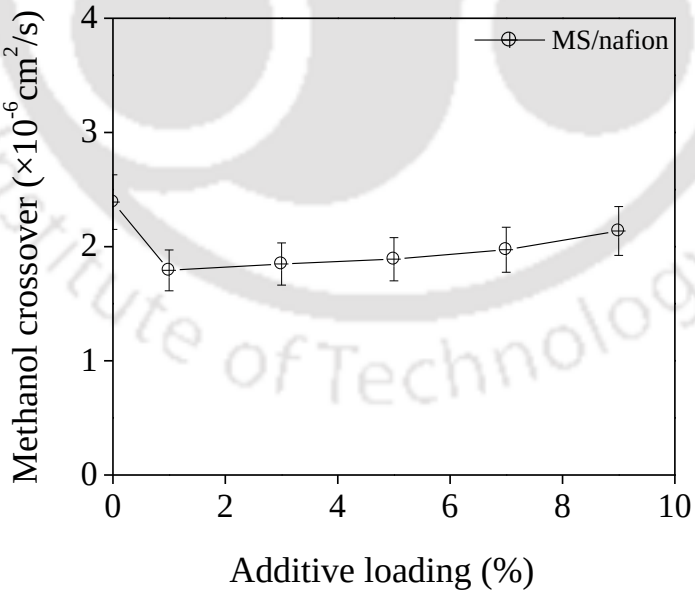

Fig. 4.47 Effect of MS loading on MCO of composite membranes

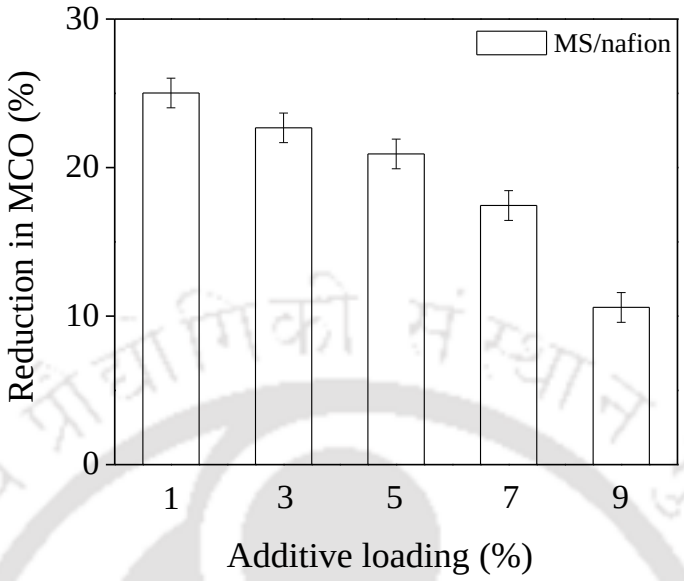

Fig. 4.48 Reduction in MCO of composite membrane at various loading of MS compared to pure cast nafion membrane

indicated by the SEM images. The decreasing tensile strength (fig. 4.33) of the MS/nafion membranes with increase in MS loading also indicates weak physical association between MS and nafion thus contributing to the effect.

Comparison of methanol uptake results (fig. 4.25 to 4.27) with MCO values (fig. 4.43, 4.45, 4.47) indicate that increase in methanol uptake not necessarily leads to an increase in MCO. The probable reason is that methanol has access to both the hydrophobic as well hydrophilic domains of the polymer. Hence, uptake accounts the methanol present in both hydrophobic as well as hydrophilic domains. MCO, on the other hand takes place primarily through the ionic clusters present in the hydrophilic domain.

The MCO of all the membranes have been tested with three more concentrations of methanol, which were 2 M, 3 M and 4 M and at three different temperatures (40, 60 and 80 °C) to investigate the effects at strong conditions. Figure 4.49 to 4.51 shows the effect of methanol concentration on the MCO of pure cast nafion membrane and the nafion composite membranes at 1% additive loading (representative results). It can be seen from the figures that increase in methanol solution concentration leads to an increase in MCO. The trend of MCO with 1 M methanol solution for pure cast nafion membrane and composite membrane with 1% loading of TiO_2, Nd_2O_3, and talc (fig. 4.49) is almost maintained at methanol solution of higher concentrations (2, 3, and 4 M). This may be attributed to the fact that the dominant factor for MCO through the membrane in the idle state is concentration gradient of the methanol across the membrane [Cruickshank and Scott, 1998].

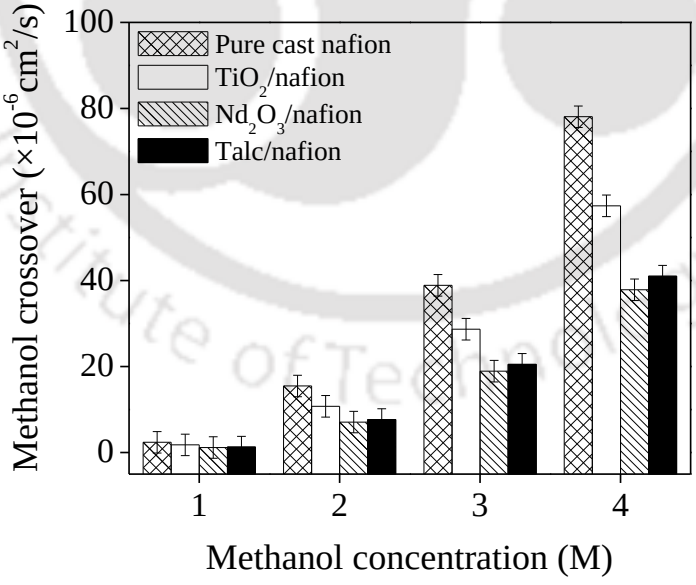

Fig. 4.49 Effect of methanol concentration on MCO of pure cast nafion and composite membrane with 1% loading of TiO_2, Nd_2O_3, and talc

Similar observations are visible for the composite membranes with ErTfO, NdTfO (fig. 4.50), and MS (fig. 4.51). The MCO of pure cast nafion membrane with 2 M, 3 M, and 4 M methanol solution increased by nearly 6.5 times, 16 times, and 33 times, respectively, compared to the MCO with 1 M methanol solution. The MCO rate of the membranes at 30 °C is a function of concentration of the methanol solution and increased almost proportionally for all the membranes when the concentration of the methanol solution was increased.

Figures 4.52 to 4.54 show the effect of temperature on MCO of pure cast nafion membrane and composite membrane with 1% loading of the additives (representative result). It can be seen that with an increase in temperature, MCO of the membranes also increases. This may be attributed to the enhanced rate of diffusion of methanol solution across the membrane with the increase in temperature [Nicotera et al., 2012]. Moreover, the solubility of water and methanol in the membrane increases with an increase in temperature, which increases the diffusion of methanol into the membrane, and thereby leads to an increase in MCO [Hansen, 2012]. For pure cast nafion membrane, the MCO increased by nearly 1.5 times, 3 times, and 4 times at 40, 60, and 80 °C, respectively, when compared to the MCO at 30 °C. A similar trend of increase in MCO is observed for the composite membranes with TiO_2, Nd_2O_3, talc, ErTfO, NdTfO, and MS, although the increase is slighter lower than that for pure cast nafion membrane, which may be attributed to the interference caused by the presence of the additives. Nevertheless, from the figures it may be inferred that with temperature variation in the idle state, the diffusion rate of the methanol solution is the dominant factor regulating the MCO across the membrane.

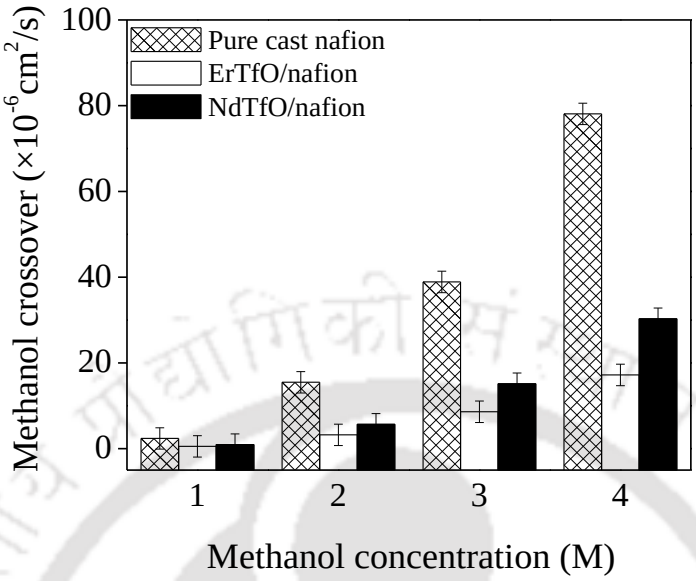

Fig. 4.50 Effect of methanol concentration on MCO of pure cast nafion and composite membrane with 1% loading of ErTfO, and NdTfO

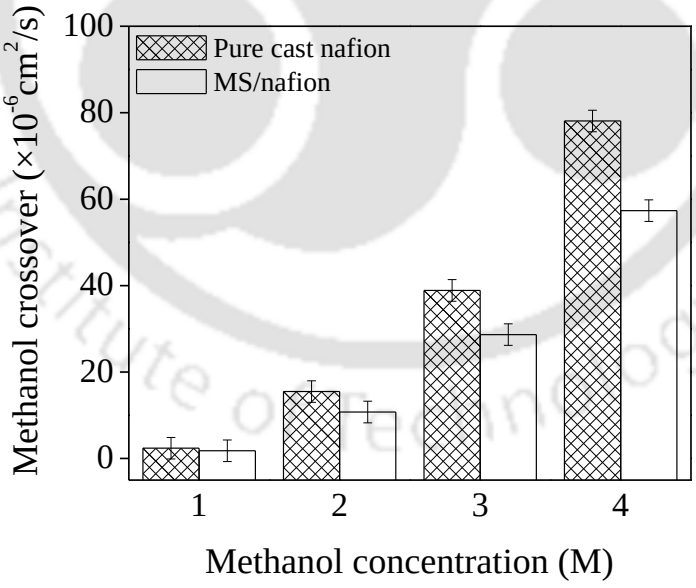

Fig. 4.51 Effect of methanol concentration on MCO of pure cast nafion and composite membrane with 1% loading of MS

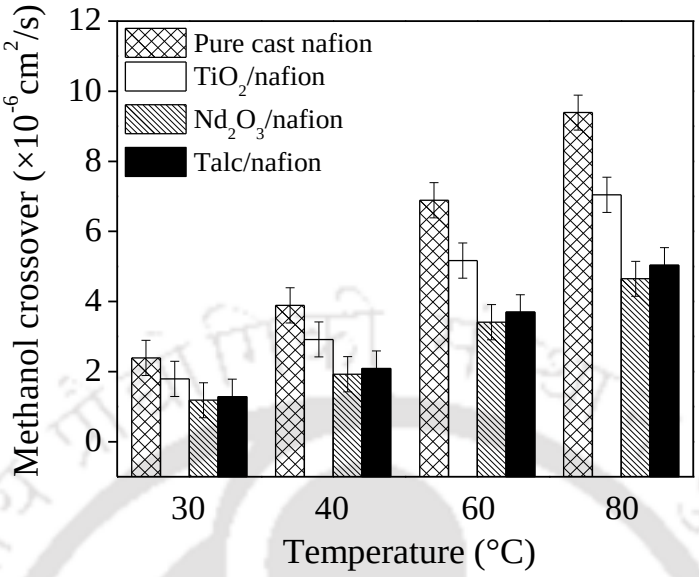

Fig. 4.52 Effect of temperature on MCO of pure cast nafion and composite membrane with 1% loading of TiO_2, Nd_2O_3, and talc

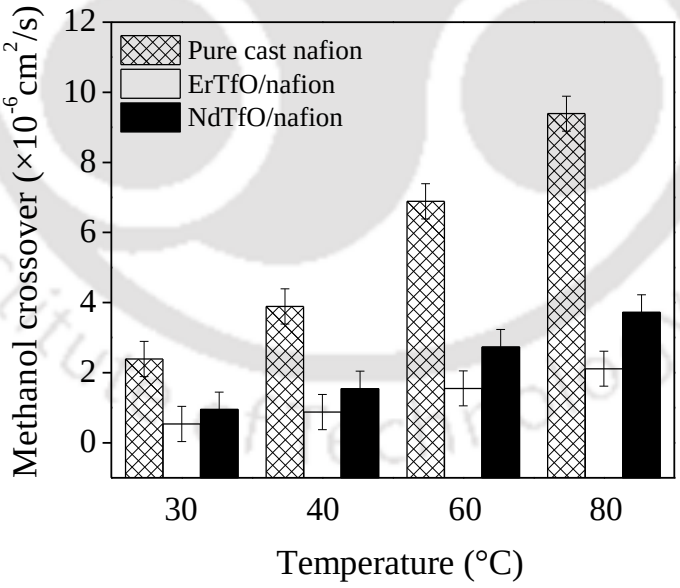

Fig. 4.53 Effect of temperature on MCO of pure cast nafion and composite membrane with 1% loading of ErTfO, and NdTfO

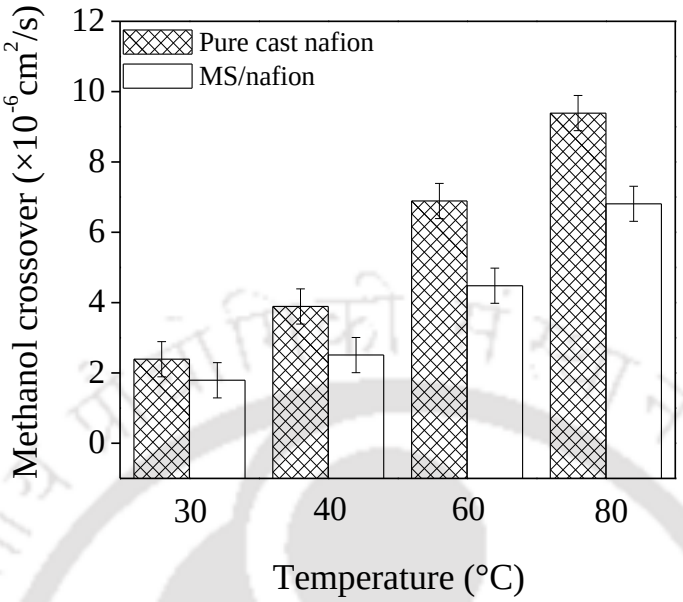

Fig. 4.54 Effect of temperature on MCO of pure cast nafion and composite membrane with 1% loading of MS

4.2.13. *Selectivity*

It has been discussed in the section 3.4.2.11 that selectivity (defined as the ratio of proton conductivity to MCO of the membrane) is the primary parameter to evaluate the suitability of the membrane in DMFC. Therefore, for better understanding, absolute selectivity (selectivity) as well as relative selectivity is shown and discussed in this section. It may be noted that for finding out the selectivity, 1 M methanol solution was used at 30 °C temperature (fig. 4.4.3, 4.45, and 4.47).

In fig. 4.55 the selectivity of composite membranes at different loading of TiO_2, Nd_2O_3, talc is evaluated. Moreover, the relative selectivity of the composite membranes with reference to pure cast nafion membrane is shown in fig. 4.56. The selectivity of 5% TiO_2/nafion

membrane is improved by 381% compared to pure cast nafion membrane followed by the composites with TiO_2 loading of 7% and 9%, which enhanced the selectivity by 283% and 243%, respectively. On the basis of the relative selectivity values, the potential TiO_2/nafion membranes would be the ones with TiO_2 loadings of 5, 7, and 9%. Nd_2O_3/nafion membranes with a loading of 5% improved the selectivity by about 199% compared to pure cast nafion, followed by 180% by the composite with 3% loading. 1% and 7% Nd_2O_3/nafion membranes showed a comparable relative selectivity of 143%. 1% talc/nafion enhanced selectivity of the composite membrane by about 110% followed by 3% and 5%, which enhanced the selectivity by about 80-90%.

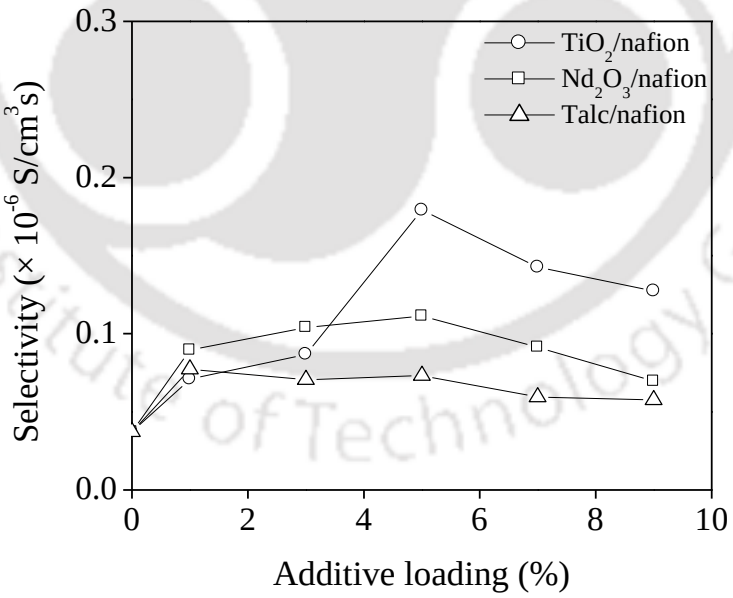

Fig. 4.55 Selectivity of pure cast nafion and composite membrane with various loading of TiO_2, Nd_2O_3, and talc

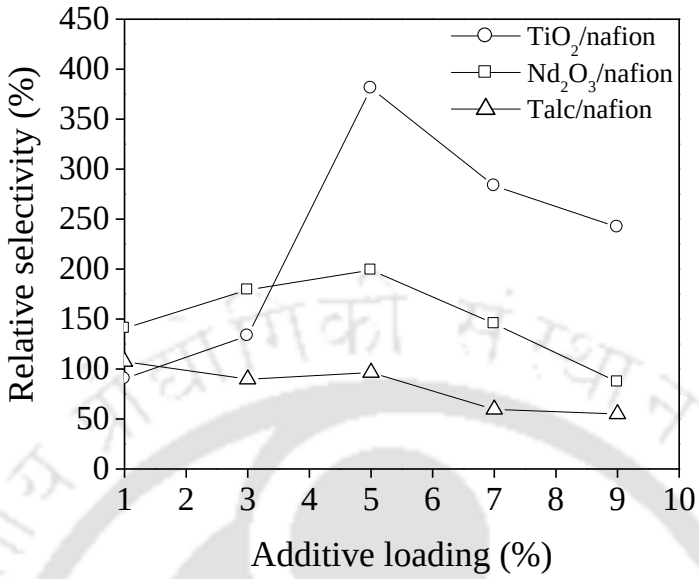

Fig. 4.56 Relative selectivity of composite membranes with respect to pure cast nafion membrane

The fig. 4.57 shows the selectivity of composite nafion membranes for ErTfO and NdTfO and fig. 4.58 shows their relative selectivities with respect to the pure cast nafion membrane. As can be seen from fig. 4.58, all the ErTfO/nafion membranes have a higher selectivity value and consequently much higher relative selectivity, which ranged in between 450% to 550% compared to pure cast nafion membrane. The 7% NdTfO/nafion membrane could enhance the selectivity of the composite membrane by about 340% compared to pure cast nafion membrane followed by the membranes with a loading of 5%, 3%, and 1% NdTfO, whose selectivity was more than pure cast nafion by 200-300%. The selectivity of 9% NdTfO/nafion membrane dropped drastically attributed to increased MCO as compared to the other composites of NdTfO (fig. 4.45).

Similarly, fig. 4.59 and fig. 4.60 show the selectivity and the relative selectivity for MS/nafion composite membranes. It can be seen that the MS/nafion membranes with a loading of 1% and 3% MS have higher selectivity (fig. 4.59), which is nearly 50% more than pure cast nafion membrane (fig. 4.60). On comparison of the selectivity of pure cast nafion with the best of each type of nafion composites, it is observed that ErTfO/nafion has the highest selectivity followed by TiO_2/nafion membranes with TiO_2 loading of 5, 7 and 9%. The high selectivity may be attributed to the sharp decrease in MCO by these nafion composite membranes relative to a moderate increase in proton conductivity. The selectivity of the best of NdTfO/nafion, Nd_2O_3/nafion, and talc/nafion composite membranes are nearly similar. However, the best selectivity shown by MS/nafion membrane is the lowest amongst all the nafion composites with various additives but nevertheless higher than that of pure cast nafion membrane.

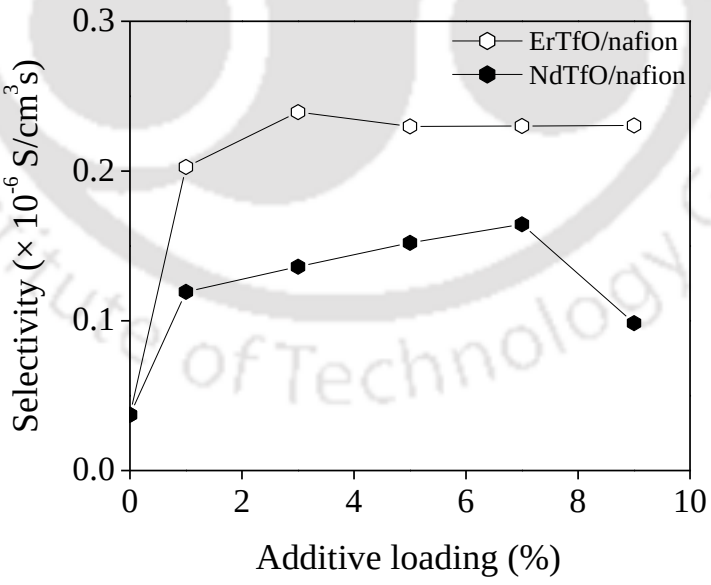

Fig. 4.57 Selectivity of pure cast nafion and composite membrane with various loading of ErTfO, and NdTfO

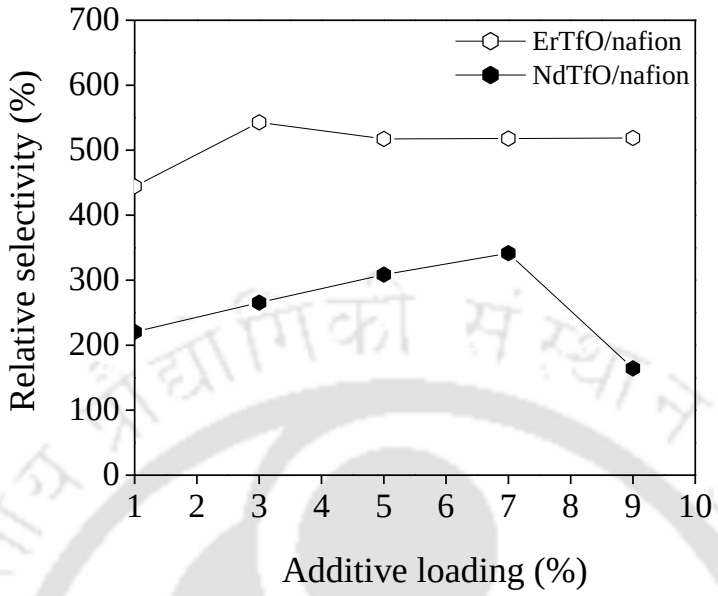

Fig. 4.58 Relative selectivity of composite membranes with respect to pure cast nafion membrane

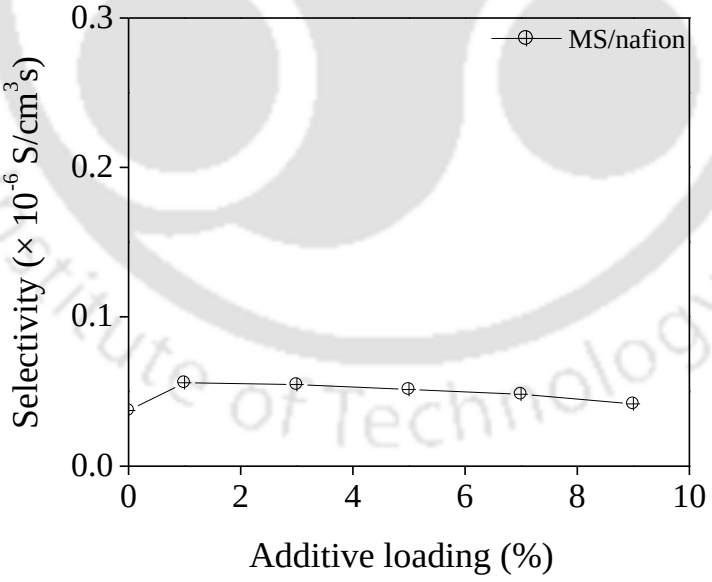

Fig. 4.59 Selectivity of pure cast nafion and composite membrane with various loading of MS

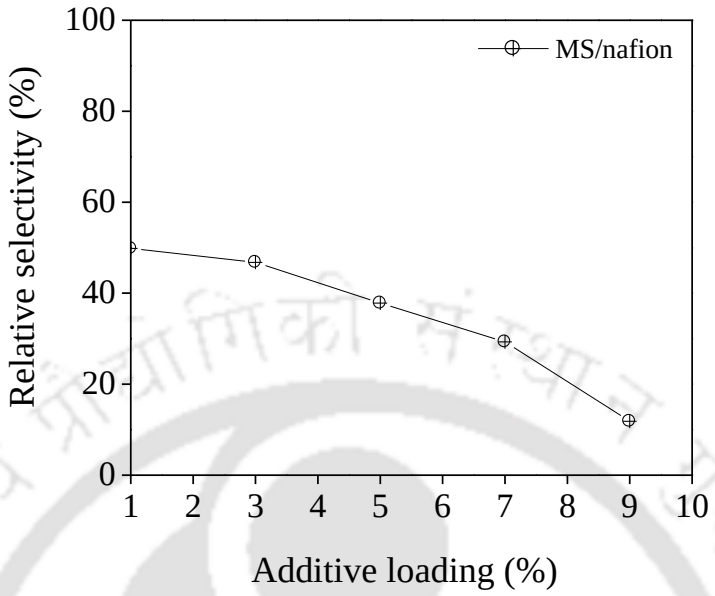

Fig. 4.60 Relative selectivity of composite membranes with respect to pure cast nafion membrane

It is essential to evaluate the performance of the membranes in DMFC environment for determining their potential for DMFC. Hence, the membranes have been further characterized by testing in a single DMFC test set-up with varying methanol concentration and at different operating temperatures. The DMFC performance of the membranes is discussed in the next section.

4.3 Performance evaluation of DMFC using membranes

4.3.1. *Effect of additive loading on DMFC performance*

Figures 4.61 to 4.72 show the DMFC performance in terms of OCV and characteristic curves for the pure cast nafion membrane and the composite nafion membranes at different loadings of TiO_2, Nd_2O_3, talc, ErTfO, NdTfO, and MS, respectively.

Open circuit voltage (OCV) has a direct relationship with the methanol crossover through the membranes. The higher the MCO, lower the OCV [Ye and Zhao, 2005]. Figure 4.61 shows a comparison of the OCV obtained in DMFC for pure cast nafion and TiO_2/nafion composite membranes along with the MCO of the membranes obtained under ex-situ conditions using 1 M methanol at 30 °C. Figure 4.61 shows the detrimental effect of MCO on OCV, which is attributed to the oxidation of crossed-over methanol at the cathode. A decrease in MCO value led to an increase in OCV.

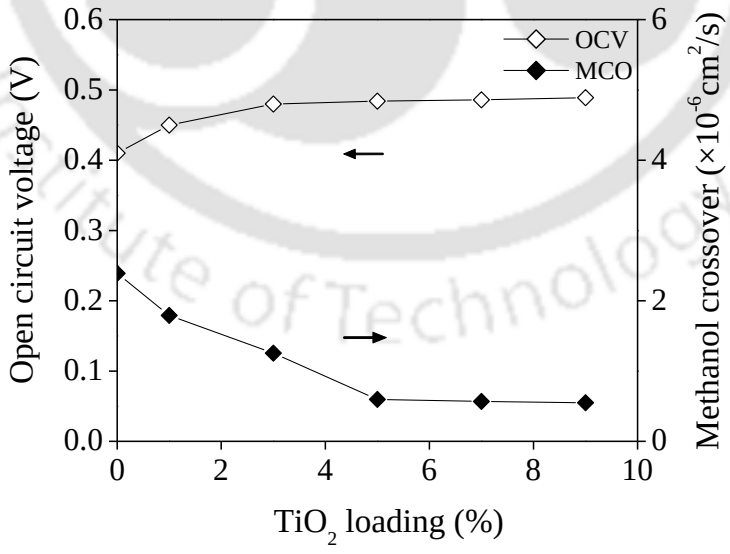

Fig. 4.61 Comparison of OCV, and MCO using membranes with various loading of TiO_2 at 30 °C using 1 M methanol at anode

Figure 4.62 shows the DMFC characteristic curves of TiO_2/nafion membranes along with that of pure cast nafion membrane. It can be seen that 5% TiO_2/nafion shows the highest power density (5.06 mW/cm^2) followed by 3% TiO_2/nafion (4.41 mW/cm^2). The power density generated by 1% TiO_2/nafion and 7% TiO_2/nafion is almost comparable. At a loading of 9% TiO_2, a decrease in performance is observed as compared to other composites. However, it may be seen that the performances of the composite are better than the pure cast nafion membrane. The highest performance is shown by 5% TiO_2/nafion owing to its maximum selectivity. However, the selectivity trend followed by other composites of TiO_2/nafion does not exactly follow the similar trend in fuel cell, which may be attributed to the proton conductivity and MCO pattern of these composites. Increase in selectivity may be either due to increase in proton conductivity or due to reduction in MCO of the membrane. The performance of the TiO_2/nafion composites almost follows the pattern of proton conductivity. Moreover, due to the higher proton conductivity, the ohmic resistance decreases and the fuel cell performance of the DMFC improves in the ohmic polarization region. Therefore, the maximum performance is achieved by the 5% TiO_2/nafion composite and the performance of the 9% TiO_2/nafion composite is slightly superior to the pure cast nafion membrane owing to the slightly improved selectivity. The lower proton conductivity of 9% TiO_2/nafion composite membrane than pure cast nafion membrane (fig. 4.38) suppressed the reduction (fig. 4.43) in MCO.

Figure 4.63 shows the variation of OCV and MCO with the change in Nd_2O_3 loading at 30 °C using 1 M methanol solution. It may be noted that the MCO, which is studied ex-situ, has

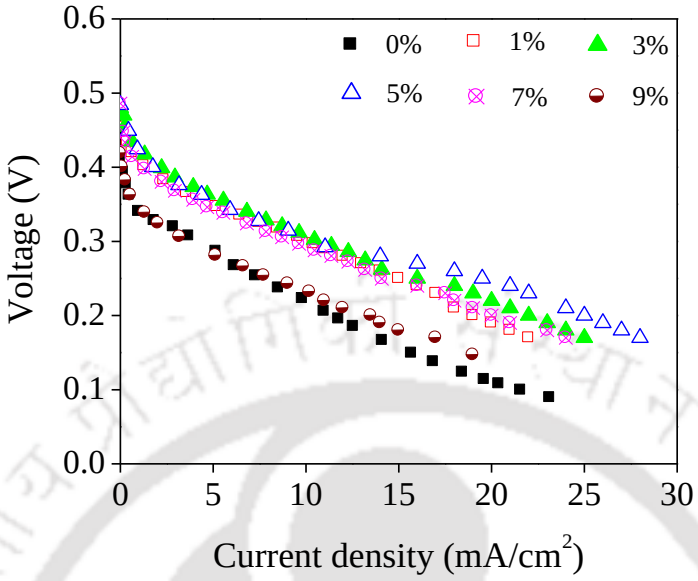

(a)

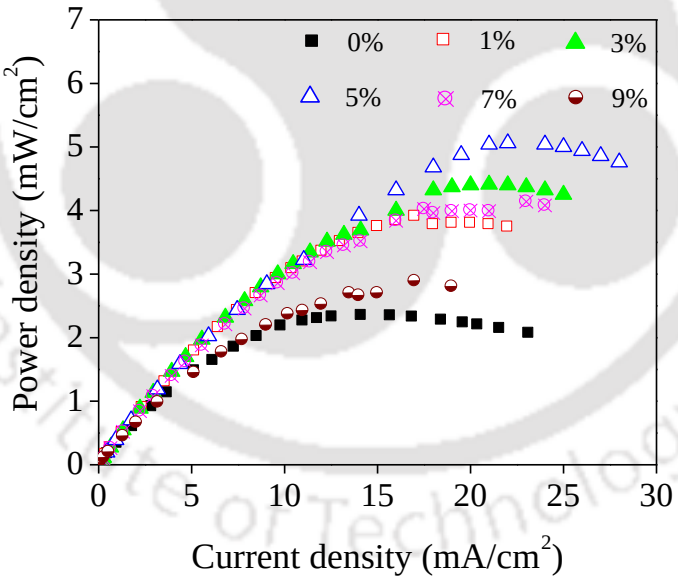

(b)

Fig. 4.62 DMFC performance curves for 1 M methanol (a) current density vs voltage, and (b) current density vs power density of membranes with various loading of TiO_2 at 30 °C

strong affect on the OCV of the DMFC. The OCV of the Nd_2O_3/nafion composite membranes increased from 1% to 5% Nd_2O_3 loading attributed to the decrease in MCO. However, with a loading of 7% and 9% Nd_2O_3, the MCO of the composite membranes slightly increased and consequently there was a decrease in the OCV owing to the oxidation of crossed-over methanol at the cathode. Nevertheless, the OCV of all the composite membranes are higher than pure cast nafion membrane.

Figure 4.64 shows a comparison of the DMFC performance of pure cast nafion membrane with Nd_2O_3/nafion composite membranes. Due to similarity in the proton conductivity values, the Nd_2O_3/nafion membranes with 1%, 3%, 5%, and 7% Nd_2O_3 exhibited nearly similar performance in the ohmic polarization region at lower current densities (fig. 4.64a).

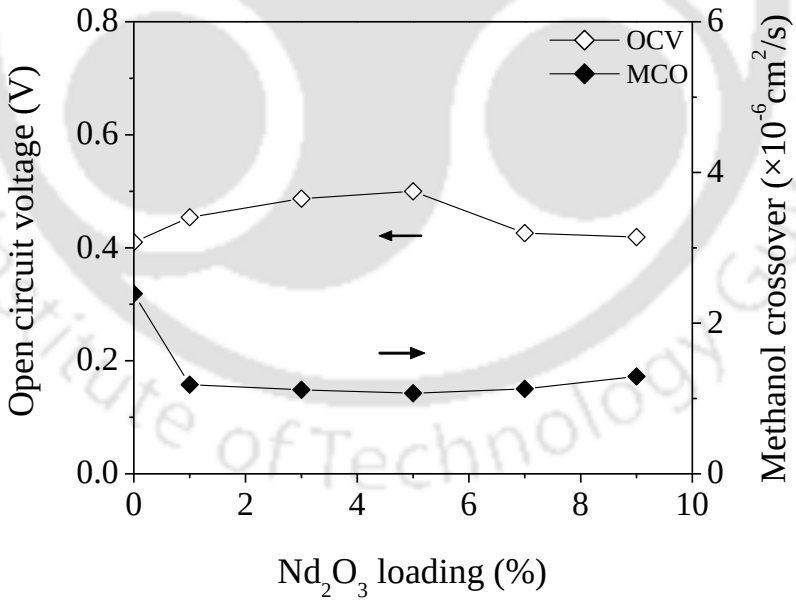

Fig. 4.63 Comparison of OCV, and MCO using membranes with various loading of Nd_2O_3 at 30 °C using 1 M methanol at anode

However, at higher current density, the later portion of the ohmic polarization changes for different composites. The performances shown by 1% and 3% Nd_2O_3 loading are quite comparable. The performance of Nd_2O_3/nafion membrane with 9% Nd_2O_3 and pure cast nafion membrane in the initial portion of the ohmic polarization region is almost similar but changes significantly at higher current density. At higher current densities, the performance is highest for the Nd_2O_3/nafion membranes with 3% Nd_2O_3 loading (4.84 mW/cm^2) followed by 1% Nd_2O_3 loading (4.56 mW/cm^2). The maximum power densities of Nd_2O_3/nafion membranes with 5% (3.80 mW/cm^2), and 7% Nd_2O_3 loading (3.61 mW/cm^2) are also almost similar, attributed to the comparative selectivity values. At higher current densities, the performance of the 9% Nd_2O_3/nafion membrane (4.08 mW/cm^2) is better than pure cast nafion membrane (2.33 mW/cm^2), and 5%, and 7% Nd_2O_3/nafion membranes. This may be due to reduced MCO of the composite membrane than pure cast nafion membrane and comparative selectivity values with that of 5%, and 7% Nd_2O_3/nafion composite membranes.

Figure 4.65 shows the additive loading on OCV and MCO for talc/nafion composite membranes at 30 °C using 1 M methanol solution. The composite membrane with 1% talc loading reduced the MCO by nearly 46% compared to that of pure cast nafion membrane. Further increase in talc loading could reduce the MCO compared to pure cast nafion membrane but the value was greater than that of 1% talc/nafion composite membrane. Hence the maximum OCV was obtained with 1% talc/nafion membrane. Beyond 1% talc loading, there is a gradual decrease in the OCV of the composite membranes attributed to the gradual increase in the corresponding MCO values.

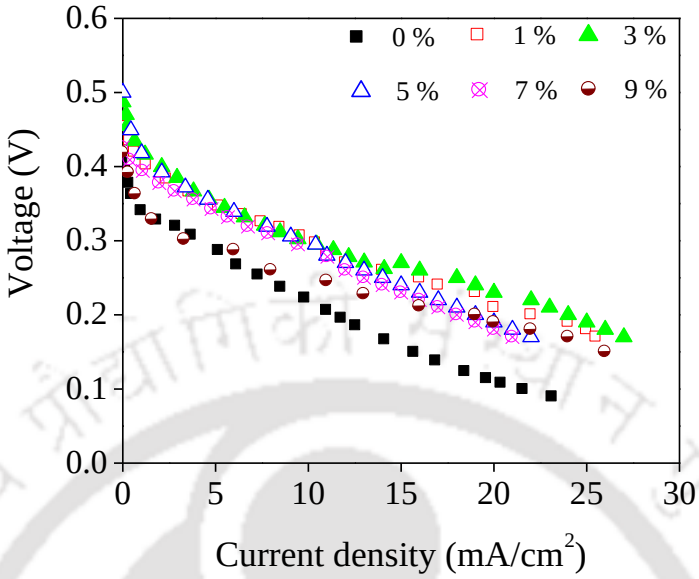

(a)

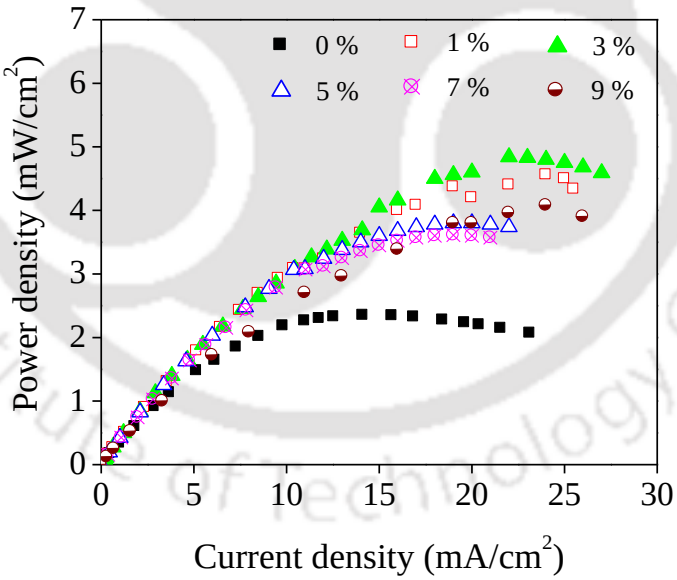

(b)

Fig. 4.64 DMFC performance curves for 1 M methanol (a) current density vs voltage, and (b) current density vs power density of membranes with various loading of Nd_2O_3 at 30 °C

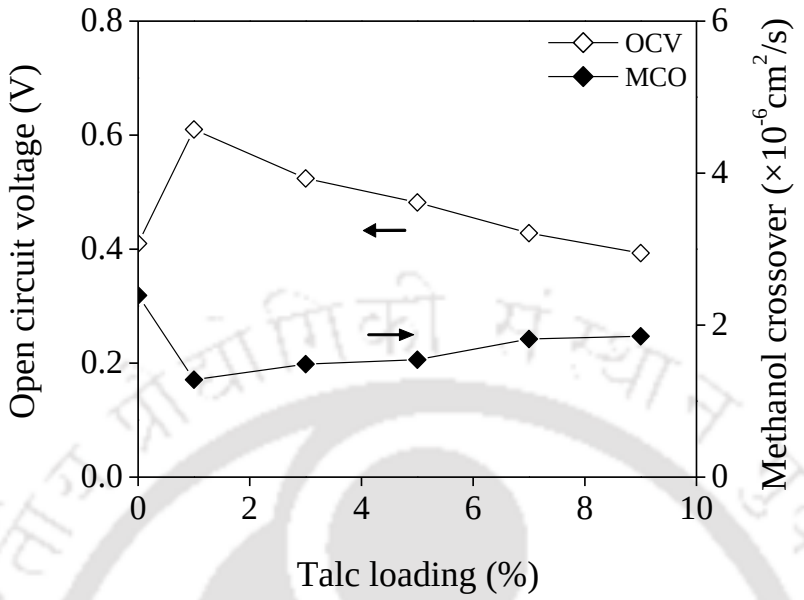

Fig. 4.65 Comparison of OCV, and MCO using membranes with various loading of talc at 30 °C using 1 M methanol at anode

Figure 4.66 shows the DMFC performance curves of talc/nafion composite membranes and that of pure cast nafion membranes for comparison. The nafion composite with 1% talc loading exhibited a marked increase in performance (7.98 mW/cm^2), which may be attributed to its better selectivity owing to its improved proton conductivity, reduced MCO, and the contribution of SiO_2 and MgO components of talc. Talc contains both SiO_2 and MgO. Improvement in fuel cell performance by composite nafion membranes containing SiO_2 as the additive have been reported by others and discussed in detail in chapter 2 of the thesis. Magnesium oxide (MgO), the other oxide in talc has been successfully used for modification of Pt/C catalyst for direct oxidation of ethanol in direct alcohol fuel cell (DAFC) [Xu et al., 2005]. It was found that the presence of MgO as an electrocatalyst improve the kinetic processes, giving the exchange current density of 1.8×10^{-2} mA/cm^2 for ethanol oxidation on

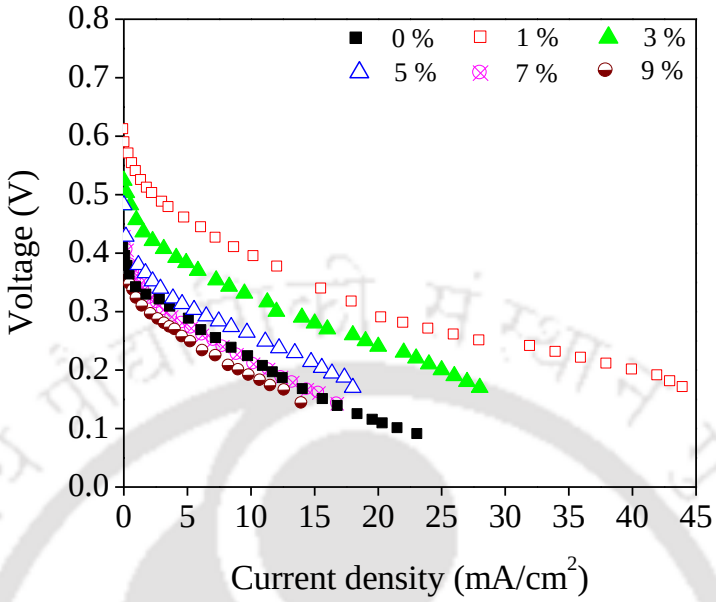

(a)

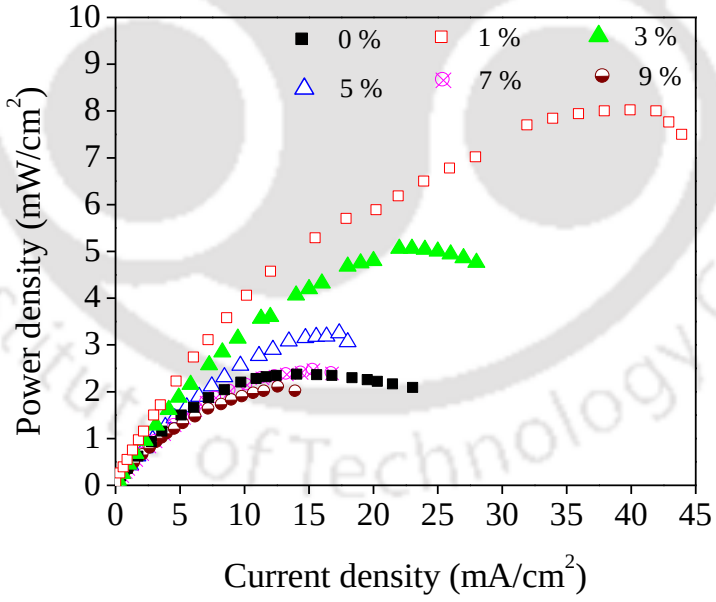

(b)

Fig. 4.66 DMFC performance curves for 1 M methanol (a) current density vs voltage, and (b) current density vs power density of membranes with various loading of talc at 30 °C

Pt–MgO/C instead of 3.3×10^{-4} mA/cm^2 on Pt/C. The best result was found on Pt–MgO/C electrode with Pt to MgO weight ratio of 4:1. The presence of the magnesium oxide in talc further reduced the poisoning effect of CO to the Pt catalyst during fuel cell performance with the talc modified nafion membranes. According to Xu et al., (2005), MgO plays a similar role as does Ru in Pt/Ru/C catalyst during alcohol oxidation by the bi-functional mechanism in DAFC. Platinum acts as the main catalyst for catalyzing the dehydrogenation of alcohol during the oxidation reaction and oxygen-containing species (OH_{ads}) can be formed on the MgO surface, similar to Ru surface, at lower potentials. These oxygen-containing species react with CO-like intermediate species on Pt surface to release the active sites for further alcohol oxidation [Prabhuram and Manoharan, 1998].

Inspite of the above positive effects of talc as an additive and the high proton conductivity values and reduced MCO values of the talc nafion membranes compared to pure cast nafion membrane, the fuel cell performance of talc/nafion membranes beyond 1% talc loading gradually decreased and 9% talc/nafion membrane showed inferior performance (2.09 mW/cm^2) to pure cast nafion membrane (2.33 mW/cm^2). SEM images of talc powder show its falky nature (fig. 4.2c). At lower percentage of loading (say 1%), the talc particles might have been distributed uniformly and in plane of the composite membrane with no overlapping, which may be the reason that the talc/nafion membrane with 1% talc loading exhibited the lowest MCO. Further increase in talc loading results in an increase in MCO (fig. 4.43), which may be due to overlapping and agglomeration of talc particles causing tilting of the flaky particles and thus facilitates MCO and might have also contributed to some extend of percolation in fuel cell operating conditions. Thus, there was a gradual

decrease in the fuel cell performance, when talc loading increased beyond 1%. The contribution of higher proton conductivity values and lower MCO is suppressed as a result.

Figure 4.67 shows the effect of ErTfO loading on OCV and MCO of ErTfO/nafion composite membranes. Modification of nafion with ErTfO led to a remarkable reduction in the MCO values of the composite membranes and hence a marked increase in the OCV values for all the ErTfO/nafion composite membrane is observed.

Figure 4.68 shows the DMFC performance curves of pure cast nafion and ErTfO/nafion membranes. The ErTfO/nafion composite membranes show markedly better performance than pure cast nafion membrane attributed to the excessive reduction of MCO by these composite membranes. It can be seen that the relative selectivity (fig. 4.58) of ErTfO is significantly increased as compared to pure cast nafion membrane. It is due to the high proton conductivities and low MCO shown by the ErTfO/nafion membranes as compared to pure cast nafion membrane. Thus the overall performance of the ErTfO/nafion composite membranes is significantly high. The maximum power density is obtained with 5% ErTfO/nafion membrane (8.02 mW/cm^2) followed by the composite membranes with 3% (7.52 mW/cm^2), 1% (7.31 mW/cm^2), and 7% (7.31 mW/cm^2) ErTfO loading. The membrane with 9% ErTfO loading shows a slight reduction in power density (6.02 mW/cm^2) attributed to the reduction in the proton conductivity.

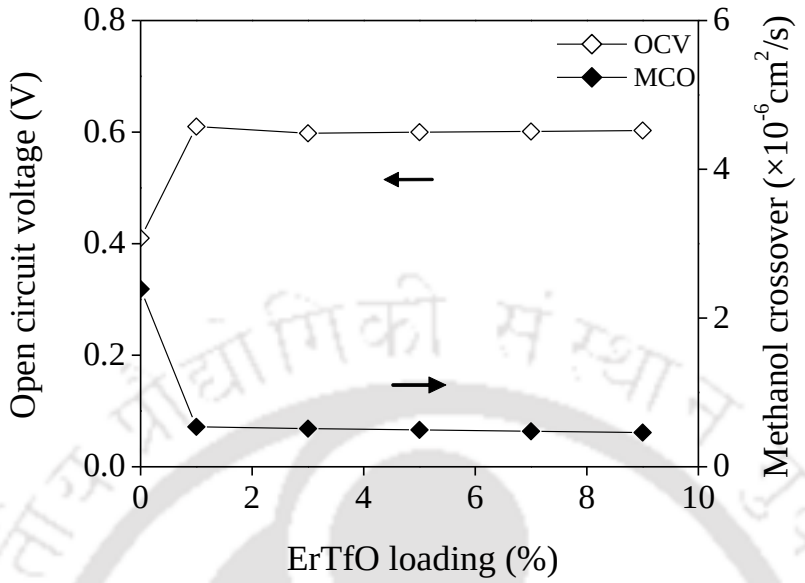

Fig. 4.67 Comparison of OCV, and MCO using membranes with various loading of ErTfO at 30 °C using 1 M methanol at anode

Figure 4.69 shows the effect of NdTfO loading on OCV and MCO of NdTfO/nafion composite membranes, which is being compared to that of pure cast nafion membrane. Modification of nafion with NdTfO decreased the MCO of the composite membranes compared to pure cast nafion membrane upto NdTfO loading of 7%, consequently resulting in improved OCV values. However, the nafion composite with 9% NdTfO loading exhibited increased MCO (fig. 4.45) as discussed in section 4.2.12., and thereby resulting in reduced OCV values.

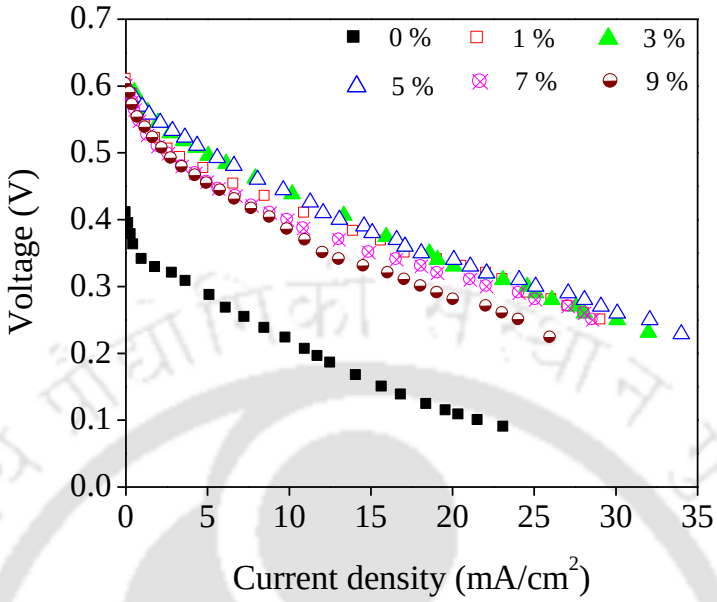

(a)

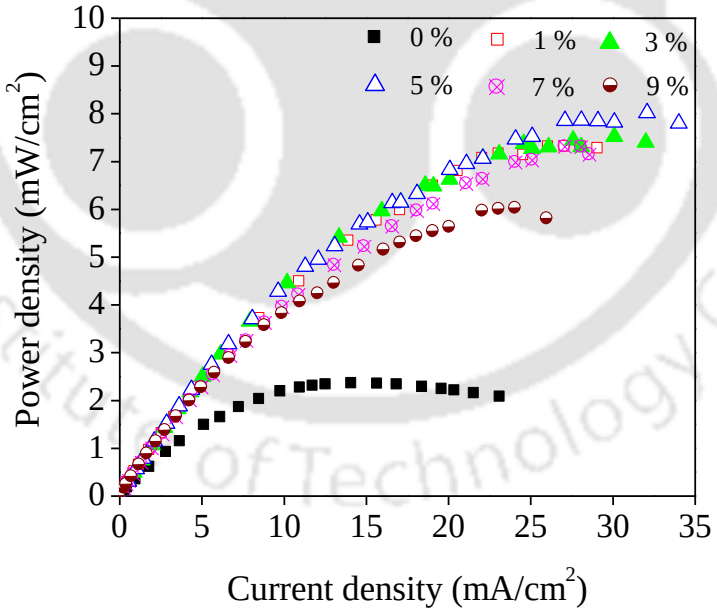

(b)

Fig. 4.68 DMFC performance curves for 1 M methanol (a) current density vs voltage, and (b) current density vs power density of membranes with various loading of ErTfO at 30 °C

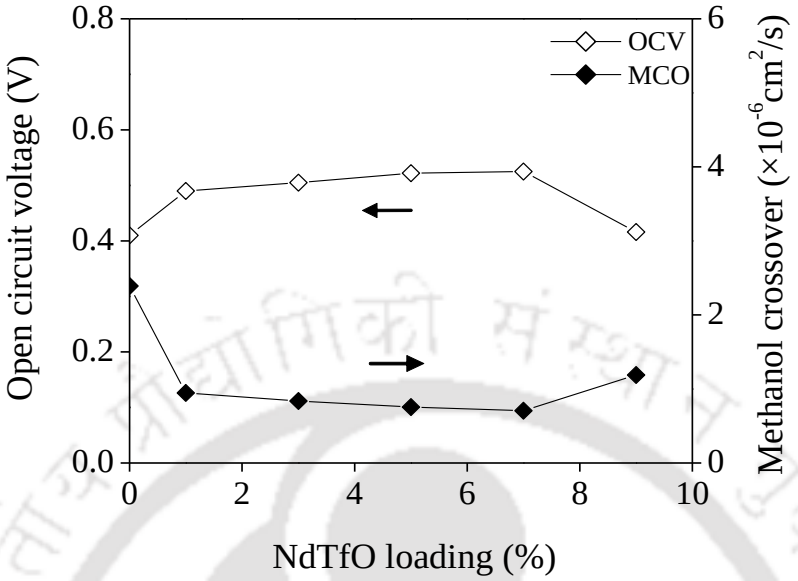

Fig. 4.69 Comparison of OCV, and MCO using membranes with various loading of NdTfO at 30 °C using 1 M methanol at anode

Figure 4.70 shows a comparison of the DMFC performance of NdTfO/nafion membranes with pure cast nafion membrane. The improved performance of the NdTfO/nafion membranes with 1%, 3%, 5%, and 7% NdTfO loading followed a trend almost similar to the improvement in proton conductivity as well as decreased MCO of the composite membranes. It can be seen in the fig. 4.70a that the 3% NdTfO/nafion membrane shows the highest performance (6.13 mW/cm^2), followed by NdTfO/nafion membrane with NdTfO loading of 5% (5.64 mW/cm^2), 7% (4.62 mW/cm^2), and 1% (4.17 mW/cm^2). The performance of the membrane with 9% NdTfO loading (2.55 mW/cm^2) was almost similar to pure cast nafion membrane (2.33 mW/cm^2) attributed to enhanced MCO of 9% NdTfO/nafion composite membrane.

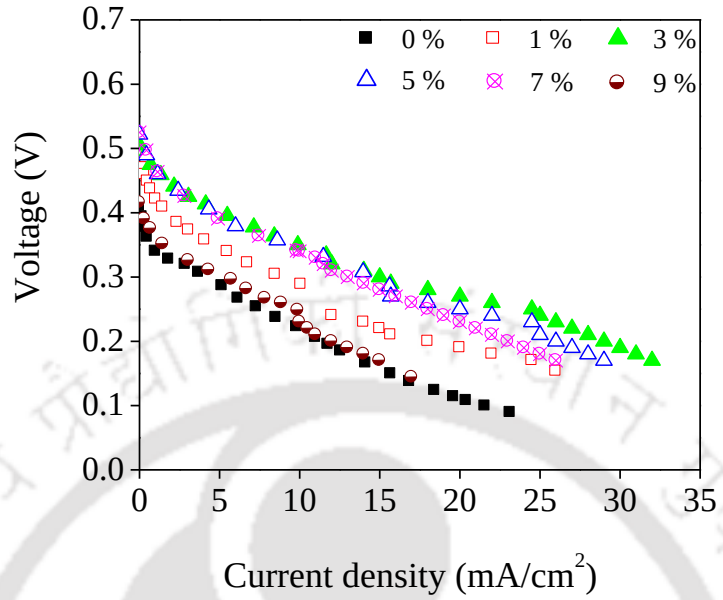

(a)

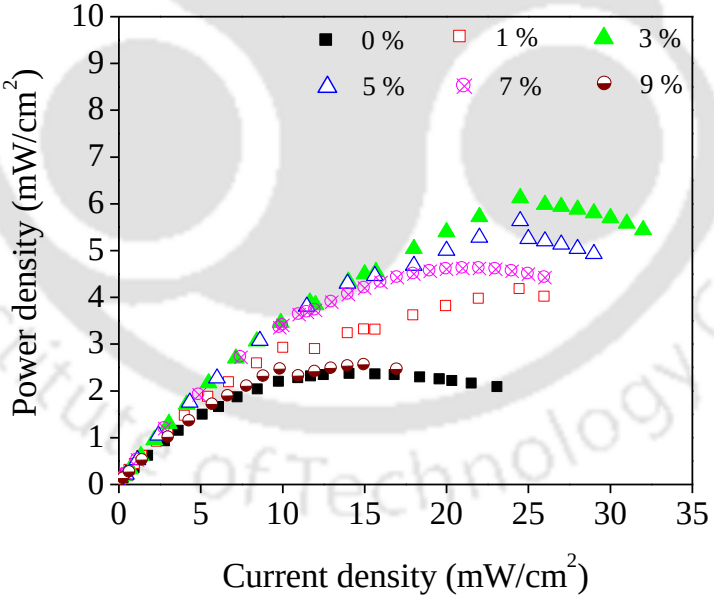

(b)

Fig. 4.70 DMFC performance curves for 1 M methanol (a) current density vs voltage, and (b) current density vs power density of membranes with various loading of NdTfO at 30 °C

Figure 4.71 shows the MS loading vs OCV and MCO plots of the composite membranes, which is being compared to that of pure cast nafion membrane. MS/nafion membrane with a loading of 1% MS could reduce the MCO by nearly 25% attributed to the size selective property of MS. However, increase in MS loading beyond 1% could not reduce the MCO of the composite membranes further, attributed to the poor physical compatibility of MS with nafion as discussed previously. Thus, the OCV of 1% MS/nafion membrane was the highest followed by a gradual decrease in the OCV for the composite membranes with higher percentage of MS loading.

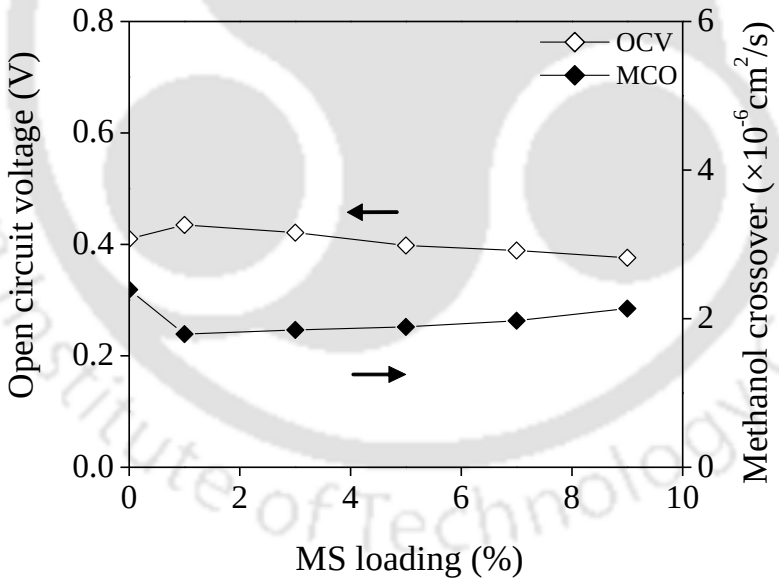

Fig. 4.71 Comparison of OCV, and MCO using membranes with various loading of MS at 30 °C using 1 M methanol at anode

Figure 4.72 shows the DMFC performance of MS/nafion membranes with varying percentage of MS loading compared with that of pure cast nafion membrane. As expected, MS/nafion membranes could inhibit MCO reflected by the improved performance of the composites with lower percentage of loading. However, as already discussed in section 4.2.12, due to formation of agglomerates, MS/nafion composites of high quality in terms of physical indication could not be obtained, which was found in the SEM images (fig. 4.11). The increase in MCO of the composites with higher percentage of loading also further confirmed the supposition. However, for lower MS loadings, the slight improvement in proton conductivity and slight reduction of MCO influenced the performance of MS/nafion composites. Therefore, 1% MS/nafion composite showed better performance as compared to pure cast nafion membrane. The other compositions could also improve the performance, especially at higher current densities. Maximum power density could be obtained with 1% MS/nafion membrane (4.08 mW/cm^2) followed by the composite with 3% MS loading (3.76 mW/cm^2). The slight improvement in performance was found for the composites with 5% (3.40 mW/cm^2), 7% (3.76 mW/cm^2), and 9% MS loading (3.06 mW/cm^2) over pure cast nafion membrane (2.33 mW/cm^2).

Figure 4.73 shows the DMFC performance curves for the best performing composite membranes in DMFC using TiO_2, Nd_2O_3, and talc additives and compared with the pure cast nafion membrane. It can be seen that the 1% talc/nafion membrane generated the maximum power density followed by 5% TiO_2/nafion, and 3% Nd_2O_3/nafion membranes. However, the performances of 5% TiO_2/nafion and 3% Nd_2O_3/nafion are almost similar. The selectivity

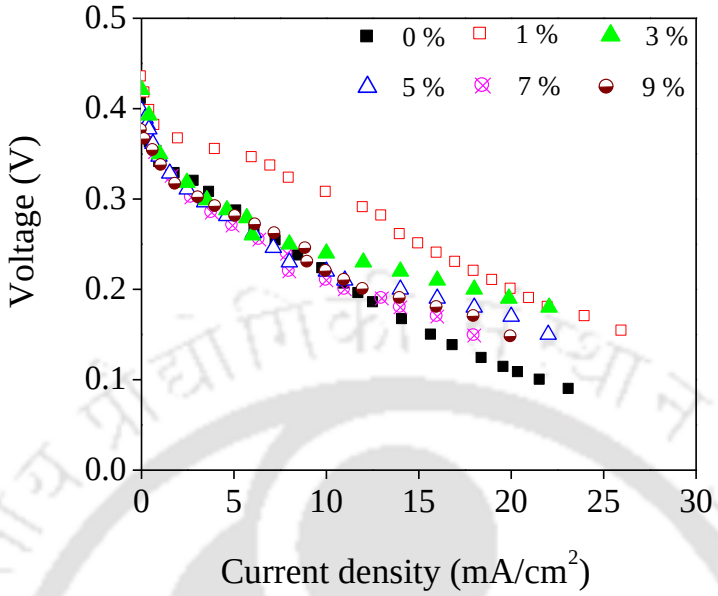

(a)

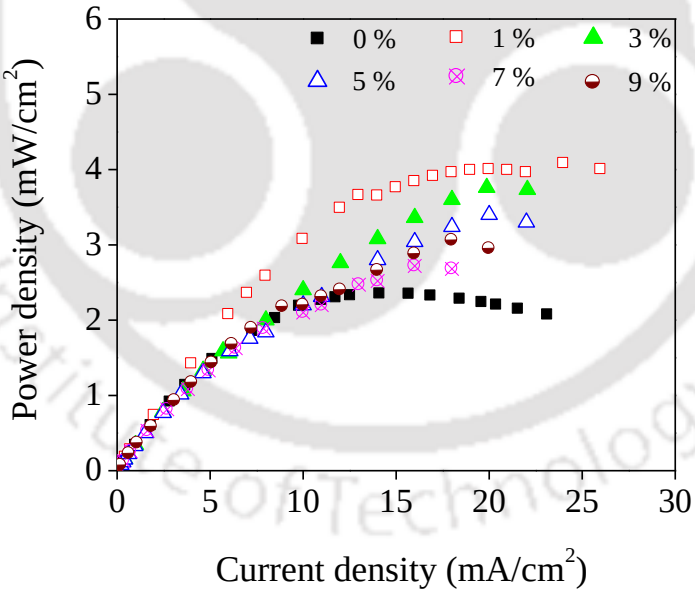

(b)

Fig. 4.72 DMFC performance curves for 1 M methanol (a) current density vs voltage, and (b) current density vs power density of membranes with various loading of MS at 30 °C

values of 5% TiO_2/nafion membrane were comparatively higher than that of 3% Nd_2O_3/nafion attributed to reduced MCO. However, the fuel cell performance of 5% TiO_2/nafion and 3% Nd_2O_3/nafion are almost at par with each other and may be attributed to the other factors governing fuel cell performance like methanol uptake, membrane swelling, and proton conductivity, which was inferior for TiO_2/nafion membranes compared to Nd_2O_3/nafion membranes (fig. 4.26, 4.29, 4.38). The exceedingly superior performance by the 1% talc/nafion membrane may be justified by the fact that in addition to high proton conductivity and reduced MCO, using talc/nafion composite membrane has the additional advantage of methanol oxidizing capability as discussed previously.

Figure 4.74 shows the DMFC performances for the best performing composite membrane in DMFC using ErTfO and NdTfO. The MCO of 5% ErTfO/nafion is lower than 3% NdTfO/nafion membrane and thus exhibited higher OCV. The performance of 5% ErTfO/nafion is better than 3% NdTfO/nafion, which may be attributed to the higher selectivity of 5% ErTfO/nafion membranes compared to 3% NdTfO/nafion membranes (fig. 4.57 and fig. 4.58). The similar comparison for MS/nafion membrane is already shown in fig. 4.72 and thus not being reported here.

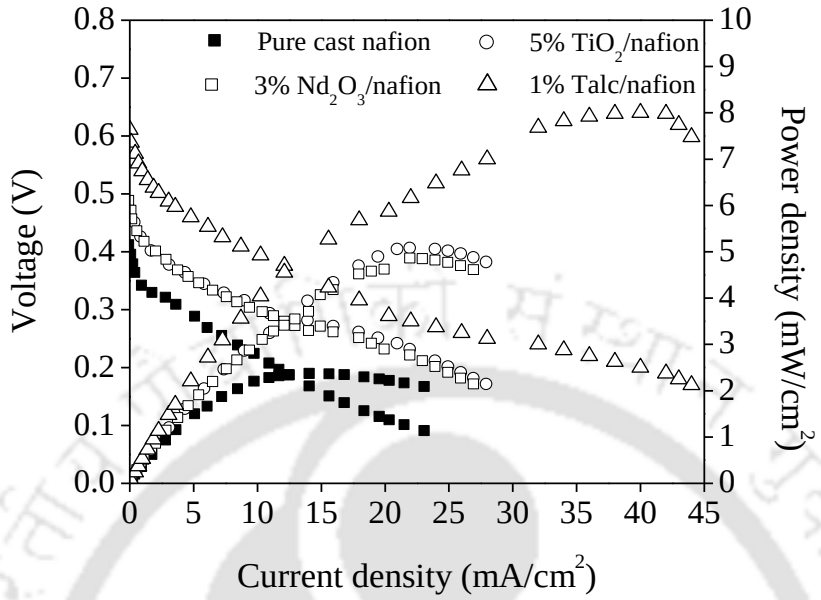

Fig.4.73 Comparison of DMFC performances of pure cast nafion membrane and nafion composite membranes using TiO_2, Nd_2O_3 and talc

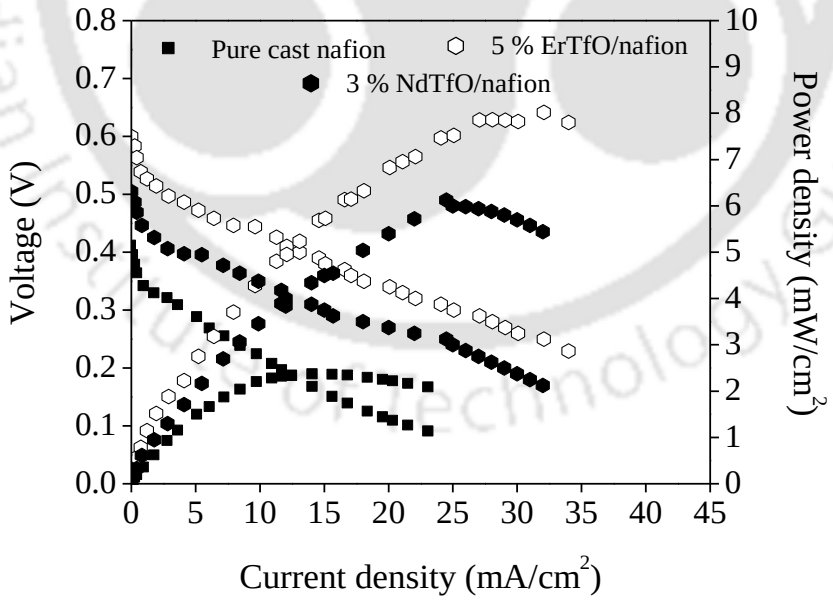

Fig.4.74 Comparison of DMFC performances of pure cast nafion membrane and nafion composite membranes using ErTfO and NdTfO

4.3.2. *Effect of methanol concentration on DMFC performance using composite nafion membranes*

The effect of methanol concentration on MCO has already been discussed in section 4.2.12 (figs 4.49, 4.50, and 4.51). It is observed that increase in methanol concentration leads to an increase in the MCO attributed to the increased concentration gradient of methanol across the membrane. The crossed-over methanol to the cathode side not only reduces the fuel utilization but also depresses the cathode potential as well as poisons the cathode electrocatalyst [Ye and Zhao, 2005]. Moreover, the permeated methanol on the cathode reacts electrochemically with oxygen at Pt-based oxygen reduction electrocatalyst, leading to the consumption of oxygen even under open-circuit conditions [Wang et al., 1996]. Therefore, in this section, the effect of methanol concentration on DMFC performance is studied with pure cast nafion membrane and nafion composites with the best combination of each additive.

Figure 4.75 to 4.81 shows the performance curves of pure cast nafion and the nafion composites using methanol solution concentrations varying from 1 to 4 M at 30 °C. The OCV of the cell at different methanol concentrations along with the maximum power density attained is summarized in table 4.8. It may be observed that an increase of methanol solution concentration leads to a drop in the OCV because of increase in MCO from anode to the cathode leading to reduction in the O_2 reduction performance at the cathode and creation of a larger mixed overpotential on the cathode [Umeda et al., 2011]. However, on comparison of the power densities, it is observed that increased methanol concentration increases the power density, which may be attributed to increase in temperature at the local site on the electrode

due to exothermic reaction of oxygen reduction at the cathode [Chen and Yang, 2003]. Thus, for each membrane the maximum power density is obtained at a higher methanol concentration in all cases. However, it may be noted that the increase in the DMFC performance at higher methanol concentration is not appreciable. The increment does not follow the methanol concentration increament. The reason is that, higher the methanol concentration, higher is the methanol crossover. The increased MCO has severe detrimental effect on the DMFC performance and suppresses the advantages of using higher methanol concentration. Table 4.8 shows that amongst the composite membranes the maximum power density of 11.33 mW/cm^2 is obtained with 1% talc/nafion followed by 5% ErTfO/nafion membrane (9.31 mW/cm^2), and 3% NdTfO/nafion membrane (7.42 mW/cm^2). The power densities of 5% TiO_2/nafion (6.60 mW/cm^2), 3% Nd_2O_3/nafion (6.36 mW/cm^2), and 1% MS/nafion (5.38 mW/cm^2) are comparable.

In order to further evaluate the effect of temperature, the DMFC performance is evaluated at higher temperature as discussed in the subsequent section.

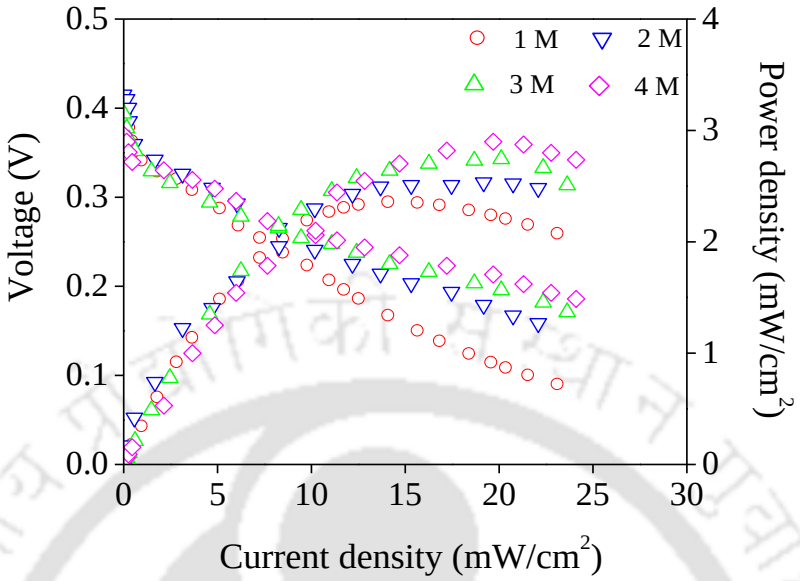

Fig. 4.75 Effect of methanol concentration on DMFC performance with pure cast nafion membrane at 30 °C

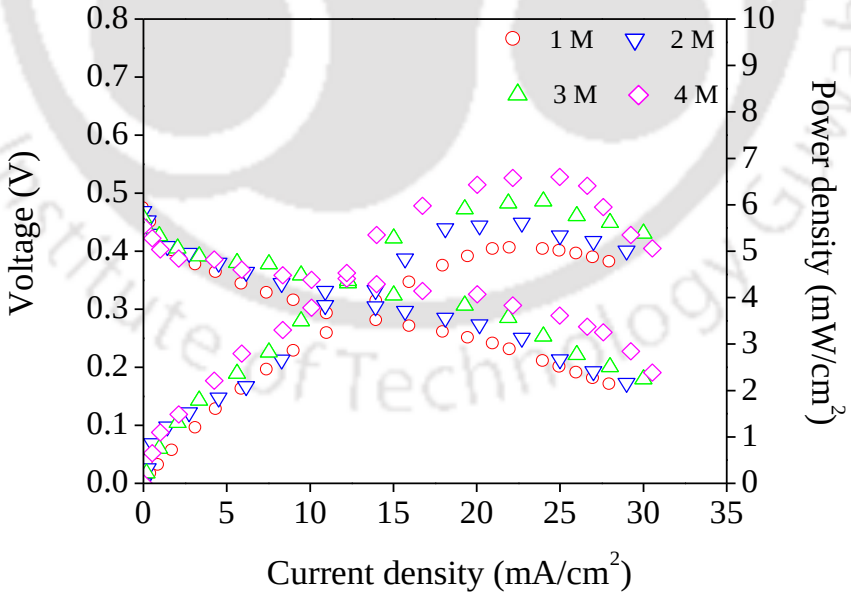

Fig. 4.76 Effect of methanol concentration on DMFC performance with 5% TiO_2/nafion membrane at 30 °C

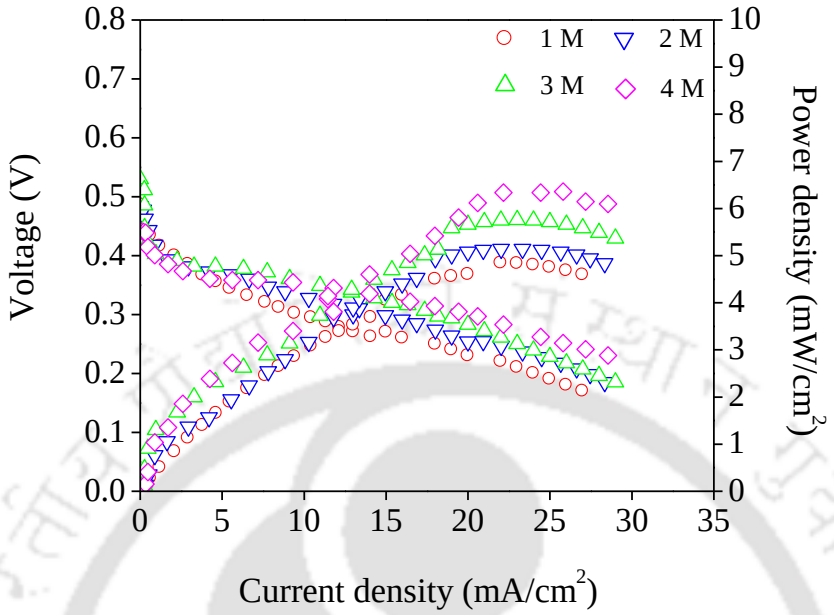

Fig. 4.77 Effect of methanol concentration on DMFC performance with 3% Nd_2O_3/nafion membrane at 30 °C

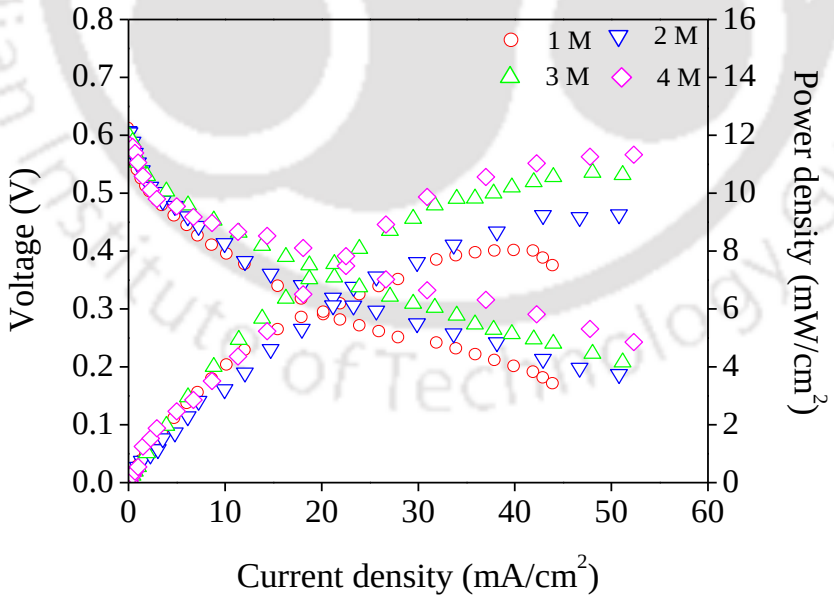

Fig. 4.78 Effect of methanol concentration on DMFC performance with 1% talc/nafion membrane at 30 °C

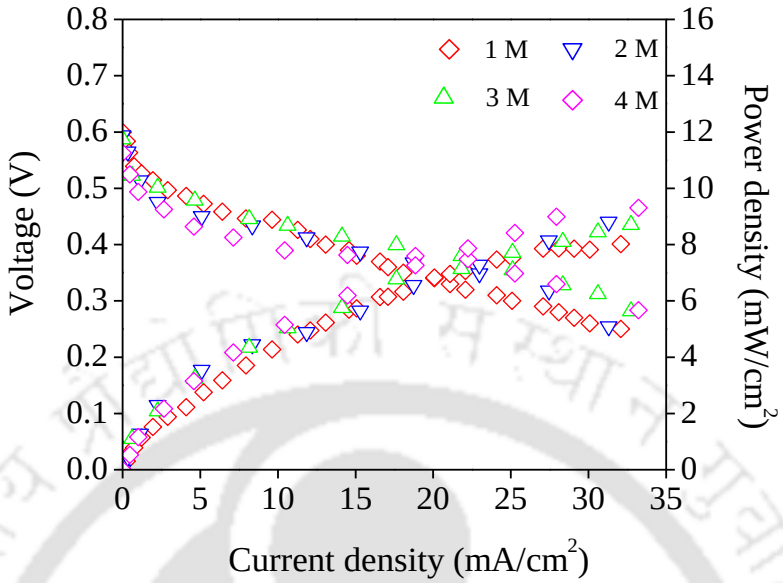

Fig. 4.79 Effect of methanol concentration on DMFC performance with 5% ErTfO/nafion membrane at 30 °C

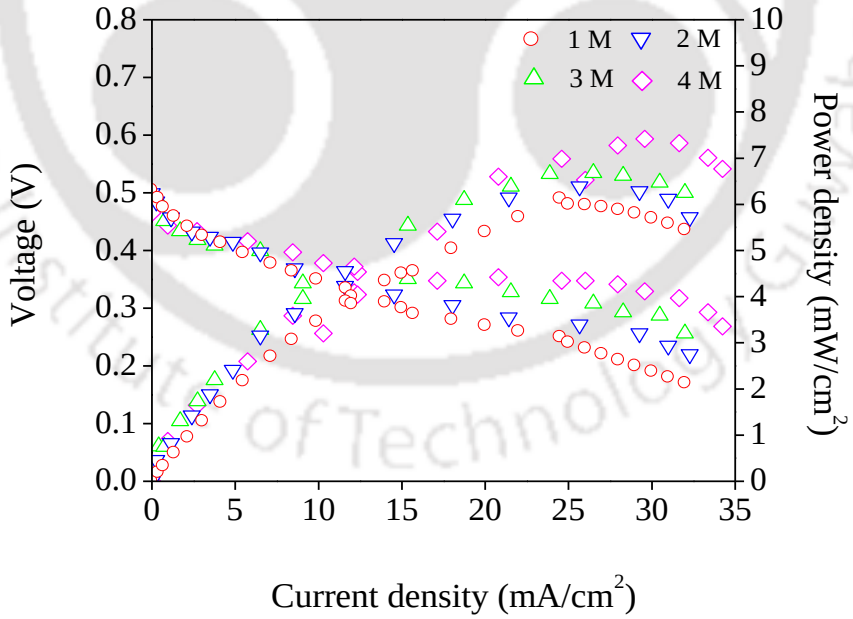

Fig. 4.80 Effect of methanol concentration on DMFC performance with 3% NdTfO/nafion membrane at 30 °C

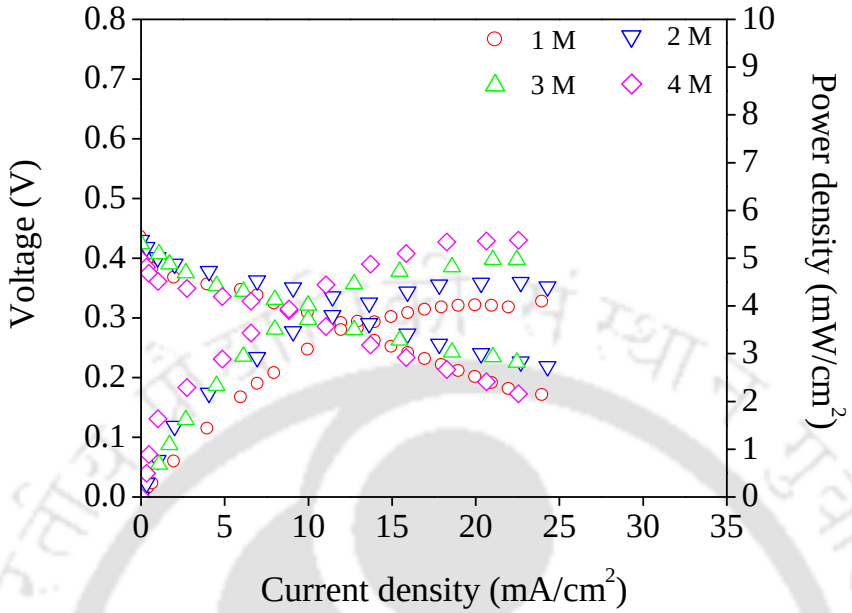

Fig. 4.81 Effect of methanol concentration on DMFC performance with 1% MS/nafion membrane at 30 °C

4.3.3. *Effect of temperature on DMFC performance using composite nafion membranes*

The effect of temperature on MCO has been discussed in section 4.2.12 (figs 4.52 to 4.54). It is observed that increase in temperature leads to an increase in the MCO through the membranes. In this section, the effect of temperature on the DMFC performance is studied with pure cast nafion membrane and nafion composite membranes with the best combination of TiO_2, Nd_2O_3, talc, ErTfO, NdTfO, and MS as discussed earlier. The fuel cell performance is studied at four different temperatures (30, 40, 60 and 80 °C) using 1 M methanol solution as feed. Figures 4.82 to 4.88 show the DMFC performance curves for each type of membrane at different temperature using 1 M methanol. The OCV values of the DMFC using various membranes at different temperature and their maximum power densities are given in table 4.9.

Table 4.8 Effect of methanol concentration on DMFC performance using different membranes

Membrane type	Methanol concentration (M)	OCV (V)	Maximum power density (mW/cm^2)
Pure cast nafion	1	0.410	02.35
	2	0.405	02.53
	3	0.394	02.74
	4	0.370	02.90
5% TiO_2/nafion	1	0.484	05.06
	2	0.469	05.61
	3	0.457	06.03
	4	0.443	06.60
3% Nd_2O_3/nafion	1	0.487	04.84
	2	0.484	05.14
	3	0.473	05.76
	4	0.442	06.36
1% Talc/nafion	1	0.611	07.98
	2	0.607	09.51
	3	0.597	10.71
	4	0.584	11.33
5% ErTfO/nafion	1	0.601	08.02
	2	0.594	08.81
	3	0.587	08.70
	4	0.563	09.31
3% NdTfO/nafion	1	0.505	06.13
	2	0.499	06.39
	3	0.489	06.68
	4	0.465	07.42
1% MS/nafion	1	0.435	04.08
	2	0.430	04.50
	3	0.424	04.97
	4	0.398	05.38

Increases fuel cell temperature should have resulted in decrease in the OCV values because of higher MCO. However, in fuel cell conditions it is observed that increase in the cell temperature results in increased OCV, which may be attributed to improved electrocatalyst activity at high temperature [Ye and Zhao, 2005]. Increase in temperature increases the methanol oxidation kinetics at the anode, which counteracted the MCO rate across the membrane to the cathode side and consequently led to an increase in the fuel cell performance [Pilatpwsky et al., 2011]. An increase in the operating temperature is beneficial to fuel cell performance because of the increase in reaction kinetics and usually lower cell resistance arising from the higher ionic conductivity of the electrolyte. In addition, the CO tolerance of electrocatalyst improves as the operating temperature increases. Consequently, the power density improves with increase in the cell temprerature. All the composite membranes show improved performance at higher temperature compared to pure cast nafion membrane. A maximum power density of 92.48 mW/cm^2 at 80 °C, is obtained with 1% talc/nafion membrane followed by that with 5% ErTfO/nafion membrane (80.85 mW/cm^2). The power densities of 5% TiO_2/nafion (73.10 mW/cm^2) and that of 3% NdTfO/nafion membrane (70.31 mW/cm^2) are comparable. The maximum power densities obtained with 3% Nd_2O_3/nafion (65.30 mW/cm^2) and 1% MS/nafion (61.70 mW/cm^2) are almost similar. Thus the performance of the membranes improved when studied at higher temperatures.

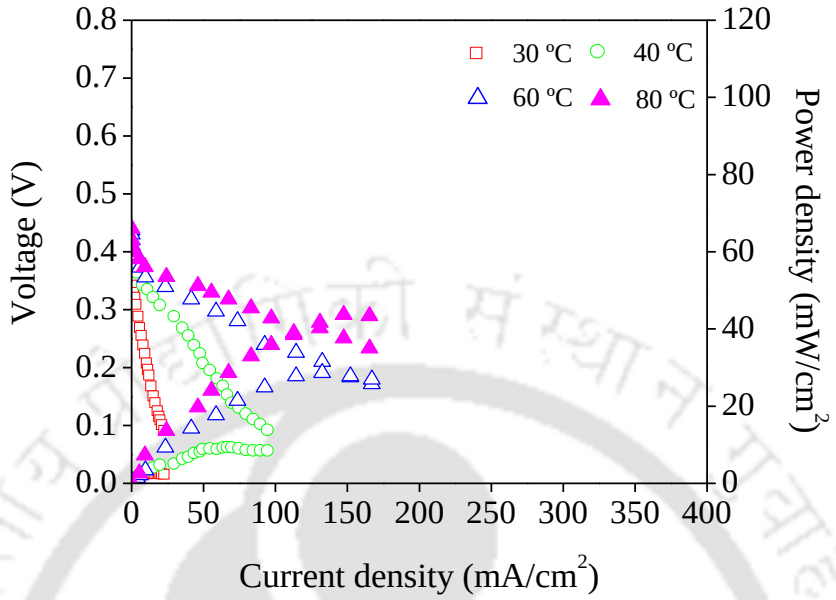

Fig. 4.82 Effect of temperature on DMFC performance with pure cast nafion membrane using 1 M methanol

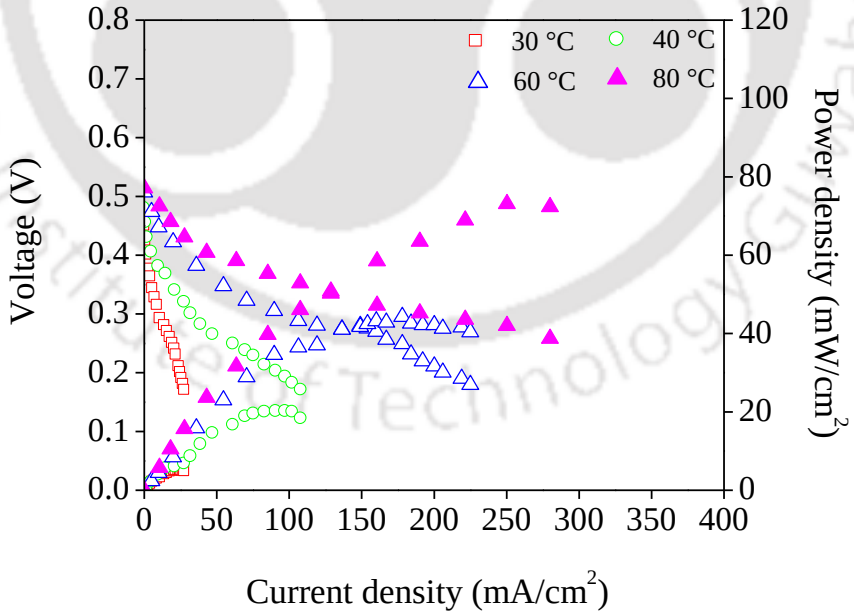

Fig. 4.83 Effect of temperature on DMFC performance with 5% TiO_2/nafion membrane using 1 M methanol

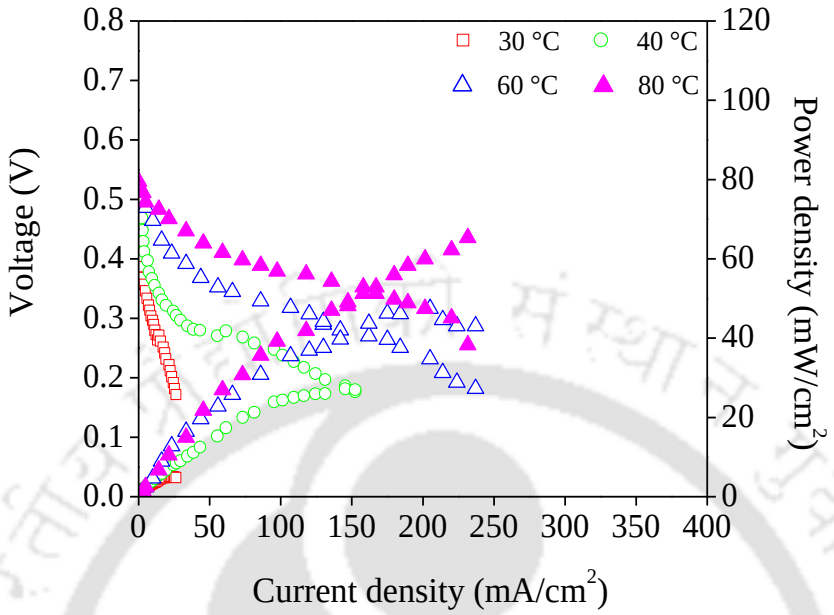

Fig. 4.84 Effect of temperature on DMFC performance with 3% Nd_2O_3/nafion membrane using 1 M methanol

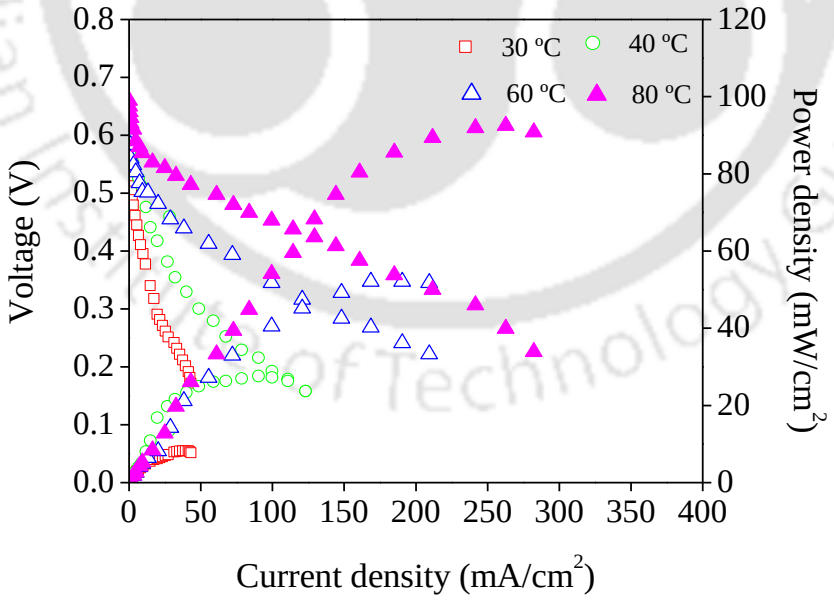

Fig. 4.85 Effect of temperature on DMFC performance with 1% talc/nafion membrane using 1 M methanol

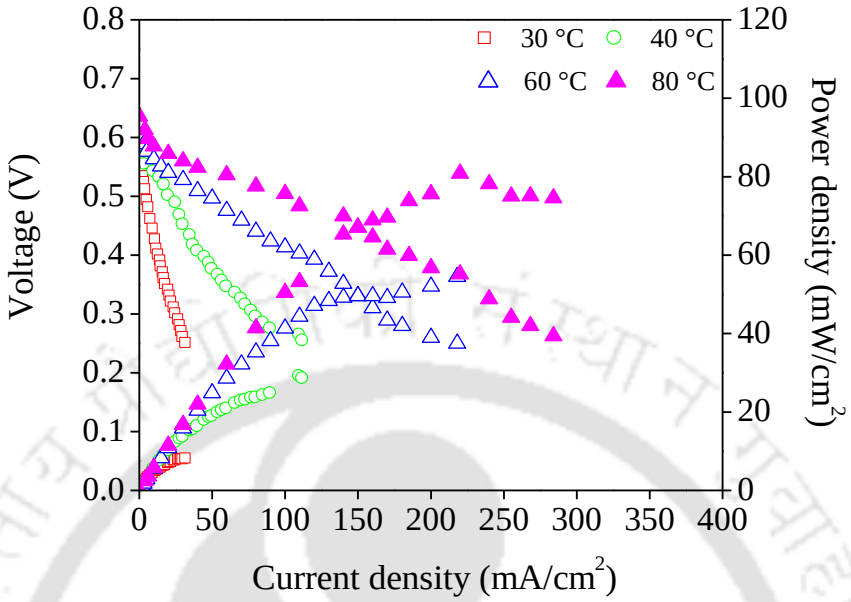

Fig. 4.86 Effect of temperature on DMFC performance with 5% ErTfO/nafion membrane using 1 M methanol

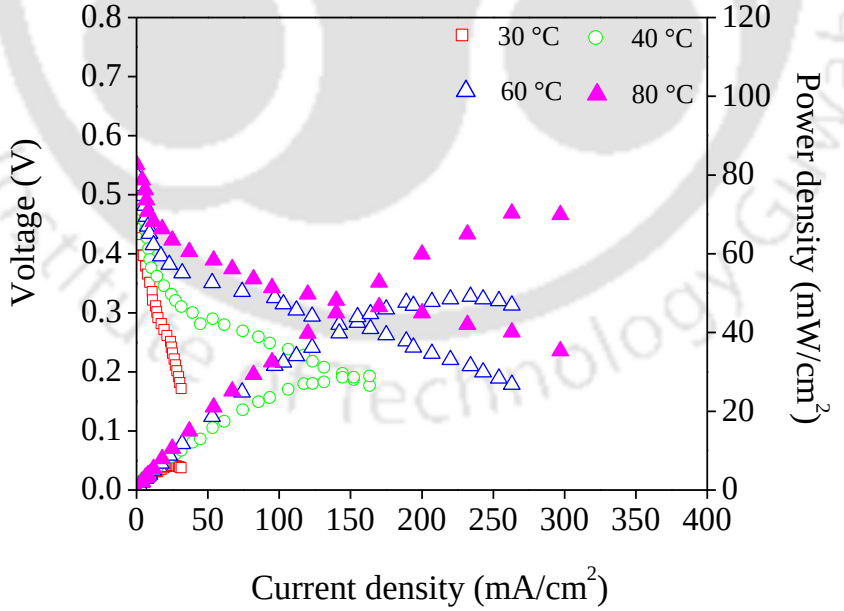

Fig. 4.87 Effect of temperature on DMFC performance with 3% NdTfO/nafion membrane using 1 M methanol

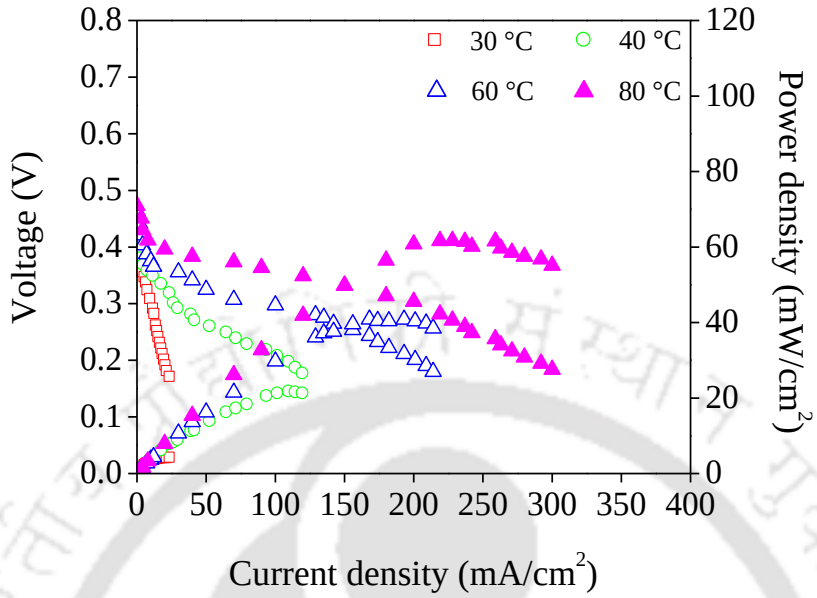

Fig. 4.88 Effect of temperature on DMFC performance with 1% MS/nafion membrane using 1 M methanol

\

Table 4.9 Effect of temperature on DMFC performance using different membranes

Membrane type	Temperature (ºC)	OCV (V)	Maximum power density (mW/cm^2)
Pure cast nafion	30	0.410	02.35
	40	0.424	09.09
	60	0.437	28.62
	80	0.440	43.69
5% TiO_2/nafion	30	0.484	05.06
	40	0.480	20.11
	60	0.507	44.31
	80	0.514	73.10
3% Nd_2O_3/nafion	30	0.487	04.84
	40	0.504	26.98
	60	0.523	47.45
	80	0.537	65.30
1% Talc/nafion	30	0.611	07.98
	40	0.622	27.39
	60	0.643	52.07
	80	0.664	92.48
5% ErTfO/nafion	30	0.601	08.02
	40	0.615	29.07
	60	0.624	54.50
	80	0.636	80.85
3% NdTfO/nafion	30	0.505	06.13
	40	0.522	28.71
	60	0.534	49.11
	80	0.551	70.31
1% MS/nafion	30	0.435	04.08
	40	0.450	21.60
	60	0.464	40.81
	80	0.473	61.70

Chapter 5

Reduction of Crossed-over Methanol Effect at Cathode using Hybrid Pt/laccase

Chapter 5: Reduction of Crossed-over Methanol Effect at Cathode using Hybrid Pt/laccase

It is seen in the previous chapter that modification of nafion with the inorganic additives reduced methanol crossover (MCO) through the membrane upto a significant extent; the maximum reduction in MCO being nearly 80% with erbium triflate/nafion membranes (ErTfO/nafion). Though a major portion of the MCO is reduced but still the methanol, which is reaching to cathode side affect the DMFC performance. The DMFC results in the previous chapter show significant improvement in DMFC performance when composite membrane is used in place of pure cast nafion membrane. However, there is further scope for the improvement of the DMFC performance by tackling the crossed-over methanol to the cathode side [Mustain et al., 2006, Chetty et al., 2009].

It is known that application of selective oxygen reduction catalyst at cathode, which do not oxidize methanol such as macrocyclic complexes [Sun and Barton, 2006], transition metal chalcogenides [Reeve et al., 2000], and platinum alloys [Xiong and Manthiram, 2004; Mustain et al., 2006] may be an alternative option to tackle the crossed-over methanol problem. Additionally, laccase, an enzymatic bioelectrocatalyst, also proves to be a potential candidate for use in the cathode of DMFC for ORR. Laccase (EC 1.10.3.2; benzenediol: oxygen oxidoreductase) is an extracellular blue copper enzyme in plants and fungi, which catalyses the oxidation of biphenols and the four-electron reduction of molecular oxygen to water. Figure 5.1 shows the structure of laccase. It contains four copper atoms, denoted as T1, T2, and T3 according to their spectroscopic properties [Madhavi and Lele, 2009]. The copper center T1 can be reduced at high potential by redox mediators, and direct electron transfer from electrodes. While substrates are

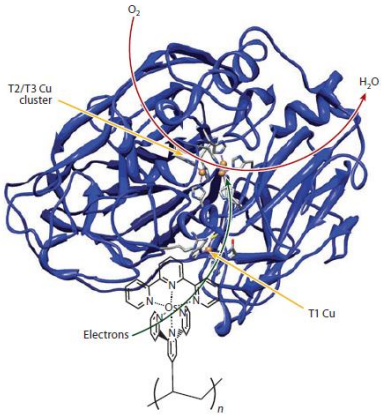

Fig. 5.1 Structure of laccase [Meredith and Minteer, 2012]

oxidized at T1, further internal electron transfer leads to the reduction of molecular O_2 at the T2/T3 cluster [Szamocki et al., 2009] as shown in the fig. 5.1. The catalytic ability of laccase to activate the four-electron reduction of oxygen has promoted their study in cathodes for bio-fuel cells. Chen et al., (2001) has done an extensive review on the electro-chemistry of laccases from different sources. Laccase has excellent selectivity and maximum activity at low temperatures and has primarily been employed in the context of air-saturated physiological solutions. Studies have demonstrated laccase as biocatalytic cathode and for the reduction of O_2 to water [Soukharev et al., 2004]. Mano et al., (2002) showed that a laccase catalyzed composite electrode can achieve O_2 reduction current densities exceeding 5 mA/cm^2 at 0.7 V (SHE) in air-saturated, pH 5, 0.2 M citrate buffer at 37.5 °C. The laccase (from *Rhusvernificera*) biocathode with an enzyme loading of 0.224 mg/cm^2 provided methanol crossover tolerance and provided a high operational current density of 50.0 mA/cm^2 and a maximum power density of 8.5 mW/cm^2 in a DMFC operated at 40% methanol solution. The laccase biocathode showed a lifetime of 290 h in the DMFC [Gellett et al., 2010]. However, such high performance was achieved in DMFC having anion exchange membrane. Considering the above findings, it has been

conceptualized that the laccase may be a potential candidate for the cathode catalyst, where crossed-over methanol effect may be mitigated.

Therefore, in an attempt to evaluate the use of laccase in the present DMFC system, the experiments were conducted to reduce the effect of crossed-over methanol on the cathode side of the DMFC set-up by hybridizing platinum with laccase. Multi-walled carbon nanotubes (MWCNT) have been used for immobilization of laccase on the electrode surface [Saxena et al., 2011] as well as to provide good electronic communication with active sites of the laccase [Das et al., 2014]. Besides, application of MWCNT is anticipated to maintain porosity of the hybrid electrode and facilitate better enzyme substrate interaction. Osmium polyvinyl pyridine (OsO_4-P4VP), known as potential electron transfer mediator between redox enzymes and electrodes, is used in the present study. Three types of cathode electrodes (Pt, laccase, and Pt/laccase) are fabricated in the present work for a comparative study and evaluated both by electrochemical technique as well as tested in the DMFC set-up to evaluate the methanol tolerance at the cathode.

5.1. *Fabrication of electrodes*

The Pt electrode was fabricated as described in section 3.5.1. For the laccase electrode and Pt/laccase electrode, the microporous layer (MPL) was made by applying nafion/carbon powder over the Toray carbon paper to get a hydrophilic microporous layer over the carbon paper. 10 mg OsO_4-P4VP in 1 mL ethyl benzene was sonicated for 1 h and then 1 mg MWCNT was added to it. The mixture was sonicated again for 1 h and then spread over the MPL and incubated at 140 °C overnight. The laccase solution prepared in 0.1 M sodium citrate buffer (pH 4.8) was then spread over the OsO_4-P4VP/MWCNT layer and allowed to freeze dry to get a loading of 2 mg/cm^2 of laccase.

Pt/laccase hybrid cathode was fabricated using layer by layer method. The Pt/OsO_4-P4VP/MWCNT layer was formed over the microporous layer, which was on the C-paper. Finally, laccase solution was spread over the porous Pt/OsO_4-P4VP/MWCNT layer so that the enzyme can percolate through the layer for effective Pt/laccase composite electrode.

The MEA for Pt at cathode was fabricated as described in section 3.5.1. For preparation of the MEAs containing laccase or Pt/laccase on the cathode side, the cathode was placed in contact with the membrane without pressing and heat treatment, in order to avoid damaging the biomaterial, since enzymes do not tolerate high pressure and temperature.

5.2. *Characterization techniques*

All electrochemical experiments were carried out in an electrochemical cell containing 25 mL of pH 4.8, 0.1 M citrate buffer at 25 °C. The cyclic voltammetry (CV) measurements were performed using a Potentiostat/Galvanostat (Autolab, PGSTAT 302N). The working electrode was prepared as discussed in the previous section. However, glassy carbon disc was used instead of C-paper as the support to the catalyst film. Potentials were measured relative to a silver-silver chloride reference electrode but the results are reported with respect to standard hydrogen electrode (SHE). The counter electrode was a platinum wire. Methanol tolerance of the electrode was studied by cyclic voltammetry in the voltage range of -1 to +1 at a scan rate of 50 mV/s at different concentrations of methanol for oxygen saturated solution. The electrodes were also used to evaluate the performance of direct methanol fuel cell as described in section 3.5.3. However, the nafion-117 was used as polymer electrolyte membrane for the fuel cell performance.

The stability of the Pt/laccase was found using cyclic voltammetry. The CV was performed using electrode on a regular interval and on remaining time the electrode was stored at 4 °C [Das et al., 2014].

5.3. *Results and discussion*

5.3.1. *Scanning electron microscopy (SEM) analysis*

Figure 5.2 shows the SEM images of the electrodes. Figure 5.2a shows the SEM image of the carbon paper. It can be seen that the carbon paper has a non-woven structure with many small and large pores through it. Figure 5.2b shows the SEM image of the microporus layer (MPL) over the carbon paper. The MPL facilitates electrical conductivity and also forms a support for the catalyst. Figure 5.2c shows the SEM image of the Pt electrode. The distribution of the Pt catalyst layer over the MPL is visible. The porosity of the electrode is maintained and is visible from the image at higher magnification (inset, fig. 5.2c). Fig 5.2d shows the SEM image of the electrode after addition of OsO_4–P4VP–MWCNT layer. The surface appears highly porous and uniform, which may be attributed to the presence of MWCNT. Figure 5.2e shows the SEM image of the electrode after addition of laccase. The difference in the surface morphology is clear. It can be seen that the porous structure is covered uniformly by the laccase layer.

5.3.2. *Cyclic voltammetry of electrode*

Figures 5.3 to 5.5 show the cyclic voltammograms (CV) of Pt, laccase, and Pt/laccase electrode, respectively. It may be noted that for clarity of various peaks the voltage axis shows the potential range from 0.2 V to 1.2 V. Figure 5.3 shows the effect of methanol on oxygen reduction reaction by platinum electrode. It is observed that the peak decreases from 0.49 mA/cm^2 to 0.33 mA/cm^2 with the introduction of methanol. The decrease in the

oxygen reduction current density is due to non-tolerance of Pt-electrode to methanol solution. With increase in methanol concentration the current density for ORR decreases further.

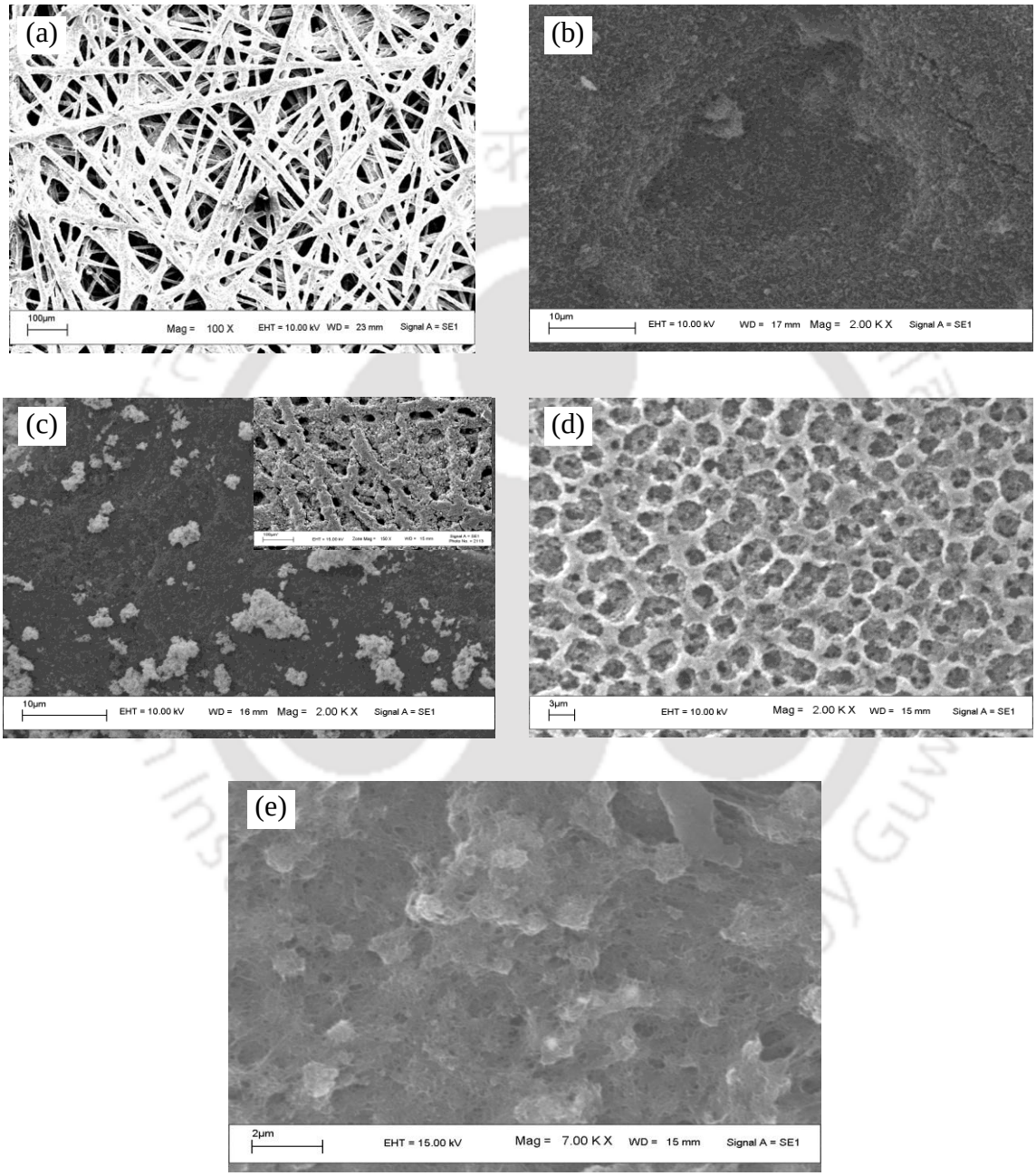

Fig. 5.2 SEM images of (a) C-paper, (b) MPL, (c) Pt electrode, (d) Pt electrode with OsO_4-P4VP-MWCNT, and (e) Pt-OsO_4-P4VP-MWCNT with laccase

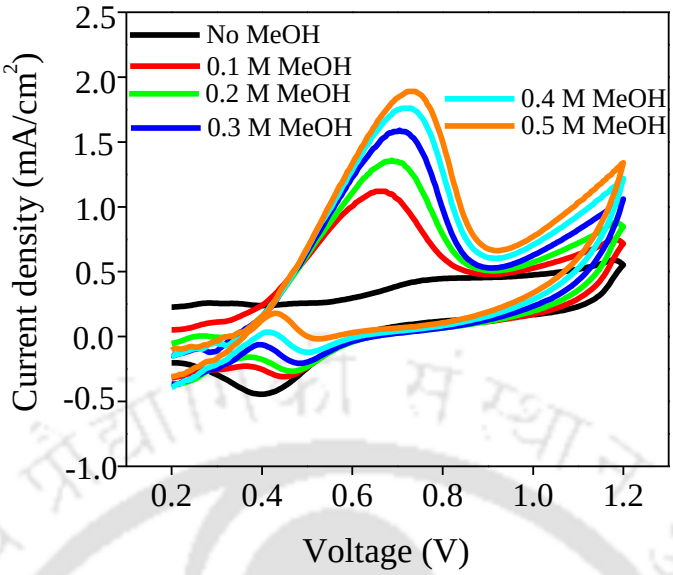

Fig. 5.3 Cyclic voltammetry using platinum on glassy carbon electrode

Figure 5.4 shows the effect of methanol on the oxygen reducing reaction capacity of laccase cathode. It is observed that increase in methanol concentration hardly affect the performance of the laccase electrode and indicates the tolerance of laccase to methanol. However, the performance of laccase electrode is inferior to platinum electrode towards oxygen reduction reaction especially without methanol.

Figure 5.5 shows the CV of Pt/laccase electrode. It is observed that the oxygen reduction peak slightly decreases with increase in methanol concentration. However, fig. 5.6 shows only a portion of CV to have better clarity to compare the peaks. On comparison with the Pt electrode (fig. 5.3) it is observed that presence of laccase reduces the loss in current density attributed to its methanol tolerance as compared in the fig. 5.6. Moreover, it seems that the platinum along with laccase increases the oxygen reduction reaction too. It can also be seen that with increase in methanol concentration there is positive shift in oxidation and reduction peak potentials for the Pt (fig. 5.3) and Pt/laccase electrode (fig. 5.5).

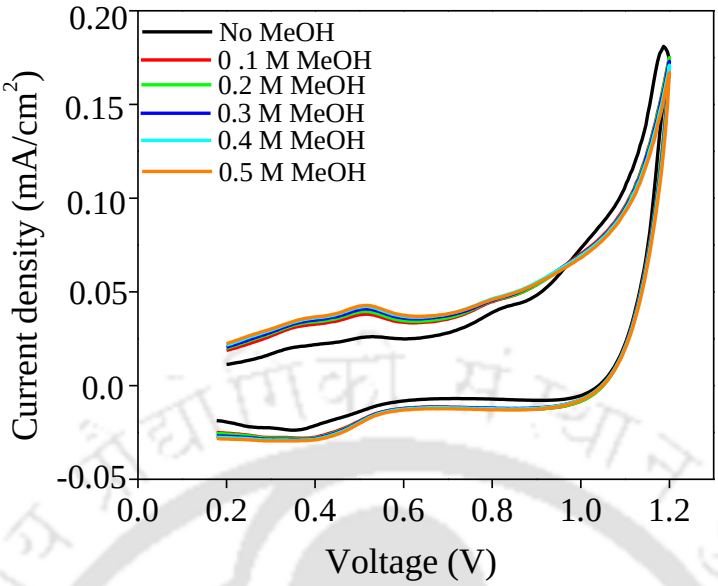

Fig. 5.4 Cyclic voltammetry using laccase/OsO_4-P4VP on glassy carbon electrode

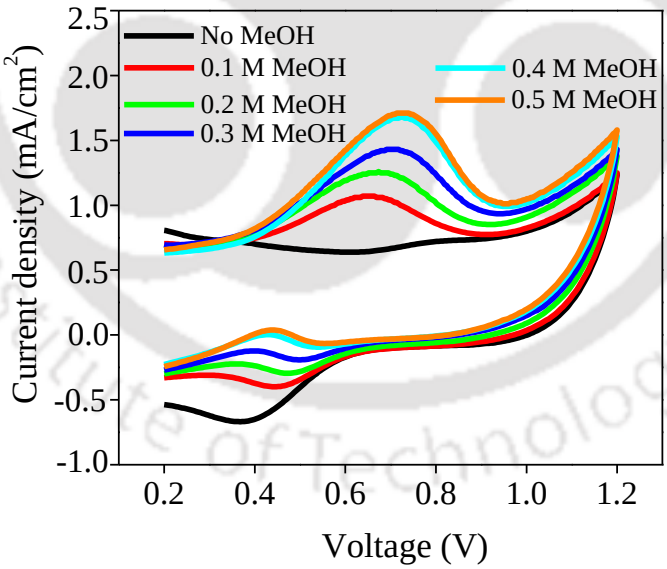

Fig. 5.5 Cyclic voltammetry using Pt/laccase on glassy carbon electrode

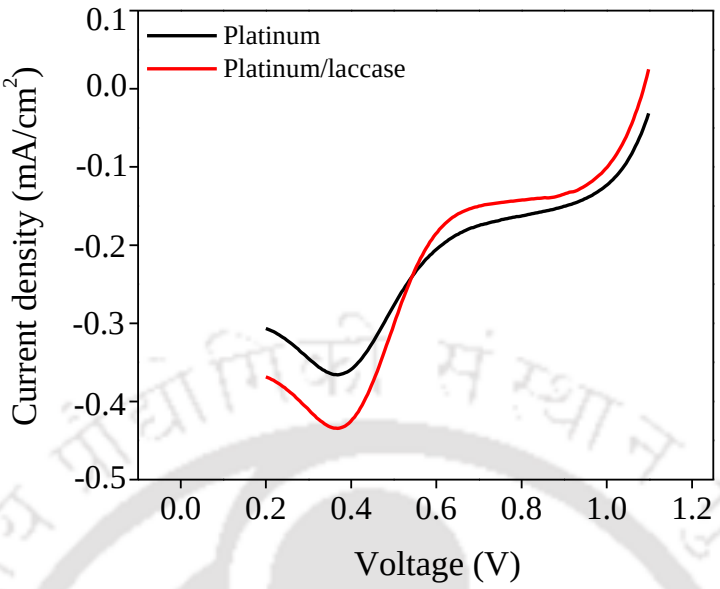

Fig. 5.6 Comparison of ORR peaks of Pt and Pt/laccase cathode using 0.1 M MeOH

The shift in methanol oxidation peak potential with increase in methanol concentration may be attributed to the reduction in electro-catalytic activity of the Pt electrode due to poisoning affect of CO generated during methanol oxidation and its subsequent adsorption on the active sites of Pt electrode [Kashyout et al., 2011]. On comparison it is observed that the shift is lower for Pt/laccase electrode compared to Pt electrode, attributed to the presence of laccase. Shifting of the oxygen reduction peak potential towards positive direction is an indication of increased electro-catalytic activity [Ding, 2010]. On comparison it is observed that the shifting in reduction peak potential is more for the Pt/laccase compared to Pt electrode, indicating its superiority over Pt electrode for ORR.

5.3.3. *Stability of Pt/laccase electrode*

Enzyme stability is always a great concern when employing it in any kind of application. Hence, the stability of the Pt/laccase electrode was checked as discussed previously and the data is reported for day 0 and day 32. The loss of performance after 32 days was found to be around 31% as shown in fig. 5.7. The loss in catalytic activity is attributed to the loss in enzyme activity.

5.3.4. *Performance evaluation of the electrodes in DMFC*

Figure 5.8 shows the OCV achieved in a single cell DMFC set-up with Pt/Ru as the anode whereas at cathode Pt or laccase or Pt/laccase, was used, after 36 hours of operation with nafion-117 at 25 °C using 1 M methanol. The DMFC cell with laccase as the cathode catalyst gives the highest OCV attributed to its tolerance to methanol. Incorporation of laccase/Pt catalyst as the cathode increased the OCV of the cell compared to that with Pt cathode. This shows that use of laccase along with Pt can improve the methanol tolerance of Pt cathode catalyst.

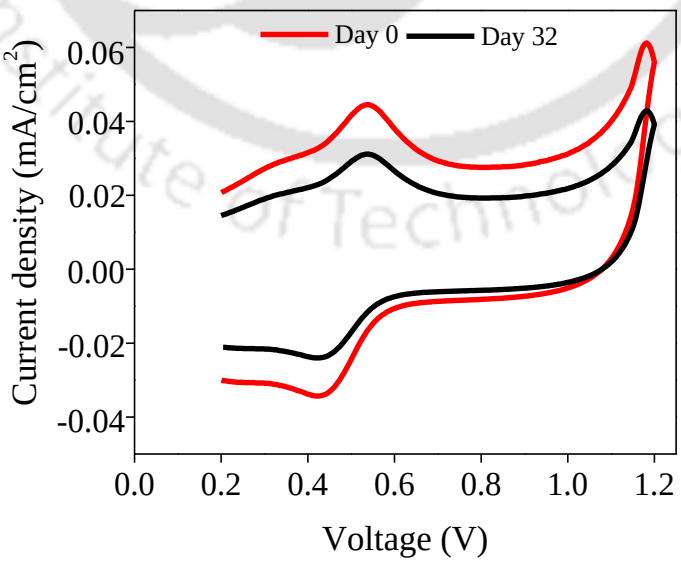

Fig. 5.7 Stability of Pt/laccase cathode (O_2 feed, pH: 4.8, 25 °C)

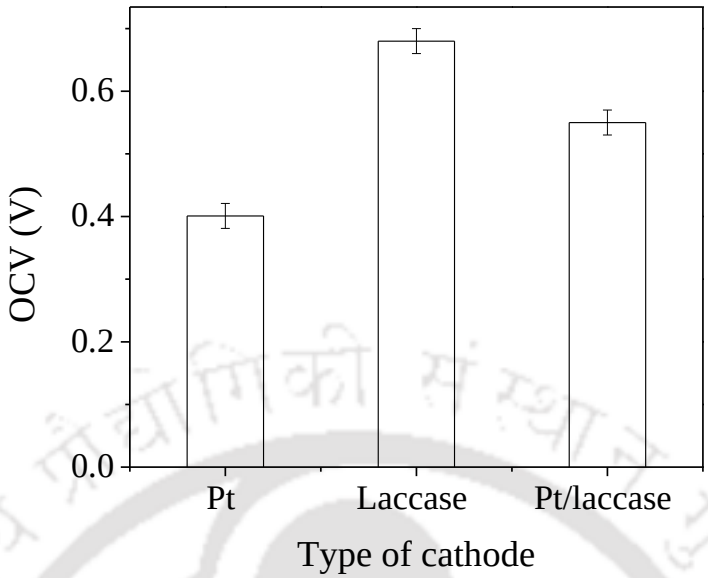

Fig. 5.8 Open circuit voltage of Pt/Ru anode and different cathode catalyst at 25 °C using 1 M methanol solution

The DMFC performance with the three types of cathode catalyst is shown in fig. 5.9. The performance achieved with Pt/laccase cathode is improved compared to the performance of Pt cathode catalyst. The DMFC performance with laccase as the cathode catalyst gives the lowest performance, which may be attributed to the difference in nature of Pt and laccase. The platinum surface can host thousands of reactions at once while each laccase molecule can only react with one oxygen molecule at a time [Blandford, 2011]. Moreover, laccase to function as efficiently as possible, it needs to have its reaction needs met such as, a good supply of oxygen (fast gas diffusion), a constant concentration of hydrogen ions (buffered pH), and a well-connected electrical structure for electron shuttling [Blandford, 2011]. On-membrane deposition of the cathodic catalyst

layers may also help to improve the performance by lowering the internal resistance of the cell [Chaparro et al., 2011] .

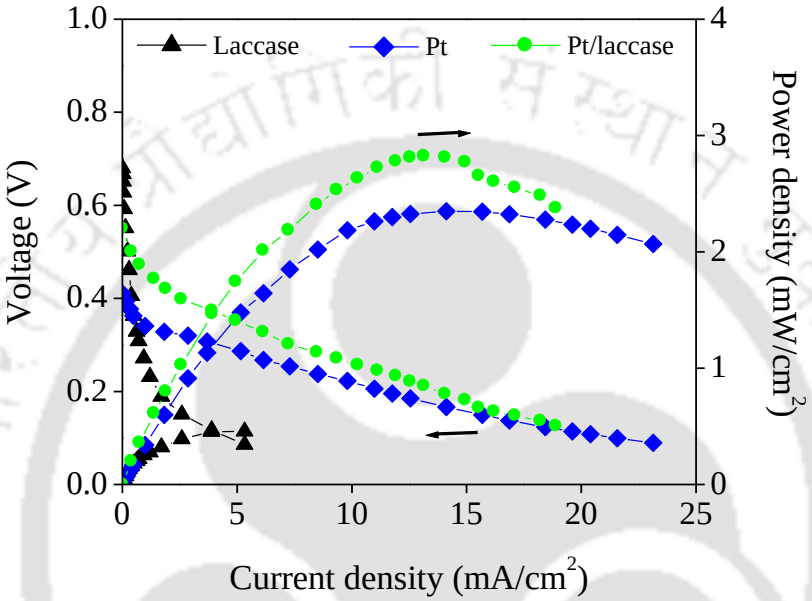

Fig. 5.9 DMFC performance using Pt, laccase, and Pt/laccase as the cathode catalyst

Chapter 6

Conclusions and Future Scope

Chapter 6: Conclusions and Future Scope

6.1. Conclusions

Composite nafion membranes were synthesized by casting method using six different types of inorganic additives, namely titanium dioxide (TiO_2), neodymium oxide (Nd_2O_3), magnesium silicate hydroxide ($H_2Mg_3(SiO_3)_4$) or talc, erbium trifluoro methane sulphonic acid (ErTfO), neodymium trifluoro methane sulphonic acid (NdTFO), and molecular sieve (MS). The additives were characterized for particle size, crystallinity, BET surface area, and morphology. The synthesized nafion composite membranes along with pure cast nafion membrane were extensively characterized by SEM, XRD, TGA, FTIR, ion exchange capacity (IEC), water uptake, methanol uptake, swelling, tensile strength, oxidative stability, proton conductivity, and methanol crossover (MCO). The membranes were later tested in a single cell DMFC test set up at 30 °C and with a methanol concentration of 1 M methanol. Further, the best combination of the nafion composite of each kind of additive was tested in a DMFC with varying methanol concentration (1, 2, 3, and 4 M) and at different temperatures (30, 40, 60, and 80 °C). A summary of the findings is given below.

- From particle size analysis of the additives, the volume median diameter [D(v,0.5)] for TiO_2, Nd_2O_3, talc, and MS particles was found to be 21.30 µm, 06.39 µm, 20.37 µm, and 07.39 µm, respectively. The results were in close agreement with the SEM images of the particles .The particle size of ErTfO and NdTfO has not been reported as these additives dissolves into the nafion solution.
- All the additives, except NdTfO, exhibited sharp X-ray diffraction peaks attributed to their crystalline nature. However, the XRD plots of nafion composite membranes showed that TiO_2 and talc could significantly contribute towards the

crystallinity of the composite membranes. The characteristic crystalline peaks of Nd_2O_3, MS, and ErTfO could not be observed for the corresponding nafion composite membranes. However, the broad peaks observed for the nafion composites with Nd_2O_3, MS, and ErTfO is attributed to some kind of chemical interaction of the Nd_2O_3 with the polymer, formation of agglomerates in case of MS/nafion membranes, and due to the dissolution of the triflate salts in the nafion solution.

- The crystal size of the additives determined from Debey Scherrer equation was 34.65 nm, 26.65 ± 8, 36.08,19.8, and 27.90 ± 3 for TiO_2, Nd_2O_3, talc, ErTfO, and MS respectively. Due to the absence of sharp peaks in case of NdTfO powder, the Scherrer formula could not be used.
- The BET surface areas of the additives were 6.54, 5.71, 3.07, 11.37, 9.63, and 4.02 m^2/g for TiO_2, Nd_2O_3, talc, ErTfO, NdTfO, and MS, respectively.
- SEM images of the membranes indicated the formation of dense nafion composite membranes with relatively uniform distribution of the additives (TiO_2, Nd_2O_3, talc, and MS). In case of ErTfO and NdTfO, the presence of additives could not be observed due to dissolution of the additives in the nafion. None of the nafion composite membranes exhibited presence of pores or cracks. Agglomerate formation was seen in a few of the cases attributed to both hygroscopic nature of the additives and poor physical compatibility between the additive and the nafion.
- Analysis of the TGA thermograms of the nafion composite membranes indicated that all the composite membranes retained more than 90% of its weight up to a temperature of about 310 °C. Above 310 °C, the composite membranes started to decompose and lost weight quite rapidly. The decomposition behavior below 300 °C was attributed to the loss of bound and unbound water and rapid weight loss at

and above 310 °C was attributed to loosening of sulfonic acid groups present in the membrane. Though the nafion composite membranes showed slight loss in thermal degradation temperature as compared to pure cast nafion but the degradation temperature of the composites was well beyond the desirable fuel cell operation temperature (25-80 °C).

- FTIR analysis of the nafion composite membranes showed shifting of peaks for S-O stretching and water stretching frequency to higher wavenumbers and broader peak for water bending vibration for the composite membranes compared to pure cast nafion membrane. It was indicative of structural changes in the nafion polymer due to incorporation of the additives, increase in hydrogen bond association as well as increase in water content.
- Ion exchange capacity was higher for the composite membranes compared to pure cast nafion membrane as inclusion of additives increased the number of ion exchange domains in the composite membranes. The porous structure of the molecular sieves accommodating loosely held H^+ contributed to the higher IEC. The OH groups in TiO_2, Nd_2O_3, and talc contributed to this effect whilst the SO_3^- group of the triflic acid was responsible in case of ErTfO and NdTfO.
- Water uptakes of the composite membranes were higher than pure cast nafion in general and followed a trend similar to IEC. The increased water content in the composite membranes was also indicated by the FTIR profile of the membranes. Methanol uptake of the composite membranes followed a trend similar to water uptake with a slight increase in uptake percentage for methanol, attributed to the presence of hydrophobic and hydrophilic domains in the structure of the nafion membrane; water being the most polar has high accessibility to the hydrophilic

domains, which covers about 25 to 35% of the membrane mass; methanol being less polar than water has accessibility to both the hydrophilic and hydrophobic domains. The methanol uptake also increased with the increased methanol concentration.

- Overall the percentage of swelling in the membranes was in the range of 10(±5)%. This is desirable for fuel cell applications as the water retained by the inorganics would keep the membrane in the hydrated state even when the fuel cell is turned off and thereby prevent delamination as well as cracks in the MEA.
- The tensile strengths of talc/nafion membranes and MS/nafion membranes were lower than that of pure cast nafion membrane (16 MPa vs ~ 14 MPa). Incorporation of these two additives into pure cast nafion apparently weakened the integrity of the nafion membrane and reduced its tensile strength. The TiO_2/nafion composite membranes showed insignificant effect on tensile strength compared to pure cast nafion membrane. Nafion membrane with 1% loading of Nd_2O_3, ErTfO, and NdTfO had a higher tensile strength than pure cast nafion membrane. However, the tensile strength slowly decreased with increased loading above 1%. The increased stiffness of the membrane at higher loading of TiO_2 and Nd_2O_3 particles into the polymer matrix might have resulted in the decreased tensile strength. In case of the inorganic triflate/nafion membranes, the higher cross-linking at higher loading apparently increased the stiffness of the membrane and reduced its tensile strength.
- Comparison of the oxidative stability of the membranes showed that the composite membranes with lower additive loadings was chemically more stable than pure cast nafion membrane though, the optimum percent of loading varied for each type of additive. The lowest degradation or highest stability was found

for 1% TiO_2, 7% Nd_2O_3, and 5% talc loading in nafion composite membrane. MS/nafion composite membrane too showed the highest stability at 5% MS loading. This is attributed to the weakening of chemical bonds of the polymer due to incorporation of the additive. In case of ErTfO/nafion and NdTfO/nafion membranes, increase in additive loading beyond 1% reduced the stability of the composite membranes. It was attributed to the weakening of chemical bonds of the polymer due to increased cross linking and subsequent oxidation degradation of the sulfonated polychains in the presence of H_2O_2.

- Proton conductivity of the composite membranes improved significantly attributed to the increase in water uptake of the composite membranes and the presence of additional proton exchange domains associated with the additives. At an optimum loading of the additives, the relative proton conductivity as compared to pure cast nafion membrane was improved by 42.7% by TiO_2/nafion, 33.71% by Nd_2O_3/nafion, 26.97% by talc/nafion, 38.2% by ErTfO/nafion, 31.46% by NdTfO/nafion, and 13.48% by MS/nafion composite membranes. However, the trend of higher water uptake leading to higher values of proton conductivity was not followed strictly.
- All the composite membranes could reduce MCO as compared to pure cast nafion membrane but the maximum reduction was achieved by ErTfO/nafion membranes (ranging 77.5% to 80.75%) followed by TiO_2/nafion membranes (ranging 25% to 77%), NdTfO/nafion membranes (ranging 50.26% to 70.5%), talc/nafion membranes (ranging 22.43% to 46.36%), Nd_2O_3/nafion membranes (ranging 46% to 55.28%) and MS/nafion membranes (ranging 10.6% to 25%). The MCO of the membranes was also evaluated at different concentrations of methanol (2 M, 3 M and 4 M) and at different temperatures (40, 60 and 80 °C). It has been observed

that increase in methanol concentration as well temperature led to the increase in MCO attributed to concentration gradient of the methanol solution across the membrane and increased diffusion kinetics.

- Based on the selectivity value, the membranes may be ranked as ErTfO/nafion>TiO_2/nafion>NdTfO/nafion>Talc/nafion>Nd_2O_3/nafion>MS/nafion >pure cast nafion. Amongst ErTfO/nafion membranes, 3% ErTfO/nafion membrane showed the highest selectivity and for TiO_2/nafion and Nd_2O_3/nafion membranes the composite with 5% loading showed the highest selectivity. In case of talc/nafion and MS/nafion, the composite with 1% loading exhibited the highest selectivity and for NdTfO/nafion membranes the composite with 7% loading showed the highest selectivity.
- The composite membranes exhibited higher power density than pure cast nafion membrane attributed to the decrease in MCO while maintaining the proton conductivity. The composite membranes with lower MCO showed a higher OCV. The maximum power density with 1 M methanol and at 30 °C was obtained with 5% ErTfO/nafion (8.02 mW/cm^2), followed by 1% talc/nafion membrane (7.98 mW/cm^2), and 3% NdTfO/nafion (6.13 mW/cm^2), which may be considered amongst the best performing membranes. The other three type of composite membranes also showed relatively better performance than pure cast nafion membrane with a power density of 5.06 mW/cm^2 with 5% TiO_2/nafion, 4.84 mW/cm^2 with 3% Nd_2O_3/nafion, and 4.08 mW/cm^2 with 1% MS/nafion.
- The effect of methanol concentration on the single cell DMFC performance was studied with pure cast nafion and nafion composite membranes at 30 °C. Increased methanol concentration led to decreased OCV, attributed to simultaneous increase of MCO from anode to the cathode, leading to mixed

potential at the cathode. However, it was observed that increased methanol concentration increased the current density. Thus, for each membrane the maximum power density was obtained at 4 M methanol concentration.

- The effect of temperature on the single cell DMFC performance was studied using pure cast nafion and nafion composite membranes with 1 M methanol and at 30, 40 60 and 80 °C. It was observed that increase in cell temperature resulted in an increase in the OCV value attributed to increase in methanol oxidation reaction at the anode. The drop in voltage with increase in current density decreased as the fuel cell temperature increased. Consequently, the power density improved with increased cell temperature. However, in case of pure cast nafion membrane the increase in power density was more prominent at lower temperatures. The difference between the power densities at 60 and 80 ºC with pure cast nafion is much less compared to nafion composite membranes, which may be attributed to the initiation of dehydration of pure cast nafion membrane at higher temperature. It was observed that the composite membranes show improved performance at higher temperature compared to pure cast nafion attributed to enhancement in hydration capacity. The pattern of the best performing membrane slightly altered when studied at varying methanol concentration and at varying temperatures, from which it was clear that apart from proton conductivity, and MCO, other parameters like swelling, and water holding capacity at higher temperature forms the combinatorial deciding factor for the membrane performance.
- An attempt was made to improve DMFC performance by use of a methanol tolerant enzyme (laccase) in combination with Pt at the cathode. Though laccase showed high tolerance to methanol, DMFC performance with laccase and osmium in polymer (OsP_4VP) did not improve DMFC performance compared to Pt

cathode. However, use of laccase in combination with Pt in the cathode showed improved performance than Pt alone. From the study, it was inferred that employing hybrid Pt/laccase cathode in a DMFC might be a potential technique of alleviating the adverse effect of crossed-over methanol from anode to cathode.

Finally, the table 6.1 summarizes the performance exhibited by various nafion composite membranes and compared with the pure cast nafion membrane.

6.2. Future scope

- Hybrid Pt/laccase electrode showed tolerance to methanol compared to single Pt cathode. Further studies may be carried out along with composite nafion membrane to evaluate the performance of the DMFC.
- PEMFC performance using hydrogen as the fuel and nafion composite membranes with ErTfO, NdTfO, talc, and Nd_2O_3 as the additive has not been reported previously. Hence, these composite membranes may be tried for high temperature PEMFC.

Table 6.1- Comparison of properties of nafion membranes

Membrane	Water uptake (%)	IEC (meq/g)	Swelling (%)	Thermal stability (°C)	Mechanical stability (MPa)	Chemical stability (% wt. loss/day)	Proton conductivity (S/cm)	MCO (cm^2/s)	Maximum DMFC performance (mW/cm^2)
Pure cast nafion membrane	23.27	0.91	5.32	up to 310 °C (approx.)	15.92	0.271	0.089	2.39×10^{-6}	2.35, 9.09, 28.62, 43.69, 1 M methanol, 30, 40, 60, and 80 °C, respectively
5% TiO_2/nafion membrane	33.91	0.92	7.21	-do-	16.08	0.264	0.107	0.60×10^{-6}	5.06, 20.11, 44.31, 73.10, 1 M methanol, 30, 40, 60, and 80 °C, respectively
3% Nd_2O_3/nafion membrane	28.51	1.00	7.14	-do-	36.86	0.233	0.116	1.12×10^{-6}	4.84, 26.98, 47.45, 65.30, 1 M methanol, 30, 40, 60, and 80 °C, respectively
1% Talc/nafion membrane	23.82	1.1	8.68	-do-	15.62	0.179	0.099	1.28×10^{-6}	7.98, 27.39, 52.07, 92.48, 1 M methanol, 30, 40, 60, and 80 °C, respectively
5% ErTfO/nafion membrane	31.13	1.33	8.89	-do-	17.50	0.130	0.114	0.50×10^{-6}	8.02, 29.07, 54.50, 80.85, 1 M methanol, 30, 40, 60, and 80 °C, respectively
3% NdTfO/nafion membrane	24.87	1.13	6.11	-do-	14.27	0.209	0.114	0.84×10^{-6}	6.13, 28.71, 49.11, 70.31, 1 M methanol, 30, 40, 60, and 80 °C, respectively
1% MS/nafion membrane	26.04	1.02	8.82	-do-	14.86	0.233	0.100	1.79×10^{-6}	4.08, 21.60, 40.81, 61.70, 1 M methanol, 30, 40, 60, and 80 °C, respectively

References

References

- Adachi G., Imanaka N., and Tamura S., Ionic Conducting Lanthanide Oxides, Chem. Rev., 102 (2002) 2405-2430.
- Adjemian K.T., Lee S.J., Srinivasan S., Benziger J., and Bocarsly A.B., Silicon oxide nafion composite membranes for proton-exchange membrane fuel cell operation at 80-140°C, J. Electrochem. Soc., 149 (2002) A256–A261.
- Affoune A.M., Yamada A., and Umeda M., Conductivity and surface morphology of nafion membrane in water and alcohol environments, J. Power Sources, 148 (2005) 9–17.
- Ahmad H., Kamarudin S.K., Hasran U.A., and Daud W.R.W., Overview of hybrid membranes for direct-methanol fuel-cell applications, Int. J. Hydrogen Energy, 35 (2010) 2160-2175.
- Alcaide F., Alvarez G., Miguel O., Querejeta A., and Boyano I., Effect of gas diffusion layer composition on the performance of liquid direct methanol fuel cell, ECS Trans., 25:1 (2009) 891-897.
- Amirinejad M., Madaeni S.S., Rafiee E., and Amirinejad S., Cesium hydrogen salt of heteropolyacids/Nafion nanocomposite membranes for proton exchange membrane fuel cells, J. Membr. Sci., 377 (2011) 89– 98.
- Amjadi M., Rowshanzamir S., Peighambardoust S.J., and Sedghi S., Preparation, characterization and cell performance of durable nafion/SiO_2 hybrid membrane for high-temperature polymeric fuel cells, J. Power Sources, 210 (2012) 350– 357.
- Andujar J.M., and Segura F., Fuel cells: History and updating. A walk along two centuries, Renewable Sustainable Energy Rev., 13:9 (2009) 2309-2322.
- Antonucci P.L., Aric´o A.S., Cret´ı P., Ramunni E., and Antonucci V., Investigation of a direct methanol fuel cell based on a composite nafion-silica electrolyte for high temperature operation, Solid State Ionics, 125 (1999) 431–437.
- Appleby A.J., Fuel cell technology: Status and future prospects, Energy, 21:7-8 (1996) 521–653.
- Arbizzani C., Donnadio A., Pica M., Sganappa M., Varzi A., Casciola M., and Mastragostino M., Methanol permeability and performance of nafion-zirconium

phosphate composite membranes in active and passive direct methanol fuel cells, J. Power Sources, 195 (2010) 7751–7756.

- Aricò A.S., Baglio V., Di Blasi A., Modica E., Antonucci P.L., and Antonucci V., Surface properties of inorganic fillers for application in composite membranes-direct methanol fuel cells, J. Power Sources, 128 (2004) 113–118.
- Babu K.S., Vijayan C., and Haridoss P., Properties of size-tuned PbS nanocrystals stabilized in a polymer template, Mater. Res. Bull., 42 (2007) 996–1003.
- Bacon F.T., Fuel cells, past, present and future, Electrochimica Acta, 14:7 (1969) 569-585.
- Bacon F.T., The development and practical application of fuel cells, Int. J. Hydrogen Energy, 10:7-8 (1985) 423-430.
- Baglio V., Aric`o A.S., Di Blasi A., Antonucci V., Antonucci P.L., Licoccia S., Traversa E., and Fiory S.F., Nafion–TiO_2 composite DMFC membranes: physico-chemical properties of the filler versus electrochemical performance, Electrochim. Acta, 50 (2005) 1241–1246.
- Baglio V., Arico A.S., Di Blasi A., Antonucci P.L., Nannetti F., Tricoli V., and Antonucci V., Zeolite-based composite membranes for high temperature direct methanol fuel cells, J. Appl. Electrochem., 35:2 (2005) 207-212.
- Baglio V., Di Blasi A., Aricò A.S., Antonucci V., Antonucci P.L., Fiory S.F., Licoccia S., and Traversa E., Influence of TiO2 nanometric filler on the behaviour of a composite membrane for applications in direct methanol fuel cells, J. New Mat. Electrochem. Systems, 7 (2004) 275-280.
- Barbora L., Acharya S., and Verma A., Synthesis and ex-situ characterization of nafion/TiO_2 composite membranes for direct ethanol fuel cell, Macromol. Symp, 277 (2009a) 177-189.
- Barbora L., Acharya S., Kaalva S., Difoe A., and Verma A., Nafion/TiO_2 for direct methanol fuel cell, Int. J. Chem. Sci., 5:4 (2007) 1579-1589.
- Barbora L., Acharya S., Singh R., Scott K., and Verma A., A novel composite nafion membrane for direct alcohol fuel cells, J. Membr. Sci., 326 (2009b) 721-726.
- Barbora L., and Verma A., Enhanced performance of direct methanol fuel cell using talc modified nafion membrane, International Journal of Innovative Research and Development, 7 (2012) 128-133.

- Barbora L., Singh R., Shroti N., and A. Verma, Synthesis and characterization of neodymium oxide modified nafion membrane for direct alcohol fuel cells', Mater. Chem. Phys., 122 (2010) 211–216.
- Basak P.R., Kaushik N., and Biswas S., Methanol as energy carrier, Search, 13:2 (2010).
- Bauer F., and Porada M.W., Microstructural characterization of Zr-phosphate–nafion membranes for direct methanol fuel cell (DMFC) applications, J. Membr. Sci, 233 (2004) 141-149.
- BauerF., and Willert-Porada M., Characterisation of zirconium and titanium phosphates and direct methanol fuel cell (DMFC) performance of functionally graded Nafion$^{(R)}$ composite membranes prepared out of them, J. Power Sources, 145 (2005) 101–107.
- Bian C., Yu Y., Xue G., Synthesis of conducting polyaniline/TiO_2 composite nanofibres by one-step in-situ polymerization method, J. Appl. Polym. Sci., 104 (2007) 21–26.
- Blanford C.F., Three-dimensional laccase electrodes for miniaturised fuel cell power sources, EPSRC Pioneering research and skills, Energy, Fuel Cell Technologies, EP/G00434X/2,The University of Manchester.
- Casciola M., Bagnasco G., Donnadio A., Micoli L., Pica M., Sganappa M., and Turco M., Conductivity and methanol permeability of Nafion–zirconium phosphate composite membranes containing high aspect ratio filler particles, Fuel Cells, 09 (2009) 394-400.
- Casciola M., Capitani D., Comite A., Donnadio A., Frittella V., Pica M., Sganappa M., and Varzi A., Nafion–Zirconium Phosphate Nanocomposite Membranes with High Filler Loadings: Conductivity and Mechanical Properties, Fuel Cells, 8 (2008) 217-224.
- Casciola M., Capitani D., Donnadio A., Frittella V., Pica M., and Sganappa M., Preparation, proton conductivity and mechanical properties of Nafion 117–zirconium phosphate sulphophenylphosphonate composite membranes, Fuel Cells, 09 (2009) 381-386.
- Chaparro A.M., Aparicio P.F., Folgado M.A., Martín A.J., Daza L., Catalyst layers for proton exchange membrane fuel cells prepared by electrospray deposition on nafion membrane, J. Power Sources 196 (2011) 4200–4208.

- Chen C.Y., and Yang P., Performance of an air-breathing direct methanol fuel cell. Short communication, J. Power Sources, 123 (2003) 37–42.
- Chen C.Y., Rodriguez J.I.G, Duke M.C., Costa R.F.D., Dicks A.L., and Costa J.C.D., Nafion/polyaniline/silica composite membranes for direct methanol fuel cell application, J. Power Sources, 166 (2007) 324–330.
- Chen C.Y., Wu C.S., and Chu P.J., Nafion/exfoliated-ZrP hybrid membrane for DMFC applications, Joint International Meeting, Electrochemical Society, Abstract 2031, 2004.
- Chen J.H., Asano M., Yamaki T., and Yoshida M., Preparation and characterization of chemically stable polymer electrolyte membranes by radiation-induced graft copolymerization of four monomers into ETFE films, J. Membr. Sci., 269 (2006) 194-204.
- Chen T., Barton S.C., Binyamin G., Gao Z., Zhang Y., Kim H.H., and Heller A., A Miniature Biofuel Cell, J. Am. Chem. Soc., 123 (2001) 8630-8631.
- Chetty R., Kundu S., Xia W., Bron M., Schuhmann W., Chirila V., Brandl W., Reinecke T., and Muhler M., PtRu nanoparticles supported on nitrogen-doped multiwalled carbon nanotubes as catalyst for methanol electrooxidation, Electrochim. Acta, 54 (2009) 4208-4215.
- Chiou J.S., Lin T.M., She K.Y., and Chen W.M., Enrichment of ammonia concentration from aqua-ammonia vapors by using 3A molecular sieve, Energy Convers. Manage., 50 (2009) 2665–2669.
- Choi P., Jalani N.H., and Datta R., Thermodynamics and proton transport in nafion II. proton diffusion mechanisms and conductivity, J. Electrochem. Soc., 152 (3) (2005) E123-E130.
- Choi W.C., Kim J.D., and Woo S.I., Modification of proton conducting membrane for reducing methanol crossover in a direct-methanol fuel cell, J. Power Sources, 96 (2001) 411-414.
- Coutinho D., Yang Z., Feng F., Ferraris J.P., and Balkus Jr. K.J., Proton conducting polyaniline molecular sieves composites, Prepr. Pap.-Am. Chem. Soc., Div. Fuel Chem., 49:2 (2004) 524-525.
- Coutinho D., Yang Z., Ferraris J.P., and Balkus Jr. K.J., Proton conducting polyaniline molecular sieve composites, Microporous Mesoporous Mater., 81 (2005) 321–332.

- Cruickshank J. and Scott K., The degree and effect of methanol crossover in the direct methanol fuel cell, J. Power Sources, 70 (1998) 40-47.
- Curtin D.E., Lousenberg R.D., Henry T.J., Tangeman P.C., and Tisack M.E., Advanced materials for improved PEMFC performance and life, J. Power Sources, 131 (2004) 41–48.
- Dacur F.N., and Sruousr A.N.R. R. P. Y., Pressure-temperature studies of anatase, brookite, rutile and TiO-II, The American Mineralogist, 53 (1968).
- Daiko Y., Klein L.C., Kasuga T., and Nogamia M., Hygroscopic-oxides/nafion hybrid electrolyte for direct methanol fuel cells, J. Membr. Sc, 281 (2006) 619–625.
- Dakhel A.A., Electrical conduction processes in neodymium oxide thin films prepared on Si(100) substrates, J. Alloys Compd., 376 (2004) 38-42.
- Dan X., Yang W., Yang Z., Gang Z., Ke S., Wei L.S., and Hui N., Hybird membrane with high proton conductivity and selectivity based on speek for direct methanol fuel cells, Chem. Res. Chin. Univ., 26:6 (2010) 1031-1034.
- Das P., Barbora L., Das M., Goswami P., Highly sensitive and stable laccase based amperometric biosensordeveloped on nano-composite matrix for detecting pyrocatechol inenvironmental samples, Sens. Actuators, B, 192 (2014) 737– 744.
- Datta J., Dutta A., and Biswas M., Enhancement of functional properties of PtPd nano catalyst in metal-polymer composite matrix: Application in direct ethanol fuel cell, Electrochem. Commun., 20 (2012) 56-59.
- Deluca N.W., and Elabd Y.A., Polymer electrolyte membranes for the direct methanol fuel cell: A review, J. Polym. Sci., Part B: Polym. Phys., 44:16 (2006) 2201-2225.
- Demirbas A., In: Biohydrogen for future engine fuel demands fuel cells, Springer, London, England, (2009) 221-239.
- D'Epifanio A., Navarra M.A., Weise F.C., Mecheri B., Farrington J., Licoccia S., and Greenbaum S., Composite nafion/sulfonated zirconia membranes: effect of the filler surface properties on proton transport characteristics, Chem. Mater. 9;22 (2010) 813-821..
- Di Noto V., Piga M., Lavina S., Negro E., Yoshida K., Ito R., and Furukawa T., Structure, properties and proton conductivity of

nafion/[(TiO_2)·(WO_3)0.148]ψTiO_2 nanocomposite membranes, Electrochim. Acta, 55 (2010) 1431.

- Di Noto V., Piga M., Piga L., Polizzi S., and Negro E., J., New inorganic–organic proton conducting membranes based on nafion and [(ZrO_2)·(SiO_2)0.67] nanoparticles: Synthesis vibrational studies and conductivity, J. Power Sources, 178 (2008) 561-574.
- Difoe A., Verma A., and Saha U. K., A Preliminary design approach for 1 kW direct methanol fuel cell system, J. Mech. Engg., 1 (2008) 30-46.
- Dillon R., Srinivasan S., Aricò A.S., and Antonucci V., International activities in DMFC R&D: status of technologies and potential applications, J. Power Sources, 127:1–2 (2004) 112-126.
- Dimitrova P., Friedrich K.A., Stimming U., and Vogt B., Modified nafion based membranes for use in direct methanol fuel cells, Solid State Ionics, 150 (2002) 115-122.
- Dimitrova P., Friedrich K.A., Stimming U., and Vogt B., Transport properties of ionomer composite membranes for direct methanol fuel cells, J. Electroanal. Chem., 532 (2002) 75-83.
- Ding K.Q., Electrocatalysis of Cyclic Voltammetrically Prepared Co-MnO_2 Composite towards Oxygen Reduction Reaction (ORR). Jnl Chinese Chemical Soc., 57 (2010) 1309–1314.
- Easton B.E. (2003) Chemical Modification of Fuel Cell Catalysts and Electrochemistry of Proton Exchange Membrane Fuel Cell Electrodes (Ph.D) Memorial University of Newfoundland, St. John's, Newfoundland, Canada.
- Easton E.B., Langsdorf B.L., Hughes J.A., Sultan J., Qi Z.G., Kaufman A., and Pickup P.G., Characteristics of polypyrrole/nafion composite membranes in a direct methanol fuel cell, J. Electrochem. Soc., 150:10 (2003), C735-C739.
- England W.A., Cross M.G., Hamnett A., Wiseman P.J., and Goodenough J.B., Fast proton conduction in inorganic ion-exchange compounds, Solid State Ionics, 1 (1980) 231-249.
- Falk M., An infrared study of water in perfluorosulfonate (Nafion) membranes, Can. J. Chem., 58 (1980) 1495-1501.

- Fang X., Shen P.K., Song S., Stergiopoulos V., and Tsiakaras P., Degradation of perfluorinated sulfonic acid films: An in-situ infrared spectro-electrochemical study, Polym. Degrad. Stab., 94 (2009) 1707–1713.
- Fu R.Q., Woo J.J., Seo S.J., Lee J.S., and Moon S.H., Covalent organic/inorganic hybrid proton-conductive membrane with semi-interpenetrating polymer network: preparation and characterizations, J. Power Sources, 179 (2008) 458-466.
- Fujishima A., Rao T.N., and Tryk D.A., TiO_2 photocatalysts and diamond electrodes, Electrochim. Acta, 45 (2000) 4683–4690.
- Gellett W., Schumacher J., Kesmez M., Le D., and Minteer S.D., High current density air-breathing laccase biocathode, J. Electrochem. Soc., 157 (2010) B557-B562.
- Gierke T.D., Munn G.E., and Wilson F.C., The morphology in nafion perfluorinated membrane products, as determined by wide- and small-angle X-ray studies, J. Polym. Sci., Part B: Polym. Phys., 19 (1981) 1687-1704.
- Glushkova V.B. and Suglobov D.N., Infrared spectra of the products of the reaction of Nd_2O_3 with water, J. Struct. Chem., 6:6 (1965) 804-808.
- Godino M.P., Barragán V.M., Villaluenga J.P.G., Ruiz-Bauzá C., and Seoane B., Water and methanol transport in Nafion membranes with different cationic forms. Alkali monovalent cations, J. Power Sources, 160 (2006) 181-186.
- Gosalawit R. , Chirachanchai S., Shishatskiy S., and Nunes S.P., Krytox-montmorillonite-nafion nanocomposite membrane for effective methanol crossover reduction in DMFCs, Solid State Ionics, 178 (2007) 1627–1635.
- Gross D., Fuel Cells: 170 years of technology development and Space Age experience, Cleantech magazine Fuel Cell Special, 2010.
- Ha S., Larsen R., and Masel R.I., Performance characterization of Pd/C nanocatalyst for direct formic acid fuel cells, J. Power Sources, 144 (2005) 28-34.
- Hankins D., Moskowitz J.W., and Sillinger F.H., Water molecule interactions, J. Chem. Phys., 53 (1970) 4544-4554.
- Hansen C.M.. (2012). Solubility Parameters: An introduction. In: Hansen C.M. Hansen Solubility Parameters: A User's Handbook. USA: CRC Press. 1-24.
- Heitner-Wirguin, C., Recent Advances in Perfluorinated Ionomer Membranes. J. Membr. Sci., 120 (1996) 1-33.

- Hobson L.J., Nakano Y., Ozu H. and Hayase S., Targeting improved DMFC performance, J. Power Sources, 104 (2002) 79-84.
- Hogarth M.P. and Ralph T.R., Catalysis for low temperature fuel cells, Platinum Met. Rev., 46:4 (2002) 146–164.
- Holmberg B.A., Wang X., and Yan Y., Nanocomposite fuel cell membranes based on Nafion and acid functionalized zeolite beta nanocrystals, J. Membr. Sci., 320 (2008) 86–92
- Horkay F., Tasaki I., and Basser P.J., Effect of monovalent-divalent cation exchange on the swelling of polyacrylate hydrogels in physiological salt solutions, Biomacromolecules, 2 (2001) 195-199.
- Hou H., Sun G., Wu Z., Jin W., and Xin Q., Zirconium phosphate/Nafion115 composite membrane for high-concentration DMFC, Int. J. Hydrogen Energy, 33 (2008) 3402 – 3409.
- http://www.eia.gov/forecasts/ieo/pdf/0484 (2013) (accessed 13th December, 2013)
- http://www.fuelcelltoday.com/media/1713685/fct_review_2012
- Inanaga J., Yokoyama Y., and Hanamoto T., Lanthanoid(III) triflates as new glycosylation catalysts, selective and efficient activation of 1-o-methoxyacetyl sugars, Tetrahedron Lett., 34 (1993) 2791-2794.
- Jiang R.C., Kunz H.R., and Fenton J.M., Composite silica/nafion membranes prepared by tetraethylorthosilicate sol–gel reaction and solution casting for direct methanol fuel cells, J. Membr. Sci., 272 (2006) 116–124.
- Jin Y., da Costa D.J.C., Lu G.Q., Proton conductive composite membrane of phosphosilicate and polyvinyl alcoho, Solid State Ionics, 178 (2007) 937-942.
- Jones D.J., and Roziere J., Fuel Cells I, Advances in the development of inorganic–organic membranes for fuel cell applications, J. Nanosci. Nanotechnol., 215 (2008) 219-264.
- Jun Y., Mu P., and Runzhang Y., Nafion/silicon oxide composite membrane for high temperature proton exchange membrane fuel cell, Mater. Sci., 22 (2007) 478-481.
- Jung D.H., Cho S.Y., Peck D.H., Shin D.R., and Kim J.S., Performance evaluation of a nafion/silicon oxide hybrid membrane for direct methanol fuel cell, J. Power Sources, 106 (2002), 173-177.

- Kadirgan F., and Savadogo O., Methanol Crossover through Modified Nafion Proton Exchange Membrane, Russ. J. Electrochem., 40 (2004) 1141-1145.
- Kang S., Peck D.H., Park, Y.C., Jung D.H., Jang J. H., Lee H.R.J., Hydroscopic strontium hydroxide/nafion composite membrane for a direct methanol fuel cell, Phys. Chem. Solids, 2008, 69, 1280-1283.
- Kashyout A.B, Nassr A B.A.A., Giorgi L.,and Maiyalagan T., Youssef B.A.B., Electrooxidation of methanol on carbon supported Pt-Ru nanocatalysts prepared by ethanol reduction method, Int. J. Electrochem. Sci., 6 (2011) 379 – 393.
- Katsuhara Y., Aramaki M., Ishii A., Kume T., Kawashima C., and Mitsumoto S., Fluorine chemistry at Central Glass:Review, J. Fluorine Chem., 127 (2006) 8–17.
- Ke˛pin´ski L., Zawadzki M., and Mis´ta W., Hydrothermal synthesis of precursors of neodymium oxide nanoparticles, Solid State Sci., 6 (2004) 1327-1336.
- Kim D.S., Shin K.H., Park H.B., and Lee Y.M., Preparation and Characterization of Sulfonated Poly(phthalazinone ether sulfone ketone) (SPPESK)/Silica Hybrid Membranes for Direct Methanol Fuel Cell Applications, Macromol. Res., 12 (2004) 413-421.
- Kim T.K., Kang M., Choi Y.S., Kim H.K., Lee W., Chang H., and Seung D., Preparation of Nafion-sulfonated clay nanocomposite membrane for direct menthol fuel cells via a film coating process, J. Power Sources, 165(2007) 1-8.
- Kim Y., Lee J.S., Rhee C.H., Kim H.K., and Chang H., Montmorillonite functionalized with perfluorinated sulfonic acid for proton-conducting organic-inorganic composite membranes, J. Power Sources, 162 (2006) 180-185.
- Kim Y.J., Choi W.C., Woo S.I., and Hong W.H., Proton conductivity and methanol permeation in nafion/ORMOSIL prepared with various organic silanes, J. Membr. Sci, 238 (2004) 213-222.
- Kim Y.M, Park K.W, Choi J.H., Park I.S., and Sung Y.E., A Pd-impregnated nanocomposite Nafion membrane for use in high-concentration methanol fuel in DMFC, Electrochem. Commun., 5 (2003) 571–574.
- Kim Y.S, Cho H.S., Song M.K., Ghil L.J., Kang J.S., and Rhee H.W., Characterization of nafion/zirconium sulphophenyl phosphate nanocomposite membrane for direct methanol fuel cells, J. Nanosci. Nanotechnol., 8:9 (2008) 4640-4643.

- Kobayashi S., Rare earth metal trifluoromethanesulfonates as water-tolerant Lewis-acid catalysts in organic synthesis, Synlett, 9 (1994) 689-701.
- Kreuer K.D., On the development of proton conducting polymer membranes for hydrogen and methanol fuel cells, J. Membr. Sci, 185 (2001) 29-39.
- Kujawski W., Nguyen Q.T., and Neel J., Infrared investigations of sulfonated ionomer membranes. I. Water–alcohol compositions and counter ions effects, J. Appl. Polym. Sci., 44 (1992) 951-958.
- Kumutha K. and Alias Y., FTIR spectra of plasticized grafted natural rubber–$LiCF_3SO_3$ electrolytes, Spectrochim. Acta Part A, 64 (2006) 442-447.
- Laporta M., Pegoraro M., and Zanderighi L., Perfluorosulfonated membrane (Nafion): FT-IR study of the state of water with increasing humidity, Phys. Chem. Chem. Phys., 1 (1999) 4619-4628.
- Larminie J., and Dicks A.. (2000). Proton exchange membrane fuel cells. In: Larminie J., and Dicks A. Fuel Cell Systems Explained. West Sussex, England : John Wiley & Sons. 69-72.
- Lee P.C., Han T.H. , Kim D.O., Lee J.H., Kang S.J., Chung C.H., Lee Y., Cho S.M., Choi H.G., Kim T., Lee E., and Nam J.D., In situ formation of platinum nanoparticles in Nafion recast film for catalyst-incorporated ion-exchange membrane in fuel cell applications, J. Membr. Sci., 322 (2008) 441–445.
- Li J., Ye D.D., Zhu X., Liao Q., Ding Y.D., and Tian X., Effect of wettability of anode microporous layer on performance and operation duration of passive air-breathing direct methanol fuel cells, J. Appl. Electrochem., 39 (2009) 1771–1778.
- Li X., and Sabir I., Review of bipolar plates in PEM fuel cells: Flow-field designs, Int. J. Hydrogen Energy, 30 (2005) 359 – 371.
- Liang Z.X., Zhao T.S., and Prabhuram J., Diphenyl silicate incorporated nafion membranes for reduction of methanol crossover in direct methanol fuel cells, J. Membr. Sci., 283 (2006) 219-224.
- Lide D.R. (1998) Handbook of Chemistry and Physics, Raton B., FL: CRC Press, 471.
- Lin F. (2006) Preparation and characterization of polymer TiO_2 nanocomposites via in-situ polymerization (M.Sc.), University of Waterloo, Waterloo, Ontario, Canada.

- Lin J.J., Chang Y.C., and Cheng I.J., Novel mechanism for layered silicate clay intercalation by poly(oxypropylene)-segmented carboxylic acid, Macromol. Rapid Commun., 25 (2005) 508-512.
- Lin Y., Li H., Liu C.P., Xing W., and Ji X.L., Surface-modified nafion membranes with mesoporous SiO_2 layers via a facile dip coating approach for direct methanol fuel cells, J. Power Sources, 2008;185:904–8.
- Lin Y.F., Yen C.Y., Hung C.H., Hsiao Y.H., and Ma C.C.M., A novel composite membranes based on sulfonated montmorillonite modified nafion for DMFCs, Short communication, J. Power Sources, 168 (2007) 162–166.
- Lin Y.F., Yen C.Y., Ma C.C.M., Liao S.H., Hung C.H., and Hsiao Y.H., Preparation and properties of high performance nanocomposite proton exchange membrane for fuel cell, J. Power Sources, 165 (2007) 692-700.
- Lin Y.S., and Seshadri S. (2011) Preparation chemistry of inorganic membranes, In. Xu R., Yan W., Pang W., Huo Q., Modern Inorganic Synthetic Chemistry Elsevier, Amsterdam, 507-524.
- Lindermeir A., Rosenthal G., Kunz U., and Hoffmann U., On the question of MEA preparation for DMFCs, J. Power Sources, 129 (2004) 180–187.
- Liu F., Yi B., Xing D., Yu J., Zhang H., Nafion/PTFE composite membranes for fuel cell applications, J. Membr. Sci, 212 (2003) 213–223.
- Liu J., Wang H., Cheng S., and Chan K.Y., Nafion–polyfurfuryl alcohol nanocomposite membranes for direct methanol fuel cells, J. Membr. Sci, 246 (2005) 95-101.
- Liu Z., Guo B., Huang J., Hong L., Han M., and Gan L.M., Nano-TiO_2-coated polymer electrolyte membranes for direct methanol fuel cells, J. Power Sources, 157 (2006) 207–211.
- Lobato J., Cañizares P., Ubeda D., Pinar F.J., Rodrigo M.A., Testing PtRu/CNF catalysts for a high temperature polybenzimidazole-based direct ethanol fuel cell. Effect of metal content, Appl. Catal., B, 106 (2011) 174-180.
- Lobato J., Canizares P., Rodrigo M.A., Úbeda D., Pinar F.J., Enhancement of the fuel cell performance of a high temperature proton exchange membrane fuel cell running with titanium composite polybenzimidazole-based membranes, J. Power Sources 196 (2011) 8265–8271.

- Lowry S.R. and Mauritz K.A., An investigation of ionic hydration effects in perfluo- rosulfonate ionomers by Fourier transform infrared spectroscopy, J. Am. Chem. Soc., 102 (1980) 4665-4667.
- Luan Y., Zhang Y., Zhang H., Li L., Li H., and Liu Y., Annealing effect of perfluorosulfonated ionomer membranes on proton conductivity and methanol permeability, J. Appl. Polym. Sci., 107 (2008) 396-402.
- Ludvigsson M., Lindgren J., and Tegenfeldt J., FTIR study of water in cast nafion films, Electrochim. Acta, 45 (2000) 2267-2271.
- Lvov S.N., Fedkin M.V., Chalkova E., and Pague M.V., Composite membrane based PEMFCs for operationg at elevated temperature and reduced relative humidity, Prepr. Pap.-Am. Chem. Soc., Div. Fuel. Chem., 49:2 (2004) 606-607.
- Ma Z.Q., Cheng P., and Zhao T.S., A palladium-alloy deposited nafion membrane for direct methanol fuel cells, J. Membr. Sci, 215 (2003) 327-336.
- Madhavi V., and Lele S.S., Laccase: Properties and applications, BioResources, 4:4 (2009) 1694-1717.
- Mahreni A.B., Mohamad A.B., Kadhum A.A.H., Daud W.R.W., and Iyuke S.E., Nafion/silicon oxide/phosphotungstic acid nanocomposite membrane with enhanced proton conductivity, J. Memb. Sci., 327 (2009) 32-40.
- Malherbe R.R.M.A., (2009) The Physical Chemistry of Materials: Energy and Environmental Applications, CRC Press, 522.
- Mano N., Mao F., and Heller A., A Miniature Biofuel Cell Operating in A Physiological Buffer, J. Am. Chem. Soc., 124 (2002) 12962–12963.
- Martinot Eric, and Sawin Janet, Renewables global status report 2009 update
- Meredith M.T., and Minteer S.D., Biofuel cells: enhanced enzymatic bioelectrocatalysis, Annu. Rev. Anal. Chem. 2012. 5:157–79.
- Merwe E.M., and Strydom C. A., Hydration of medium reactive magnesium oxide using hydration agents, J. Therm. Anal. Calorim., 84 (2006) 467-471.
- Mizuno K., Mabuchi K., Miyagawa T., Matsuda Y., Kita S., Kaida M., and Shindo Y., IR study of hydrogen bonds in halogeno-alcohol–water mixtures, J. Phys. Chem. A, 101 (1997) 1366-1369.
- Mohamadbeigy K. , Forsat K. , and Binesh R., Experimental studying on gas dewatering by molecular sieve, Pet. Coal, 49:1 (2007) 41-45.

- Mokhtaruddin S.R., Mohamad A.B., Shyuan L.K., Kadhum A.A.H., and Akhmad M., Preparation and characterization of nafion-zirconia composite membrane for PEMFC, Adv. Mat. Res., (2011) 239 – 242.
- Mustain W.E., Kepler K., and Prakash J., CoPdx oxygen reduction electrocatalysts for polymer electrolyte membrane and direct methanol fuel cells, Electrochim. Acta, 52 (2006) 2102-2108.
- Nadykto A.B., and Yu F., Uptake of neutral polar vapor molecules by charged clusters//particles: Enhancement due to dipole-charge interaction, J. Geophys. Res., 108:23 (2003) 4717-4723.
- Nagao M., Hamano H., Hirata K., Kumashiro R., and Kuroda Y., Hydration process of rare-earth sesquioxides having different crystal structures, Langmuir, 19 (2003) 9201-9209.
- Nam S.E., Kim S.O., Kang Y., Lee J.W., and Lee K.H., Preparation of Nafion/sulfonated poly(phenylsilsesquioxane) nanocomposite as high temperature proton exchange membranes, J. Membr. Sci., 322 (2008) 466-474.
- Navarra M.A., Croce F., and Scrosati B., New high temperature superacid zirconia doped nafion composite membranes, J. Mater. Chem., 17 (2007) 3210-3215.
- Neburchilov V., Martin J., Wang H., and Zhang J., A review of polymer electrolyte membranes for direct methanol fuel cells, J. Power Sources, 169 (2007) 221-238.
- Neto A.O., Vasconcelos T.R.R., Da Silva R.W.R.V., Spinace´M.L.E.V., Electro-oxidation of ethylene glycol on PtRu/C and PtSn/C electrocatalysts prepared by alcohol-reduction process, J. Appl. Electrochem., 35 (2005) 193-198.
- Nguyen T., and Wang X., Multifunctional composite membrane based on a highly porous polyimide matrix for direct methanol fuel cells, J. Power Sources, 195 (2010) 1024-1030.
- Nicotera K., Angjeli L., Coppola, Aricò A.S., and Baglio V., NMR and electrochemical investigation of the transport properties of methanol and water in Nafion and clay-nanocomposites membranes for DMFCs, Membranes, 2 (2012) 325-345.
- Offer G.J., Shearing P., Golbert J.I., Brett D.J.L, Atkinson A., and Brandon N.P., Using electrochemical impedance spectroscopy to compensate for errors when

measuring polarization curves during three-electrode measurements of solid oxide fuel cell electrodes, Electrochim. Acta, 53 (2008) 7614-7621.

- O'Hayre R., Cha S.W., Colella W., and Odian F.B.P.G. (2004) Fuel cell fundamentals, 2nd Ed., Principles of Polymerization, Wiley-Interscience, 464.
- Othman M.H.D., Ismail A.F., and Mustafa A., Recent development of polymer electrolyte membranes for direct methanol fuel cell application-a review, Malaysian Polymer Journal, 5:2 (2010) 1-36.
- Park H., Kim Y., Hong W.H., Choi Y.S., and Lee H., Influence of morphology on the transport properties of perfluorosulfonate ionomers/polypyrrole composite membrane, Macromolecules, 38 (2005) 2289-2295.
- Park J., Wang L., Advani S.G., and Prasadz A.K., Durability analysis of nafion/hydrophilic pretreated PTFE membranes for PEMFCs, J. Electrochem. Soc., 159:12 (2012) F864-F870.
- Park Y.S. and Yamazaki Y., Low water uptake content and low water/methanol transport in CP/nafion hybrid membrane with high non-hydrogen bonding, J. Membr. Sci., 261 (2005) 58-66.
- Park Y.S. and Yamazaki Y., Novel Nafion/hydroxyapatite composite with high crystallinity and low methanol crossover for DMFC, Polym. Bull., 53 (2005) 181-192.
- Pereira F., Valle K., Belleville P., Morin A., Lambert S., and Sanchez C., Adavance mesostructured hybrid silica-nafion membranes for high performance PEM fuel cell, Chem. Mater., 20 (2008) 1710-1718.
- Pilatowsky I., Romero R.J., Isaza C.A., Gamboa S.A., Sebastian P.J., and Rivera W., (2011) Energy and Co-generation. Co-generation Fuel Cell-Sorption Air conditioning Systems. Green Energy and Technology, Springer-Verlag London Limited, 1-24.
- Prabhuram J., and Manoharan R., Investigation of methanol oxidation on unsupported platinum electrodes in strong alkali and strong acid, J. Power Sources, 74 (1998) 54-61.
- Prabhuram J., Zhao T.S., Liang Z.X., Yang H., and Wong C.W., Pd and Pd-Cu alloy deposited nafion membranes for reduction of methanol crossover in direct methanol fuel cells, J. Electrochem. Soc., 152:7, (2005) A 1390-A1397.

- Raj A.M.E., Nehru L.C., Jayachandran M., and Sanjeeviraja C., Spray pyrolysis deposition and characterization of highly (100) oriented magnesium oxide thin films, Cryst. Res. Technol., 42 (2007) 867-875.
- Ramani V., Kunz H.R., and Fenton J.M., Effect of particle size reduction on the conductivity of nafion/phosphotungstic acid composite membranes, J. Membr. Sci., 266 (2005) 110-114.
- Ramaswamy S., Huang H., Bandrau R. (2013) Application of adsorption in biorefineries, Separation and Purification Technologies in Biorefineries Adsorption, England: John Wiley & Sons Ltd. 647-662.
- Read J.F., The hydrogen–oxygen reaction on lanthanide oxides. I. Hydrogen and oxygen adsorption on some lanthanide oxides, Can. J. Chem., 50:4 (1972) 490-496.
- Reeve R.W., Christensen P.A., Dickinson A.J., Hamnettand A., and Scott K., Methanol-tolerant oxygen reduction catalysts based on transition metal sulfides and their application to the study of methanol permeation, Electrochim. Acta, 45 (2000) 4237–4250.
- Ren S., Li C., Zhao X., Wu Z., Wang S., Sun G., Xin Q., and Yang X., Surface modification of sulfonated poly(ether ether ketone) membranes using Nafion solution for direct methanol fuel cells, J. Membr. Sci, 247 (2005) 59-63.
- Ren S., Sun G., Li C., Song S., Xin Q., and Yang X., Sulfated zirconia–nafion composite membranes for higher temperature direct methanol fuel cells, J. Power Sources,157:2 (2006) 724-726.
- Rhee H., Kim H.K., Chang H., and Lee J.S., Nafion/sulfonated montmorillonite composite: a new concept electrolyte membrane for direct methanol fuel cells, Chem. Mater., 17 (2005) 1691-1697.
- Rhim J.W., Park H.B., Lee C.S., Jun J.H., Kim D.S., and Lee Y.M., Crosslinked poly(vinyl alcohol) membranes containing sulfonic acid group: proton and methanol transport through membranes, J. Membr. Sci., 238 (2004) 143-151.
- Rice C., Ha S., Masel R.I., Waszczuk P., Wieckowski A., and Barnard T., Direct formic acid fuel cells, J. Power Sources, 111 (2002) 83-89.
- Rill C., Bauer M., Bertagnolli H., and Kickelbick G., Microemulsion approach to neodymium, europium, and ytterbium oxide/hydroxide colloids--effects of

precursors and preparation parameters on particle size and crystallinity, J. Colloid Interface Sci., 325 (2008)179-186.

- Rodgers M.P., Shi Z.Q., and Holdcroft S., Transport properties of composite membranes containing silicon dioxide and nafion, J. Membr. Sci., 325 (2008) 346–56.
- Ruslimie C.A., Razali M.H., and Khairul W.M., Effect of HTAB concentration on the synthesis of nanostructured TiO_2 towards its catalytic activities, The Malaysian Journal of Analytical Sciences, 14:1 (2010) 41-49.
- Sacc`a A., Carbone A., Passalacqua E., D'Epifanio A., Licoccia S., Traversa E., Sala E., Traini F., and Ornelas R., Nafion–TiO_2 hybrid membranes for medium temperature polymer electrolyte fuel cells (PEFCs), J. Power Sources, 152 (2005) 16–21.
- Sandhu S.S., Crowther R.O., and Fellner J.P., Prediction of methanol and water fluxes through a direct methanol fuel cell polymer electrolyte membrane, Electrochim. Acta, 50 (2005) 3985-3991.
- Sanni A.S. (2011) Development of zeolites and zeolite membranes from ahoko nigerian kaolin (Ph.D), University of Manchester, Manchester, U.K.
- Santiago E.I., Isidoro R.A., Dresch M.A., Matos B.R., Linardi M., and Fonseca F.C., Nafion–TiO_2 hybrid electrolytes for stable operation of PEM fuel cells at high temperature, Electrochim. Acta, 54 (2009) 4111–4117.
- Satterfield M.B., Majsztrik P.W., Ota H., Benziger J.B., and Bocarsly A., Mechanical properties of nafion and titania/nafion composite membranes for polymer electrolyte membrane fuel cells, J. Polym. Sci.: Part B: Polym. Phys., 44 (2006) 2327–2345.
- Saxena U., Das M., Ahmed S., Barbora L., Borthakur M., Verma A., Bora U., and Goswami P., Multiwalled carbon nanotube-based enzyme electrode for total cholesterol estimation in human serum, J. Exp. Nanosci., 6:1 (2011) 84-95.
- Sethuraman V., Weidner J.W., A. Haug T., Motupally S., and Protsailo L.V., Hydrogen Peroxide Formation Rates in a PEMFC Anode and Cathode: Effect of Humidity and Temperature, J. Electrochem. Soc., 155 (2008) B50-B57.
- Shao Z.G., and Hsing I.M., Nafion membrane coated with sulfonated poly(vinyl alcohol)-nafion film for direct methanol fuel cells electrochem, Solid-State Lett., 5:9 (2002) A185-A187.

- Shao Z.G., Xu H., Li M., and Hsing I.M., Hybrid nafion inorganic oxides membrane doped with heteropolyacids for high temperature operation of proton exchange membrane fuel cell, Solid State Ionics, 177 (2006) 779–785.
- Shen Y., Xi J.Y., Qiu X.P., and Zhu W.T., A new proton conducting membrane based on copolymer of methyl methacrylate and 2-acrylamido-2-methyl-1-propanesulfonic acid for direct methanol fuel cells, Electrochim. Acta, 52 (2007) 6956–61.
- Shroti N., Barbora L. , and Verma A., Neodymium triflate modified nafion composite membranefor reduced alcohol permeability in direct alcohol fuel cell, Int. J. Hydrogen Energy, 36 (2 0 1 1) 14907-14913.
- Si Y., Lin J.C., Kunz H.R., and Fenton J.M., $Zr(HPO_4)_2$-nafion composite membranes for direct methanol fuel cells, Meeting of the Electrochemical Society, Philadelphia, PA, 2002.
- Silva C.J.R., and Smith M.J., Preparative effects on poly(ethylene oxide) based polymer electrolytes of lanthanide salts, Electrochim. Acta, 40 (1995) 2389-2392.
- Silva M.M., Zea de Bermudez V., Carlos L.D., and Smith M.J., Neodymium doped sol-gel processed polymer electrolytes, Ionics, 4 (1998)170-174.
- Silva V.S., Ruffmann B., Silva H., Mendes A., Madeira M., and Nunes S., Zirconium oxide modified sulfonated poly(ether ether ketone) membranes for direct methanol fuel cell applications, Mater. Sci. Forum, 455-456 (2004) 587-591.
- Silva V.S., Ruffmann B., Vetter S., Mendes A., Madeira L.M., and Nunes S.P., Characterization and application of composite membranes in DMFC, Catal. Today, 104 (2005) 205-212.
- Siracusano S., Baglio V., Navarra M.A., Panero S., Antonucci V., and Aricò A.S., Investigation of composite nafion/sulfated zirconia membrane for solid polymer electrolyte electrolyzer applications, Int. J. Chem. Sc., 7 (2012) 1532-1542.
- Smitha B., Sridhar S., and Khan A.A., Solid polymer electrolyte membranes for fuel cell applications-a review, J. Membr. Sci., 259 (2005) 10–26.
- Song C., and Zhang J. (2008) Electrocatalytic Oxygen Reduction Reaction. In: Zhang J. PEM Fuel Cell Electrocatalysts and Catalyst Layers Fundamentals and Applications, Springer.

- Soukharev V., Mano N., and Heller A., A four-electron O_2-electroreduction biocatalyst superior to platinum and a biofuel cell operating at 0.88 V, J. Am. Chem. Soc., 126 (2004) 8368–8369.
- Staiti P., Arico A.S., Baglio V., Lufrano F., and Passalacqua E., Antonucci V., Hybrid nafion-silica membranes doped with heteropolyacids for application in direct methanol fuel cells, Solid State Ionics, 145 (2001) 101-107.
- Stone C., and Morrison A.E., From curiosity to 'power to change the world, Solid State Ionics, 152-153 (2002) 1–13.
- Su L.J., Li L., Li H., Tang J.K., Zhang Y.M., Yu W., and Zhou C.X., Preparation of polysiloxane modified perfluorosulfonic acid composite membranes assisted by supercritical carbon dioxide for direct methanol fuel cell, J. Power Sources, 194 (2009) 220-225.
- Su L.J., Pei S.P., Li L., Li H., Zhang Y.M., Yu W., and Zhou C.X., Preparation of polysiloxane/perfluorosulfonic acid nanocomposite membranes in supercritical carbon dioxide system for direct methanol fuel cell, Int. J. Hydrogen Energy, 34 (2009) 6892-6901.
- Sun H., Sun G., Wang S., Liu J., Zhao X., Wang G., Xu H., Hou S., and Xin Q., Pd electroless plated nafion membrane for high concentration DMFCs, J. Membr. Sci, 259 (2005) 27-33.
- Sungpet A., Reduction of alcohol permeation through nafion by polypyrrole, J. Membr. Sci, 226 (2003) 131-134.
- Surampudi S., Narayanan S.R., Vamos E., Frank H., Halpert G., LaConti A., Kosek J., Prakash G.K.S., and Olah G.A., Advances in direct oxidation methanol fuel cells, J. Power Sources, 47 (1994) 377-385.
- Szamocki R., Flexer V., Levin L., Forchiasin F., and Calvo E.J., Oxygen cathode based on a layer-by-layer self-assembled laccase and osmium redox mediator, Electrochim. Acta, 54 (2009) 1970-1977.
- Tang H., Pan M., Jiang S., Wan Z., and Yuan R., Self-assembling multi-layer Pd nanoparticles onto nafion membrane to reduce methanol crossover, Colloids Surf., A, 262 (2005) 65-70.
- Tang H., Wan Z., Pan M., and Jiang S.P., Self-assembled nafion–silica nanoparticles for elevated-high temperature polymer electrolyte membrane fuel cells, Electrochem. Commun., 9 (2007) 2003-2008.

- Tay S.W., Zhang X., Liu Z., Hong L., and Chan S.H., Composite nafion membrane embedded with hybrid nanofillers for promoting direct methanol fuel cell performanceOriginal Research Article, J. Membr. Sci., 321 (2008) 139-145.
- Tazi B., and Savadogo O., Effect of various heteropolyacids (HPAs) on the characteristics of Nafion®-HPAS membranes and their H_2/O_2 polymer electrolyte fuel cell parameters, J. New. Mat. Electrochem. Systems, 4 (2001) 187-196.
- Tazi B., and Savadogo O., Parameters of PEM fuel-cells based on new membranes fabricated from Nafion®, silicotungstic acid and thiophene, Electrochim. Acta, 45 (2000) 4329-4339.
- Thamaphat K., Limsuwan P., and Ngotawornchai B., Phase characterization of TiO_2 powder by XRD and TEM, Kasetsart J. (Nat. Sci.), 42 (2008) 357 – 361.
- Townsend R.P., and Harjula R., Ion Exchange in Molecular Sieves by Conventional Techniques, Molecular Sieves, 3 (2002) 1-42.
- Tricoli V., and Nannetti F., Zeolite-nafion composites as ion conducting membrane materials, Electrochim. Acta, 48 (2003) 2625-2633.
- Tricoli V., Proton and methanol transport in poly(perfluorosulfonate) membranes containing Cs^+ and H^+ cations, J. Electrochem. Soc., 145 (1998) 3798-3801.
- Tsai J.C., Cheng H.P., Kuo J.F., Huang Y.H., and Chen C.Y., Blended nafion/SPEEK direct methanol fuel cell membranes for reduced methanol permeability, J. Power Sources, 189 (2009) 958–965.
- Tseng T. F. , County H., Hsein T., County H., Chen T.H., County H., Hao H., Count H., Wei C., and Hsinchu C., Epoxy resin blend, United States Patent Application Publication (2012) 1-4 US 2012/0055704.
- Uchida H., Mizuno Y., and Watanabe M., Suppression of methanol crossover in Pt-dispersed polymer electrolyte membrane for direct methanol fuel cells, Chem. Lett., (2000)1268-1269.
- Umeda M., Sayama K., and Inou M., Temperature and methanol concentration dependences of direct methanol fuel cell performance measured by single cell having reference electrode, J. Renewable Sustainable Energy, 3 (2011) 043107-043109.
- Vaivars G., Maxakato N.W., Mokrani T., Petrik L., Klavins J., Gericke G., and Linkov V., Zirconium Phosphate Based Inorganic Direct Methanol Fuel Cell, Mater. Sci., 10 (2004) 162–165.

- Velankar S.S., Richard V.L., and Vaia A., Swelling induced delamination causes folding of surface-tethered polymer gels, Appl. Mater. Interfaces, 4 (2012) 24−29.
- Viswanathan, and Helen M., Is nafion, the only Choice?, Bulletin of the Catalysis Society of India, 6 (2007) 50-66.
- Wand G., Fuel cells history, Part 1, Johnson Matthey plc., 14, Retrieved 2008-10-06.
- Wang J.T., Wasmus S., and Savinell R.F., Real-time mass spectrometric study of the methanol crossover in a direct methanol fuel cell, J. Electrochem. Soc., 143:4 (1996) 1233-1239.
- Wang L., and Kumar R.V., Thick film miniaturized HCl gas sensor, Sens. Actuators, B, 98 (2004) 196-203.
- Wang M., Guo H., and Ma C., Dynamic Characteristics of a Direct Methanol Fuel Cell, J. Fuel Cell Sci. Technol., 3 (2006) 202-207.
- Wang Y., Chen K.S., Mishler J., Cho S.C., and Adroher X.C., A review of polymer electrolyte membrane fuel cells: Technology, applications, and needs on fundamental research, Appl. Energy, 88 (2011) 981–1007.
- Wang B. Wang Q., Li L., Morphology and properties of highly talc- and $CaCO_3$-filled poly(vinyl alcohol) composites prepared by melt processing J. Appl. Polym. Sci., 130: 5 (2013) 3050–3057.
- Watanabe M, Uchida H., and Emori M., Polymer electrolyte membranes incorporated with nanometer-size particles of Pt and/or metal-oxides: experimental analysis of the self-humidification and suppression of gas-crossover in fuel cells, J. Phys. Chem. B, 102 (1998) 3129-3137.
- Watanabe M., Uchida H., Seki Y., Emori M., and Stonehart P., Self-humidifying polymer electrolyte membranes for fuel cells, J. Electrochem. Soc., 143:12 (1996) 3847-3852.
- Website[1] http://en.wikipedia.org/wiki/Fuelcell (last accessed on 13th December, 2013)
- Wongkaew A., Jansome W., Khemchan S., Sawaengmit N., and Mitpapan S., Synthesis of nanoparticles of mixed oxides containing titanium cerium silver and silicon: phase transformation, Energy Research Journal, 1:2 (2010) 73-77.

- Wu R.J., Sun Y.L., Lin C.C., Chen H.W., and Chavali M., Composite of TiO_2 nanowires and nafion as humidity sensor material, Sens. Actuators, B, 115 (2006) 198–204.
- Wu Z., Sun G., Jin W., Hou H., Wang S., and Xin Q., Nafion® and nano-size TiO_2–SO_4^{2-} solid superacid composite membrane for direct methanol fuel cell, J. Membr. Sci., 313 (2008) 336–343.
- Xi J., Wu Z., Qiu X., and Chen L., Nafion/SiO_2 hybrid membrane for vanadium redox flow battery, J. Power Sources, 166 (2007) 531-536..
- Xiong L. and Manthiram A., Synthesis and characterization of methanol tolerant Pt/TiOx/C nanocomposites for oxygen reduction in direct methanol fuel cells, Electrochim. Acta, 49: 24 (2004) 4163-4170.
- Xu C.W., Shen P.K., Ji X., Zeng R., and Liu Y., Enhanced activity for ethanol electrooxidation on Pt–MgO/C catalysts, Electrochem. Commun., 7 (2005) 1305-1308.
- Xu W., Lu T., Liu C., and Xing W., Low methanol permeable composite Nafion/silica/PWA membranes for low temperature direct methanol fuel cells, Electrochim Acta, 50 (2005) 3280-3285.
- Yang C., Srinivasan S., Aricò A.S., Cretì P., Baglio V., and Antonucci V., Composite nafion/zirconium phosphate membranes for direct methanol fuel cell operation at high temperature, Electrochem. Solid-State Lett., 4:4 (2001) A31-A34.
- Yang C., Srinivasan S., Bocarsly A.B., Tulyani S., and Benziger J.B., A comparison of physical properties and fuel cell performance of Nafion and zirconium phosphate/Nafion composite membranes, J. Membr. Sci., 237 (2004) 145–161.
- Ye Q., and Zhao T. S., Abrupt decline in the open-circuit voltage of direct methanol fuel cells at critical oxygen feed rate, J. Electrochem. Soc., 152:11 (2005) A2238-A2245.
- Yeager H.L., and Steck A., Cation and water diffusion in nafion exchange membranes: influence of polymer structure, J. Electrochem. Soc., 128:9 (1981) 1880-1884.

- Yen C.Y., Lee C.H., Lin Y.F., Lin H.L., Hsiao Y.H., Liao S.H., Chuang C.Y., and Ma C.C.M., Sol–gel derived sulfonated-silica/nafion composite membrane for direct methanol fuel cell, J. Power Sources,173 (2007) 36-44.
- Yeo T.L., Sun T., Grattan K.T.V., Parry D., Lade R., and Powell B.D., Characterization of a polymer-coated fibre Bragg grating sensor for relative humidity sensing, Sens. Actuators, B, 110 (2005) 148–156.
- Yoon S.R., Hwang G.H., Cho W.I, Oh I.H., Hong S.A., and Ha H.Y., Modification of polymer electrolyte membranes for DMFCs using Pd films formed by sputtering, J. Power Sources, 106 (2002) 215-223.
- Zaidi S.M.J.. (2009). Research trends in polymer electrolyte membranes. In: Zaidi S.M.J., and Matsuura T. Polymer Membranes for Fuel Cells. Canada: Springer. 7-19.
- Zawodzinski T.A., Deroin C., Radzinski S., Sherman J., Smith V.T., Springer T.E., Gottesfeld S., Water-uptake by and transport through nafion-117 membranes, J. Electrochem. Soc., 140 (1993) 1041-1047.
- Zhang H., and Shen P.K., Recent Development of Polymer Electrolyte Membranes for Fuel Cells, Chem. Rev., 112 (2012) 2780−2832.
- Zhang T. (2005) Valveless piezoelectric micropump for fuel delivery in direct methanol fuel cell (DMFC) devices (Ph.D), University of Pittsburgh, U.S.A.
- Zhou W.J., Song S.Q., Li W.Z., Sun G.Q., Xin Q., Kontou S., Poulianitis K., and Tsiakaras P., Pt-based anode catalysts for direct ethanol fuel cells, Solid State Ionics, 175 (2004) 797-803.

Annexure A

Annexure A

A.a *SEM of membranes*

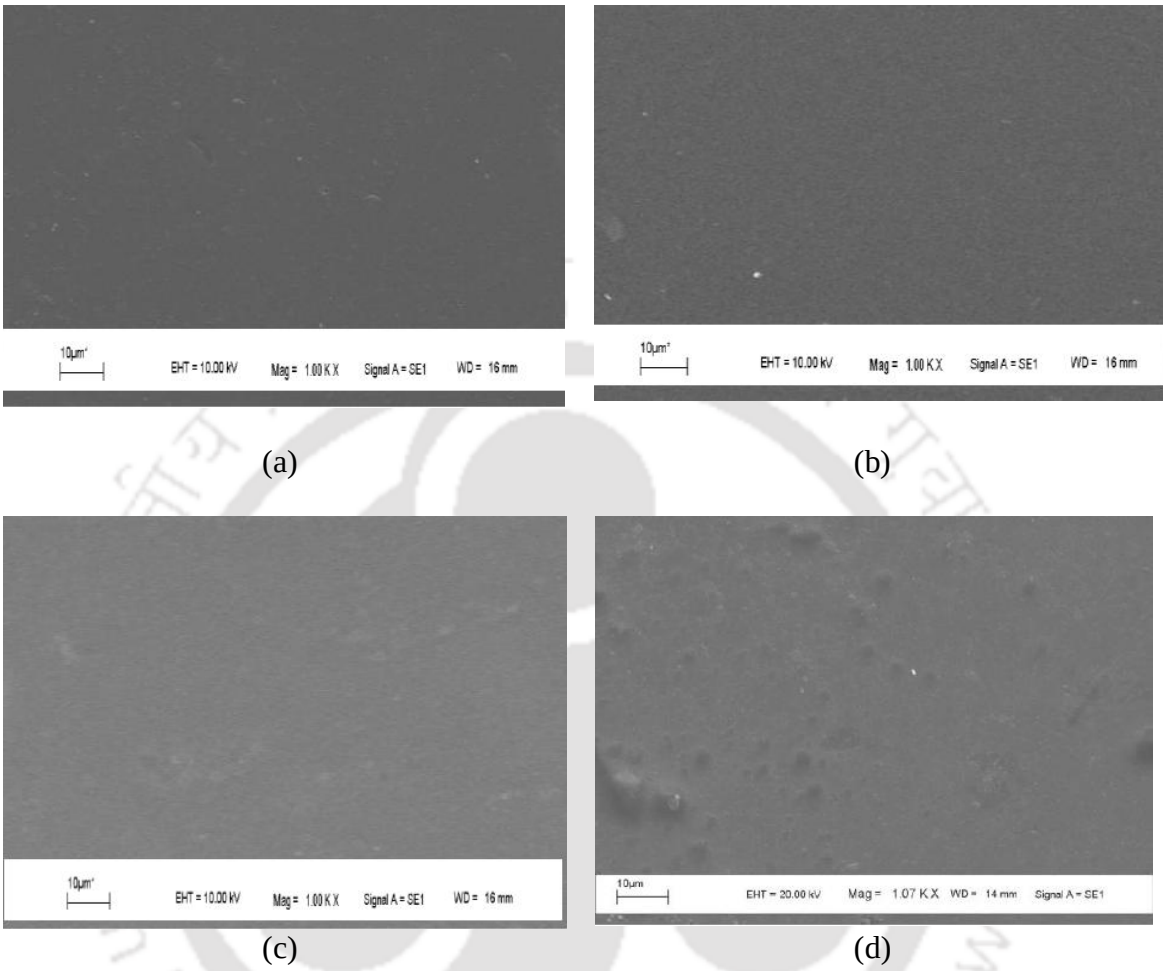

Figure A.1: SEM image of (a) 3% ErTfO/nafion, (b) 5% ErTfO/nafion, (c) 7% ErTfO/nafion, and (d) 9% ErTfO/nafion composite membranes

Figures A.1 and A.2 shows the SEM images of ErTfO/nafion and NdTfO/nafion membranes with an additive loading of 3%, 5%, 7%, and 9% for each membrane type. As discussed in section 4.2.1, the surface morphology of ErTfO/nafion and NdTfO/nafion composites bear similarity in appearance with that of pure cast nafion membrane and the increase in additive loading did not show any marked difference in surface morphology, which may be attributed to the miscibility of the additives in nafion solution.

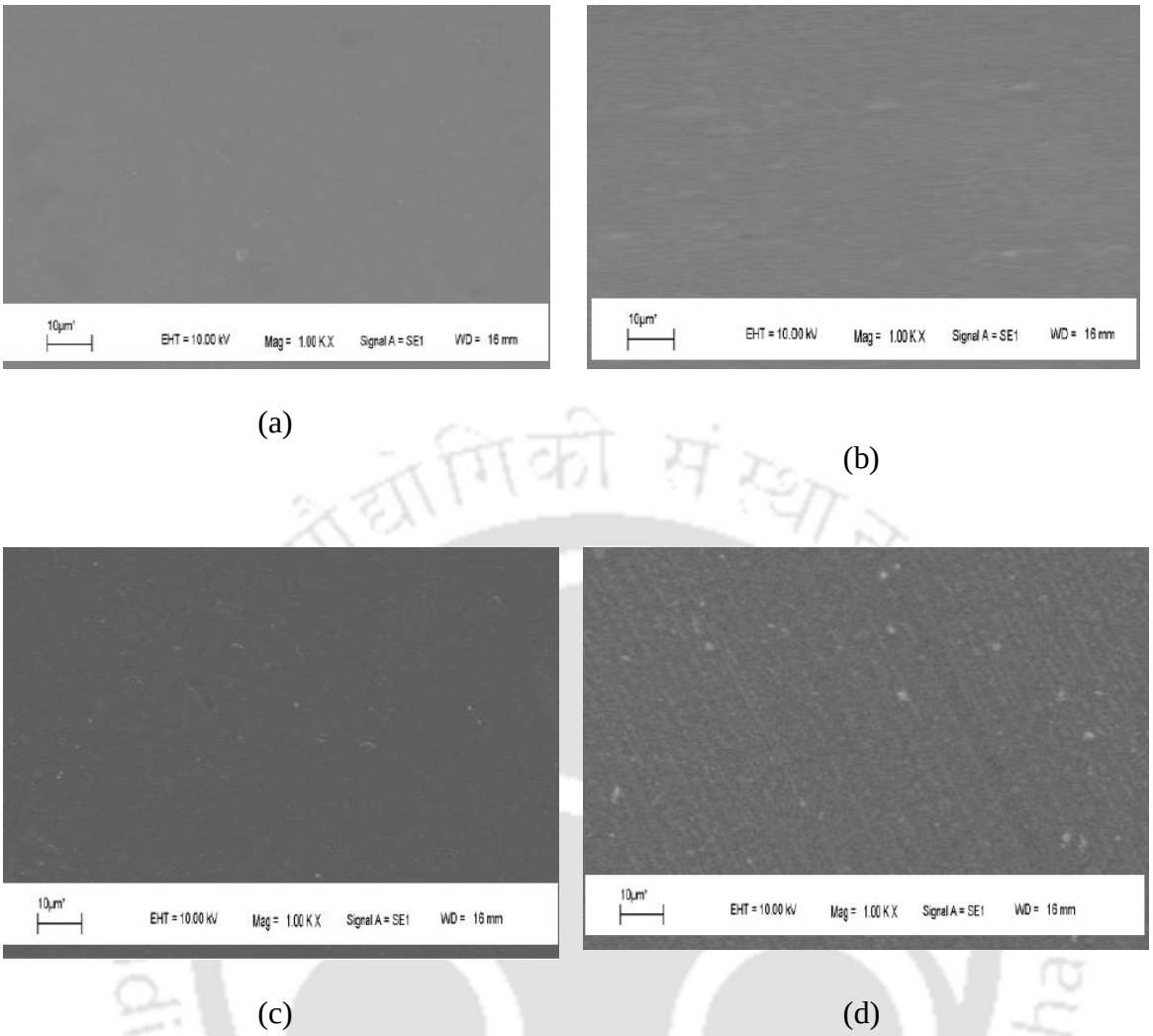

Figure A.2: SEM image of (a) 3% NdTfO/nafion, (b) 5% NdTfO/nafion, (c) 7% NdTfO/nafion, and (d) 9% NdTfO/nafion composite membranes

A.b: ***TGA of membranes***

Figures A.3 to A.8 shows the thermogram of the nafion composites with a loading of 3%, 5%, 7%, and 9% of TiO_2, Nd_2O_3, talc, ErTfO, NdTfO, and MS, respectively. It can be seen from the thermograms that the nafion composite membranes with the various type of additives at a loading of 3%, 5%, 7%, and 9% are thermally stable and at par with pure cast nafion membrane. Thus, incorporation of the additives did not reduce the thermal stability of nafion membrane.

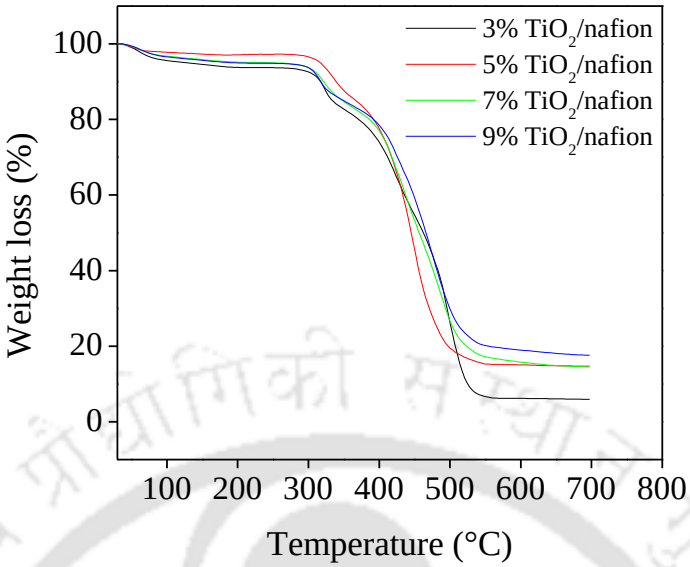

Figure A.3: Thermogram of TiO_2/nafion composite membranes with a loading of 3%, 5%, 7%, and 9% TiO_2

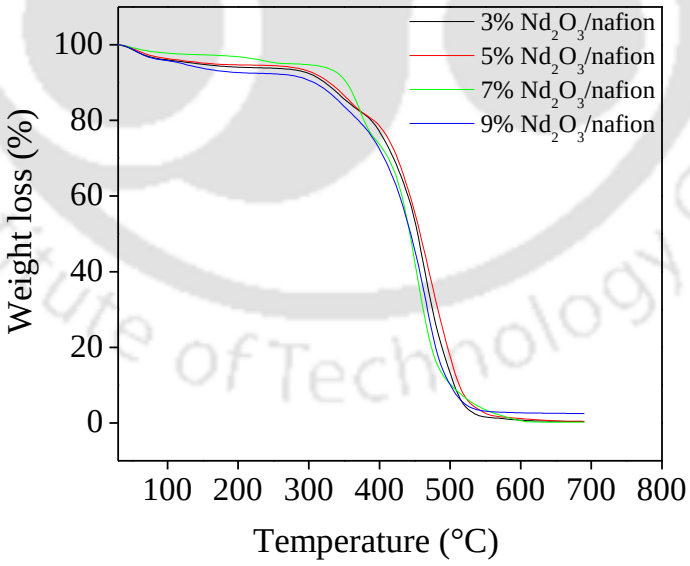

Figure A.4: Thermogram of Nd_2O_3/nafion composite membranes with a loading of 3%, 5%, 7%, and 9% Nd_2O_3

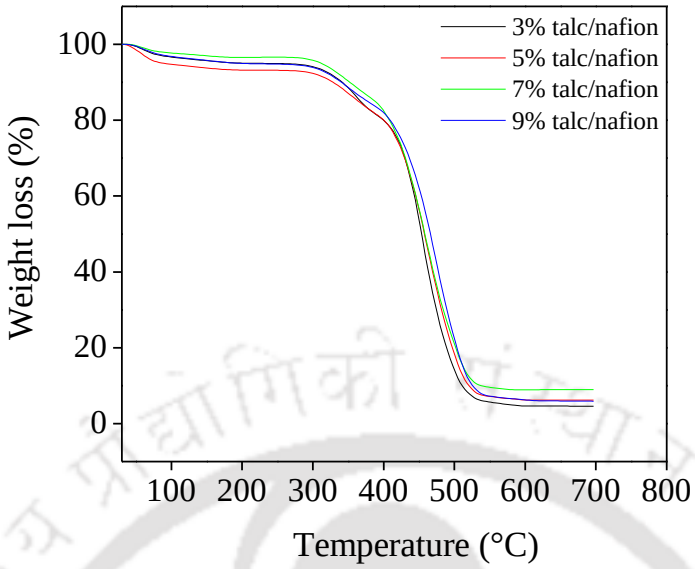

Figure A.5: Thermogram of talc/nafion composite membranes with a loading of 3%, 5%, 7%, and 9% talc

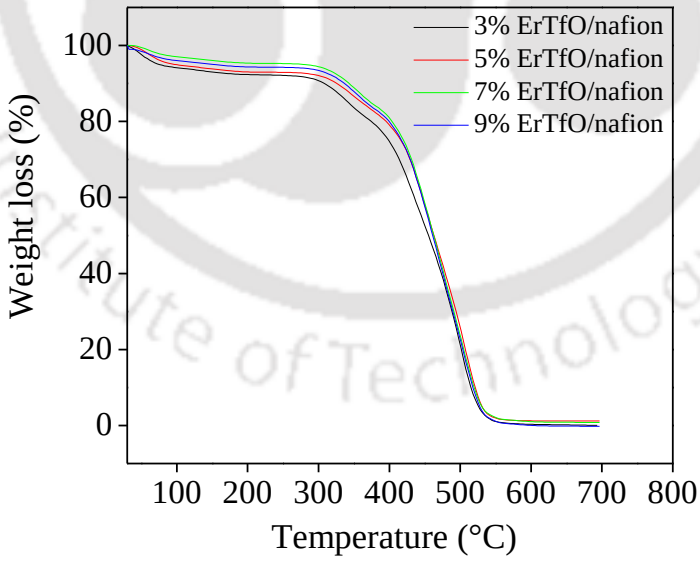

Figure A.6: Thermogram of ErTfO/nafion composite membranes with a loading of 3%, 5%, 7%, and 9% ErTfO

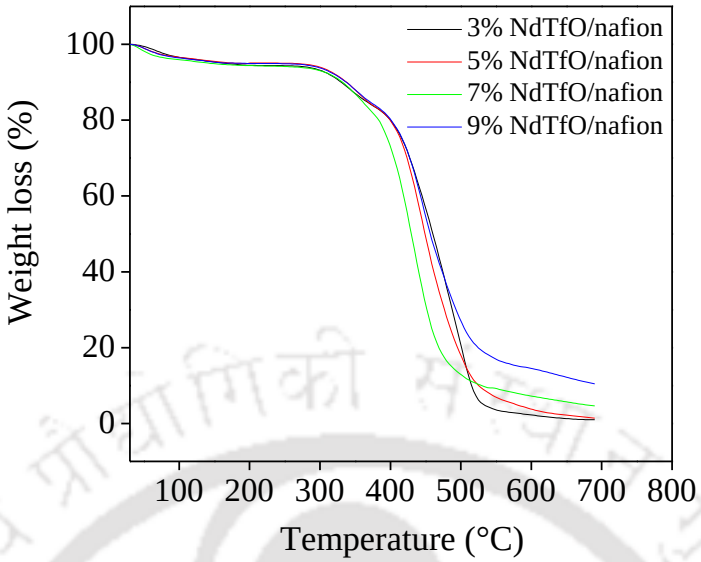

Figure A.7: Thermogram of NdTfO/nafion composite membranes with a loading of 3%, 5%, 7%, and 9% NdTfO

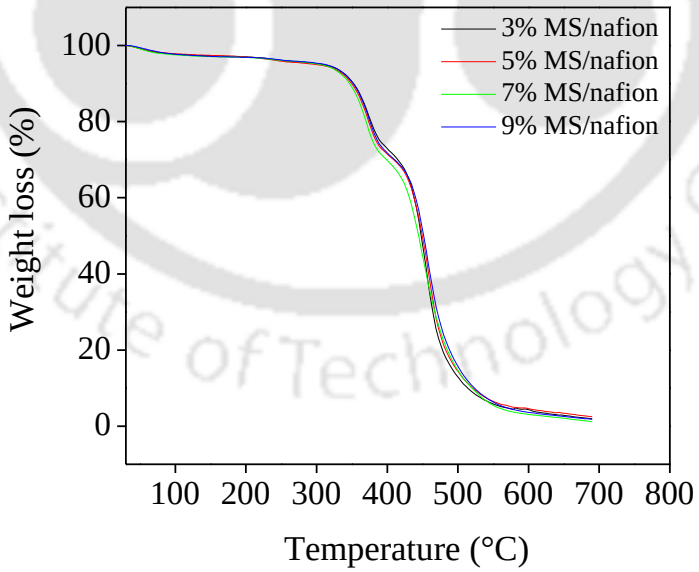

Figure A.8: Thermogram of MS/nafion composite membranes with a loading of 3%, 5%, 7%, and 9% MS

A.c: *FTIR of membranes*

Figure A.9 shows the FTIR spectra of 1% talc/nafion membrane highlighting the peaks for Si-OH (960 cm^{-1}) and Si-O-Si(1084 cm^{-1} and 1035 cm^{-1}), which were visible only for the talc/nafion membrane and were absent for pure cast nafion membrane [Jung et al., 2002]. Similarly, the Mg-O absorption peaks expected in the 400-600 cm^{-1} region (fig. A.10) was observed only for the talc/nafion membrane and was absent for pure cast nafion membrane [Raj et al., 2007].

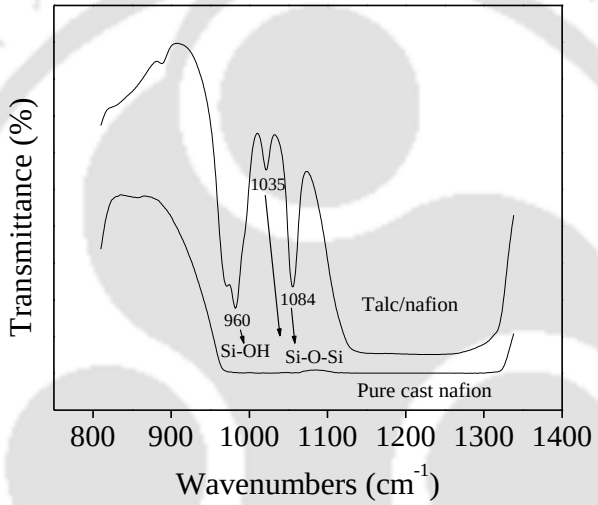

Figure A.9: FTIR spectra of characteristic peaks of Si-O-Si and Si-OH

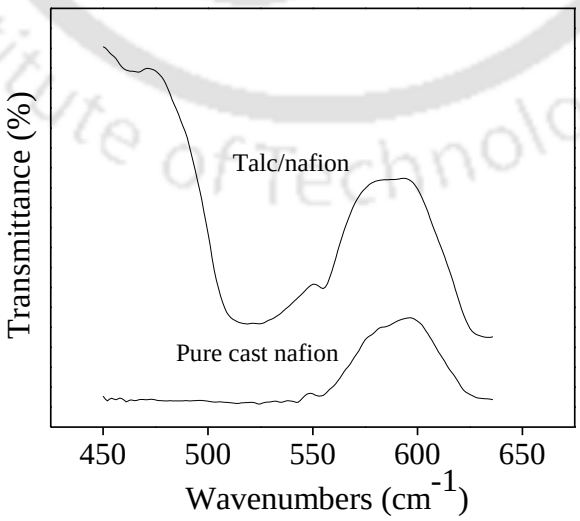

Figure A.10: FTIR spectra of characteristic peak of Mg-O

Research output

Journal publications

1. L. Barbora and A.Verma, 'Enhanced performance of direct methanol fuel cell using talc modified nafion membrane', International Journal of Innovative Research and Development, 7 (2012) 128-133.
2. N. Shroti, L. Barbora, R. Singh and A. Verma, 'Neodymium triflate modified nafion composite membrane for reduced alcohol permeability in direct alcohol fuel cell', International Journal of Hydrogen Energy, 36:22 (2011) 14907-14913.
3. L. Barbora, R. Singh, N. Shroti and A. Verma, 'Synthesis and characterization of neodymium oxide modified nafion membrane for direct alcohol fuel cells', Materials Chemistry and Physics 122 (2010) 211–216.
4. L. Barbora, S. Acharya and A. Verma, 'Synthesis and ex-situ characterization of nafion/TiO_2 composite membranes for direct ethanol fuel cell', Macromolecular Symposia, 277 (2009) 177–189.
5. L. Barbora, S. Acharya, R. Singh, K. Scott and A. Verma, 'A novel composite nafion membrane for direct alcohol fuel cells', Journal of Membrane Science, 326 (2009) 721–726.
6. L. Barbora, S. Acharya, S. Kaalva, A. Difoe and A. Verma, 'Nafion/TiO_2 composite membrane for direct methanol fuel cell', International Journal of Chemical Science, 5 (2007) 1579-1589.

Presentation in International Conference

1. L. Barbora, N. Shroti, R. Singh and A. Verma, FUCETECH 2009, 11-13 Nov., 2009, Mumbai.

2. L. Barbora, S. Acharya and A. Verma, POLYCHAR-World Forum of Advanced Materials, 17-21 Feb., 2008, Lucknow.
3. L. Barbora and A. Verma, International Seminar and Workshop on Energy, Sustainability, and Development, 12-14 Oct., 2012, Sibsagar, Assam.

Presentation in National Conference

1. L. Barbora, S. Acharya, R. Singh and A. Verma, CHEMCON 2009, in the 62nd Annual Meeting of Indian Institute of Chemical Engineers, 27-30 December, 2009, Visakhapatnam.
2. L. Barbora, S. Acharya, R. Singh and A. Verma, CHEMCON 2008, in the 61th Annual Meeting of Indian Institute of Chemical Engineers, 27-30 December, 2008, Chandigarh.
3. L. Barbora, S. Acharya, S. Kaalva, A. Difoe and A. Verma, National Conference on Frontiers in Chemical Engineering, 12-14 December, 2008, IIT Guwahati, Assam.

Award/Recognition

1. Ms. Lepakshi Barbora has been Awarded *Diploma of Distinction* by *World Forum on Advanced Materials (POLYCHAR16*) for her research work paper entitled, 'Composite polymer electrolyte membrane for direct ethanol fuel cell' Lucknow, 17-22 Feb, 2008.

About the author

The author has been working as a Scientific Officer in the Centre for Energy at IIT Guwahati since February, 2005, and joined the PhD programme in July, 2006 as a part time scholar. The author completed her M.Sc. in Molecular Biology and Biotechnology in 2000 from Tezpur University, Tezpur, Assam, India.

The author had worked as a Project Assistant in the project entitled 'High rate biomethanation of lignocellulosic waste and the utilization of its effluent as plant growth regulators', a project funded by MNES (now MNRE), New Delhi, in the Division of Biochemistry, RRL (now NEIST), Jorhat, Assam, from July 2001 to July 2003.She joined IIT Guwahati in July, 2003 as a Technical Assistant in the Department of Biotechnology.

The author is associated with several sponsored projects as co-principal investigator. The author published 6 research papers in several peer reviewed high impact factor international journals. She has also presented several scientific and technical research papers in national and international seminars and symposiums. At present, she is also the reviewer of several international journals.